

Axel Petzold *Editor*

Optical Coherence Tomography in Multiple Sclerosis

Clinical Applications

 Springer

Optical Coherence Tomography in Multiple Sclerosis

Axel Petzold
Editor

Optical Coherence Tomography in Multiple Sclerosis

Clinical Applications

 Springer

Editor

Axel Petzold
Department of Neuroimmunology
VU Medical Center
Expertise Center Neuro-ophthalmology
Departments of Neurology
and Ophthalmology, Amsterdam
The Netherlands, Moorfields Eye Hospital
Department of Neuro-Ophthalmology
London, UK
UCL Institute of Neurology
London
UK

ISBN 978-3-319-20969-2 ISBN 978-3-319-20970-8 (eBook)
DOI 10.1007/978-3-319-20970-8

Library of Congress Control Number: 2015949464

Springer Cham Heidelberg New York Dordrecht London
© Springer International Publishing Switzerland 2016

This work is subject to copyright. All rights are reserved by the Publisher, whether the whole or part of the material is concerned, specifically the rights of translation, reprinting, reuse of illustrations, recitation, broadcasting, reproduction on microfilms or in any other physical way, and transmission or information storage and retrieval, electronic adaptation, computer software, or by similar or dissimilar methodology now known or hereafter developed.

The use of general descriptive names, registered names, trademarks, service marks, etc. in this publication does not imply, even in the absence of a specific statement, that such names are exempt from the relevant protective laws and regulations and therefore free for general use.

The publisher, the authors and the editors are safe to assume that the advice and information in this book are believed to be true and accurate at the date of publication. Neither the publisher nor the authors or the editors give a warranty, express or implied, with respect to the material contained herein or for any errors or omissions that may have been made.

Printed on acid-free paper

Springer International Publishing AG Switzerland is part of Springer Science+Business Media
(www.springer.com)

Preface

Over the past decade optical coherence tomography (OCT) has developed from a research instrument to a clinical tool without which many clinicians will not want to do. This book, *Optical Coherence Tomography in Multiple Sclerosis: Clinical Applications*, takes into account the need for up-to-date information on current research in multiple sclerosis subgroups and multiple sclerosis associated optic neuritis. The assessment for macular edema has become obligatory for many patients suffering from multiple sclerosis who take disease modifying treatment.

This book comes in handy if you want to learn how to use or interpret retinal optical coherence tomography (OCT). The book was predominantly written for readers with a neurological or neuro-ophthalmological background. There are parts of the book that are of value for OCT technicians. Those involved in designing and conducting clinical trials will find practical and theoretical information in a clear structured format supported by simple flow-charts and addressing current regulatory authorities' standards.

Eminent specialists in the field review the data available for multiple sclerosis-associated optic neuritis (MSON), neuromyelitis optica (NMO), clinically isolated syndromes (CIS), relapsing-remitting multiple sclerosis (RRMS), and progressive multiple sclerosis (SP and PP MS). Image examples are given for characteristic findings, with one chapter entirely dedicated to OCT image interpretation of the differential diagnosis of MS and MSON mimics.

This book gives special reference to newly recognized signs that only became possible by the clinical application of OCT. Bidirectional transsynaptic axonal degeneration is the driving mechanism behind the cascade of inner retinal layer atrophy, stopping at the level of the inner nuclear layer, only to give rise to a retrograde maculopathy with its characteristic microcysts. For those readers who now feel they want to refresh their anatomical knowledge of the retina, one chapter will discuss layer by layer combining histology with OCT hyper- and hypodense bands. As this terminology already suggests, retinal OCT imaging has taken a role of similar importance to the retina as the radiological imaging for the brain.

Amsterdam, The Netherlands
London, United Kingdom

Axel Petzold, MD, PhD

Contents

1 Introduction: Clinical Application of OCT in Multiple Sclerosis	1
Sven Schippling	
2 Anatomy of the Retina and the Optic Nerve	3
Nikos Evangelou and Omar S.M. Alrawashdeh	
3 Optical Coherence Tomography (OCT)	21
Axel Petzold	
4 MS-Associated Optic Neuritis (MSON)	47
Kannan Narayana, Rachel C. Nolan, Steven L. Galetta, and Laura J. Balcer	
5 Clinical Use of OCT and MSON Mimics	59
Axel Petzold and Gordon T. Plant	
6 OCT Findings in Neuromyelitis Optica Spectrum Disorders	85
Olivier Outteryck and Patrick Vermersch	
7 OCT and Early MS: Clinically Isolated Syndromes (CIS)	97
Fiona Costello	
8 OCT in Relapsing–Remitting Multiple Sclerosis (RRMS)	113
Shiv Saidha and Peter A. Calabresi	
9 Progressive Multiple Sclerosis (SP and PP MS)	135
Friedemann Paul and Alexander U. Brandt	
10 Retrograde Maculopathy	151
Mathias Abegg	
11 Monitoring Treatment in Multiple Sclerosis	161
Shin C. Beh, Teresa C. Frohman, and Elliot M. Frohman	
12 Drug Trials in Neuroprotection	171
Elena H. Martínez-Lapiscina, Bernardo Sanchez-Dalmau, and Pablo Villoslada	
13 Role of the OCT Reading Center	185
Ferenc B. Sallo, James V.M. Hanson, Sebastian Lukas, and Sebastian Wolf	
Index	195

Contributors

Mathias Abegg, MD, PhD Universitätsklinik für Augenheilkunde, Universität Bern, Inselspital, Bern, Switzerland

Omar S.M. Alrawashdeh, MBBS (MD), PhD Clinical Neurology Unit of Clinical Neurology, Faculty of Medicine, Alkarak Hospital, Mutah University, Alkarak, Jordan

Laura J. Balcer, MD, MSCE Department of Ophthalmology, New York University Langone Medical Center, New York, NY, USA

Department of Population Health, New York University Langone Medical Center, New York, NY, USA

Department of Neurology, New York University Langone Medical Center, New York, NY, USA

Shin C. Beh, MD MS Division, Department of Neurology, University of Texas Southwestern Medical Center, Dallas, TX, USA

Alexander U. Brandt, MD NeuroCure Clinical Research Center, Department of Neurology, Charité University Medicine Berlin, Berlin, Germany

Peter A. Calabresi, MD Richard T. Johnson Division of Neuroimmunology and Neuroinfectious Diseases, Department of Neurology, Multiple Sclerosis Center, Johns Hopkins Hospital, Baltimore, MD, USA

Fiona Costello, MD, FRCP Departments of Clinical Neurosciences and Surgery (Ophthalmology), University of Calgary, Foothills Medical Centre, Calgary, AB, Canada

Nikos Evangelou, MD, FRCP, DPhil Department of Clinical Neurosciences, Medicine & Health Sciences, Nottingham University Hospital, Nottingham, UK

Elliot M. Frohman, MD, PhD, FAAN Department of Neurology & Neurotherapeutics and Ophthalmology, Multiple Sclerosis and Neuroimmunology Program and Clinical Center for Multiple Sclerosis, University of Texas Southwestern School of Medicine, Dallas, TX, USA

Teresa C. Frohman, PA-C Department of Neurology, University of Texas Southwestern Medical Center at Dallas, Dallas, TX, USA

Steven L. Galetta, MD Department of Neurology, New York University Langone Medical Center, New York, NY, USA

James V.M. Hanson, PhD Department of Neurology, Neuro-OCT Reading Centre, University Hospital Zurich, Zurich, Switzerland

Department of Ophthalmology Neuro-OCT Reading Centre, University Hospital Zurich, Zurich, Switzerland

Sebastian Lukas, Dipl. Ing. (FH) Neuroimmunology and Multiple Sclerosis Research Section, Department of Neurology, Neuro-OCT Reading Centre, University Hospital Zürich, Zürich, Switzerland

Elena H. Martínez-Lapiscina, MD, PhD Center of Neuroimmunology and Ophthalmology Department, Institute of Biomedical Research August Pi Sunyer (IDIBAPS) – Hospital Clinic of Barcelona, Barcelona, Spain

Kannan Narayana, MBBS, MD Department of Neurology, New York University Langone Medical Center, New York, NY, USA

Rachel C. Nolan, BA Department of Neurology, New York University Langone Medical Center, New York, NY, USA

Olivier Outteryck, MD Department of Neurology, University Hospital of Lille, Lille, France

Friedemann Paul, MD Department of Neurology, NeuroCure Clinical Research Center, Charité University Medicine Berlin, Berlin, Germany

Axel Petzold, MD, PhD Department of Neuro-ophthalmology, Moorfields Eye Hospital & National Hospital of Neurology and Neurosurgery, London, UK

Department of Neuroimmunology, UCL Institute of Neurology, London, UK

Departments of Neurology and Ophthalmology, Dutch Expertise Center Neuro-Ophthalmology, VU Medical Center, Amsterdam, The Netherlands

Gordon T. Plant, MA, MD, FRCP, FRCOphth Department of Neuro-ophthalmology, Moorfields Eye Hospital, St. Thomas' Hospital, National Hospital for Neurology and Neurosurgery, London, UK

Shiv Saidha, MBBCh, MD, MRCPI Division of Neuroimmunology and Neurological Infections, Department of Neurology, Johns Hopkins Hospital, Baltimore, MD, USA

Ferenc B. Sallo, MD, PhD NIHR Biomedical Research Center for Ophthalmology of Moorfields Eye Hospital and the UCL Institute of Ophthalmology, London, UK

Bernardo Sanchez-Dalmau, MD Center of Neuroimmunology and Ophthalmology Department, Institute of Biomedical Research August Pi Sunyer (IDIBAPS) – Hospital Clinic of Barcelona, Barcelona, Spain

Sven Schippling, MD Neuroimmunology and Multiple Sclerosis Research Section, Department of Neurology, University Hospital Zurich and University of Zurich, Zurich, Switzerland

Patrick Vermersch, MD, PhD Department of Neurology, Université de Lille (EA2686), Hopital Roger Salengro CHRU Lille, Lille, France

Pablo Villoslada, MD, PhD Center of Neuroimmunology and Ophthalmology Department, Institute of Biomedical Research August Pi Sunyer (IDIBAPS) – Hospital Clinic of Barcelona, Barcelona, Spain

Sebastian Wolf Department of Ophthalmology, Inselspital, University Hospital Bern, Bern, Switzerland

Introduction: Clinical Application of OCT in Multiple Sclerosis

1

Sven Schippling

Multiple sclerosis (MS) is an inflammatory and neurodegenerative disease of the central nervous system, in which several environmental factors act against the background of a complex, poly-genetic trait. Pathologically, MS is characterized by T-cell-mediated inflammation and neuro-axonal damage that lead to tissue loss. While the former may be associated with functional deficits (commonly referred to as relapses) during early, relapsing phases of the disease, the latter is thought to be the morphological correlate of sustained disability characterizing more advanced stages of the disease. Exact mechanisms leading to degeneration of neurons and axons in MS, however, are far less well understood.

Furthermore, disease subtypes as well as individual disease phenotypes are characterized by significant clinical and pathological heterogeneity. The most commonly accepted *in vivo* surrogate marker to monitor disease activity to date is magnetic resonance imaging (MRI). With the introduction of the McDonald criteria, MRI has also become vital in MS diagnosis. Proving dissemination in space and time radiologically instead of clinically has led to earlier diagnoses or increased sensitivity of the new criteria. However,

MRI findings associated with MS are largely unspecific as regards the underlying pathology. Advanced MRI sequences with potentially increased specificity for distinct pathological features—such as magnetization transfer (MTR) in case of de- and re-myelination or diffusion tensor imaging (DTI) in case of demyelination and/or axonal loss—are costly, time consuming, and not yet routinely available in many clinical settings.

It is against this background and the fact that the retinal nerve fiber layer (RNFL) consists of nonmyelinated axons that optical coherence tomography (OCT) offers a unique and novel technology to quantify the extent of neurodegenerative changes in individual MS patients. Any change to RNFL integrity can thus be supposed to reflect thinning or loss of its axons. Similarly, a loss of ganglion cell layer thickness reflects a loss of primary neurons (i.e., ganglion cells). Clinically, visual impairment is common in MS with 20–30 % of patients presenting with multiple sclerosis associated optic neuritis (MSON) as a primary symptom. Recent evidence from histopathology studies suggests that primary retinal pathology involves retinal axons and neurons despite the absence of myelin—the major target of the autoimmune response in MS. Based on patients' perceptions, visual function is the second highest-ranked bodily function next to ambulation in both early and late disease stages.

Due to the confined size of the retina as a target structure, probing fine structure/function correlations may reduce the level of variability that

S. Schippling, MD
Neuroimmunology and Multiple Sclerosis Research
Section, Department of Neurology, University Hospital
Zurich and University of Zurich, Zurich, Switzerland
e-mail: Sven.Schippling@usz.ch

seems inherent in brain and spinal cord MR imaging based on the random and sparse distribution of lesions. Since the first two-dimensional OCT images generated by Fujimoto and colleagues at the Massachusetts Institute of Technology (MIT) in 1991 [1], the technology has undergone a remarkable development witnessed by a significant body of literature both in ophthalmology and, more recently, neurology. Many of the colleagues who have pioneered the technology in the field of neurology have also contributed to this compendium. Following a number of cross-sectional studies showing retinal pathology in MS assessed by OCT, more recent papers using a longitudinal approach suggest that retinal degeneration beyond levels of physiological aging can reliably be detected in MS patients even in the absence of clinical episodes of multiple sclerosis associated optic neuritis (MSON). Recent technical developments in post-processing of OCT macular B-scans allow reliable segmentation of all—including deeper—retinal layers. Significant improvements in the technical properties, including the level of resolution and acquisition time, of recent spectral-domain OCT technology have fostered a broad application in a number of inflammatory and neurodegenerative neurological diseases, with MS still being the most intensively investigated disease model. Here, retinal measures of atrophy correlate strongly with functional visual and MRI atrophy outcomes. Consequently, assessing structural changes of the anterior visual pathway using OCT together with measures of functional integrity appears to be a unique model to investigate major pathological mechanisms relevant to the disease.

While major OCT findings in MS patients may not be specific for the disease and can be found in a number of optic neuropathies other than MS-associated MSON, the amplitude of change as well as the spatial distribution of axonal loss associated with a single MSON episode, e.g., in neuromyelitis optica (NMO), usually outweighs the magnitude of change in MS. These findings together with further improvements of the technology itself as well as post-processing of OCT images may help to further increase the specificity of the methodology.

In this compendium we have tried to put together an overview of major recent advances in

OCT technology as much as in its clinical application. In the beginning, the anatomy of the retina and visual pathway will be recapitulated followed by an overview of basic technological characteristics of OCT. Several individual chapters are then dedicated to OCT findings in different optic neuropathies as well as the different phenotypes of MS and a potential role of OCT in treatment monitoring. The level of availability of the latest OCT technology in clinical routine would in principle justify the application of OCT in multicenter clinical trials. To date, proof-of-concept phase II as well as phase III clinical trials in MS investigating regenerative or neuroprotective properties of compounds are costly and time consuming, typically requiring long-term follow-ups in order to prove efficacy. Typically, such studies involve structural (and functional) MRI of the brain and the spinal cord, although the sparse nature of lesions and the high degree of variability among patients remain challenging. Quantitative assessment of neurodegenerative changes in the optic tract using OCT might constitute an attractive alternative strategy for such studies due to the combination of a relatively small and easily accessible anatomical structure, the magnitude of change of RNFL and ganglion cell layer thickness in a first ever MSON episode, and the predictive power of retinal OCT as regards functional visual outcomes. A major prerequisite for the use of OCT as a clinical trial endpoint in a multicenter approach is to guarantee for high levels of reliability of repeated measures through rigorous quality control based on validated quality criteria. It is for this reason that we decided to close the book with a chapter on OCT reading.

We hope that we have put together an interesting compendium that may provide a useful starting point for the interested reader as well as an overview for both the clinical neurologist and the physician-scientist with an interest in the technology and its clinical application.

Reference

1. Huang D, Swanson EA, Lin CP, Schuman JS, Stinson WG, Chang W, Hee MR, Flotte T, Gregory K, Puliafito CA, Fujimoto JG. Optical coherence tomography. *Science*. 1991;254(5035):1178–81.

Nikos Evangelou and Omar S.M. Alrawashdeh

Introduction

Vision is defined as the ability of our nervous system to perceive and process information obtained from visible light. Light waves are initially perceived by photoreceptors and then converted into electric signals in a process called phototransduction [1].

The process of vision starts when light successfully travels through the eyeball to be focused on the retina. The eye, the visual organ, is a sphere formed of three layers. The outer layer is a connective tissue layer formed of the sclera posteriorly and the cornea anteriorly. The middle layer is a pigmented layer formed of the choroid. The choroid is the layer that provides nourishment to the inner photosensitive layer, which is the retina [2]. The iris and the ciliary body are the anterior continuation of the choroid layer and they contain muscles that control the amount of light and the refractive power of the lens to ensure that the optimal image quality is focused on the retina [2]. The inner layer is the retina, which

sends signals that are transmitted via the optic nerve to the brain.

The Retina

The retina embryologically belongs to the central nervous system. It is a complex structure that is derived from the ventricles around the diencephalon. The developmental process of the retina is similar to that of the cerebral cortex where multipotent neuroblastic precursors proliferate and differentiate and each cell migrates to its laminar destination producing a multilayered tissue [3]. The photosensitive part of the retina lines the posterior two-thirds of the eyeball and blends with the anterior insensitive part at a junction called the ora serrata. It has a diameter of 30–40 mm [2, 4–6] with a total area of approximately 11 cm² [4]. The posterior part of the retina is the central retina and measures about 6 mm diameter. The central retina is occupied by an elliptical area called the macula lutea, which represents an area with the highest visual acuity. The area anteriorly beyond the central retina to the junction of ora serrata is called the peripheral retina.

The retinal thickness varies, being thickest at the area of the optic disk (0.56 mm) [4, 7]. Peripheral to the optic disk, the retina is thinner and becomes about 0.1 mm at the most peripheral part near the ora serrata junction [7].

N. Evangelou, MD, FRCP, DPhil (✉)
Department of Clinical Neurosciences,
Medicine and Health Sciences, Nottingham
University Hospital, Nottingham, UK
e-mail: Nikos.Evangelou@nottingham.ac.uk

O.S.M. Alrawashdeh, MBBS (MD),
PhD Clinical Neurology
Unit of Clinical Neurology, Faculty of Medicine,
Alkarak Hospital, Mutah University, Alkarak, Jordan

The optic disk is located 3 mm medial and 1 mm superior to the macula lutea. The disk is about 1.5 mm in diameter and appears paler on ophthalmoscopy than the rest of the retina, with a central depression for the passage of central retinal vessels. The area of the optic disk is devoid of photoreceptors and therefore it is insensitive to light (detected as a blind spot during the conventional neurological examination) [5].

From the optic disk, the branches of the central retina artery and veins can be seen using the ophthalmoscope. These vessels are the only vessels of the body that can be visualized directly by the naked eye due to the transparency of the retina. Vessels are seen spreading from the optic disk to various regions of the retina except the area of the fovea, which has no vessels and thus is called the avascular zone [4].

Layers of the Retina

Layers of the retina are uninterrupted in all areas of the optic retina except the area of the optic disk where the fibers exit the retina to form the optic nerve. However, these layers are present with variable thickness throughout the retina [8].

Most textbooks describe ten histological retinal layers, which are described from the outermost layer (layer 1 near the choroid) to the innermost layer (layer 10 near the vitreous body) [9]. These layers have been described according to their appearance under the light microscope and electron microscope [10, 11]. However, *in vivo* study of retinal layers has been achieved by using retinal optical coherence tomography (OCT). Various layers of the retina can appear hyporeflective or hyperreflective with the retinal OCT (Fig. 2.1) [12].

Layer 1: Retinal Pigment Epithelium

Histologically, the retinal pigment epithelium (RPE) is composed of a single layer of low cuboidal epithelium. This layer has a neuroectodermal embryologic origin [3, 13, 14], with abundant melanosomes (melanin-containing granules)

within the cells' cytoplasm [15]. With OCT, the RPE layer appears hyperreflective [16].

The pigment epithelium forms the outer layer of the entire neural retina and extends from the optic disk forward through the ora serrata to be continuous with the epithelium of the ciliary body [2, 4]. There are about four million epithelial cells in each human retina [17]. The greatest density of these cells is in the fovea (5000/mm²) where these cells are also smaller and appear more condensed to each other. From the surface view of the retina, the retinal pigment epithelial cells appear tightly packed with regular hexagonal arrangement. This is due to the presence of tight junctions between cells. These tight junctions form a band that appears histologically as a membrane called Verhoeff's membrane [18]. Their number is reduced with age, especially at the periphery where they reach 2000/mm² in people above 40 years of age [19].

The basal surface of the RPE is separated from the underlying choroid capillaries by a membrane called Bruch's membrane [20]. Bruch's membrane is an elastic membrane that is formed of five layers: the choriocapillaris basement membrane, the outer collagenous layer, the central elastic layer, the inner collagenous layer, and the basement membrane of the RPE [5]. As the RPE, Bruch's membrane also appears hyperreflective with the OCT. In low-resolution OCT, the RPE and Bruch's membrane appear as one thick zone, but with high-resolution (spectral-domain) OCT, two hyperreflective zones separated by a thin hyporeflective band can be identified. As it appears on the OCT, the whole zone has been recently referred to as the RPE/Bruch's complex (zone 14) (Fig. 2.1) [16].

The presence of the underlying Bruch's membrane and the tightly packed epithelial cells create a barrier between the choriocapillaris and the outer retina. This barrier, usually referred to as the outer blood-retina barrier, works with the inner blood-retina barrier to control the microenvironment of the retina and to protect the retina from the immune system and systemic infections. These barriers are selective and allow for small molecules such as O₂ and CO₂ to diffuse freely [21].

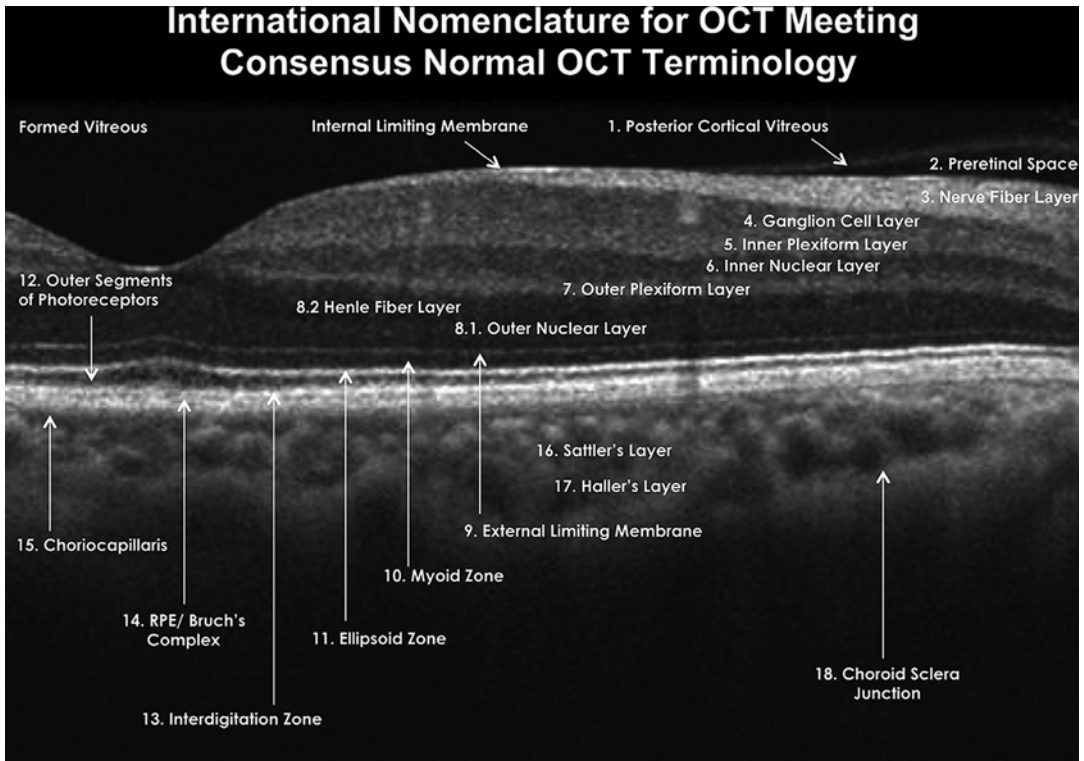


Fig. 2.1 Retinal layers as they appear on spectral domain optical coherence tomography (Reprinted with permission from Staurenghi et al. [16])

The apical surface of the cuboidal epithelium is in contact with the photoreceptors (cone and rod processes) within the subretinal space. Here, the cuboidal epithelial cells possess microvilli that project in between processes of rods and cones [19]. The subretinal space is the extracellular space between the RPE microvilli and the photoreceptors. Every single epithelial cell faces 40 photoreceptors [19]. This arrangement of the RPE microvilli and the photoreceptor processes appears with retinal OCT as a hyperreflective zone on the apical side of the RPE. This has been believed to be the reflection of Verhoeff's membrane, which represents the tight junction between RPE cells. It has been reported recently that this hyperreflective zone is in fact the outer tips of the photoreceptors with microvilli of the RPE [16, 22] and was named the interdigitation zone (zone 13) (Fig. 2.1) [22].

The connection between photoreceptors and microvilli in the interdigitation zone is important

in maintaining integrity of the retina and also in the turnover process of rod and cone molecules. In fact, the granular appearance of the RPE cells is believed to be due to lipofuscin granules, which are produced from the phagocytosis of rod and cone debris into the cytoplasm of the pigment cells of this layer [23].

Retinal epithelial cells have high metabolic activity and that explains the abundance of mitochondria, endoplasmic reticulum, and free ribosomes [24, 25]. There appears to be active transport of molecules across the basal and apical surfaces of pigment epithelial cells with the outer choroid layer capillaries and the inner photoreceptor layer, respectively. For example, retinol is an essential vitamin for the visual cycle. This vitamin is absorbed from the choriocapillaris by the retinal epithelium and then supplied to the photoreceptors. The RPE is also supportive to the photoreceptors of the retina; loss of the epithelial layer usually results in atrophy of the photoreceptors [5, 25].

Another proposed function of the retinal epithelium is absorption of light that goes through the retinal layers and prevents it from being reflected back to the photosensitive cells, thus preventing photoreceptor cells from being restimulated. It is believed that this process helps in improving the image quality [25]. In addition, the layer also absorbs the energy from the reflected light and prevents it from overheating the eye. However, very strong light initially causes damage to this layer and consequently damage to the retina [26].

Layer 2: Photoreceptor Layer

This layer contains processes of cone and rod cells that receive light signals and convert them into electric signals. Each of these processes has an outer segment and inner segment. The plasma membrane of the outer segment is arranged into hundreds of flat disks [27]. The flat disks contain photopigments that are attached to their plasma membrane. Such arrangement increases the surface area of the plasma membrane and consequently the amount of photopigments. The lamellated disks with their photopigments are disposed between microvilli of the retinal pigment epithelium to form the interdigitation zone that has been described [16]. There are no junctional complexes between microvilli and the plasma membrane of the photoreceptor disks creating the subretinal space [28]. It is a loose potential space that is liable to become a true space under certain pathological conditions when the retina becomes detached from the underlying RPE [29].

The inner segment is divided into two parts: the outer zone is packed with mitochondria making it hyperreflective under OCT examination (ellipsoid zone), and the inner zone contains smooth and rough endoplasmic reticulum and appears hyporefective with retinal OCT (myoid zone) (Fig. 2.1) [5, 27, 30].

Therefore, the photoreceptor layer appears as three distinct zones on the OCT imaging: a hyporefective zone corresponds to the outer segment (zone 12), a hyperreflective zone

corresponds to the ellipsoid zone of the inner segment (zone 11), and a hyporefective zone corresponds to the myoid zone of the inner segment (zone 10) [16, 18].

Layer 3: External Limiting Membrane

The external limiting membrane appears on the OCT as a thin hyperreflective membrane that runs perpendicular to the direction of cell bodies of cone and rods and their process (zone 9) [16, 31, 32]. The inner segments of rod and cone cells pass through the external limiting membrane to reach their cell bodies in the next layer, which is the outer nuclear layer. It is not a true membrane; the intercellular junction between the processes of the cone and rods and Müller cells appears as a membrane on radial section of the retina [33, 34]. Integrity of this membrane is important in protection of photoreceptors [35], and in maintaining visual acuity in health and disease [36, 37].

Layer 4: Outer Nuclear Layer

The outer nuclear layer is formed of the cone and rod cell bodies containing their nuclei. These cells are the photosensitive cells of the retina. This layer is thickest at the macula and around the fovea centralis, where these cells form a multicellular layer [38].

Cone cells are primarily responsible for color vision with high resolution during daylight or under good lighting. The number of cones in the human retina is 4.6 million [39]. Cone cells are distributed in the entire retina but their concentration increases gradually toward the center of the retina to become highest in the area with the greatest visual acuity (the fovea), where the concentration reaches 199,000 cones/mm². Cone concentration reduces gradually away from the fovea to become 2500 cells/mm² near the ora serrata [38]. Also, cone density is higher in the nasal retina by 40–50 % compared to the temporal retina [39]. According to their lighting sensitivity, cone cells are classified into three types:

blue, red, and green ones. The most common cells are the red cones forming 63 % of all cone cells, followed by the green cones (32 %) and the blue cone cells (5 %).

Rod cells are responsible for night vision as they are sensitive to a high range of illumination including light with low intensity. Their number is greater than cones, with a total number of 92 million. Rod density is variable throughout the retina. However, density reduces toward the center of the retina to become absent at the area of the fovea [38, 39]. The highest density of rods is a ring area 3–5 mm away from the fovea where their concentration may reach 150,000 cells/mm². Concentration of rods also reduces to 30,000/mm² toward the periphery of the retina [38].

Cells forming the outer nuclear layer, rods and cones, have a similar structure characterized by long cells with vertical orientation relative to the retinal layers. Each cell of the rods and cones has two processes that travel radially into two different directions. One of these processes is the photoreceptor portion that forms the previously described zones on OCT, which are myoid (zone 10), ellipsoid (zone 11), outer segment layer (zone 12), and part of interdigitation zone 13. The other process is the photoreceptor axons, which travel vertically to reach the outer plexiform layer forming a membrane called Henle's fiber layer. The fiber layer of Henle is prominent at the area of the macula and can be recognized using OCT as a pale fibrous band apical to cone and rod cells [40, 41]. With OCT, the outer nuclear layer and Henle's fiber layer appear as one hyporeflexive zone (zone 8), where Henle's fiber layer occupies the inner half and the rod and cone cell bodies occupy the outer half of the zone [16]. Thickness of this zone can be measured using OCT and frequently correlated to the degree of visual acuity in a number of conditions, especially at the area of the macula [42, 43]. At the macula, the zone is liable for extravasation of fluid and protein causing edema of the macula, which significantly affects visual acuity. Macular edema can be detected with OCT imaging and commonly seen in patients with diabetes [44] and as a side effect of fingolimod use in multiple sclerosis patients [45].

Layer 5: Outer Plexiform Layer

It is a complex layer of synapses between different processes of cone and rod cells and other interneurons. The photoreceptor axons end in a cone pedicles or rod spherules that have synaptic contacts with other cells in the outer plexiform layer, such as the bipolar and horizontal cells [30]. It is considered the initial step in the processing of light signals where the first synapse of these signals takes place [46]. This layer conducts signals from the outer nuclear layer to the inner nuclear layer [46, 47]. The layer contains cone pedicles and rod spherules synapsing on dendrites of bipolar cells, horizontal cells, and interplexiform cells, and the whole zone appears on OCT as a hyperreflective layer (zone 7) [16, 48, 49].

Layer 6: The Inner Nuclear Layer

This layer contains the cell bodies and nuclei of different types of interneurons: the horizontal cells, the bipolar cells, the amacrine cells, the Müller cells, and the interplexiform cells. These cells form complex connections via their processes in the inner and outer plexiform layers; it is considered the interconnection between the photoreceptors and the ganglion cells. The nearest cells to the outer plexiform layers are the horizontal cells. The amacrine cells are present near the inner plexiform layer, while other cells are located in between [50–52].

The layer appears with the OCT as a hyporeflexive zone (zone 6) [16]. Its morphology can be affected by a number of diseases. However, there is no atrophy of the inner nuclear layer in multiple sclerosis or any other central pathology leading to retrograde axonal degeneration [53–55]. Focal thickening of the internuclear layer due to microcyst formation has been reported in MS and a large range of other neurological and ophthalmological diseases [56].

Bipolar Cells

The cell bodies and nuclei of bipolar cells are located in the inner nuclear layer. Each cell body

has two processes: one is directed internally toward the inner plexiform layers and the other externally toward the outer plexiform layer. The externally directed process has dendrites that come in contact with rod spherules and cone pedicles and horizontal cell dendrites in the outer plexiform layer. Usually bipolar cell processes have more than one dendrite that is connected to a variable number of cells. Bipolar cells that contact cone pedicles are called cone bipolar cells, while those that contact rod spherules are called rod bipolar cells. Usually rod bipolar cells contact as many as 70 rod cells, whereas rod bipolar cells make contact with fewer cone cells [46, 57].

The internally directed process has dendrites that contact ganglion cell dendrites and amacrine cells in the inner plexiform layer. Simply, bipolar cells convert the analogue signals from photoreceptors to a digital signal, which is transmitted to the ganglion cells [57].

Cone bipolar cells are classified into three types: midget bipolar cells, blue bipolar cells, and diffuse bipolar cells. Midget bipolar cells are small cells that directly connect cone cells to ganglion cells; each midget cell connects one cone cell to a ganglion cell. Midget cells are believed to be responsible for high spatial resolution. Blue cells are larger than midget cells and they mediate transmission of short-wave signals. The diffuse cone bipolar cells are connected to several cone cells, up to ten cones, and they probably mediate luminosity rather than color. Rod bipolar cells receive signals from many rod cells and transmit the signal to ganglion cells indirectly by contacting dendrites of amacrine cells [46, 57, 58].

Horizontal Cells

Horizontal cell bodies and nuclei are located in the outer zone of the inner nuclear layer. Each cell has many dendrites directed toward the outer plexiform layer where these dendrites make synaptic contacts with rods and cones and with bipolar cell dendrites. These cells also have connections between each other in the outer plexiform layer via gap junctions at the tips of their dendrites. Horizontal cells are inhibitory to other cells in the outer plexiform layer. Inhibition is thought to be an important mechanism in

improving contrast and spatial resolution by inhibiting illumination from the periphery of the visual field [51, 59, 60].

Amacrine Cells

Amacrine cell bodies are located either in the inner nuclear layer with other bipolar cells or in the ganglion cell layer where they are called displaced amacrine cells [61, 62]. Some amacrine cells have been described in between dendrites of the inner plexiform layer [61]. Amacrine cells have dendrites that are directed toward the inner plexiform layer and their input is thought to be inhibitory in nature [63]. These dendrites function also as axons and transmit signals in two directions. The amacrine cells form extensive connection with axons of bipolar cells and with dendrites, axons, and cell bodies of ganglion cells and also with other amacrine cells [46].

There are as many as 30 types of amacrine cells, but they are generally classified according to the degree of their dendritic connections within the inner plexiform layer [64]. The narrow-field amacrine cells, such as amacrine II cells, connect rod bipolar cells to ganglion cells and therefore may be involved in the scotopic vision (rod pathway), while large-field starburst amacrine cells are for motion detection and light adaptation during different times of the day (circadian rhythm) [59]. According to the inhibitory neurotransmitter released, there are different types of amacrine cells: GABAergic, glycinergic [65], or neither of them. Amacrine cells have been found to release dopamine [63] and acetylcholine in the retina [65, 66].

Layer 7: Inner Plexiform Layer

This layer is another processing layer of the retina that can be visualized using the OCT as a hyperreflective band (zone 5) [16]. The layer is divided into laminae, which can be up to six laminae with different connection levels. Three main laminae are usually described according to the type of contact: (1) the outer layer contains connection between bipolar cells, ganglion cells, and some amacrine cells; (2) the middle layer

contains similar contact but with displaced amacrine cells; and (3) the inner layer contains synapses between bipolar and displaced amacrine cells [46, 47]. The layer contains synapses between dendrites of cells in the inner nuclear layer and the dendrites of ganglion cells. Therefore, this layer can be affected by pathologies of the surrounding layers. Thickness of the layer can be assessed by OCT [67] and can reflect pathological changes such as glaucoma [68, 69] and diabetes [70].

Layer 8: Ganglion Cell Layer

This layer contains the cell bodies and nuclei of mainly retinal ganglion cells and, less commonly, displaced amacrine cells in addition to few astrocytes. There are around one million ganglion cells in each retina, with more ganglion cells at the peripheral nasal retina compared to the peripheral temporal retina [71]. Ganglion cells are not present at the center of the fovea, but their number is greatest around the fovea where they form up to nine layers of ganglion cells. Ganglion cell density may reach 38,000/mm² at the center of the retina [71]. However, there is only one layer of ganglion cells in most of the peripheral retina.

Ganglion cells are the final cells in the process of transmitting visual signals from the retina to the brain. They are multipolar cells with their dendrites directed toward the outer layers, while their axons form the nerve fiber layer. Dendrites of ganglion cells are connected to bipolar cells and amacrine cells in the inner plexiform layer. Each ganglion cell dendrites make indirect contact with a large number of other photoreceptor cells [46, 58].

There are more than 20 types of ganglion cells within the human retina. The two main types that form more than 80 % of the ganglion cells are the midget ganglion cells and the parasol ganglion cells [72]. Midget ganglion cells are small cells with a small number of dendrites. They receive signals from midget bipolar cells with a ratio of 1 to 1 at the fovea. This ratio increases as we move out from the fovea. In comparison, the parasol

cells are larger with much wider dendritic connection. Axons of midget and parasol cells terminate at the lateral geniculate nucleus of the brain [73]. Another morphological and physiological classification of ganglion cells in vertebrates includes alpha, beta, and gamma ganglion cells. Alpha ganglion cells have large cell bodies, large axons, and large dendritic fields, while beta cells have smaller cell bodies, smaller axons, and smaller dendritic fields. Gamma cells are smaller heterogeneous cells that are distributed throughout the retina with low conduction velocity [74].

Ganglion cells can be stimulated directly by light without necessarily being stimulated by input from the photoreceptors. Ganglion cells contain photopigments called melanopsins, which are present in a subset of ganglion cells called intrinsically photosensitive ganglion cells [75]. These cells form only 0.3 % of all ganglion cells in the retina and they combine direct stimulation by brightness of the surroundings with signals received from rod and cone cells. Axons of these ganglion cells project to the diencephalon and midbrain. These projections are believed to play a role in certain functions of the eye, such as the circadian rhythm and the pupillary reflex. This may explain the preservation of the circadian rhythm, photosensitivity, and pupillary reflex in patients with severe loss of rod and cone photoreceptors [76].

The distance from the cell body of the retina to the brain requires an effective mechanism to transport metabolites and neurotransmitter vesicles to the axon terminals. Transportation of molecules travels through the optic disk and any interference of this transportation process beyond the optic disk usually results in optic disk swelling (papilloedema), which may lead to loss of optic nerve axons if left untreated (optic atrophy) [46].

The ganglion cell layer thickness (zone 4) can be assessed using OCT, especially at the macular area [16, 77]. The degree of atrophy in the layer correlates to clinical outcome measures of visual function in a number of diseases including multiple sclerosis [77], glaucoma [78], and optic neuritis [79].

For comparison, Table 2.1 summarizes the average size of retinal cells in relationship to the

Table 2.1 Overview of the size of retinal cell soma in relationship to the 3–7 μm axial resolution of current clinical routine OCT technology

Cell	Diameter of the soma
RGC	5–20 μm [80]
Amacrine cell	12–16 μm [81]
Horizontal cell	10 μm [82]
Bipolar cell	8 μm [83]
Cone	3.3 μm (center of retina) and 10 μm (periphery of the retina) [38]
Rod	3.0–5.5 μm [38]
Pigment epithelium	Width 14 μm at the macula and 60 μm at the periphery (height is variable) [25]

resolution of current OCT technology (3–7 μm) [25, 38, 80–83].

Layer 9: Nerve Fiber Layer

The nerve fiber layer is formed by the ganglion cell axons that travel horizontal to the retina layers. Axons converge within the layer from the entire retina to the area of the optic disk where other layers of the retina are diminished. The nerve fiber layer is thin at the periphery and becomes thicker as more fibers converge in the layer toward the optic disk [60]. Axons from the medial or nasal half of the retina usually converge radially to the area of the optic disk, which lies medial to the macula. Axons of ganglion cells of the macula, which is located just lateral to the optic disk, travel directly in a fasciculus called the papillomacular fasciculus or bundle to the optic disk. Axons from peripheral parts of the temporal retina pass above and below the macula to reach the optic disk. The axons of the papillomacular bundle (PMB) are smaller in diameter compared to axons elsewhere in the retina. The average axonal diameter of primates' PMB, as demonstrated by electron microscopy studies, was 0.4 μm [84]. The small size of axons possibly makes the PMB particularly vulnerable, explaining the frequently seen temporal thinning of the nerve fiber layer in MS. Selective loss of small axons of the optic nerve in MS with the

consequent degeneration of parvocellular cells has been reported previously. The study also demonstrated another evidence that the PMB projects mainly to the parvocellular cells [85].

Axons of the nerve fiber layer are unmyelinated as the refractile characteristic of myelin may interfere with vision. However, these axons are ensheathed by the surrounding processes of glial cells such as astrocytes and Müller cells, which are present in the nerve fiber layer [51, 86]. Few axons may possess myelin at the optic retina as a developmental anomaly, but most retinal axons acquire myelin sheath once they pass an area at the optic disk called lamina cribrosa [87].

The high reflectivity of the layer makes it apparent as a distinct zone even with low-resolution OCT (zone 3) [16, 88]. Therefore, the nerve fiber layer has been visualized and examined early during the development of OCT [88]. The nerve fiber layer is one of the important layers of the retina that can be affected by a wide spectrum of retinal diseases [89]. As the nerve fiber layer represents axons of the ganglion cells, these axons are affected greatly by the pathology of the ganglion cells. Thickness of the nerve fiber layer, especially around the optic nerve head (peripapillary), can reflect ganglion cell survival and consequently visual function [77].

Layer 10: Internal Limiting Membrane

The most interior layer of the retina is the internal limiting membrane. The membrane is formed by the expanded terminal end feet of Müller cells and astrocytes. The membrane continues anteriorly to the ora serrata and blends with the membrane that covers the inner surface of the ciliary body. Selective fluid exchange between the retina and the vitreous body takes place through the membrane. The membrane also controls migration of cells and other particles to the vitreous body [46].

Structure and thickness of the membrane vary at different parts of the retina. Thickness of the membrane is about 70 nm at the optic disk and the periphery of the retina, whereas thickness at the macula may reach 400–500 nm. The

membrane is attached to the vitreous body of the eye by an inner meshwork of fibrils. The degree of attachment with the vitreous body also varies at different regions of the retina, being loose with few fibrils at the fovea centralis [90]. However, due to the connection between this membrane and the vitreous body, the retina is significantly affected by changes in the shape of the vitreous body.

The membrane appears hyperreflective on OCT [16] and it frequently cannot be differentiated from the underlying nerve fiber layers. Occasionally a hyporeflexive narrow zone can be seen on normal OCT between the ILM and the vitreous called the preretinal space (zone 2) [16]. This space is a potential space for vitreous preretinal hemorrhage. Anterior to the preretinal space is the vitreous body, which is called posterior cortical vitreous near the center of the retina (zone 1) [16].

Retinal Glial Cells

The extensive distribution of neuroglia within layers of the retina fills the extracellular space and provides physical support to the retina. These cells appear to be important in maintaining the ionic environment around neural cells, glycogen storage, reuptake of released neurotransmitters, removal of debris, and insulating axons and neurons.

There are three types of retinal glial cells: radial glial cells that are also called Müller cells, astrocytes, and microglia. The most abundant cells in the retina among glial cells are Müller cells [91].

Müller cell bodies and nuclei are present in the inner nuclear layer. These cells extend radially and cross the layers of the retina from the most inner layer to the photoreceptive layer to form the cytoarchitectural support of the retina. The outer process extends to terminate as microvilli between the cone and rod processes. At this level, radial glial cells form the external limiting membrane, which is formed by dense zonula adherens. The inner process extends to the inner surface of the retina forming a flattened terminal foot plate. The terminal foot plate fuses with those foot plates from other Müller cells, and

probably with astrocytes, forming the internal limiting membrane [46].

Müller cells are scattered between rods and cones and between other neuronal cells in the retina. They are also scattered between blood vessels and capillaries and cover them. Their processes send lateral lamellae forming a sheath-like structure that separates retinal cells except the areas of synapses. These lamellae contact blood vessels, especially capillaries, and their basal laminae fuse with those of the vascular smooth muscle in the media of vessels or of the endothelial lining of capillaries [46, 50, 92]. Müller cells are important in maintaining the extracellular environment necessary for the proper function of retinal neurons [16, 93].

Retinal astrocytes do not belong embryologically to the retina as they migrate along the optic nerve through the optic disk. This may explain the restricted position of these cells to the nerve fiber of the retina [94]. They are scattered in the entire retina except the fovea. These cells have similar morphology to astrocytes of the central nervous system in terms of flattened cell body with numerous processes and can be readily marked with astrocytes marker glial fibrillary acidic protein [95]. The astrocytes form extensive processes that ensheath axons of the ganglion cells and they also contribute in supporting retinal capillaries by forming glia limitans [92].

Microglia migrate to the retina from the circulation and distribute in small numbers in different parts of the neural retina. They are mainly present within the inner plexiform layer. They have multiple processes that extend horizontally to retinal layers. Their function in the retina is primarily similar to their function in the central nervous system as they are able to phagocytose debris [46].

The Macula Lutea

The macula lutea appears yellow in color and its diameter measures about 5 mm [96]. At the center of the macula is a reddish depression, of a diameter of 1.5 mm, called the fovea. The area of the macula is responsible for most of the photopic vision. The yellow color is due to the presence of the yellow carotenoid pigments known as

xanthophylls [46]. The fovea appears shiny when examined with the ophthalmoscope (foveal reflex). It has the highest density of cone cells (199,000/mm²) [39], where cone cells are elongated with smaller diameter compared to cone cells in other parts of the retina. These are arranged in close proximity to each other and serve the function of the retina of obtaining high degree of spatial discrimination [39].

The previously described layers of the retina are modified in the macula, especially at the fovea. According to structure and modification of layers, four concentric zones can be recognized at the macula [43].

The perifoveal zone is the outermost part of the macula that delineates between the central retina and the peripheral retina. It is considered the transitional zone of retinal layer modification. The peripheral retina extends outside the perifovea and it is anatomically characterized by the presence of one layer of ganglion cells [97, 98]. At this zone, the ganglion cell layer starts to become multicellular. The perifovea is rich in blood vessels that start to diminish gradually when moving toward the central zones. In addition, the perifovea has a high rod-to-cone ratio of about 30–130:1. This ratio starts to reduce gradually toward the center [61].

At the parafoveal zone, which is the next zone toward the fovea, retinal vessels start to diminish and the rod-to-cone ratio becomes significantly lower than the perifoveal zone (4:1 rod-to-cone ratio). In addition, the parafoveal region has the highest thickness of the granular cell layer in the entire retina.

Next to the parafovea is the foveal slope where foveal cone axons are directed obliquely from the foveola. Processes of foveal cone photoreceptors are directed obliquely in order to synapse on the outer plexiform layer on the periphery of the fovea—a layer that is deficient at the center of the fovea. Therefore, cone pedicles or rod spherules are not present in the fovea, but rather at the periphery of the fovea. The foveal slope represents the zone of transition from the vascular to the avascular retina. The vascular capillaries only reach the margins of the fovea, leaving an area of

500 µm at the center of the fovea with no retinal capillaries (the foveal avascular zone) [46].

At the foveal slope, the ganglion cell layer and rod receptors start to diminish. The slope will end in the foveal depression where it is populated with cone photoreceptors and Müller cells only. Embryologically, the foveal morphology is produced from migration of ganglion cells to the periphery of the fovea and migration of green and red cones to the center of the fovea. Therefore, the fovea has no blue cone cells, no vessels, or other glial cells except Müller cells [39]. In addition, the fovea has no inner nuclear layer, inner plexiform layer, ganglion layer, and nerve fiber layers. Therefore, the retina is more transparent at the foveal area.

Vascular Supply of the Retina

The retina is supplied by the ophthalmic artery—the first branch of the internal carotid artery. Ophthalmic branches that contribute to the nourishment of the retina are the posterior ciliary arteries (short and long one) and the central retinal artery [99].

The posterior ciliary arteries approach the back of the eye outside the optic nerve. They penetrate the sclera at the back of the eye and branch out in the choroid into choroidal arteries. The greatest flow of these arteries is received by the choroid. The choroid is arranged into layers: the innermost layer is the choriocapillaris layer, and the outer zone is the feeding arterioles and venules. The choriocapillary layer is formed of densely arranged capillaries that are separated from the retinal epithelial layer by Bruch's membrane [100]. These layers can partly be visualized using OCT, which is depth ambiguous, where the choriocapillaris layer appears as a hyporeflective zone (zone 15) while the feeding arterioles as a hyperreflective zone. The next zones, however, are not well demarcated using the OCT and usually named according to the previous histological description [16].

The outer layers of the retina are avascular and depend on the choroid for nourishment.

Molecules are transmitted by rapid diffusion to the retinal pigment epithelium. The choroidal circulation supplies the pigment epithelial layer, the photoreceptor layer, the outer nuclear layer, and the outer plexiform layer [101]. In addition, the short ciliary arteries also contribute in supplying the optic nerve head [46, 102].

The inner retinal blood supply comes from the central retina artery and its branches. It pierces the dura and the arachnoid to enter the optic nerve 1 cm behind the eyeball and then accompanies the nerve as far as the lamina cribrosa [78]. Here the artery branches into superior and inferior retinal arteries. Each of these arteries divides into nasal and temporal arteries that supply the four quadrants of the retina. Similarly, retinal veins drain the retina and unite to form the central retinal vein at the optic disk [102–104].

The arteries and veins run at the nerve fiber layer and some arterioles penetrate down to the internal nuclear layer. Similarly, venules are formed at the internal nuclear lamina and travel radially to the nerve fiber layer where they pass parallel to the layer forming the central retinal vein [46]. The inner nuclear layer separates between two capillary beds: the inner capillary bed belongs to the circulation from the central retinal artery and the outer capillary bed belongs to the choroidal circulation. These two capillary beds are visible in OCT as hyperreflective spots on both sides of the inner nuclear layer [105].

Arteries supplying the retina are similar in structure to other arteries in the body except that there is no internal elastic lamina. Arteries usually get smaller to form arterioles that end in a network of capillaries with a nonfenestrated epithelium. Retinal capillaries do not exceed the internal nuclear layer; they are absent at the fovea but abundant at the macula lutea. At the other end of the capillary bed, venules are formed, which unite as they run superficially to the surface of the retina to form smaller veins. There is usually no anastomosis between different arterial territories, in which sudden occlusion of a certain retinal artery may result in visual field loss in the area supplied by that artery [4, 46].

The Optic Nerve

The ganglion cell axons converge horizontally through the nerve fiber layer at an area called the optic disk. The larger fibers are generally axons of ganglion cells from peripheral retina and they occupy the peripheral part of the optic nerve. Small axons come from the center of the retina and occupy the center of the optic nerve [74]. These axons are arranged in bundles (about 1200 bundles). The bundles are usually separated from each other by the supporting glia and separated from the connective tissue by a membrane of astrocytes [106].

The length of the optic nerve from the optic disk to where it ends at the optic chiasm ranges between 3.8 cm and 5.8 cm [106]. The optic nerve is formed of one million nerve fibers with their cell bodies located in the ganglion cell layer of the retina. All of these fibers are afferent from the retina to different parts of the brain [107]. Unlike peripheral nerves, the optic nerve is myelinated by oligodendrocytes and can be affected by CNS inflammatory demyelinating conditions such as MS [108].

For better understanding of the optic nerve anatomy, the nerve is divided into four anatomic regions: the optic nerve head, the intraocular part, the intracanalicular part, and the intracranial parts.

The Optic Nerve Head

The optic nerve head is where the optic nerve is formed and sometimes referred to as the optic disk or optic papilla. Normally, the optic disk or papilla is not elevated above the level of the retina as it may appear with the retinal examination. It does, in fact, have a depression at the middle called physiological cupping of the optic disk [106].

On surface view, the optic disk is an oval light area in the retina with a vertical diameter of 1.88 mm and a horizontal diameter of 1.77 mm [109]. This diameter depends largely on the diameter of the opening of the choriocleral canal. When the canal is narrow, there is usually

no physiological cupping, but with a large canal, the extra space appears as cupping. Therefore, the larger the canal, the larger the cupping. On the other hand, the angle by which axons of the retinal neurons exit the retina usually determines the shape of the optic disk [106]. In fact, size and shape of the physiological cupping vary significantly between individuals [110].

The most anterior part of the optic nerve head is the surface nerve fiber layer. It contains the nerve fibers as they enter the choriocleral canal to form the optic nerve. These nerve fibers bend, forming circular elevation at the periphery of the optic disk. The optic disk and the physiological cupping are separated from the vitreous by the internal limiting membrane. Normally the nerve fiber layer is thick at the optic disk as fibers accumulate and bend at 90° to enter the disk. This area diameter and thickness of the nerve fiber layer can be estimated using OCT imaging [111, 112]. OCT of the optic disk can be useful in assessing the degree of retinal nerve fiber loss following optic neuritis or retrograde transsynaptic axonal degeneration following lesions in the posterior optic pathways [113].

The Prelaminar Region

Beneath the nerve fiber layer, the optic nerve fibers are arranged in bundles with glial cells in between the bundles. This region contains only glial cells, which are a specialized type of astrocytes called spider cells [114]. These cells have their fibers run perpendicular to the direction of the optic nerve fibers [115]. At the periphery of the optic nerve, this layer is attached to the choroid, while centrally it is attached to the connective tissue of the central retinal vessels [115].

These glial fibers are much thinner than the normal connective tissue and form a loose layer. Many pathologists believe that this arrangement is responsible for the pathologic optic swelling. This layer is the only nutrient support of the optic nerve fibers as they bend backward into the optic nerve [106, 115].

When there is physiological cupping, the space between the internal limiting membrane

and the lamina cribrosa is filled with connective tissue. On the periphery of the prelaminar portion of the optic nerve, astrocytes separate the nerve from other layers of the retina and from the choroid. These astrocytes form a layer separating the nerve from the choriocleral canal and send connective tissue centrally to support the nerve fibers [106, 115].

The Lamina Cribrosa

The more posterior region of the optic nerve head is called the lamina cribrosa region. It is also called the scleral layer and it is convex posteriorly and concave anteriorly. This layer is formed of transverse connective tissue fibers running between nerve bundles. At the periphery of the nerve, the connective tissue of lamina cribrosa is attached to the sclera and centrally attached to the connective tissue of the central retinal vessels [116–118]. The cross section of the lamina cribrosa shows trabecular arrangement of connective tissue with openings for the transmission of nerve bundles with a central opening for the retinal vessels. The nerve fibers are still separated from the surrounding connective tissue by a membrane formed of glial cells [106, 115].

The Intraorbital Part of the Optic Nerve

This intraorbital or retrolaminar part of the optic nerve extends for 4 mm from the eyeball to the optic canal. The retrolaminar part of the optic nerve becomes thicker because the nerve fibers acquire myelin by oligodendrocytes that are present posterior to the lamina cribrosa [87, 119]. Myelination of the intraorbital optic nerve is first seen in the intracranial part of the nerve. Oligodendrocytes migrate further to myelinate the intraorbital optic nerve, which becomes fully myelinated by the age of 2 years [87]. Further migration of oligodendrocytes into the retina is prevented by the lamina cribrosa, thus preventing myelination of retinal axons [120]. The intraorbital part of the optic nerve acquires all the meninges of the central nervous system including the dura, arachnoid, and pia mater, as well as the cerebrospinal fluid and subarachnoid space.

The sheath of the optic nerve, which is formed of the dura and the arachnoid, is loose at the front where it ends anteriorly and blends with the sclera of the eyeball [119]. The underlying subarachnoid space is widest just posterior to the eyeball, producing a bulb-like appearance. Thickness of the optic nerve sheath at this part of the nerve can be assessed by ultrasound examination and can detect increases of intracranial pressure [121]. The subarachnoid space is narrower posterior to the bulb and becomes narrowest at the region of the optic canal. At the entrance to the optic canal, the optic nerve sheath is attached to the annular tendon, which is the common tendon for extraocular muscles [119].

The connective tissue and the glial tissue run in different directions in this portion of the optic nerve but become longitudinally arranged near the center of the optic nerve, where it is attached to the central retinal vessels. Peripherally the connective tissue is attached to the pia mater and attached firmly at the front to the posterior part of the lamina cribrosa [106, 115, 119]. The nerve fibers extend within the connective tissue and separated from this tissue by a layer of astrocytes. These fibrous astrocytes and other glial cells such as oligodendrocytes and microglia are scattered within the nerve bundles.

At the posterior portion of the intraorbital nerve, the ophthalmic artery is closely related to this part of the optic nerve. The pia mater has a vascular plexus that is formed by branches from the ophthalmic artery. This plexus is the main blood supply to the optic nerve [106, 107].

The Intracanalicular Part of the Optic Nerve

Within the canal, the optic nerve sheath is adherent to the periosteum of the bones. The dura and the arachnoid are also adherent to each other; they are also adherent to the pia of the optic nerve by a trabecular meshwork of connective tissue. The degree of adherence has individual variation that affects the degree of CSF flow from the intracranial side to the intraorbital side. This affects the speed by which the CSF pressure is elevated within the intraorbital part as a consequence of increased CSF pressure in the brain. Here the

ophthalmic artery has an intimate relation with the optic nerve and runs within the sheath of the optic nerve [121, 122].

The Intracranial Part of the Optic Nerve

This part of the optic nerve extends from the optic canal to the optic chiasm. It is located above the diaphragm sellae and then above the cavernous sinus. The ophthalmic artery is located inferolaterally, while the internal carotid artery is located laterally and the anterior cerebral artery superiorly. When they reach the optic chiasm, the nerve fibers decussate. Fibers from the nasal half of the retina decussate to join the contralateral temporal retinal fibers. Two optic tracts are formed from the optic chiasm and project to various parts of the central nervous system such as the lateral geniculate nucleus, the pretectal nuclei, the superior colliculi, the hypothalamus, the visual cortex, and other parts of the brain [122, 123].

References

1. Rea MS, Figueiro MG, Bullough JD, Bierman A. A model of phototransduction by the human circadian system. *Brain Res Brain Res Rev.* 2005;50(2): 213–28.
2. Kolb H. Gross anatomy of the eye. 1 May 2005 [Updated 1 May 2007]. In: Kolb H, Fernandez E, Nelson R, editors. *Webvision: The Organization of the Retina and Visual System* [Internet]. Salt Lake City: University of Utah Health Sciences Center; 1995. Available from: <http://www.ncbi.nlm.nih.gov/books/NBK11534/?report=classic>.
3. Reese BE. Development of the retina and optic pathway. *Vision Res.* 2011;51(7):613–32. doi:10.1016/j.visres.2010.07.010. Epub 2010 Jul 18.
4. Kolb H. Simple anatomy of the retina. 1 May 2005 [Updated 31 Jan 2012]. In: Kolb H, Fernandez E, Nelson R, editors. *Webvision: The Organization of the Retina and Visual System* [Internet]. Salt Lake City: University of Utah Health Sciences Center; 1995. Available from: <http://www.ncbi.nlm.nih.gov/books/NBK11533/>.
5. Reynolds J, Olitsky S, Hildebrand GD, Fielder A. Anatomy and physiology of the retina. In: *Pediatric retina*. Berlin/Heidelberg: Springer; 2011. p. 39–65.
6. Kolb H. Simple anatomy of the retina. *Webvision: The Organization of the Retina and Visual System*. Salt Lake City: University of Utah Health Sciences Center; 1995.

7. Kremser B, Troger J, Baltaci M, Kralinger M, Kieselbach GF. Retinal thickness analysis in subjects with different refractive conditions. *Ophthalmologica*. 1999;213(6):376–9.
8. Göbel W, Hartmann F, Haigis W. Determination of retinal thickness in relation to the age and axial length using optical coherence tomography. *Der Ophthalmologe Zeitschrift der Deutschen Ophthalmologischen Gesellschaft*. 2001;98(2):157–62.
9. Drake RL, Vogl W, Mitchell AWM, Gray H. Gray's anatomy for students. Philadelphia: Churchill Livingstone/Elsevier; 2010.
10. Dowling JE, Boycott BB. Organization of the primate retina: Electron microscopy. *Proc R Soc Lond B Biol Sci*. 1966;166(1002):80–111.
11. Kolb H. Organization of the outer plexiform layer of the primate retina: electron microscopy of Golgi-impregnated cells. *Philos Trans R Soc Lond B Biol Sci*. 1970;258(823):261–83.
12. Costa RA, Skaf M, Melo Jr LA, Calucci D, Cardillo JA, Castro JC, et al. Retinal assessment using optical coherence tomography. *Prog Retin Eye Res*. 2006;25(3):325–53.
13. Wolfensberger TJ. The historical discovery of the retinal pigment epithelium. In: Marmor MF, Wolfensberger TJ, editors. *The retinal pigment epithelium*. Oxford: Oxford University Press; 1998. p. 13–22.
14. Bharti K, Miller SS, Arnheiter H. The new paradigm: retinal pigment epithelium cells generated from embryonic or induced pluripotent stem cells. *Pigment Cell Melanoma Res*. 2011;24(1):21–34.
15. Peters S, Schraermeyer U. Characteristics and functions of melanin in retinal pigment epithelium. *Ophthalmologe*. 2001;98(12):1181–5.
16. Staurenghi G, Sadda S, Chakravarthy U, Spaide RF. Proposed lexicon for anatomic landmarks in normal posterior segment spectral-domain optical coherence tomography: the in*oct consensus. *Ophthalmology*. 2014;121(8):1572–8.
17. Panda-Jonas S, Jonas JB, Jakobczyk-Zmija M. Retinal pigment epithelial cell count, distribution, and correlations in normal human eyes. *Am J Ophthalmol*. 1996;121(2):181–9.
18. Spaide RF, Curcio CA. Anatomical correlates to the bands seen in the outer retina by optical coherence tomography: literature review and model. *Retina*. 2011;31(8):1609–19.
19. la Cour M, Tezel T. The retinal pigment epithelium. *Adv Organ Biol*. 2005;10:253–72.
20. Pauleikhoff D, Harper CA, Marshall J, Bird AC. Aging changes in Bruch's membrane: a histochemical and morphologic study. *Ophthalmology*. 1990;97(2):171–8.
21. Cunha-Vaz JG. The blood-retinal barriers system. Basic concepts and clinical evaluation. *Exp Eye Res*. 2004;78(3):715–21.
22. Srinivasan VJ, Monson BK, Wojtkowski M, Bilonick RA, Gorczynska I, Chen R, et al. Characterization of outer retinal morphology with high-speed, ultrahigh-resolution optical coherence tomography. *Invest Ophthalmol Vis Sci*. 2008;49(4):1571–9.
23. Marmor MF. Retinal and retinal pigment epithelial physiology. In: Regillo CD, Brown GC, Flynn HW, editors. *Vitreoretinal disease*. New York/Stuttgart: Thieme; 1999. p. 25–38.
24. Thumann G, Hoffmann S, Hinton DR. Cell biology of the retinal pigment epithelium. *Retina*. 2006;1:137–52.
25. Strauss O. The retinal pigment epithelium in visual function. *Physiol Rev*. 2005;85(3):845–81.
26. Chen L, Zhang X-W. Which lamp will be optimum to eye? Incandescent, fluorescent or led etc. *Int J Ophthalmol*. 2014;7(1):163–8.
27. Kolb H. Photoreceptors. 1 May 2005 [Updated 28 Feb 2012]. In: Kolb H, Fernandez E, Nelson R, editors. *Webvision: The Organization of the Retina and Visual System* [Internet]. Salt Lake City: University of Utah Health Sciences Center; 1995. Available from: <http://www.ncbi.nlm.nih.gov/books/NBK11522/>.
28. Mitchell CH, Reigada D. Purinergic signalling in the subretinal space: a role in the communication between the retina and the rpe. *Purinergic Signal*. 2008;4(2):101–7.
29. Matsumoto H, Miller JW, Vavvas DG. Retinal detachment model in rodents by subretinal injection of sodium hyaluronate. *J Vis Exp*. 2013;79.
30. Roof DJ, Makino CL. The structure and function of retinal photoreceptors. In: Alberts DM, Jakobiec FA, editors. *The principals and practice of ophthalmology*. 2nd ed. Philadelphia: WB Saunders Co; 2000. p. 1624–73.
31. Sheth SS, Rush RB, Natarajan S. Inner and outer retinal volumetric and morphologic analysis of the macula with spectral domain optical coherence tomography in retinitis pigmentosa. *Middle East Afr J Ophthalmol*. 2012;19(2):227.
32. Wolf-Schnurrbusch UEK, Enzmann V, Brinkmann CK, Wolf S. Morphologic changes in patients with geographic atrophy assessed with a novel spectral OCT-SLO combination. *Invest Ophthalmol Vis Sci*. 2008;49(7):3095–9.
33. Alm A, Bill A. Ocular and optic nerve blood flow at normal and increased intraocular pressures in monkeys (*Macaca irus*): a study with radioactively labelled microspheres including flow determinations in brain and some other tissues. *Exp Eye Res*. 1973;15(1):15–29.
34. Alm A, Bill A, Young FA. The effects of pilocarpine and neostigmine on the blood flow through the anterior uvea in monkeys. A study with radioactively labelled microspheres. *Exp Eye Res*. 1973;15(1):31–6.
35. Theodossiadis PG, Grigoropoulos VG, Theodossiadis GP. The significance of the external limiting membrane in the recovery of photoreceptor layer after successful macular hole closure: a study by spectral domain optical coherence tomography. *Ophthalmol J Int d'ophtalmologie Int J Ophthalmol Zeitschrift fur Augenheilkunde*. 2010;225(3):176–84.

36. Oishi A, Hata M, Shimozone M, Mandai M, Nishida A, Kurimoto Y. The significance of external limiting membrane status for visual acuity in age-related macular degeneration. *Am J Ophthalmol.* 2010; 150(1):27–32.e21.
37. Ito SI, Miyamoto N, Ishida K, Kurimoto Y. Association between external limiting membrane status and visual acuity in diabetic macular oedema. *Br J Ophthalmol.* 2011. doi:10.1136/bjophthalmol-2011-301418.
38. Jonas JB, Schneider U, Naumann GO. Count and density of human retinal photoreceptors. *Graefes Arch Clin Exp Ophthalmol.* 1992;230(6): 505–10.
39. Curcio CA, Sloan KR, Kalina RE, Hendrickson AE. Human photoreceptor topography. *J Comp Neurol.* 1990;292(4):497–523.
40. Lujan BJ, Roorda A, Knighton RW, Carroll J. Revealing Henle's fiber layer using spectral domain optical coherence tomography. *Invest Ophthalmol Vis Sci.* 2011;52(3):1486–92.
41. Otani T, Yamaguchi Y, Kishi S. Improved visualization of Henle fiber layer by changing the measurement beam angle on optical coherence tomography. *Retina.* 2011;31(3):497–501.
42. Matsumoto H, Sato T, Kishi S. Outer nuclear layer thickness at the fovea determines visual outcomes in resolved central serous chorioretinopathy. *Am J Ophthalmol.* 2009;148(1):105–110.e101.
43. Ishikawa H, Stein DM, Wollstein G, Beaton S, Fujimoto JG, Schuman JS. Macular segmentation with optical coherence tomography. *Invest Ophthalmol Vis Sci.* 2005;46(6):2012–7.
44. Antcliff RJ, Marshall J, editors. The pathogenesis of edema in diabetic maculopathy. *Semin Ophthalmol.* Informa UK Ltd; 1999.
45. Liu L, Cuthbertson F. Early bilateral cystoid macular oedema secondary to fingolimod in multiple sclerosis. *Case Rep Med.* 2012;2012:134636.
46. Hildebrand GD, Fielder AR. Anatomy and physiology of the retina. *Pediatric retina.* Heidelberg: Springer; 2011. p. 39–65.
47. Zhu M, Madigan MC, van Driel D, Maslim J, Billson FA, Provis JM, et al. The human hyaloid system: Cell death and vascular regression. *Exp Eye Res.* 2000;70(6):767–76.
48. Chen TC, Cense B, Miller JW, Rubin PAD, Deschler DG, Gragoudas ES, et al. Histologic correlation of in vivo optical coherence tomography images of the human retina. *Am J Ophthalmol.* 2006;141(6): 1165–8.
49. Schuman JS, Hee MR, Arya AV, Pedut-Kloizman T, Puliafito CA, Fujimoto JG, et al. Optical coherence tomography: a new tool for glaucoma diagnosis. *Curr Opin Ophthalmol.* 1995;6(2):89–95.
50. Newman EA. Müller cells and the retinal pigment epithelium. In: *Principles and practice of ophthalmology.* Philadelphia: W.B. Saunders Co.; 2000:1763–85
51. Ogden TE. Nerve fiber layer of the macaque retina: retinotopic organization. *Invest Ophthalmol Vis Sci.* 1983;24(1):85–98.
52. Gartner S, Henkind P. Aging and degeneration of the human macula. 1. Outer nuclear layer and photoreceptors. *Br J Ophthalmol.* 1981;65(1):23–8.
53. Gabilondo I, Martinez-Lapiscina EH, Fraga-Pumar E, Ortiz-Perez S, Torres-Torres R, Andorra M, et al. Dynamics of retinal injury after acute optic neuritis. *Ann Neurol.* 2015;77(3):517–28.
54. Balk LJ, Twisk JW, Steenwijk MD, Daams M, Tewarie P, Killestein J, et al. A dam for retrograde axonal degeneration in multiple sclerosis? *J Neurol Neurosurg Psychiatry.* 2014;85(7):782–9.
55. Bermel RA, Villoslada P. Retrograde trans-synaptic degeneration in ms: a missing link? *Neurology.* 2014;82(24):2152–3.
56. Burggraaff MC, Trieu J, de Vries-Knoppert WA, Balk L, Petzold A. The clinical spectrum of microcystic macular edema. *Invest Ophthalmol Vis Sci.* 2014;55(2):952–61.
57. Masland RH. The fundamental plan of the retina. *Nat Neurosci.* 2001;4(9):877–86.
58. Callaway EM. Structure and function of parallel pathways in the primate early visual system. *J Physiol.* 2005;566(Pt 1):13–9.
59. Fitzgibbon T, Taylor SF. Retinotopy of the human retinal nerve fiber layer and optic nerve head. *J Comp Neurol.* 1996;375(2):238–51.
60. FitzGibbon T. The human fetal retinal nerve fiber layer and optic nerve head: a Dil and DiA tracing study. *Vis Neurosci.* 1997;14(3):433–47.
61. Provis JM, Penfold PL, Cornish EE, Sandercoe TM, Madigan MC. Anatomy and development of the macula: specialisation and the vulnerability to macular degeneration. *Clin Exp Optom.* 2005;88(5): 269–81.
62. Provis JM, Sandercoe T, Hendrickson AE. Astrocytes and blood vessels define the foveal rim during primate retinal development. *Invest Ophthalmol Vis Sci.* 2000;41(10):2827–36.
63. Newkirk GS, Hoon M, Wong RO, Detwiler PB. Inhibitory inputs tune the light response properties of dopaminergic amacrine cells in mouse retina. *J Neurophysiol.* 2013;110(2):536–52.
64. Masland RH. Amacrine cells. *Trends Neurosci.* 1988;11(9):405–10.
65. Ishii T, Kaneda M. On-pathway-dominant glycinergic regulation of cholinergic amacrine cells in the mouse retina. *J Physiol.* 2014;592(Pt 19): 4235–45.
66. Whitney IE, Keeley PW, Raven MA, Reese BE. Spatial patterning of cholinergic amacrine cells in the mouse retina. *J Comp Neurol.* 2008;508(1): 1–12.
67. Mwanza JC, Durbin MK, Budenz DL, Girkin CA, Leung CK, Liebmann JM, et al. Profile and predictors of normal ganglion cell-inner plexiform layer thickness measured with frequency-domain optical coherence tomography. *Invest Ophthalmol Vis Sci.* 2011;52(11):7872–9.
68. Nakano N, Hangai M, Nakanishi H, Mori S, Nukada M, Kotera Y, et al. Macular ganglion cell layer imaging in preperimetric glaucoma with speckle noise-

- reduced spectral domain optical coherence tomography. *Ophthalmology*. 2011;118(12):2414–26.
69. Mwanza JC, Oakley JD, Budenz DL, Chang RT, Knight OJ, Feuer WJ. Macular ganglion cell-inner plexiform layer: automated detection and thickness reproducibility with spectral domain-optical coherence tomography in glaucoma. *Invest Ophthalmol Vis Sci*. 2011;52(11):8323–9.
 70. van Dijk HW, Kok PH, Garvin M, Sonka M, Devries JH, Michels RP, et al. Selective loss of inner retinal layer thickness in type 1 diabetic patients with minimal diabetic retinopathy. *Invest Ophthalmol Vis Sci*. 2009;50(7):3404–9.
 71. Curcio CA, Allen KA. Topography of ganglion cells in human retina. *J Comp Neurol*. 1990;300(1):5–25.
 72. Wurtz RH, Kandel ER. Central visual pathways. In: Eric Kandel JS, Jessel T, editors. *Principles of neural science*. New York: McGraw-Hill Companies Incorporated; 2000. p. 523–47.
 73. Davson H. Retinal structure and organization. In: Davson H, editor. *Physiology of the eye*. 5th ed. London: MacMillan; 1990. p. 205–18.
 74. Brooks DE, Komaromy AM, Kallberg ME. Comparative retinal ganglion cell and optic nerve morphology. *Vet Ophthalmol*. 1999;2(1):3–11.
 75. Benarroch EE. The melanopsin system: phototransduction, projections, functions, and clinical implications. *Neurology*. 2011;76(16):1422–7.
 76. Do MT, Yau KW. Intrinsically photosensitive retinal ganglion cells. *Physiol Rev*. 2010;90(4):1547–81.
 77. Saidha S, Syc SB, Durbin MK, Eckstein C, Oakley JD, Meyer SA, et al. Visual dysfunction in multiple sclerosis correlates better with optical coherence tomography derived estimates of macular ganglion cell layer thickness than peripapillary retinal nerve fiber layer thickness. *Mult Scler*. 2011;17(12):1449–63.
 78. Tan O, Chopra V, Lu AT, Schuman JS, Ishikawa H, Wollstein G, et al. Detection of macular ganglion cell loss in glaucoma by fourier-domain optical coherence tomography. *Ophthalmology*. 2009;116(12):2305–2314.e2301–2.
 79. Syc SB, Saidha S, Newsome SD, Ratchford JN, Levy M, Ford E, et al. Optical coherence tomography segmentation reveals ganglion cell layer pathology after optic neuritis. *Brain*. 2011;135(Pt 2):521–33.
 80. Sekirnjak C, Hottowy P, Sher A, Dabrowski W, Litke AM, Chichilnisky EJ. Electrical stimulation of mammalian retinal ganglion cells with multielectrode arrays. *J Neurophysiol*. 2006;95(6):3311–27.
 81. Kolb H. *Roles of amacrine cells*. Salt Lake City: University of Utah Health Sciences Center; 1995. Available from: webvision.med.utah.edu.
 82. Eglén SJ, Wong JC. Spatial constraints underlying the retinal mosaics of two types of horizontal cells in cat and macaque. *Vis Neurosci*. 2008;25(2):209–14.
 83. Kao YH, Sterling P. Matching neural morphology to molecular expression: Single cell injection following immunostaining. *J Neurocytol*. 2003;32(3):245–51.
 84. Ogden TE. Nerve fiber layer of the primate retina: morphometric analysis. *Invest Ophthalmol Vis Sci*. 1984;25(1):19–29.
 85. Evangelou N, Konz D, Esiri MM, Smith S, Palace J, Matthews PM. Size-selective neuronal changes in the anterior optic pathways suggest a differential susceptibility to injury in multiple sclerosis. *Brain*. 2001;124(Pt 9):1813–20.
 86. Radius RL, Anderson DR. The histology of retinal nerve fiber layer bundles and bundle defects. *Arch Ophthalmol*. 1979;97(5):948–50.
 87. Magoon EH, Robb RM. Development of myelin in human optic nerve and tract. A light and electron microscopic study. *Arch Ophthalmol*. 1981;99(4):655–9.
 88. Huang D, Swanson EA, Lin CP, Schuman JS, Stinson WG, Chang W, et al. Optical coherence tomography. *Science*. 1991;254(5035):1178–81.
 89. Schuman JS, Pedut-Kloizman T, Hertzmark E, Hee MR, Wilkins JR, Coker JG, et al. Reproducibility of nerve fiber layer thickness measurements using optical coherence tomography. *Ophthalmology*. 1996;103(11):1889–98.
 90. Heegaard S, Jensen OA, Prause JU. Structure and composition of the inner limiting membrane of the retina. Sem on frozen resin-cracked and enzyme-digested retinas of macaca mulatta Graefes. *Arch Clin Exp Ophthalmol*. 1986;224(4):355–60.
 91. Saint-Geniez M, D'Amore PA. Development and pathology of the hyaloid, choroidal and retinal vasculature. *Int J Dev Biol*. 2004;48(8–9):1045–58.
 92. Provis JM. Development of the primate retinal vasculature. *Prog Retin Eye Res*. 2001;20(6):799–821.
 93. Newman E, Reichenbach A. The muller cell: a functional element of the retina. *Trends Neurosci*. 1996;19(8):307–12.
 94. Watanabe T, Raff MC. Retinal astrocytes are immigrants from the optic nerve. *Nature*. 1988;332(6167):834–7.
 95. Chang ML, Wu CH, Jiang-Shieh YF, Shieh JY, Wen CY. Reactive changes of retinal astrocytes and muller glial cells in kainate-induced neuroexcitotoxicity. *J Anat*. 2007;210(1):54–65.
 96. Kincaid MC, Green WR. Anatomy of the vitreous, retina, and choroid. In: Regillo CD, Brown GC, Flynn HW, editors. *Vitreoretinal disease*. New York, Stuttgart: Thieme; 1999.
 97. Provis JM, Diaz CM, Dreher B. Ontogeny of the primate fovea: A central issue in retinal development. *Prog Neurobiol*. 1998;54(5):549–80.
 98. Hendrickson AE. Primate foveal development: A microcosm of current questions in neurobiology. *Invest Ophthalmol Vis Sci*. 1994;35(8):3129–33.
 99. Ojima M. [Studies on the angioarchitecture of the optic nerve. (1) relation to the ciliary arterial

- circulation (author's transl)]. *Nihon Ganka Gakkai Zasshi*. 1977;81(7):642–9.
100. Olver JM. Functional anatomy of the choroidal circulation: Methyl methacrylate casting of human choroid. *Eye (Lond)*. 1990;4(Pt 2):262–72.
 101. Hayreh SS. Segmental nature of the choroidal vasculature. *Br J Ophthalmol*. 1975;59(11):631–48.
 102. Henkind P, Levitzky M. Angioarchitecture of the optic nerve. I The papilla. *Am J Ophthalmol*. 1969;68(6):979–86.
 103. Awai T. Angioarchitecture of intraorbital part of human optic nerve. *Jpn J Ophthalmol*. 1985;29(1):79–98.
 104. Levitzky M, Henkind P. Angioarchitecture of the optic nerve. II. Lamina cribrosa. *Am J Ophthalmol*. 1969;68(6):986–96.
 105. Wang Q, Kocaoglu OP, Cense B, Bruestle J, Jonnal RS, Gao W, et al. Imaging retinal capillaries using ultrahigh-resolution optical coherence tomography and adaptive optics. *Invest Ophthalmol Vis Sci*. 2011;52(9):6292–9.
 106. Hayreh S. Structure of the optic nerve. In: *Ischemic optic neuropathies*. Berlin/Heidelberg: Springer; 2011. p. 7–34.
 107. Laterza A, Nappo A. Optic nerve: a concise review of the anatomy, pathophysiology and principal acquired disorders. *Ital J Neurol Sci*. 1987;8(6):529–35.
 108. Marques IB, Matias F, Silva ED, Cunha L, Sousa L. Risk of multiple sclerosis after optic neuritis in patients with normal baseline brain mri. *J Clin Neurosci*. 2014;21(4):583–6.
 109. Quigley HA, Brown AE, Morrison JD, Drance SM. The size and shape of the optic disc in normal human eyes. *Arch Ophthalmol*. 1990;108(1):51–7.
 110. Tsai CS, Zangwill L, Gonzalez C, Irak I, Garden V, Hoffman R, et al. Ethnic differences in optic nerve head topography. *J Glaucoma*. 1995;4(4):248–57.
 111. Samarawickrama C, Wang JJ, Huynh SC, Pai A, Burlutsky G, Rose KA, et al. Ethnic differences in optic nerve head and retinal nerve fiber layer thickness parameters in children. *Br J Ophthalmol*. 2009;94(7):871–6.
 112. Dzhumataeva ZA. Ethnic differences in the parameters of the head of the optic nerve: Data of optical coherent tomography. *Vestn Oftalmol*. 2007;123(3):29–30.
 113. Costello F, Coupland S, Hodge W, Lorello GR, Koroluk J, Pan YI, et al. Quantifying axonal loss after optic neuritis with optical coherence tomography. *Ann Neurol*. 2006;59(6):963–9.
 114. Anderson DR. Ultrastructure of the optic nerve head. *Arch Ophthalmol*. 1970;83(1):63–73.
 115. Hayreh SS, Vrabec F. The structure of the head of the optic nerve in rhesus monkey. *Am J Ophthalmol*. 1966;61(1):136–50.
 116. Burgoyne CF, Downs JC, Bellezza AJ, Suh JK, Hart RT. The optic nerve head as a biomechanical structure: a new paradigm for understanding the role of iop-related stress and strain in the pathophysiology of glaucomatous optic nerve head damage. *Prog Retin Eye Res*. 2005;24(1):39–73.
 117. Birch M, Brotchie D, Roberts N, Grierson I. The three-dimensional structure of the connective tissue in the lamina cribrosa of the human optic nerve head. *Ophthalmologica*. 1997;211(3):183–91.
 118. Hernandez MR, Luo XX, Igoe F, Neufeld AH. Extracellular matrix of the human lamina cribrosa. *Am J Ophthalmol*. 1987;104(6):567–76.
 119. Levin L. Optic nerve. In: Kaufman PL, Alm A, Adler FH, editors. *Adler's physiology of the eye: clinical application*. St. Louis: Mosby; 2003. p. 603–38.
 120. Perry VH, Lund RD. Evidence that the lamina cribrosa prevents intraretinal myelination of retinal ganglion cell axons. *J Neurocytol*. 1990;19(2):265–72.
 121. Blaivas M, Theodoro D, Sierzenski PR. Elevated intracranial pressure detected by bedside emergency ultrasonography of the optic nerve sheath. *Acad Emerg Med*. 2003;10(4):376–81.
 122. Hayreh SS. The sheath of the optic nerve. *Ophthalmologica*. 1984;189(1–2):54–63.
 123. Hayreh SS, Dass R. The ophthalmic artery: I. origin and intra-cranial and intra-canalicular course. *Br J Ophthalmol*. 1962;46(2):65–98.

Axel Petzold

Introduction

Spectral-domain optical coherence tomography (SD-OCT) has matured from a research instrument to a tool used in clinical routine [1–3]. The combination of OCT data with confocal scanning laser ophthalmoscopy (cSLO) or infrared (IR) has enabled all of us to take an image of the surface (cSLO/IR) and depth (OCT) of the retina, then sit down and talk about it. The axial resolution of commercial SD-OCT machines is in the 4–7 μm range. As you have learned from the previous chapter, a retinal ganglion cell (RGC) has a thickness of about 5–20 μm (see Table 2.1). Therefore SD-OCT does permit us to make observations on a quantitative scale that reaches the cellular level in individual retinal layers. In other words,

SD-OCT permits the visualization of neurodegeneration in vivo at a hitherto unparalleled structural resolution. All you need to know is how to acquire the technical skills to do so. This is not only fun but also highly satisfactory, both in clinical care and in research.

How to Assess a Patient Using OCT

This section describes the three key factors relevant to obtaining a good OCT: a suitable environment, a comfortable patient, and a competent examiner.

The Setup

Create an examination situation in which the patient and you feel comfortable and confident. A relationship of mutual trust will help to obtain best results, particularly if unforeseen problems appear during the assessment.

A well-suited setup is an air-conditioned room with dimmable light levels. The air stream should not blow into the patient's face in order to avoid dry eyes, which can cause frequent blinking during the OCT assessment. Position the patient and examiner so that both can best do their tasks. The patient should not be visually distractible and may therefore best face a wall. The examiner should be able to always keep an eye on the patient but will,

Electronic supplementary material The online version of this chapter (doi:[10.1007/978-3-319-20970-8_3](https://doi.org/10.1007/978-3-319-20970-8_3)) contains supplementary material, which is available to authorized users.

A. Petzold, MD, PhD
Department of Neuro-ophthalmology,
Moorfields Eye Hospital & National Hospital
of Neurology and Neurosurgery, London, UK

Department of Neuroimmunology,
UCL Institute of Neurology, London, UK

Dutch Expertise Center Neuro-Ophthalmology,
Departments of Neurology and Ophthalmology,
VU Medical Center, Amsterdam, The Netherlands
e-mail: a.petzold@ucl.ac.uk, a.petzold@vumc.nl,
axel.petzold@moorfields.nhs.uk

in a busy work environment, also need to interact with colleagues. This can be achieved by the examiner facing the entrance to the examination room (Fig. 3.1). This setup also allows to minimize the effect of stray light to the patient's eyes in case of an open entrance or incidental opening of the door. The OCT examination is best performed in a darkened room, particularly in patients in whom the pupils were not pharmacologically dilated.

To enable assistance to patients through a third person, provide sufficient space around the patient's place. Finally, the examination room should have wheelchair access.

For teaching purposes allow sufficient space behind the OCT machine on the examiner's side.

The Patient

The patient is in a vulnerable role. Their emotions may be influenced by the disease. Insecurity and anxiety may create challenges for a good assessment (Box 3.1). Reasons can be physical disabilities affecting mobility and communication but also bad experiences with past investigations. Building and maintaining trust is a good way to help overcome these issues.

Patients suffering from multiple sclerosis may have symptoms that can complicate the OCT

Box 3.1

The main task for the patient is to fixate a small visual target during the examination, which requires keeping the eye, head, and body still.

assessment. These problems should be recognized prior to the OCT assessment. Some symptoms may require additional assistance and protocol modifications, which are best discussed prior to starting the assessment.

1. *Vision*: inability to maintain visual fixation because of a central visual field defect, poor visual acuity, and/or nystagmus.
2. *Hearing*: inability to follow auditory directions during the examination.
3. *Mobility*: pathology affecting the cerebellar function and pyramidal and extrapyramidal systems may all make it difficult for a patient to sit comfortably throughout the OCT assessment and maintain a still head position.
4. *Cognition*: impaired cognitive function may not only limit what a patient understands about the assessment and the ability to follow directions but also influence the patient's behavior during the OCT assessment itself. Patients

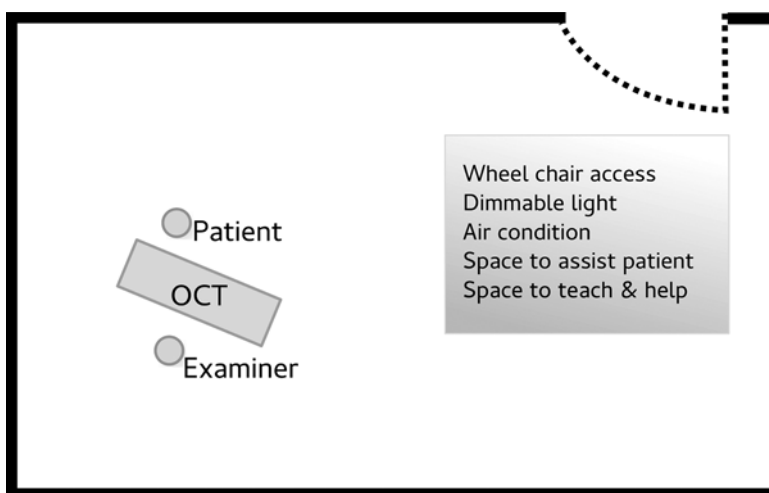


Fig. 3.1 The setup should allow for good OCT examination conditions. Patients may require wheelchair access and additional help during the assessment for which there needs to be sufficient space. Dimmable light permits the OCT examination to be performed in a darkened room.

The effect of stray light from an open door/entrance should be minimized by positioning the patient and examiner appropriately. Allow for sufficient space on the examiner's side too to permit teaching and technical help with challenging situations

may be easily distractible, look around, keep talking, grow fidgety, or tire out during the assessment. Loss of praxic skills and higher visual functions pose a challenge too.

5. *Face, lid, and eye:* anatomical constraints of the face may make it impossible for the OCT lens to be moved close enough to the eye to obtain an OCT image. A ptosis of narrow palpebral fissure may require extra assistance. Makeup and long eyelashes may dirty the OCT lens. Small pupils (<2 mm) may require pharmacological pupil dilation; this may also be of help in some cases with opacities in the light pathway, such as cataract or floaters.

In general terms, the OCT assessment is relatively straightforward in patients suffering from multiple sclerosis compared to patients with movement disorders, dementia, rapidly progressive neurodegenerative disorders, or pathology causing impaired vision and blindness.

The Examiner

The role of the examiner(s) depends on the professional background. The examiner can be an OCT technician, physician, nurse, trainee, or student. A trainee will require teaching, both hands on and theoretical. An OCT technician may want to discuss medical questions potentially arising from certain images. A nurse or physician may require technical assistance. Therefore the position of the examiner should be clear to the patient.

The examiner should be able to communicate in lay terms what the OCT assessment includes (Box 3.2). The examiner should be able to answer the patient's question: "Will my eye be touched?" The examiner needs to give the appropriate

Box 3.2

The task of the examiner is to obtain high-quality OCT data, which requires giving directions.

instructions to aid the patient in maintaining visual fixation and keeping the eye, head, and body still. The examiner needs to recognize when extra assistance is needed for the patient. Likewise, an examiner needs to know when to call for help with OCT image acquisition, handling, and storage.

As a general rule, always explain to the patient what you want to do before you do it. Like with other paramedical tests, be very cautious about what you say to a patient with regard to the images just obtained. Your words may cause distress and harm. The errors of overreporting are likely to be greater than the errors of underreporting. There is no harm in asking for more time to discuss the images with your colleagues first.

The Machine

Common to all OCT devices on the market is that a light signal is focused through a lens to the retina. Next, light scattered back from the retina is captured by the same lens. Finally, the OCT image is composed with the aid of device-specific hardware and software. For brevity, this chapter takes examples predominantly derived from one SD-OCT device. There are differences between the many commercial devices, but the OCT market is developing so rapidly that it will not be possible to have an updated pragmatic chapter on all.

All one needs to do to obtain a good OCT image is to place the lens correctly. Practically, this is similar to the handling of a slit lamp. If you have never used a slit lamp or ophthalmoscope, think of the opening scene from a James Bond movie (Fig. 3.2).

Which OCT Do You Want to Own?

The OCT market is rapidly expanding. Both commercially developed and in-house-developed devices contribute to the data available. Access to in-house devices will remain exclusive to a few research centers. In contrast, the commercial sector has developed an impressive "shopping list," which was recently reviewed by Fiona Costello [4]. Device-specific features for spectral-domain and swept-source OCT are reproduced and

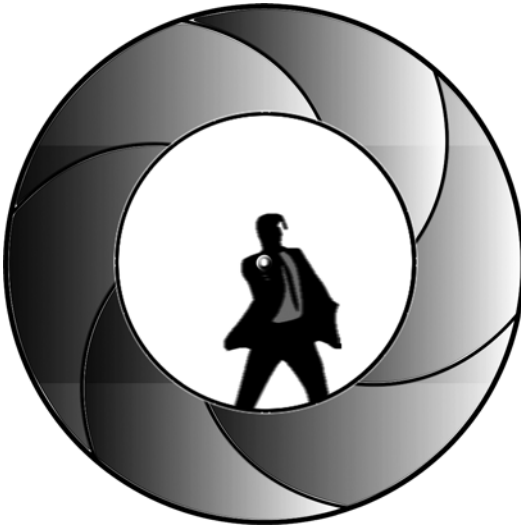


Fig. 3.2 A mnemonic aid for correct placement of the OCT light beam is the gun barrel sequence that features in almost every 007 film. The OCT light beam should enter the center of the pupil

updated from reference [4]. At the time of writing, most literature on OCT in multiple sclerosis and optic neuritis is based on data from the Cirrus and Spectralis devices:

1. Cirrus (Zeiss)TM combines advanced software features that enable good-quality scan acquisition. The FastTracTM option reduces eye motion artifacts. The Guided Progression AnalysisTM permits for longitudinal comparison of retinal layer thickness changes. The FoveaFinderTM ensures that the Early Treatment Diabetic Retinopathy Study (ETDRS) grid is centered on the fovea. The AutoCenterTM centers the ring scans on the optic nerve head. Automated seven-layer segmentation is possible. Finally, HD-OCT technology enables sharing of data with networked review stations.
2. The SPECTRALIS (Heidelberg Engineering) is a multimodality device combining the advantages of a confocal scanning laser ophthalmoscope (cSLO) with the benefits of achieving cross-sectional images of the retina with a spectral domain-based optical coherence tomography (OCT) module. Besides the standard infrared (IR)-based fundus image, the SPECTRALIS offers up to six different imaging modalities in the highest stage of expansion. The MulticolorTM feature combines three wavelengths (IR, green, blue) to generate a true detailed color fundus image, while the autofluorescence (BluepeakTM) allows the structural assessment of the retina as well as gathering metabolic information of the lipofuscin distribution in the retinal pigment epithelium (RPE), which is of relevance for ophthalmologic disease. Next, there is an option for fluorescence angiography (FA) and indocyanine green angiography (ICGA) in combination with a noncontact ultra-wide-field (UWF) lens peripheral angiography. The anterior segment (ASM) lens extends the capability to image the cornea, sclera, and chamber angles. An important feature is the active eye-tracking system (TruTrackTM), which compensates involuntary eye movements and blinking at time of scanning without need for post-processing. This technique allows a precise point-to-point registration of the fundus image and OCT scan. Moreover, the eye-tracking system is the base for the rescan (AutoRescanTM) function, which uses the baseline exam to place the follow-up exam on precisely the same position on the retina before acquiring the follow-up scan. This enables reliable longitudinal data. Recent software developments not only correct to circumvent rotatory problems (e.g., head tilt) but also adjust the scans individually on the retina. The so-called anatomic positioning system (APS) uses the center of the fovea and the Bruch membrane opening (BMO) as distinct reference points in the retina. Taking head tilt and cyclotorsion into account during acquisition allows for an individual classification of the scans. Finally there is the option for 11-layer segmentation on B-scans individually and as a batch as relevant for clinical studies.
3. IVue (Optovue). Designed to be easy and fast, the machine includes a foot switch and touch screen. There is also the option for imaging of the anterior segment including corneal thickness measurements. Color-coded retinal layer segmentation and mapping includes the GCL,

- GCC, and the option for 3D “en face” visualization.
4. Angiovue (Optovue). During the writing of this chapter, the first OCT device on the market to permit for 3D visualization of the retinal vasculature became available. This technology does not permit investigation for leakage, and the potential role for optic neuritis and multiple sclerosis remains to be seen. Possibly diseases like Susac syndrome or anterior ischemic optic neuropathy (AION) and paracentral acute middle maculopathy (PAMM) are of greater interest.
 5. 3D OCT 1000/2000 (Topcon). Longitudinal image acquisition is possible, enabling comparison over time. Both 3D and 2D OCT viewing options can be combined with the fundus image (FastMap™ software). There is the option to manually pinpoint the location of an OCT image in the fundus image (Pin-Point™). Images are viewed through the EyeRoute® Image Management System.
 6. DRI OCT Atlantis (Topcon). A very quick swept-source OCT with follow-up function. Has the advantage of invisible scan lines, which makes it easier for the patient to focus on the target. A large 12 mm-wide screen for scanning. Automated 7-layer segmentation.
 7. OCT/SLO (Optos). It is possible to combine SLO and retinal tracking before, during, and after acquisition of the OCT scan. Registered follow-up is possible with the SLO “Lock and Track” function. There is the option to align 3D topographies to the SLO image, which permits correction for artifacts due to rotation and shift. Longitudinal comparisons, including retinal thickness, is possible with aid of the “Auto – Compare” feature. All images can be viewed remotely using the “Viewer Software.”
 8. Copernicus HR (Optopol Technology). Longitudinal image comparison possible. Option for 3D visualization and volume maps. There is a disk damage likelihood scale (DDLS) for the optic nerve, which is based on the rim/disk (r/d) ratio and optic nerve size. Imaging of the anterior segment is possible at a 3 μm resolution. Remote viewing of images from a central database is possible.
 9. Canon OCT HS-100. Longitudinal imaging is possible using SLO tracking of retinal images. Option for enhanced depth imaging of the choroid. Option to import retinal camera images, which then can be aligned and overlaid with the SLO image. Ten-layer retinal segmentation.
 10. RS-3000 (Nidek). Longitudinal imaging using multifunctional follow software is possible for this SD-OCT device, which enables averaging up to 120 images. Option for selectable OCT sensitivity aids improved visualization with a range of ocular pathologies. Eye-tracking capabilities including torsion. Reports can be customized.

Infrared (IR) and (Confocal) Scanning Laser Ophthalmoscopy (c)SLO

There are two options: an IR camera or a scanning laser ophthalmoscope (SLO). The SLO scans the image line per line, similar to how old-fashioned television screens used to build up an image. In most devices this is a bit slower than the IR camera (about 16 images per second compared to 24 images per second), but scanning speeds can be increased. The speed of both IR and (c)SLO enables video recording. One advantage of the SLO and confocal SLO (cSLO) images is the high resolution. Taken together, the image quality of (c)SLO is better than for IR. In (c)SLO there is a small depth of focus and scattered light is better suppressed. Therefore patients find (c)SLO more comfortable (less bright light exposure). There are good 3D imaging capabilities. Finally, imaging with smaller pupil sizes becomes possible.

IR

IR is used by the following OCT devices: Stratus, 3D OCT 2000, iVue, and Copernicus HR. (c)SLO is used by Spectralis, Cirrus, DR 1, RS-3000, OCT SLO, and Canon OCT HS-100.

Pupil Size Requirements

A preference in a neurological clinic is not to dilate the pupil pharmacologically. In most patients it will be possible to obtain good-quality

OCT scans without the need to dilate the pupil. The pupil size should be measured at the same light level at which the OCT images will be acquired. At time of writing, the following pupil size requirements apply:

- ≥ 2 mm: Spectralis, Cirrus
- ≥ 2.5 mm: 3D OCT, DR 1, RS-3000
- ≥ 3 mm: iVue, OCT SLO, Copernicus HR, Cannon OCT HS-100
- ≥ 3.2 mm: Stratus

Light Source

The axial resolution of OCT is related to the bandwidth of light. A finer axial resolution is achieved with a wider span of wavelengths in the light. The current light source range is 820–1050 nm.

- 820 nm: Stratus
- 830 nm: OCT SLO
- 840 nm: Cirrus, 3D OCT 2000, iVue
- 850 nm: Copernicus
- 855 nm: Canon OCT HS-100
- 870 nm: Spectralis
- 880 nm: RS-3000
- 1050 nm: DR 1

Resolution

For all devices the axial resolution (3–10 μm) is better than the transverse resolution (12–20 μm). The reported axial resolution is:

- 3 μm : Canon OCT HS-100, Copernicus HR
- 5 μm : Cirrus, iVue
- 6 μm : 3D OCT 2000
- 7 μm : Spectralis, RS-3000
- 8 μm : DR 1
- 10 μm : OCT SLO, Stratus

Scanning Speed

The number of A-scan obtained per second determines the scanning speed. High scanning speed reduces the likelihood of motion artifacts. Scanning speed will become more and more

important with the advance of Doppler OCT. The exquisite images of the retinal vasculature obtained by, for example, the Angiovue is only possible due to the high scanning speed of 70,000 A-scans/s. At time of writing, scanning speeds are:

- 400 A-scans/s: Stratus
- 25,000 A-scans/s: iVue
- 27,000 A-scans/s: Cirrus
- 40,000 A-scans/s: Spectralis
- 50,000 A-scans/s: 3D OCT 2000
- 52,000 A-scans/s: Copernicus HR
- 53,000 A-scans/s: RS-3000
- 70,000 A-scans/s: Angiovue, Canon OCT HS-100
- 100,000 A-scans/s: DR 1

Basic OCT Protocol

As a minimal requirement, one needs to capture (1) the area where all axons leave the eye, the optic nerve head, and (2) the area most relevant for our vision, the macula. A basic OCT protocol therefore comprises a volume scan of the macula and optic nerve head. Some patients with MS will have difficulties maintaining the visual fixation needed to acquire a good-quality volume scan. A volume scan may take too long for these patients. Therefore if speed matters, a ring scan around the optic nerve head may be used instead of the volume scan. The basic OCT scan protocol, which should be possible in most patients with MS, is summarized in Fig. 3.3.

Start OCT Scan

This section was written for the Spectralis device (Fig. 3.4) and reproduced from reference [5]. For other devices the reader is referred to the device-specific instruction manuals.

1. First, prepare the software by entering the patient details into the database. In case of

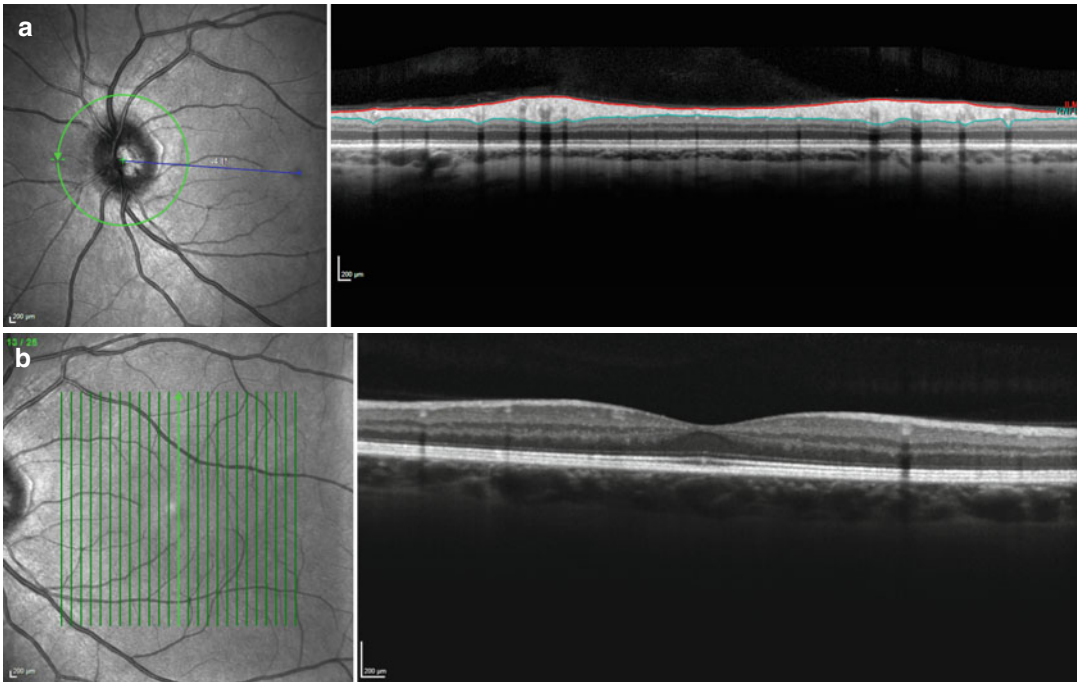
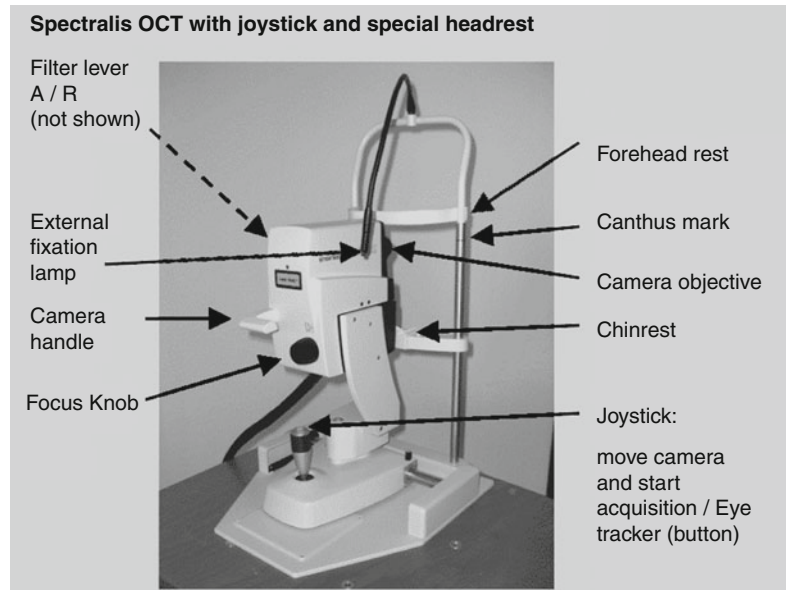


Fig. 3.3 Basic OCT protocol for patients with MS. (a) Ring scan of the optic nerve head and (b) volume scan of the macula

Fig. 3.4 Heidelberg Spectralis OCT



a follow-up examination, a patient record will already have been created and you will only need to specify the OCT operator taking the image.

2. Second, prepare the hardware. (1) Pull the OCT camera head back, (2) clean the parts coming in contact with the patient (forehead and chin rest), (3) remove the lens cap and wipe

the lens if not clean, (4) adjust the height of the table to a comfortable position for the patient, (5) adjust the height of the patient's head so that the marker indicating the canthus (Fig. 3.4) comes to the patient's eye, and (6) ask if the patient is ready to go or if there are any questions. The patient should already know that the eye will not be touched.

3. Third, start the OCT acquisition window. There will be a short device calibration period before you can click on the yellow square to the bottom right of the screen to start imaging. Now the cSLO image will appear in the window to the left of the screen. A few seconds later, the OCT signal will be seen in the window to the right of the screen.
4. Fourth, repeat explaining to the patient that a fixation target will appear. This is a blue light. Some patients will see a series of vertically displaced blue lights for optical reasons. In this case ask them to look at the brightest one, which typically is the bottom one. Some patients will not be able to see the internal fixation target. If this is the case, (1) use the external fixation target consisting of a lamp, (2) use your finger (or alternative) as a target, or (3) give verbal instructions where to look (right, left, up, down). Be aware that good visual fixation will help to get quick and high-quality OCT images. Patients are permitted to blink and move eyes in between for their own comfort. A teary dry eye is no good for OCT imaging.
5. Fifth, in the acquisition window select "Axonal." The advantage of the axonal setting is that it was developed specifically for neurological conditions. The OCT B-scan lines are orientated vertically, which permits capture of all axons cross-sectionally.
6. Now you are ready to choose from the "Preset" buttons. For a basic protocol, you will only need the macular volume scan and ring scan. It is your choice which one you start with. My personal preference is to start with the macular volume scan because the patient finds it easier to fixate.

The Macular Volume Scan

1. First, click on one of the macular volume scans from the preset buttons. Scans with a low ART¹ (e.g., 9) are quicker than scans with a high ART (e.g., 40–100) and better suited to detect small microcysts but less suited for high-quality retinal layer segmentation. A high ART takes longer and may be less suited for patients with difficulties to maintain visual fixation or to sit comfortably for long in the required position.
2. Second, use the "007 technique" (Fig. 3.2) on the cSLO to get the retina in focus. The OCT image will appear once you have advanced the OCT camera head close enough to the patient's eye. If the OCT image "flips over" on the top of the screen you will need to move the camera a bit back again. Do not touch the eye.
3. Third, once you have a good cSLO image and OCT signal, activate the device-specific "Eye-Tracker." To do so, you need to either (i) press the joystick button for about 2 s (basic Spectralis device) or (ii) press the round button below the touch screen (all other Spectralis devices).
4. Fourth, place the volume scan with the mouse over the macula.
5. Fifth, once you start scanning by either (a) pressing the joystick button shortly or (b) pressing the "Acquisition" button on the touch screen, make absolutely sure to observe the OCT live image to the bottom of the screen. Always keep the scan as much horizontally aligned as you can. While the device is acquiring several images to obtain a good signal-averaged image, you may need to continue adjusting the live image with tiny up/down/right/left movements of the joystick.
6. Once the image is complete, continue with the ONH ring scan.

¹ART stands for averaging of scans. The averaging algorithm takes eye movements into account. A "smoother" but not always necessarily "better" OCT B-scan will be obtained with a high ART number.

The ONH Ring Scan

1. First, click on “RNFL-N” (indicating the ONH ring scan) from the preset buttons. Adjust the ART according to the patient’s abilities and image post-processing needs. Higher ART means longer scanning time.
2. Second, ask the patient to fixate on the new target, which is now closer to her nose.
3. Third, once the ONH is clearly visible in the cSLO window and there is also a good OCT signal, start the device-specific “Eye-Tracker” function as described previously.
4. Fourth, place the ring scan around the ONH using the mouse drag-and-drop option. Note that the ring scan needs to be well centered [6, 7]. Also use the mouse to move the blue line on the cSLO image over the foveola.
5. Fifth, start the OCT image acquisition by pressing the device-specific button as described earlier.

Advanced OCT Protocol

Advanced options help to increase anatomical information and modification of imaging modalities.

From an anatomical perspective, the ONH is particularly interesting. There is a large anatomical variation of the ONH between subjects.

Principally, an ONH volume scan (Fig. 3.5) is best suited to capture this and also permits for image post-processing including extraction of a ring scan and analysis of the lamina cribrosa where myelination of the optic nerve axons starts. An option is between a very fast ring scan and a longer volume scan is an ONH star scan (Fig. 3.6). Either scan combined with the EDI function may permit capture of the lamina cribrosa. For comparison, the EDI function was enabled in Fig. 3.5, but not in Fig. 3.6. Consequently the lamina cribrosa is captured better in the former.

The nerve fibers of the so-called papillomacular bundle (PMB) are more vulnerable compared to other axons in the retina [8]. The diameter of axons in the PMB is only around $0.4\ \mu\text{m}$ but up to $2.5\ \mu\text{m}$ fibers elsewhere in the retina [9]. There is an option to scan for the approximate area of the PMB (Fig. 3.7). But because there is no exact anatomical definition to the extent and course of the PMB [10], an ONH volume scan, together with a volume scan of the area projecting from the ONH to the macula (Fig. 3.7), might be valuable.

From an image modality perspective, autofluorescence (Fig. 3.8) is interesting in a clinical neuro-ophthalmology setting but has, to the best of my knowledge, not yet delivered any valuable information in MS. Likewise, there are options for multicolored laser beams in the cSLO image (Fig. 3.9) that to date do not add to the investiga-

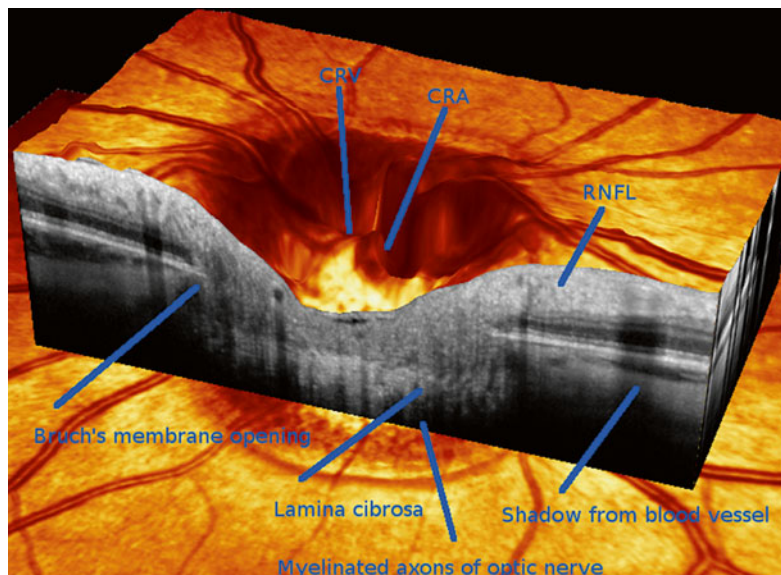


Fig. 3.5 An ONH volume scan with EDI enabled. The cSLO image of the retina is shown in pseudo-colors and the OCT image in grey. This 3D image was constructed of $n=73$ vertical B-scans. Anatomical landmarks are indicated: CRA central retinal artery, CRV central retinal vein, RNFL retinal nerve fiber layer

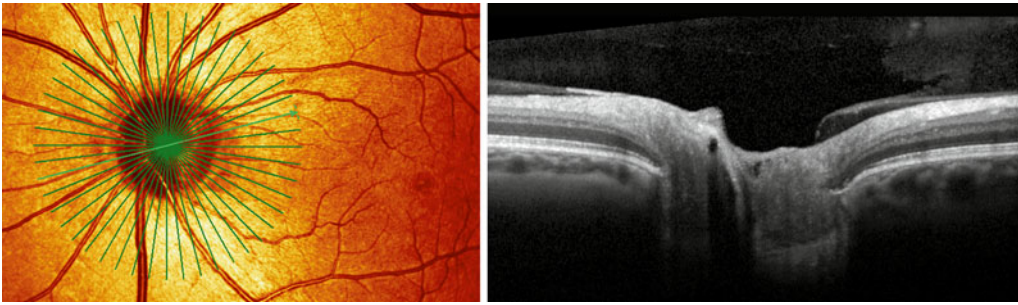


Fig. 3.6 An ONH star scan without EDI. Compared to the volume scan, the star scan is quicker due to the lower number of B-scans ($n=24$), which are acquired at different angles

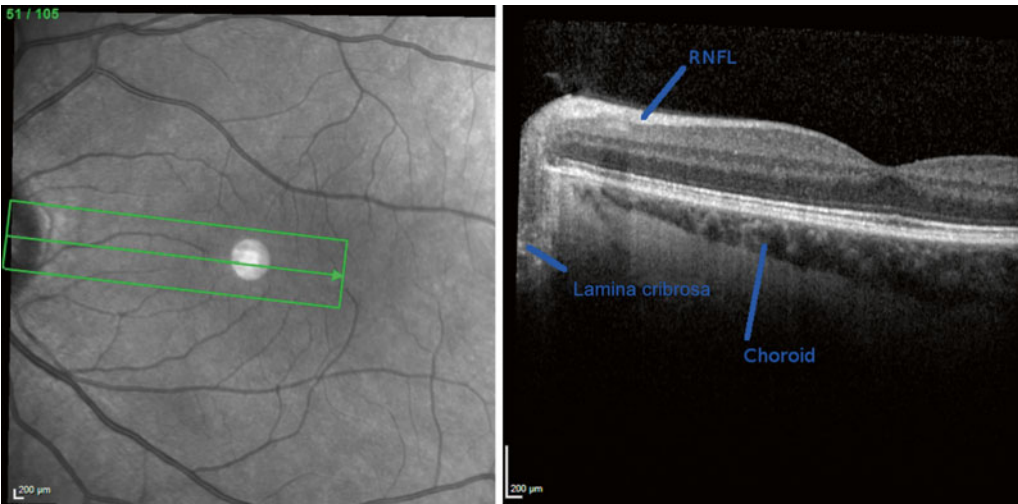


Fig. 3.7 A volume scan placed over the area between the foveola and ONH, which captures part of the papillomacular bundle (PMB). This is a high-resolution scan of $n = 105$ B-scans. A circular artifact is seen to the middle of the cSLO image due to a light reflex



Fig. 3.8 Autofluorescence (AF) of the fundus revealing buried optic disk drusen



Fig. 3.9 Multicolor cSLO

tion of patients with MS. In contrast, the option to perform fluorescence angiography is relevant and will be of value in a subset of patients with possible optic neuritis to determine leakage. Recent developments include so-called Doppler OCT, which makes use of image motion information during acquisition. Essentially, this represents a conceptually diametrically opposed paradigm to classical OCT image acquisition, which tries to average only structurally stable parts of the retina. Blood vessels pulsate and move and thus angio-OCT permits detection of the retinal vasculature. A predicted shortcoming is that angio-OCT will not show leakage from the retinal vasculature.

Another interesting option is the use of polarization-sensitive OCT (PS-OCT). It was proposed to test if change of birefringence in the RNFL precedes loss of RNFL [2]. The underlying pathological mechanism is thought to reflect on change of the most abundant structural protein of the axon: neurofilaments. Mechanisms described in MS are neurofilament aggregate formation, posttranslational modifications (phosphorylation, nitrosylation, glycosylation), and proteolysis. There may be a role for tubulin too; but because tubulin proteins are expressed in almost all cell types [11], data are likely to be contaminated unless obtained in a cell-type-specific cell culture model. Credit really goes to Mark Kupersmith who was first to make use of the clinically most suited model to test such a hypothesis: anterior ischemic optic neuropathy (AION), where the onset of symptoms is well defined and the outcome definite [12]. Reproduction of these data, which were acquired with scanning laser polarimetry, with PS-OCT will be informative. If indeed PS-OCT signal change can be related in translational studies to proteomic data, such as neurofilament phosphorylation and aggregate formation as an early sign of axonal pathology, then it might be possible to test neuroprotective treatment options that may reverse damage to proteins prior to axonal loss occurring.

Retinal Layer Segmentation

There is no doubt that the development and validation of algorithms for segmentation of retinal layers has risen to the top of the image post-processing agenda. Automated segmentation will be relevant to acquire quantitative normative data for individual data that will inform on layer-specific pathology. For multiple sclerosis the most relevant layers to assess neurodegeneration are the RNFL, GCL, IPL, and potentially the INL. The latter two can be segmented individually but are sometimes presented jointly as GCIP (see Chap. 9 by Paul and Brandt in this book). The advantage of the macular GCL is that optic disk edema does not mask onset and progression of atrophy. This is interesting for longitudinal monitoring of patients with multiple sclerosis and optic neuritis [3, 13].

Recognize Common Pitfalls

My experience with quality control reading in clinical trials and investigator-driven studies is that there are only very few common technical mistakes and most issues relate to adherence to the manual and scanning protocol(s). Therefore a slightly patronizing advice is to only go ahead if the answer to the following three questions is “yes”:

1. Is the patient comfortable and correctly positioned?
2. Can the patient fixate?
3. Do you know which protocol to run?

Then there are common pitfalls, which can be minimized by following the “do’s” and avoiding the “don’ts”:

1. Three “do’s” to remember:
 - (a) Keep the ring scan still while the averaging (ART) is ongoing, and only press the button to acquire the image after averaging is complete (horizontal bar under ART).

- (b) Most people are good in getting the first scan well aligned. But please keep an eye on the live imaging window during acquisition of the volume scan. A volume scan is composed of a number of B-scans. Make sure that you do not inadvertently “cut off” subsequent B-scans by either moving the camera too much or not at all.
 - (c) Keep the scan horizontally aligned in the live image window. If this should not be possible, please make sure that you keep the direction of the tilt on subsequent scans. This is particularly relevant for the ring scans.
2. Three “don’ts” to remember:
- (a) Do not be trigger active. Premature pressure of the acquisition button will result in low-quality images such as illustrated in Figs. 3.10, 3.11, and 3.12.
 - (b) A cutoff B-scan as shown in Fig. 3.13.
 - (c) A scan with poor illumination that is also not horizontally aligned in the live window (seen as a change of the signal intensity of the OPL/ONL) as illustrated in Fig. 3.14 [14] and Fig. 3.11. If this is the only scan

you can get, do not change the position of the measurement beam (seen as a change of the OPL/ONL signal) on subsequent visits.

Implement Quality Control (QC)

The rationale for implementation of quality control is that the small degree of retinal layer atrophy caused by neurodegeneration can easily be masked by artifacts [6, 15]. To be able to separate one from the other, implementation of QC is mandatory.

Atrophy Measures Are Influenced by QC Issues

As already stated, the annual atrophy rate of the peripapillary RNFL in MS is about 1–2 μm per year compared to about 0.1 μm in healthy individuals, based on time-domain OCT data on a group level [16]. Using spectral-domain OCT data and advanced retinal layer segmentation, an annual atrophy rate of 1.1 μm was shown for the peripap-

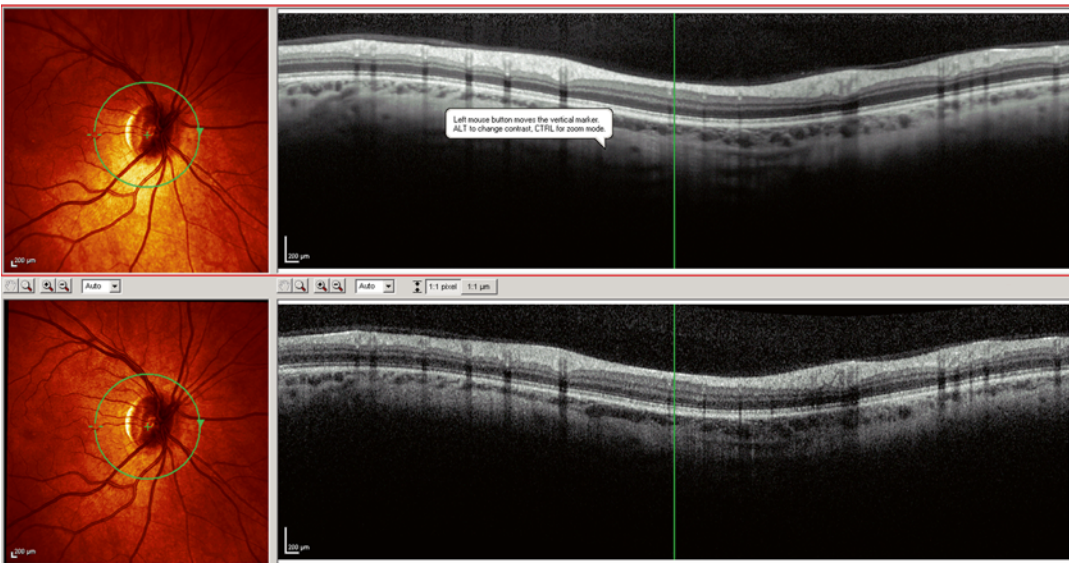


Fig. 3.10 A good-quality baseline OCT is shown on the top as a reference scan. For the follow-up, the operator was “trigger active” and acquired the OCT scan before

sufficient averaging was done. Another QC problem with this ring scan is that it was not well centered. This scan does fail QC

illary RNFL and a matching $1.1\ \mu\text{m}$ for the macular ganglion cell complex (GCL and IPL) [17].

In a clinical setting seeing individual patients, the question might arise if any atrophy had occurred since the last visit. Figure 3.15 illustrates two subsequent scans from one subject taken 1 year apart. Clearly, the bold black line taken at follow-up suggests $12\ \mu\text{m}$ atrophy of the peripapillary RNFL. But closer inspection demonstrates a change of signal intensity in the OPL/ONL (blue lines). This is a well-known measurement artifact due to tilted OCT measurement beam placement [14]. Therefore it would be wrong to report progressive atrophy in this particular case.

Other recognized artifacts include displacement of the peripapillary ring scan (over $3.4\ \mu\text{m}$) [18] and poor signal quality (around $10\ \mu\text{m}$) [19].

On a group level, as relevant to clinical trials and cohort studies, one needs to realize that the small degree of atrophy in neurodegeneration can easily be masked by preventable artifacts. A set of internationally validated QC criteria emphasize seven key points that require attention [7].

OSCAR-IB

Mnemonics were chosen to remember the seven key QC points for retinal OCT scans, OSCAR-IB [6, 7]. These criteria were originally developed

for the peripapillary ring scan but equally apply to volume scans [20]. These criteria are summarized in Table 3.1 [6] and will be discussed one by one in the following seven sections:

O Criterion

Obvious reasons leading to QC failure are protocol violations. Like with a photograph, an optically sharp image is required. So failure to focus the image causes QC failure. Other causes encountered are a dirty lens, obscurations in the optical pathways (lens opacities, vitreous hemorrhage, or a strong cellular reaction in the anterior segment), and a very small pupil size ($<2\ \text{mm}$ for most current devices). Software issues include a lack of averaging of OCT B-scans either because the averaging mode was turned off or because the OCT images were taken too quickly (“trigger active”). An example for an OCT scan that was cut off is shown in Fig. 3.13. Such a scan will fail QC.

S Criterion

The signal strength needs to be sufficient for a good-quality OCT B-scan with appropriate contrast between layers as required for image post-processing. The signal strength required can vary.

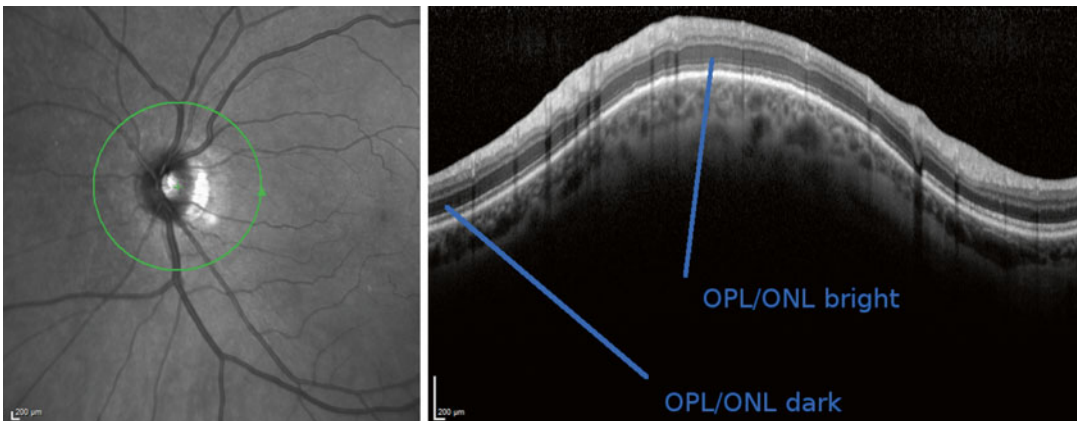


Fig. 3.11 During acquisition of this ring scan, the OCT laser beam was not centrally placed. Consequently the OCT image, typically seen in the live imaging window,

appears as a curved line. This is always associated with the OPL/ONL sign [14]. Both layers are inhomogeneously illuminated

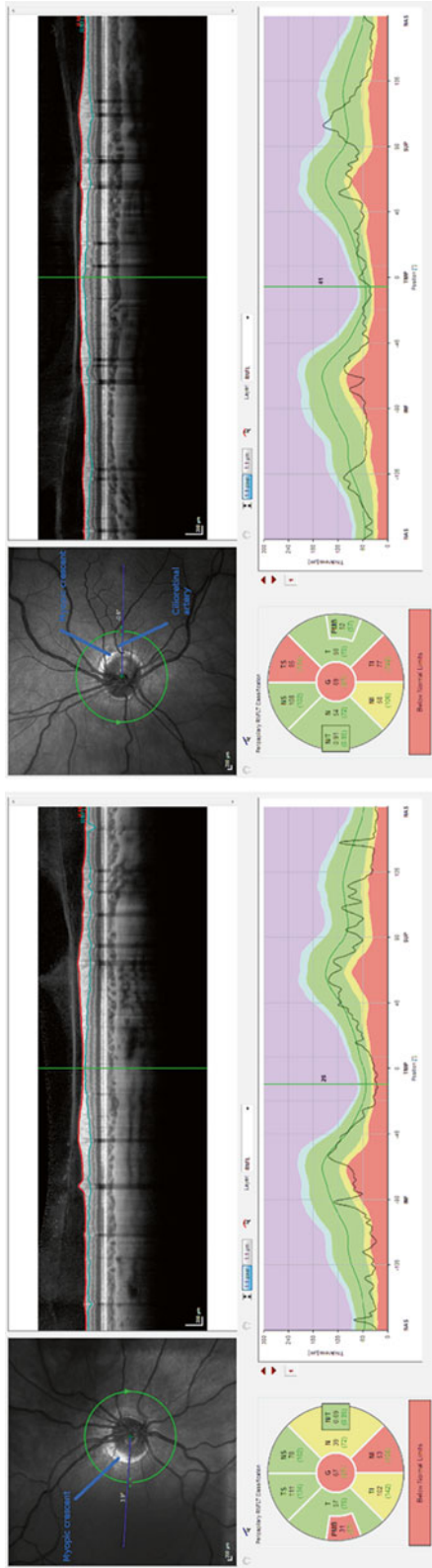


Fig. 3.12 Artifactual peripapillary RNFL thinning in a subject with -8 diopters myopia in both eyes. A myopic crescent can be seen on the cSLO images. There is a cilioretinal artery in the left eye

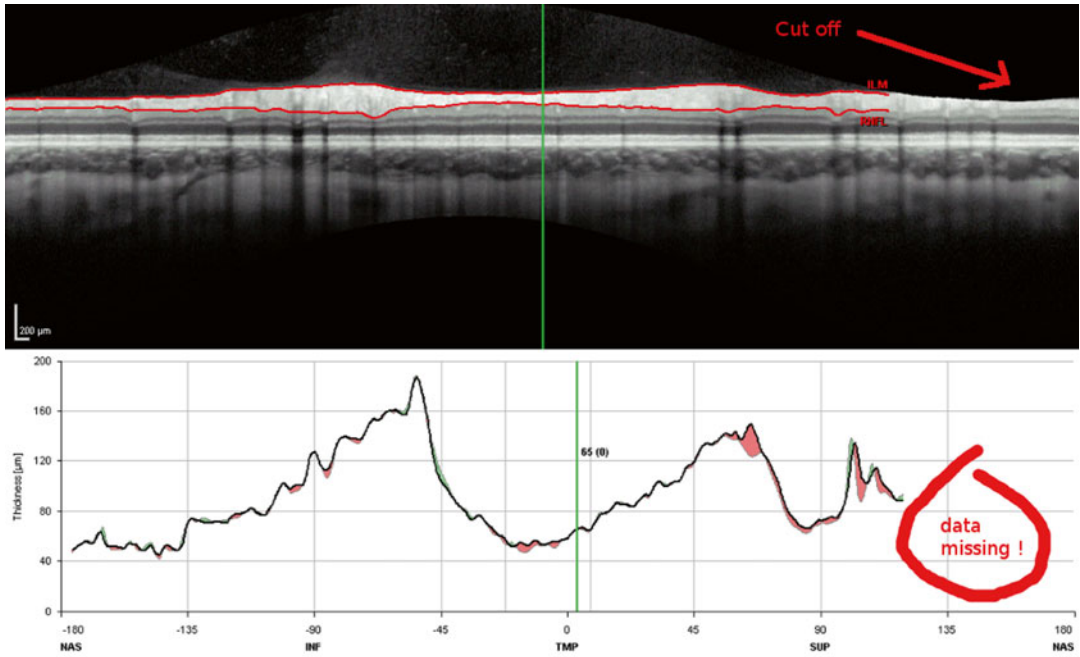


Fig. 3.13 This ring scan taken at follow-up was partly cut off. No data can be calculated for the nasal sector. This scan does not fulfill QC criteria

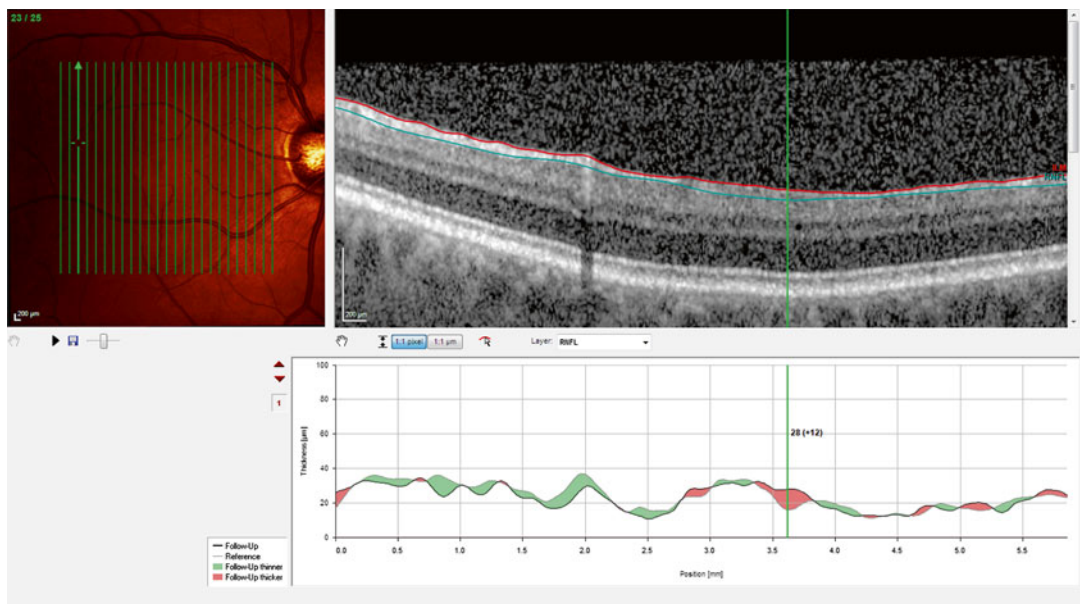


Fig. 3.14 An unequally illuminated OCT volume scan due to poor scanning technique. This scan should be QC rejected

For segmentation of the RNFL from a young healthy eye, the signal strength required will be lower if compared to what is needed for segmentation of the outer retinal layers from an elderly patient with cataract- and age-related macular

degeneration. As a rule of thumb, if one is able to visually distinguish the different retinal layers in the averaged OCT image, the signal is sufficient. Usually an OCT scan fails QC for the S criterion not in isolation but because algorithm failures

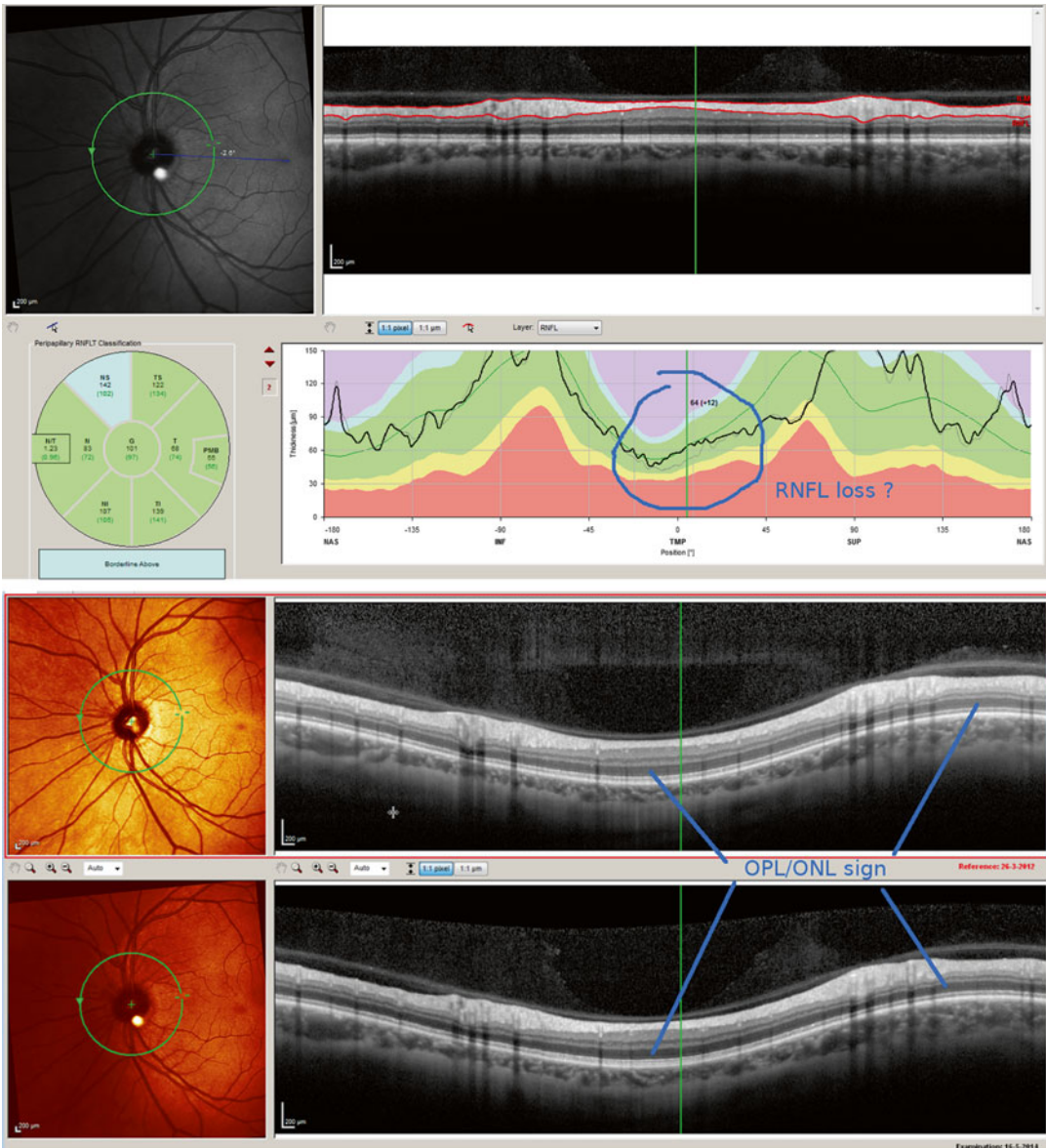


Fig. 3.15 In this 45-year-old man with a 19-year history of MS, the follow-up OCT ring scan (top of image) suggests a localized loss of the RNFL in the papillomacular bundle of around 12 μm (blue circle) over the past 2 years. This is clearly more than what would be expected from aging alone. Comparison of the OCT B-scan at

baseline (red square, 26-MAR-2012) and follow-up (16-MAY-2014) shows change of signal intensity in the OPL/ONL. This is caused by change of the OCT measurement beam pathway and the reason for artifactual PMB thinning. This patient never had an episode of MSON

(A criterion) also follow. Figure 3.16 shows an example of a poor signal strength OCT. This example highlights that QC criteria, originally thought to be relevant for the RNFL, will be even more relevant for the widespread use of segmentation algorithms.

Table 3.1 Seven key QC points using the mnemonic OSCAR-IB

Item	Criteria
O	Any obvious problems?
S	Sufficient signal?
C	Well-centered OCT scan?
A	Any algorithm failure(s)?
R	Signs for retinal pathology?
I	Good illumination of the retina?
B	Consistent beam placement?

The table has been shortened from Ref. [6]

C Criterion

Correct centration of a ring or volume scan is relevant, too. In a clinical setting, a poorly centered ring scan can make it impossible to see whether or not there is relevant RNFL loss. Figure 3.17 shows the ring scan taken from a patient with MS. It is impossible to say from this scan if there was any loss of RNFL in the PMB. This ring scan was placed too close to the temporal/superior optic disk margin. Such a loss was clinically anticipated because of persistent poor color vision following an episode of MSON, implying pathology of the parvocellular projections [21].

On a group level, even a small degree of displacement may introduce a measurement artifact of more than 3.4 μm for the RNFL [18].

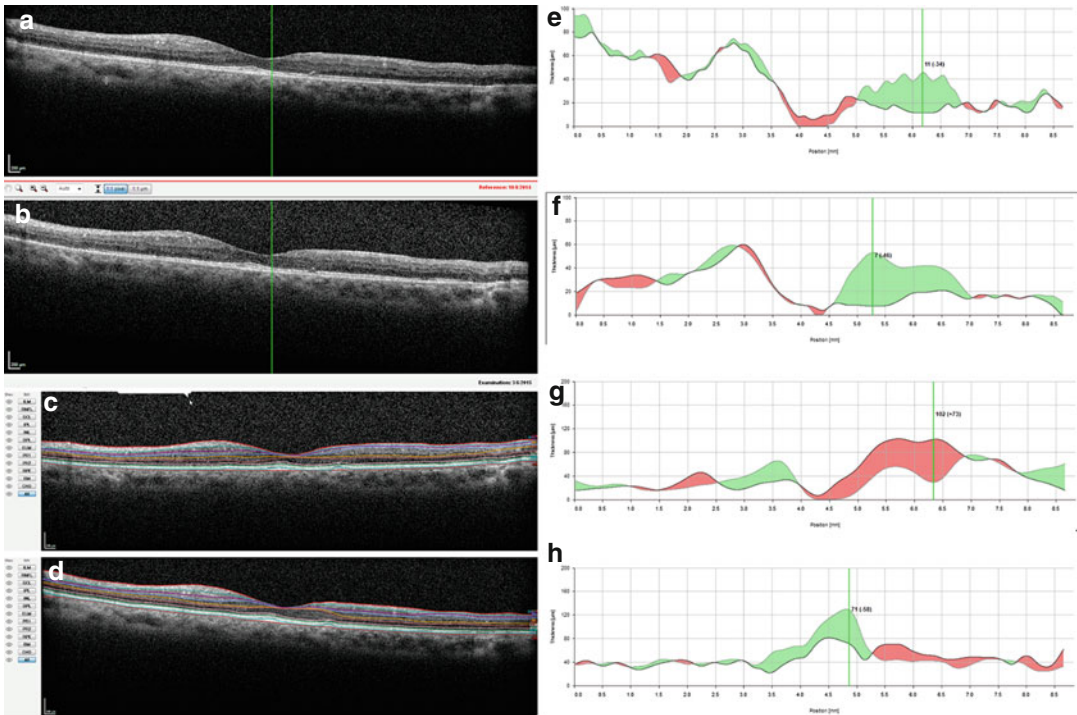


Fig. 3.16 This poor signal strength OCT gives rise to a grainy and noisy image with associated algorithm failures for several layers. (a) The OCT B-scan at baseline and (b) follow-up. Clearly there is a difference in contrast between retinal layers. Following automated segmentation (c) at baseline and (d) follow-up, artifactual differences in layer thicknesses are suggested. The artifactual change of indi-

vidual retinal layer thicknesses is shown for (e) the RNFL (maximal error 34 μm , indicated by green reference line), (f) the GCL (maximal error 46 μm , indicated by green reference line), (g) the INL (maximal error 73 μm , indicated by green reference line), and (h) the ONL (maximal error 58 μm , indicated by green reference line)

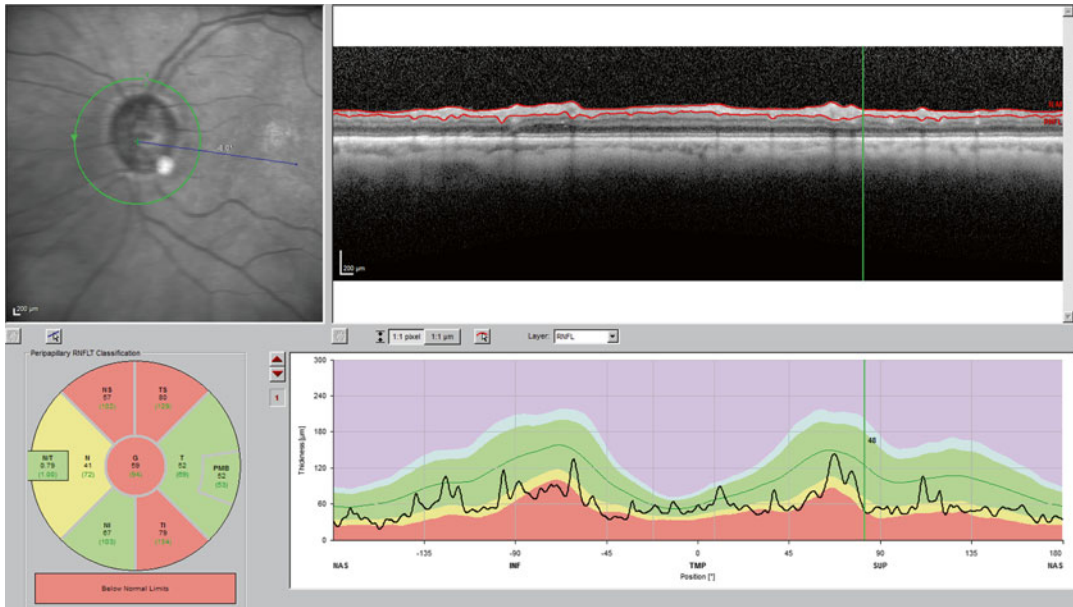


Fig. 3.17 This ring scan was not well centered. Consequently RNFL thickness values cannot be compared to the normal range (*green-shaded area*). This scan is also poorly focused (O criterion). This scan fails QC

Likewise poor centration of the macular volume scan over the foveola causes artifactual retinal thickness maps. Figure 3.18 illustrates this in one clinical case with MSON. In some cases it may still be possible to manually readjust for measurement areas, such that at least part of the data can be used. If the misplacement was too extreme, even image post-processing may fail.

Note that re-centration by image post-processing may be possible for the macular scan, which consists of many OCT B-scans, but not for the ring scan of which there is only one. In a clinical setting, this may be relevant for choice of OCT image protocol in patients with poor fixation. A quick large area volume scan might be preferred over a ring scan to increase the chance to cover the relevant area.

A Criterion

Reasons for algorithm failures are a poor signal strength, poor illumination, retinal pathology, inconsistent OCT beam placement, and blood vessel artifacts, to name but a few. Figure 3.19 shows an algorithm failure due to the presence of an epiretinal gliosis. Such an error can be manually corrected by image post-processing. In a clinical

setting, it is always advised to visually inspect if the RNFL was segmented correctly. Blindly relying on values can lead to misinterpretation. In the case shown, there was a significant degree of atrophy that could easily have been overlooked.

For clinical trials and cohort studies, most algorithm failure can almost always be corrected at a later stage if the other OSCAR-OB QC criteria are met.

R Criterion

Presence of retinal pathology which can influence retinal layer thickness measurements can introduce a bias into the data. Therefore retinal pathology needs to be carefully excluded, particularly for cross-sectional studies comparing groups. A typical example for an MS clinic might be presence of myopia. In subjects with severe (>6 diopters) myopia, the elongation of the eyeball leads to RNFL thinning. This is illustrated in Fig. 3.12. Conversely there might be artifactual RNFL thickening in a subject with hyperopia or presence of drusen. In some cases hyperopia can be misinterpreted as papilledema.

A list of retinal pathology that can effect retinal layer thickness measurements and therefore

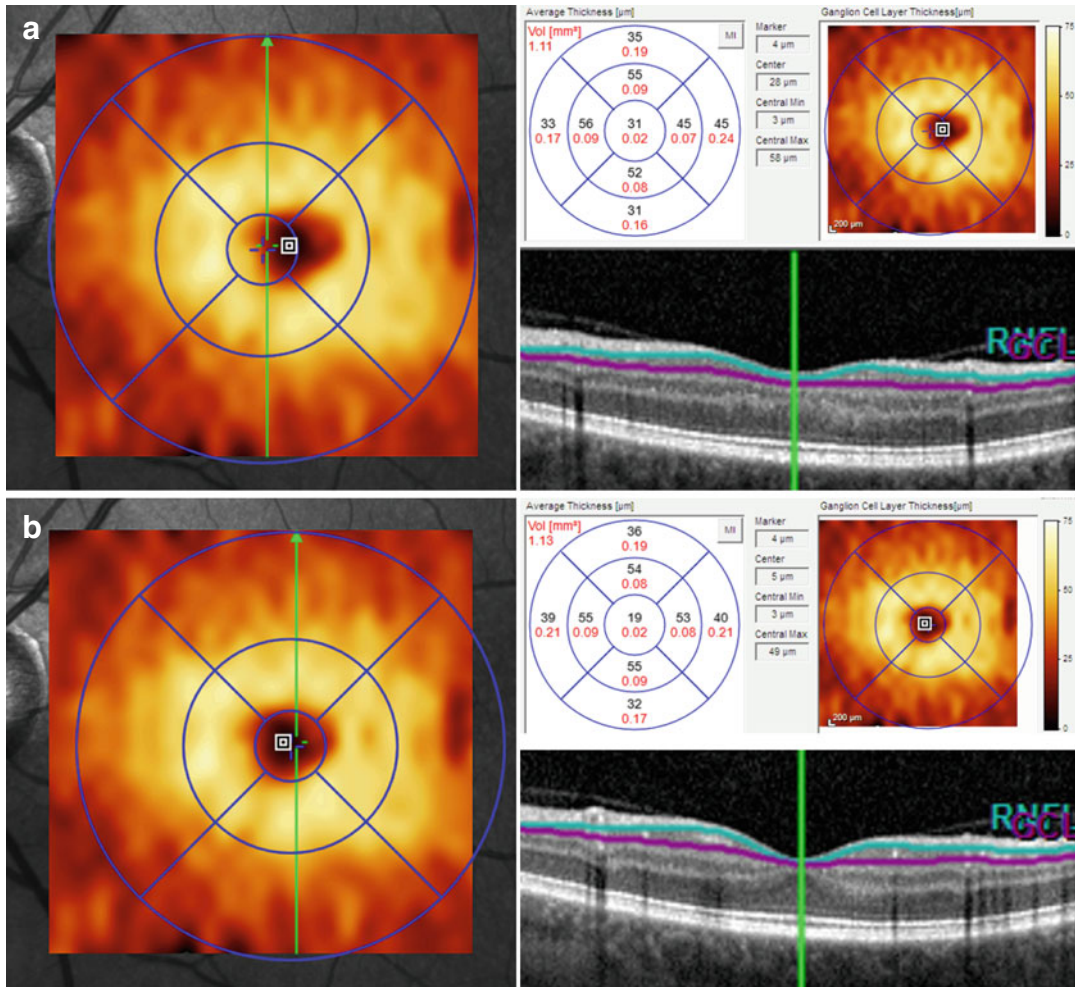


Fig. 3.18 This macular volume scan was placed too far to the left. (a) The EDTRS grid was not centered over the foveola. This led to an artifactual macular thickness map for the GCL (between *bluish* and *purple* lines in OCT). (b) Manual replacement of the EDTRS grid still permits for these scan data to be used. The OCT B-scan now

shows that the center of measurement is placed well within the foveola. The *small black/white square* placed over the foveola in the cSLO image is a marker used as a reference. Quantitative data from this marker is shown in the *red framed box* to the *upper right* in (a) and (b)

requires to be considered is given in Table 3.2 [6]. The risk for bias due to retinal pathology might be less in longitudinal studies that consider change of retinal layer thickness over time compared to cross-sectional studies.

I Criterion

Poor illumination of poor signal go frequently, but not always, hand in hand. Poor illumination

can be an image that is either generally too dark or unequal. Illumination was embraced as one of the first QC criteria in the ophthalmological literature [15]. An unequally illuminated image is shown in Fig. 3.14. As can be seen, there is a drop of signal in the poorer-illuminated areas and algorithm failures follow. In a clinical setting, it is always worthwhile remembering that floaters are a frequent cause for entoptic phenomena and can also be the root for unequal illumination as they cast shadows (Fig. 3.20).

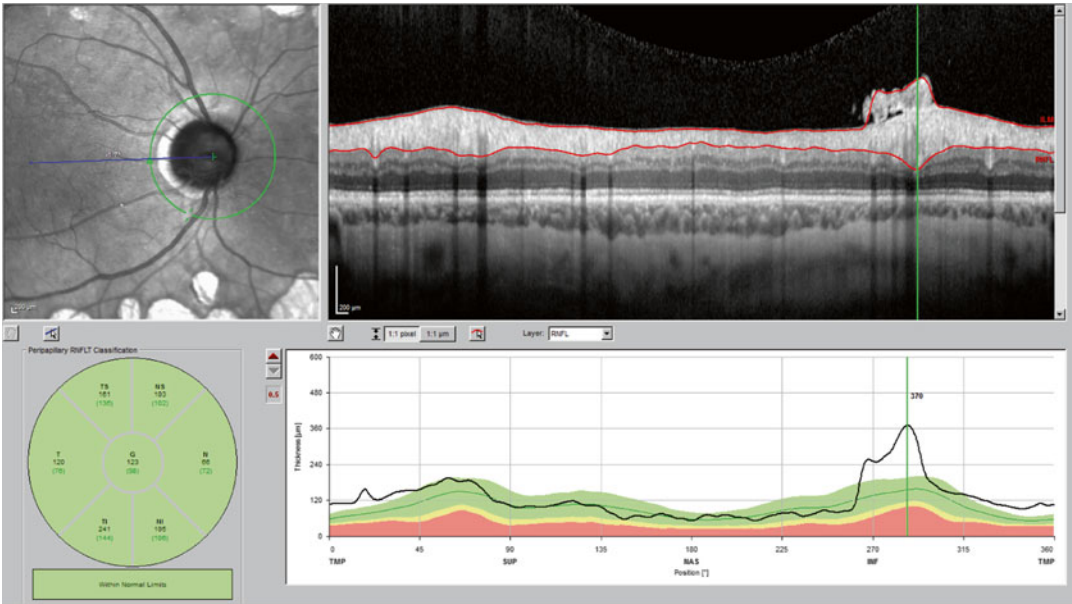


Fig. 3.19 (a) Algorithm failure due to presence of epiretinal gliosis (*vertical green reference line*). This shows a 34-year-old man with a diabetes mellitus type 1 and diabetic retinopathy for which he received laser treatment (*white spots on cSLO image*)

Table 3.2 Pathology of the retina to be considered by the OSCAR-IB criteria

Summary	Diseases
Structural	Drusen, cysts, detachment, large disks, small crowded disks, presence of myelinated axons, nevus, tumor, peripapillary atrophy, optic disk edema, more than 6 diopters of myopia or hyperopia
Vascular	AION and PION, NA-AION and NA-PION, PAMM, GCA, CRAO, CRBO, AVM, cotton wool spots, CVA affecting the optic pathways
Immune	Paraneoplastic, MAR, NMO, CAR, SLE, uveitis, birdshot retinochoroiditis
Infectious	Viral, bacterial, fungus, HIV, Lyme, secondary syphilis
Hereditary	Leber’s, DOA, albinism, cone dystrophy, retinitis pigmentosa
Iatrogenic	Retina surgery, photocoagulation, solar retinopathy, central serous chorioretinopathy, Purtscher’s retinopathy, optic nerve sheath fenestration, brain surgery affecting the optic pathways
Metabolic/toxic	Diabetes; vit. A deficit; alcohol-, tobacco-, and malnutrition-induced amblyopia; amiodarone, chloroquine, vigabatrin
Other	Glaucoma, macular degeneration, acute posterior multifocal placoid pigment epitheliopathy, acute macular neuroretinopathy

Table reproduced and modified with permission from Tewarie et al. [6].

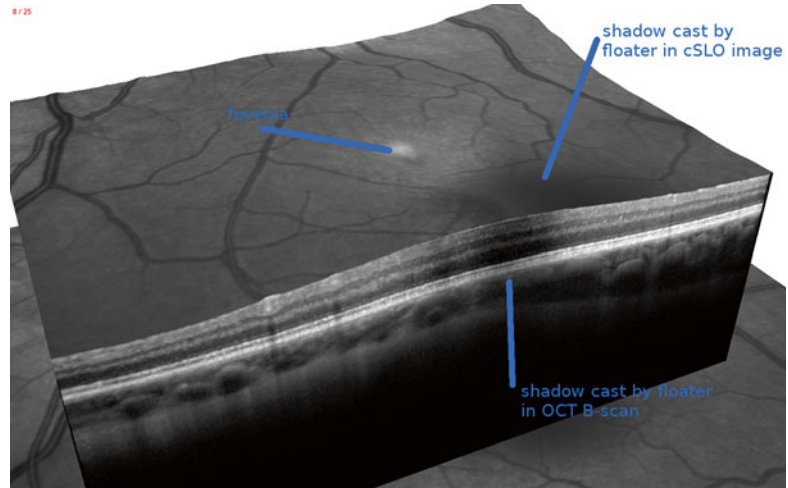
B Criterion

Finally, there is one artifact that is not readily recognized: the influence of the light pathway. The easiest way to avoid this error is to always keep the OCT B-scan in the live image horizontally aligned.

To understand the B criterion, it is best to try it out by performing an OCT scan to oneself or watching the online provided as supplementary data from reference [14].

If the measurement beam is horizontally or vertically displaced, the OCT B-scan appears to be wavy (Fig. 3.21) [14]. Localised measurement

Fig. 3.20 An unequally illuminated OCT volume scan due to a floater. The floater can be seen casting a shadow in the cSLO image and in the OCT B-scan. This scan should be QC accepted



artifacts due to poor beam placement are in the range of 9–40 μm for the peripapillary RNFL. Likewise data from the macular are affected by off-center beam placement [22]. Therefore recognition of this error is relevant in a clinical setting to avoid data misinterpretation, which might influence patient management. Likewise clinical trials and cohort studies will need to carefully QC check their longitudinal data for the B criterion.

A simple sign that can alert to change of measurement beam placement between two examinations is the signal intensity of the OPL/ONL. This is shown in Fig. 3.22 [14].

Concluding Remarks on OSCAR-IB

The mnemonic was chosen to help the OCT operator in preparing scan acquisition. Make sure to follow the right protocol with appropriate B-scan averaging and have a well-focused image (O).

While scanning, ensure that the ring and volume scans are well centered over the area of interest (C). Take care that the image is sufficiently bright and equally illuminated (I). Have the OCT scan horizontally aligned in the live window (B).

After the scan is completed and the patient is still present, check for presence of algorithm failures (A) and relevant retinal pathology (R). In some cases immediate re-imaging will be helpful. In a clinical setting, this may be relevant for following up on retinal pathology. In a clinical trial

setting, this will prevent the undesirable situation to have to call a patient back, because a reading center does not accept OCT scans that fail QC (see chapter 13).

On a practical level, these straightforward, transparent, and validated QC criteria [6, 7] are best implemented by training and auditing team and service.

Train Your Team

It might not be possible or desirable to scan all patients yourself in a busy neurological outpatient clinic. Most teams have trained OCT operators who can have a wide educational background, frequently with some knowledge of retinal photography.

Training involves letting people make mistakes. Once an OCT operator understands how to reproducibly make a certain mistake, for example, with the B criterion, such a mistake will more readily be recognized in a real-life setting.

Next to obtaining good-quality OCT scans, it is necessary to have a complete set of scans. If a protocol contains only a ring scan and a macular volume scan, recognition of other pathologies should trigger further, more appropriate scans.

To give one example, optic disk drusen may give rise to pseudopapilledema (Fig. 3.23a). An apt operator who then performs an optic nerve head volume scan (Fig. 3.23b) and autofluorescence

Fig. 3.21 Off-center placement of the OCT measurement beam results in tilted images. Here we show the OCT live image obtained by the optic nerve head ring scan. (a) The reference scan with the measurement beam (yellow dot) being placed centrally in the pupil (black circle). This results in a correct, horizontal OCT live image. Note: the live image will not be visible to the reading center (note that the live image was taken as a screenshot during the imaging and appears in print in lower quality than in reality. Please see Video 3.1 in the supplementary material for a live coverage image acquisition). (b) Temporal off-center placement of the measurement beam results in a centrally convex live image. (c) Nasal off-center placement results in a centrally concave OCT live image. (d) Rostral off-center placement results in a rising wave, which is mirrored by (e) caudal off-center placement (a falling wave). Please note that for didactic purposes the off-center placement of the measurement beam is shown for an idealized situation with a central fixation target for a perfectly aligned right subject's eye from the OCT operator's point of view (Image reproduced with permission from Balk et al. [14])

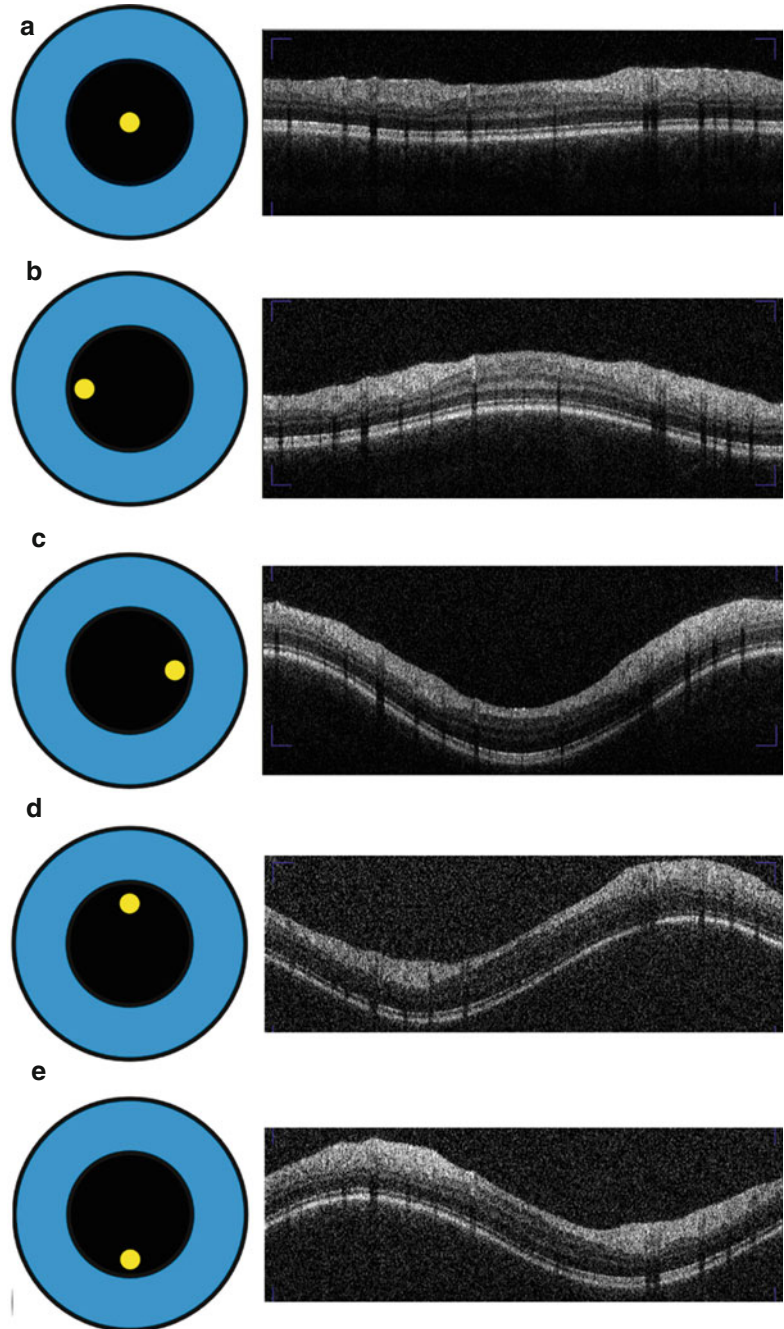
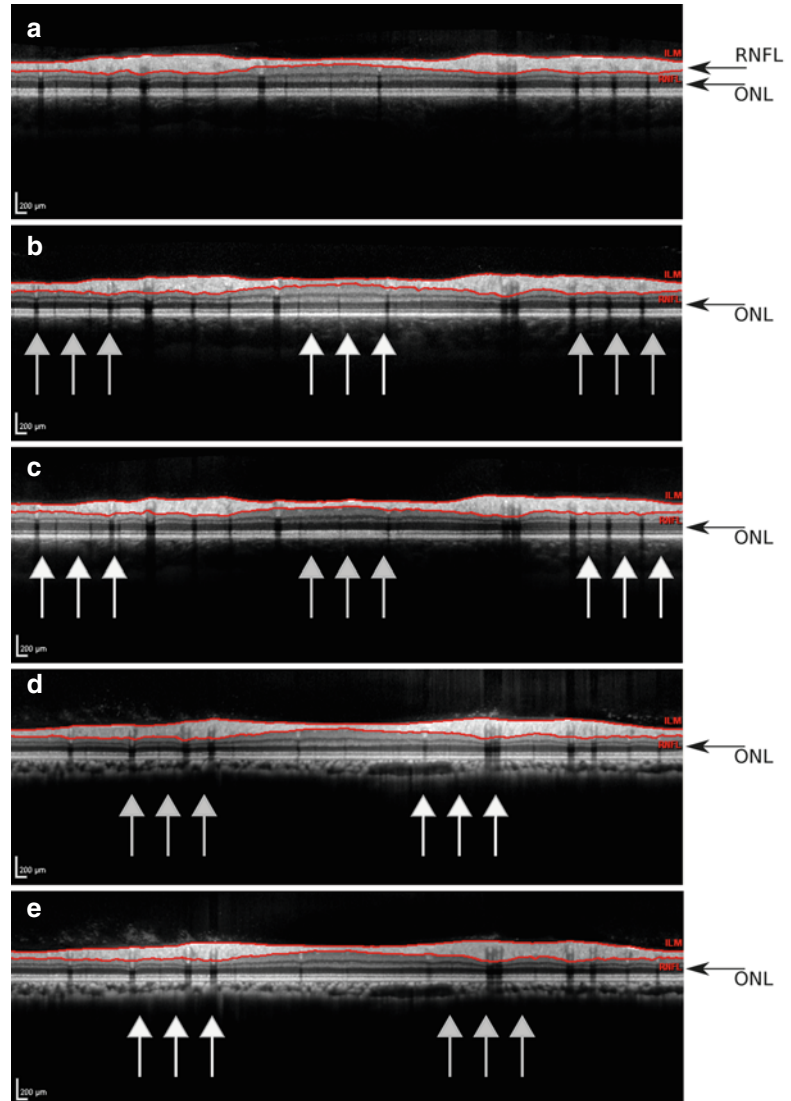


(Fig. 3.8) will add valuable information to clinical decision-making.

Little can be more annoying than to realize that a patient will need to be called back because an incomplete series of scans was acquired. In a clinical trial setting, this will inevitably lead to

rejection from an OCT reading center (see chapter 13). In clinical practice, there might be a failure to recognize relevant pathology. In practice, a simple checklist helps to make sure that all relevant scans are done. An example for such a checklist is given in Fig. 3.24.

Fig. 3.22 Inhomogeneous reflectivity of the outer part of the ONL indicates off-center placement of the OCT measurement beam. (a) The averaged summary scan obtained from the correctly, horizontally orientated live images of the reference scan. This image shows a homogeneous reflectivity of the outer ONL (black arrow). The automated segmentation identifies the borders of the RNFL (red/gray lines). Note: this is the image that is sent to the reading center and used for automated calculation of the RNFL thickness. (b) Temporal off-center placement results in an inhomogeneous outer ONL reflectivity. The ONL reflectivity is increased for the centrally elevated part in the live image (white arrows) and decreased in the periphery (gray arrows). (c) Nasal off-center placement. (d) Rostral off-center placement. (e) Caudal off-center placement (Image reproduced with permission from Balk et al. [14])



Audit Your Service

There are good reasons to regularly check if a clinical service provided delivers what it is supposed to deliver. As with all other paraclinical tests, the OCT is an extension of the clinical judgment. Clinicians generally have an idea what they want to see on the OCT image, even if they are not familiar with all the details of the different OCT machines. Independent to what OCT device is used, the images need to be of an acceptable quality. Longitudinal monitoring of patients will require appropriate use of follow-up functions. Do

the OCT images obtained have an influence on clinical decision-making? This can be reassurance about a suspected pathology but also redirect the diagnostic workup to a different pathology. Were all OCT requests made necessary? These parts of the general workflow can be assessed in an audit.

A first-level audit frequently will have to deal with quality control issues and training of personnel. At different institutions, the initial quality control failure rate may be unexpectedly high. This does not need to come as a surprise because many departments will have made use of OCT as an instrument to discover rather substantial levels

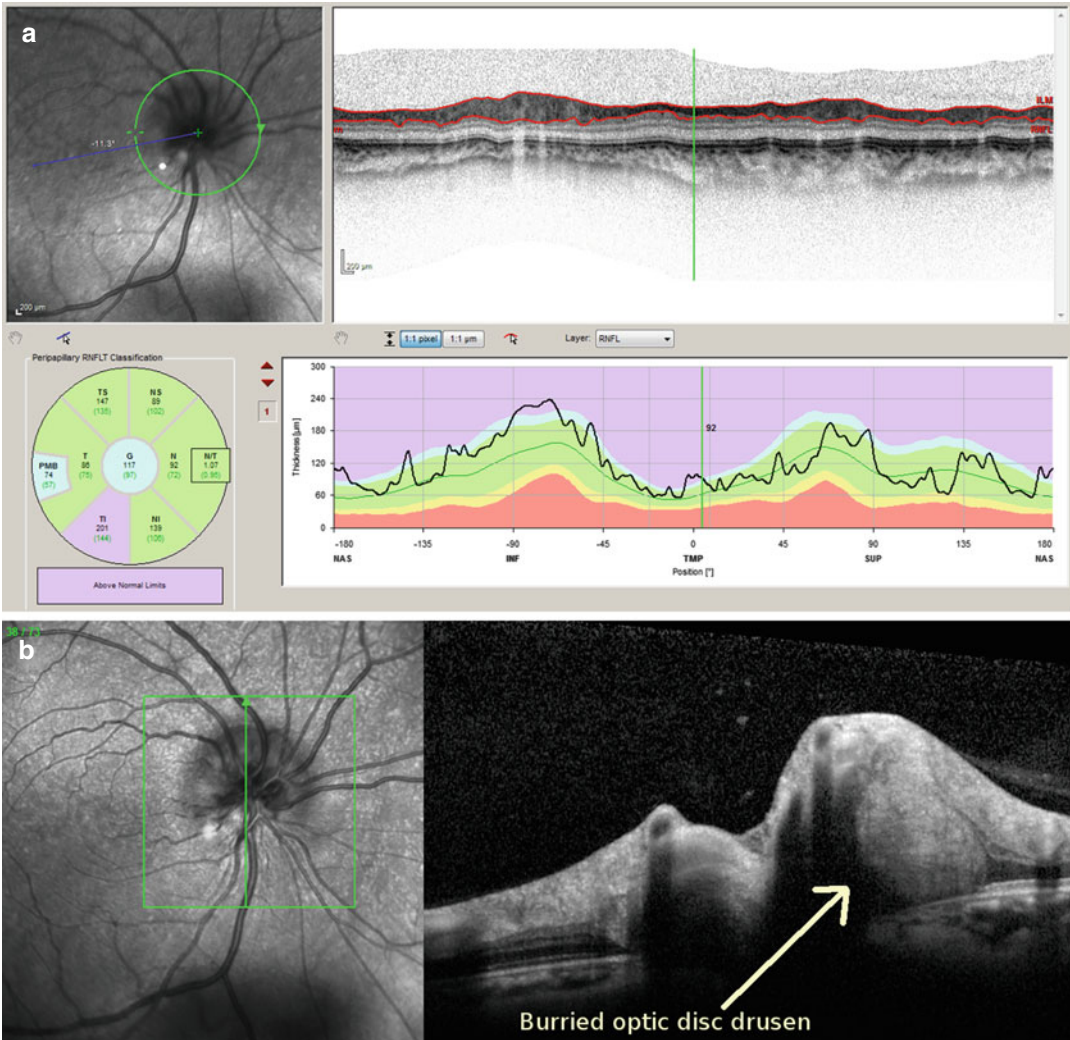


Fig. 3.23 Artfactual RNFL thickening in presence of optic disk drusen. (a) ONH ring scan and (b) ONH volume scan. Drusen are indicated by the *arrow*

of pathology. The need for highly accurate OCT imaging as relevant for assessment of neurodegeneration would not necessarily have been part of OCT operator training. The outcome of a first-level audit is likely to result in a team discussion and additional training.

Permit for sufficient time for improvements to consolidate. Next, implement an audit circle.

A reaudit will show if these measures have contributed to improving the overall quality of scans. People will have gained more experience and new ideas that may materialize in on-site

protocols or standard operating procedures (SOPs). The outcome of a second-level audit may then be how to smooth the workflow, to optimize access to OCT scan results including use of remote viewing stations and to streamline OCT reporting.

Another reaudit at this stage should enable to assess the impact the OCT scans have on clinical decision-making and patient management. This will be important, because of the rapid development of technology, to help with the careful use of resources and potentially to contribute to developing and refining the clinical questions asked.

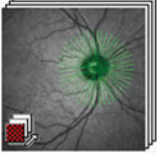
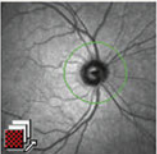

Patient scan checklist (tick boxes for scans completed)		
OCT	Baseline (marked as reference scan)	
Scan	OD	OS
		
		
		

Fig. 3.24 Patient scan checklist

Conclusion

Retinal OCT has developed from a research tool [1, 2] to a validated tool recommended for clinical use [3, 13]. But good clinical practice will require adherence to QC [23, 6, 7, 20]. This chapter provided an overview of lessons learned from hands-on teaching of retinal OCT to a broad audience at a number of centers, both neurological and ophthalmological, and international teaching courses.

References

1. Frohman E, Costello F, Zivadinov R, et al. Optical coherence tomography in multiple sclerosis. *Lancet Neurol.* 2006;5:853–63.
2. Petzold A, de Boer JF, Schippling S, et al. Optical coherence tomography in multiple sclerosis: a systematic review and meta-analysis. *Lancet Neurol.* 2010;9:921–32.
3. Saidha S, Calabresi PA. Optical coherence tomography should be part of the routine monitoring of patients with multiple sclerosis: yes. *Mult Scler.* 2014;20:1296–8.
4. Costello FE. Optical coherence tomography technologies: which machine do you want to own??. *J Neuroophthalmol.* 2014;34(Suppl):S3–9.
5. Petzold A. Optical coherence tomography to assess neurodegeneration in multiple sclerosis. *Methods Mol Biol.* 2014;153 ff. doi:10.1007/7651_2014_153
6. Tewarie P, Balk L, Costello F, Green A, Martin R, et al. The OSCAR-IB consensus criteria for retinal OCT quality assessment. *PLoS One.* 2012;7, e34823.
7. Schippling S, Balk L, Costello F, et al. Quality control for retinal OCT in multiple sclerosis: validation of the OSCAR-IB criteria. *Mult Scler.* 2014;21(2): 163–70.
8. Uthoff W. Untersuchungen über den Einfluss des chronischen Alkoholismus auf das menschliche Sehorgan. *Archiv für Ophthalmologie.* 1886;32:95–188.
9. Ogden TE. Nerve fiber layer of the primate retina: morphometric analysis. *Invest Ophthalmol Vis Sci.* 1984;25:19–29.
10. Plant GT, Perry VH. The anatomical basis of the caecocentral scotoma. New observations and a review. *Brain.* 1990;113(Pt 5):1441–57.

11. Petzold A. CSF biomarkers for improved prognostic accuracy in acute CNS disease. *Neurol Res.* 2007; 29:691–708.
12. Kupersmith MJ, Anderson S, Durbin MK, Kardon RH. Scanning laser polarimetry, but not optical coherence tomography predicts permanent visual field loss in acute non-arteritic anterior ischemic optic neuropathy. *Invest Ophthalmol Vis Sci.* 2013;54:5514–9.
13. Petzold A, Wattjes MP, Costello F, et al. The investigation of acute optic neuritis: a review and proposed protocol. *Nat Rev Neurol.* 2014;10:447–58.
14. Balk LJ, de Vries-Knoppert WAEJ, Petzold A. A simple sign for recognizing off-axis OCT measurement beam placement in the context of multicentre studies. *PLoS One.* 2012;7(11), e48222.
15. Domalpally A, Danis RP, Zhang B, et al. Quality issues in interpretation of optical coherence tomograms in macular diseases. *Retina.* 2009;29: 775–81.
16. Talman LS, Bisker ER, Sackel DJ, et al. Longitudinal study of vision and retinal nerve fiber layer thickness in multiple sclerosis. *Ann Neurol.* 2010;67:749–60.
17. Balk L, et al. Retinal ganglion cell injury in MS occurs most rapidly early in the course of disease. *Multiple Sclerosis J.* 2014;20(S1):PS8.3.
18. Gabriele ML, Ishikawa H, Wollstein G, et al. Optical coherence tomography scan circle location and mean retinal nerve fiber layer measurement variability. *Invest Ophthalmol Vis Sci.* 2008;49:2315–21.
19. Balasubramanian M, Bowd C, Vizzeri G, et al. Effect of image quality on tissue thickness measurements obtained with spectral domain-optical coherence tomography. *Opt Express.* 2009;17:4019–36.
20. Petzold A, Balcer L, Calabresi P, et al. OCT in a multi-centre setting: quality control issues. In: Calabresi P, Balcer L, Frohman E, editors. *Optical coherence tomography in neurological disease.* New York: Cambridge University Press; 2015. p. 103–13.
21. Evangelou N, Konz D, Esiri MM, et al. Size-selective neuronal changes in the anterior optic pathways suggest a differential susceptibility to injury in multiple sclerosis. *Brain.* 2001;124:1813–20.
22. Hariri A, Lee SY, Ruiz-Garcia H, et al. Effect of angle of incidence on macular thickness and volume measurements obtained by spectral-domain optical coherence tomography. *Invest Ophthalmol Vis Sci.* 2012;53:5287–91.
23. Hutchinson M. Optical coherence tomography should be part of the routine monitoring of patients with multiple sclerosis: commentary. *Mult Scler.* 2014;20:1302–3.

Kannan Narayana, Rachel C. Nolan,
Steven L. Galetta, and Laura J. Balcer

Background

The Optic Neuritis Treatment Trial (ONTT) [1–5] is a landmark study in the field of neuro-ophthalmology that systematically described the clinical course of typical inflammatory optic neuritis (ON) and the subsequent risk of multiple sclerosis (MS). ON may be the presenting feature (i.e., the first clinical demyelinating event) in up to 20 % of patients with multiple sclerosis [6]. The presence of magnetic resonance imaging (MRI)-detected lesions and cerebrospinal fluid (CSF) oligoclonal bands (OCB) was found to predict later development of MS, as defined at the time of the trial as a second clinical demyelinating event [7, 8]. As such, the

risk of development of clinically definite MS (CDMS) after an episode of isolated unilateral ON was 22 % at 10 years with normal brain MRI, as opposed to 56 % of those with one or more brain MRI lesions at baseline in the ONTT [8]. Visual acuity loss in ON is mostly mild to moderate, progressing over days. Visual recovery usually starts within a month [5]. Remarkably, 86 % of affected eyes in the ONTT had visual acuity of 20/25 or better at the 10-year follow-up [9], suggesting an excellent visual prognosis. However, several observations in the ONTT merit attention: two thirds of fellow eyes [4] showed an abnormality on one or more tests of visual function at enrollment (color vision, contrast sensitivity, and visual field testing). Furthermore, 11 % of patients with 20/20 vision in the affected eye at baseline had deficits in vision-specific quality of life (QOL) even at 5–8 years following the acute event. Thus, visual acuity testing alone may be an inadequate clinical measure of visual dysfunction in MS-associated optic neuritis (MSON) or in MS even without an ON history.

Visual symptoms in MS may result from a variety of pathological processes, including inflammation, demyelination, and axonal degeneration in the afferent visual pathways [10, 11]. Subclinical optic neuropathy and involvement of the optic chiasm or post-chiasmatal regions of the optic tract also have been documented [12–14].

Electronic supplementary material The online version of this chapter (doi:[10.1007/978-3-319-20970-8_4](https://doi.org/10.1007/978-3-319-20970-8_4)) contains supplementary material, which is available to authorized users.

K. Narayana, MBBS, MD (✉) • R.C. Nolan, BA
S.L. Galetta, MD
Department of Neurology, New York University
Langone Medical Center, New York, NY, USA
e-mail: knarayana@gmail.com

L.J. Balcer, MD, MSCE
Department of Neurology, New York University
Langone Medical Center, New York, NY, USA

Department of Ophthalmology, New York University
Langone Medical Center, New York, NY, USA

Department Population Health, New York University
Langone Medical Center, New York, NY, USA

Diagnosis of optic neuropathy in MS is made on clinical grounds in most instances, and, when in doubt, visually evoked potentials and visual fields may be helpful. Fluorescein angiography (FA) is not routinely performed in MS subjects. Microcystic macular edema (MME) is a relatively new finding seen in multiple conditions that cause retinal or optic nerve injury, including MS subjects. In contrast to a fluorescein leakage seen with the retinal condition of cystoid macular edema, microcystic macular edema may not always be seen on FA. Over the last 15 years, progress has been made in the qualitative and quantitative assessment of visual function in MS. Studies have found that measures of low-contrast vision, particularly low-contrast letter acuity, demonstrate the greatest

capacity to capture visual impairment [15–18]. Vision-specific QOL, as measured by the 25-item National Eye Institute Visual Functioning Questionnaire (NEI-VFQ-25) and the more recently studied 10-item Neuro-Ophthalmic Supplement to the NEI-VFQ-25, has correlated with low-contrast acuity and with the structural changes seen in OCT (Table 4.1) [19–22].

Optical Coherence Tomography (OCT) in MS

Optical coherence tomography (OCT) is a noninvasive technique that allows for tissue-level in vitro imaging of the optic nerve head and retina.

Table 4.1 Mean reference values from recent investigations of vision, quality of life, and OCT in MS*

	Disease-free controls	All MS	MS, no history of MSON	MS, history of MSON
High-contrast visual acuity (VA), ETDRS, number of letters correct	59 ± 6 (n = 52 eyes)	53 ± 10 (n = 559 eyes)	55 ± 7 (n = 301 eyes)	52 ± 12 (n = 252 eyes)
Binocular testing	62 ± 4 (n = 26 pts)	58 ± 7 (n = 273 pts)	59 ± 6 (n = 147 pts)	57 ± 8 (n = 123 pts)
Low-contrast letter acuity (2.5 %), number of letters correct	35 ± 6 (n = 52 eyes)	25 ± 12 (n = 550 eyes)	27 ± 11 (n = 296 eyes)	23 ± 13 (n = 248 eyes)
Binocular testing	44 ± 4 (n = 26 pts)	34 ± 11 (n = 273 pts)	36 ± 9 (n = 147 pts)	32 ± 11 (n = 123 pts)
Low-contrast letter acuity (1.25 %), number of letters correct	21 ± 9 (n = 52 eyes)	13 ± 11 (n = 550 eyes)	15 ± 11 (n = 296 eyes)	11 ± 11 (n = 248 eyes)
Binocular testing	32 ± 5 (n = 26 pts)	23 ± 11 (n = 271 pts)	25 ± 11 (n = 146 pts)	21 ± 12 (n = 122 pts)
NEI-VFQ-25 composite score, best score = 100	98 ± 2 (n = 27 pts)	85 ± 15 (n = 264 pts)	88 ± 14 (n = 142 pts)	82 ± 15 (n = 119 pts)
10-item neuro-ophthalmic supplement to the NEI-VFQ-25, best score = 100	97 ± 5 (n = 28 pts)	78 ± 18 (n = 256 pts)	83 ± 16 (n = 137 pts)	73 ± 18 (n = 117 pts)
Time-domain (TD) OCT				
Peripapillary RNFL thickness, μm	104.5 ± 10.7 (n = 219 eyes)	92.5 ± 16.7 (n = 1,058 eyes)	95.6 ± 14.5 (n = 730 eyes)	85.7 ± 19.0 (n = 328 eyes)
Total macular volume, mm ³	6.84 ± 0.36 (n = 219 eyes)	6.54 ± 0.51 (n = 1,058 eyes)	6.63 ± 0.48 (n = 730 eyes)	6.36 ± 0.53 (n = 328 eyes)
Spectral-domain (SD) OCT				
Peripapillary RNFL thickness, μm	93.0 ± 9.0 (n = 48 eyes)	83.1 ± 12.9 (n = 529 eyes)	86.4 ± 10.9 (n = 287 eyes)	79.1 ± 14.1 (n = 236 eyes)
Ganglion cell + inner plexiform layer (GCL + IPL), μm	88.9 ± 6.9 (n = 61 eyes)	84.1 ± 8.4 (n = 239 eyes)	87.0 ± 6.6 (n = 150 eyes)	79.7 ± 9.2 (n = 87 eyes)
Macular volume cube, mm ³	10.1 ± 0.4 (n = 50 eyes)	9.8 ± 0.6 (n = 509 eyes)	9.9 ± 0.5 (n = 282 eyes)	9.7 ± 0.6 (n = 221 eyes)

*Data above from a collaboration between NYU, Johns Hopkins, and UT Southwestern Dallas

Abbreviations: MS multiple sclerosis, ETDRS early treatment diabetic retinopathy study, NEI-VFQ-25 25-Item National Eye Institute Visual Functioning Questionnaire, TD time-domain (OCT-3 platform), SD spectral-domain (Cirrus platform), OCT optical coherence tomography, RNFL retinal nerve fiber layer

OCT provides a unique opportunity to image the unmyelinated axons arising from the retinal ganglion cells (axons not myelinated anterior to the lamina cribrosa). By measuring the thickness of the peripapillary RNFL (commonly referred to for simplicity as the RNFL), OCT provides the ability to quantitate the amount of axonal loss associated with optic nerve injury and is a means to monitor the neurodegenerative process. In addition, OCT can be used to measure total macular volume (TMV), which may provide an estimate of neuronal integrity (ganglion cell integrity) at the retinal level. The development of computerized OCT image segmentation techniques has added to the ability to image distinct neuronal populations including the ganglion cell layer (GCL).

OCT in Patients with History of MSON

Autopsy studies have shown that up to 94–99 % of patients with MS have detectable optic nerve lesions [23, 24]. The earliest application of OCT technology to the study of MSON was reported by Parisi et al. in 1999 [25]. In that study, which utilized first-generation OCT, RNFL thickness was reduced by an average of 46 % in the eyes with history of MSON as compared to control subjects and by an average of 28 % in comparison to fellow eyes of patients with a history of MSON. Even in the clinically unaffected eyes of patients with MS, there was a 26 % reduction in RNFL thickness when compared to disease-free control eyes (whose average RNFL thickness is approximately 100–110 microns). In 2005, Trip et al. [26] reported similar findings, with 33 % reductions in RNFL thickness in the eyes of the patients with a history of MSON compared with eyes of matched controls and a 27 % reduction when the MSON-affected and unaffected eyes of the same patients with MS were compared. They also showed total macular volume loss by 11 % in the eyes of patients with a history of MSON when compared to control eyes ($p < 0.001$) and by 9 % in the MSON-affected versus the unaffected eyes of the same patients ($p < 0.001$). Thus, OCT was able to show both RNFL thinning and macu-

lar retinal volume loss, suggesting the occurrence of both axonal and neuronal cell loss in the eyes of patients with MS with and without acute MSON (see Case Studies 1 and 2).

In 2010, Petzold et al. [27] performed a meta-analysis of OCT studies in the MS and MSON literature with available data ($n = 63$ studies). The authors found an average RNFL thinning of 20.38 μm (95 % CI 17.91–22.86, $n = 2,063$, $p < 0.0001$) in eyes with MSON, while thinning was 7.08 μm on average (5.52–8.65, $n = 3,154$, $p < 0.0001$) in MS eyes without MSON. The estimated degree of RNFL thinning in patients with MS was greater than the extent expected by normal aging. Normal RNFL thickness may be in the range of 110–120 μm by the age of 15 years, with an estimated physiological loss of only about 0.017 % per year in retinal thickness (approximately 10–20 μm loss over 60 years) [28]. RNFL thickness in the Petzold et al. meta-analysis [27] also was found to correlate with visual and neurological functioning.

OCT in Acute MSON and Retrobulbar Neuritis

In 2006, Costello et al. [29] reported that the majority of patients with acute MSON (approximately 75 %) will sustain 10–40 μm of RNFL loss within a period of approximately 3–6 months (see Case Study 3). Importantly, RNFL thinning down to a level of 75–80 μm was found to be a “threshold level” below which there was a corresponding decline in visual function, as measured by automated perimetry [29], and below which visual dysfunction persisted.

In the acute setting of ON, Pro et al. [30] demonstrated mild OCT RNFL thickening in 8 subjects who were thought clinically to have retrobulbar ON (i.e., no obvious optic disk swelling on ophthalmoscopy). In most of these cases, increased RNFL thickness was subtle and not beyond the range of normal (100.7 μm in ON-affected eyes, versus 92.9 μm in unaffected fellow eyes). The unaffected eyes in this study remained stable, while thinning was demonstrated in the affected eyes with ON. This thinning was seen as early as 2–4 months after

the onset of the visual loss. The findings of this study, as well as clinical experience, suggest that mild optic disk swelling is present even in cases of suspected retrobulbar ON based on ophthalmoscopic examination.

OCT Changes in the Subacute Phase and During Recovery from MSON

The time course of RNFL axonal loss following an episode of acute MSON may be important for determining the “window of opportunity” for potential intervention with neuroprotective or repair therapies. From the available data, it appears that most of the RNFL thinning occurs in MSON within the first 1–3 months. This observation suggests that significant and rapid axonal degeneration follows primary demyelination of the optic nerve [27, 29]. Stabilization of RNFL thickness is evident by 6 months following onset of MSON [29, 31].

Henderson et al. [31], in a study of 23 patients with acute clinically isolated unilateral MSON, performed comprehensive visual assessments. The mean time to 90 % loss of RNFL thickness from baseline values for MSON-affected eyes was 2.38 months. Ninety-nine percent of the RNFL thickness loss occurred by a mean of 4.75 months. The time of first OCT-detectable RNFL atrophy compared to the baseline fellow eye value was 1.64 months (95 % CI, 0.96–2.32; listed $p < 0.05$). Eyes with poor recovery had a significantly greater decline of RNFL thickness from baseline to 3 months ($p = 0.002$). Macular volumes also declined significantly to the time of last follow-up.

OCT in Different Types of MS

Costello et al. [32] demonstrated that the pattern of OCT RNFL thinning may be able to distinguish MS disease subtypes. They found that RNFL comparisons involving MS eyes with a history of ON (MSON eyes) yielded greater differences between MS subtypes than did comparisons of unaffected eyes. For MSON eyes in this study, patients with clinically isolated syndrome (CIS)

had the highest overall RNFL thickness values (mean 87.8 μm), while patients with secondary progressive MS (SPMS) had the greatest degree of thinning compared to control reference values (mean RNFL thickness 70.8 μm). For MS non-MSON eyes, RNFL thickness was reduced in patients with primary progressive MS (PPMS, average 94.3 μm $p = 0.04$), relapsing remitting MS (RRMS, average 99.6 μm , $p = 0.02$), and SPMS (average 84.7 μm , $p < 0.0001$) relative to eyes of patients with CIS (average RNFL thickness 105.7 μm). RNFL thickness may thus represent an important structural marker of disease progression.

Galetta et al. [33] have shown that even patients with “benign MS” may have RNFL axonal loss that is similar to that of typical MS. In these studies, definitions of “benign MS” were an EDSS score of ≤ 3 and a ≥ 15 -year disease duration. Importantly, those with benign MS had associated reductions of vision-specific QOL as well as impairments of low-contrast letter acuity. While overall neurologic impairment in benign MS may be mild, visual dysfunction may actually account for a substantial degree of disability.

RNFL Thickness in the Asymptomatic Fellow Eye

Thinning of RNFL has been observed not only in the eyes with a history of MSON but also in the asymptomatic fellow eyes of MS patients [34–39]. Average RNFL thickness values for fellow eyes in MSON have ranged from 91.1 to 109.3 μm . In MS patients with no history of acute MSON, the average RNFL thickness was between 93.9 and 110.9 μm . These findings suggest that MS can cause subclinical visual pathway disease with associated axonal loss (see Case Study 3).

RNFL Thinning and Visual Loss

One of the most important findings that have resulted from the use of OCT in MS is the correlation between RNFL thinning and visual loss,

as measured by low-contrast letter acuity [22]. In 2006, Fisher et al. [34] published a cross-sectional study that compared RNFL thickness among MS eyes with a history of ON (MSON eyes), MS eyes without a history of ON (MS non-MSON eyes), and eyes of disease-free controls. They found that RNFL thickness was reduced significantly among MS patients (92 μm) versus controls (105 μm , $p < 0.001$, generalized estimating equation models, accounting for age) and particularly reduced in MSON eyes (85 μm , $p < 0.001$). Furthermore, lower visual function scores were associated with reduced average overall RNFL thickness in MS eyes; for every one line decrease in low-contrast letter acuity or contrast sensitivity score, the mean RNFL thickness decreased by 4 μm . These findings supported the validity of low-contrast visual assessment and suggested a potential role for OCT in MS trials that examine neuroprotective and other disease-modifying therapies [40]. Several other investigations have demonstrated correlations between RNFL thinning and visual loss [26, 41–43]. For example, Costello et al. [44] found that RNFL thickness after an episode of isolated ON cannot be used to predict the risk of MS.

Relation of RNFL Thickness and MRI Findings

Conventional MRI techniques may not specifically reflect axonal damage in the anterior visual pathway, and also may not demonstrate findings of subclinical optical neuropathy or neurodegenerative effects on the retina. The process of RNFL thinning correlates with the atrophy (thinning in caliber) of the optic nerve, which may be visualized on conventional MRI. Studies have shown a significant correlation of RNFL thickness with the conventional and normalized volumes of brain white and gray matter [39, 45]. The correlation between RNFL thickness and MRI measurements of brain atrophy was more significant in the subset of patients with no history of MSON than in those patients with history of MSON [45].

Overall, RNFL thickness measurements are a likely correlate of brain atrophy in MS [34]; ongoing studies are examining the role for ganglion cell layer thickness as a neuronal structural marker that relates to overall and gray matter atrophy by brain MRI.

Longitudinal Data

In a longitudinal study with a mean follow-up of 18 months, Talman et al. [46] found that degree of RNFL thinning was significantly related to length of follow-up; this was consistent with a progressive RNFL thinning over time in some patients with MS. For this cohort of patients examined between 0.5 and 4.5 years, an average of 2 microns of RNFL thickness was lost per year of follow-up ($p < 0.001$). This relation was similar for MSON eyes (1.4 μm , $p = 0.005$) and MS non-MSON eyes (2.4 μm , $p < 0.001$). Percentage decreases in RNFL thickness from baseline were highest for the temporal quadrant (3.1 %), followed by the nasal quadrant (2.5 %). RNFL thinning was also associated with clinically significant visual loss by low-contrast letter acuity, most correlated with the low-contrast letter acuity at the 2.5 % level. These findings are likely to influence how we manage MS-associated visual loss and serve as a backdrop for understanding the relative contributions of MSON versus axonal loss in the absence of MSON in MS.

Segmentation and Recent Trends

With the rapid advancement in the OCT technology, segmentation of some of the retinal layers is now possible for use in the clinical setting. Walter et al. [47] found that thinning of the ganglion cell layer (GCL) plus inner plexiform layer (IPL, single interneuron layer that is inseparable from the GCL by OCT) was greatest among patients with the highest degrees of visual loss and decrements in vision-specific QOL. This study confirmed an important role for neuronal loss, measured by

GCL+IPL thickness, in determining visual disability in MS. Gabilondo et al. similarly studied retinal changes in optic neuritis utilizing segmentation techniques. The change in the ganglion cell layer and inner plexiform layer (GCIPL) thickness in the first month predicted the visual impairment by 6 months [48].

There is a significant interest as to whether race/ethnicity has a significant role in the visual pathway dysfunction in relation to MS. Kimbrough et al. [49] provided evidence that African-American MS patients have accelerated visual pathway damage and visual disability, as compared to Caucasian subjects: they had faster RNFL thinning and worse LCVA per year of disease progression. Moss et al. [50] performed a secondary analysis of the ONTT and found that black race/ethnicity seems to be associated with worse scores of contrast sensitivity and visual acuity outcomes in affected eyes during a 15-year period following acute optic neuritis.

OCT and Psychophysics

Low-contrast acuity

Low-contrast letter acuity is a visual outcome measure that is being used for clinical trials in MSON and has demonstrated validity and the capacity to show treatment effects in MS trials.

Acute MSON causes functional visual impairment that is best captured by clinical measures of low-contrast letter acuity (perception of gray letters of progressively smaller size on a white background) and contrast sensitivity (perception of gray letters of a single large size on a white background) [16, 51, 52].

Results from the Optic Neuritis Treatment Trial (ONTT) and multiple other cohorts indicate that some degree of persistent visual loss occurs regardless of corticosteroid treatment for acute MSON. Permanent deficits result from irreversible neuronal and axonal degeneration. Identification of agents that protect axons and

neurons and defining the therapeutic window even more precisely are the essential next steps in improving the visual outcome of acute MSON.

Color Vision

Henderson et al. studied patients with acute unilateral optic neuritis and found both color vision and low-contrast letter scores were associated with RNFL thinning and predictive of axonal loss on SD-OCT [53]. Additionally, color vision deficits were correlated with RNFL thinning on SD-OCT in MS patients both with and without optic neuritis in a study by Villoslada et al. [54].

Conclusion

Acute ON in the setting of MS (MSON) is a strong contributor to anterior visual pathway axonal and neuronal loss as measured by OCT RNFL and GCL+IPL thickness. Studies of heterogeneous MS cohorts have also demonstrated evidence for subclinical visual loss in the absence of MSON. Both groups of patients have reductions in vision-specific QOL and visual function, consistent with an unmet need for neuroprotection and repair agents in MS as well as MSON.

Representative Case Studies

Case 1 MS patient with unilateral MSON

A 35-year-old female with a history of MS diagnosed 2 years prior presenting as optic neuritis in the right eye was treated with IV steroids for 7 days, with partial resolution of symptoms. The patient had been on Tysabri® (natalizumab) for 2 years at time of imaging. Exam showed a corrected visual acuity of 20/40 (6/12) in the right eye, 20/16 (6/4.8) in the left eye, a right RAPD, and a pale right disk. OCT revealed RNFL of 57 microns OD (Video 4.1) and 100 microns OS

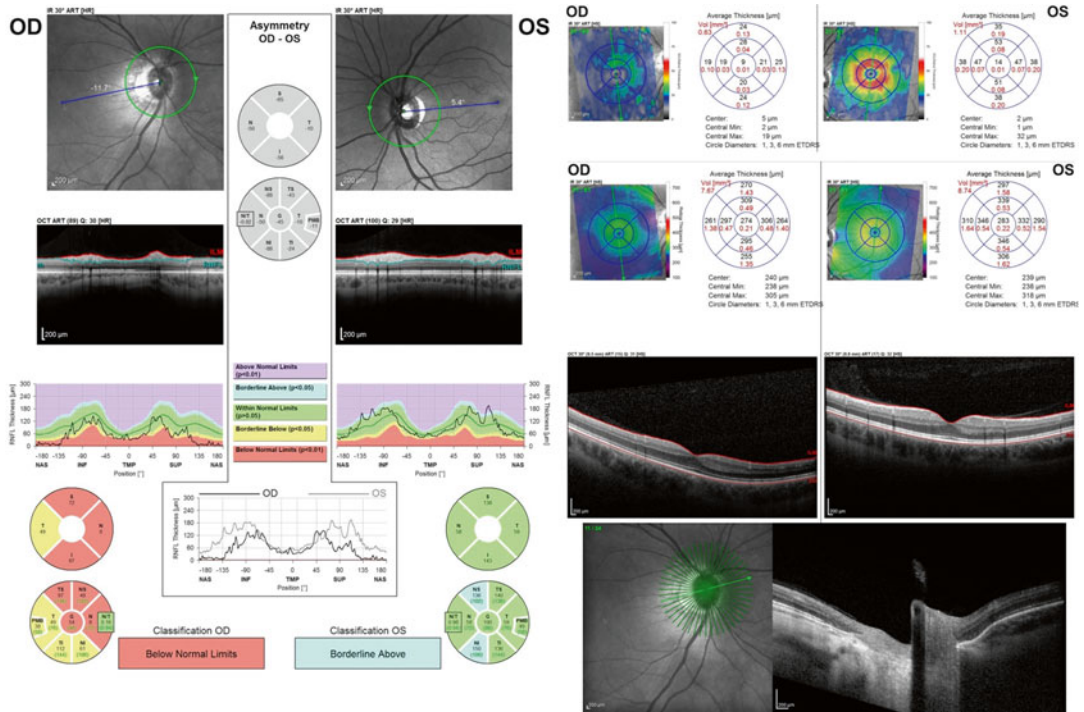


Fig. 4.1 RNFL thickness (*left*), GCL thickness (*top right*), macular volume (*middle right*), myopic scleral crescent (*bottom right*)

(Video 4.2) and macular thinning OD (7.67 mm³ versus 8.74 mm³ in the left eye) and ganglion cell layer loss (0.63 mm³ OD versus 1.11 mm³ OS). Patient is myopic with characteristic myopic crescents and tilted disks (Fig. 4.1).

Case 2 Longitudinal optic neuritis

A 25-year-old female presented with painful monocular vision loss in her right eye. Exam showed red desaturation, central scotoma, and visual acuity of 20/400 (6/120) in that eye. Left eye visual function was within normal limits. Patient was diagnosed with RRMS and optic neuritis and followed with OCT over the next 3 years. Visual acuity improved to 20/15 (6/4.8). Peripapillary RNFL, macular ganglion cell layer, and macular volume thinning were evident in the right eye, with an initial decline stabilizing by 4.5 months, followed by a slower but steady decline over the next 3 years (Fig. 4.2).

Case 3 Subtle optic disk swelling during acute ON discovered by OCT

A 30-year-old female with RRMS and past history of acute MSON in her right eye presented with complaints of eye pain in the right eye only 2 days prior. This was most evident if she moved the eye to an extreme direction or pushed the eye into the orbit. Patient stated that the pain was exactly like that experienced at the start of her first episode of MSON. Fundus photos showed a subtle, mildly hyperemic, and bland blurring of the disk margins (Fig. 4.3). OCT images were less subtle with a concentric thickening of RNFL in the right eye that was not readily evident on ophthalmoscopy. MRI showed a T2 hyperintense and enhancing lesion in the intracanalicular segment of the right optic nerve consistent with acute optic neuritis. Patient was treated for 3 days with IV steroids with visual improvement.

Normalized RNFL Thickness

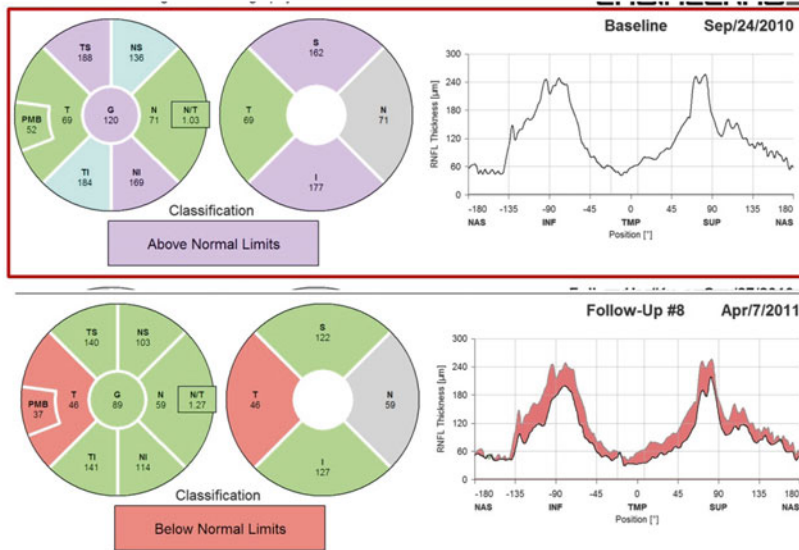
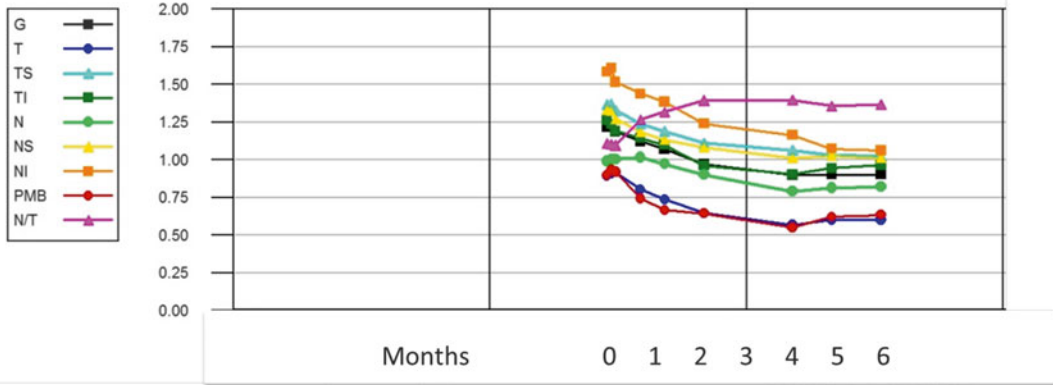


Fig. 4.2 Normalized RNFL thickness loss by quadrants over first 6 months after acute MSON (*top*). Comparison of RNFL thickness map from baseline to imaging 6 months later (*bottom*) (Images courtesy of Sam Arnow and Ari Green, MD at University of California San Francisco).

G global, *T* temporal, *TS* temporal superior, *TI* temporal inferior, *N* nasal, *NS* nasal superior, *NI* nasal inferior, *PMB* papillomacular bundle, *N/T* nasal-to-temporal quadrant ratio, *S* superior, *I* inferior, *N* nasal

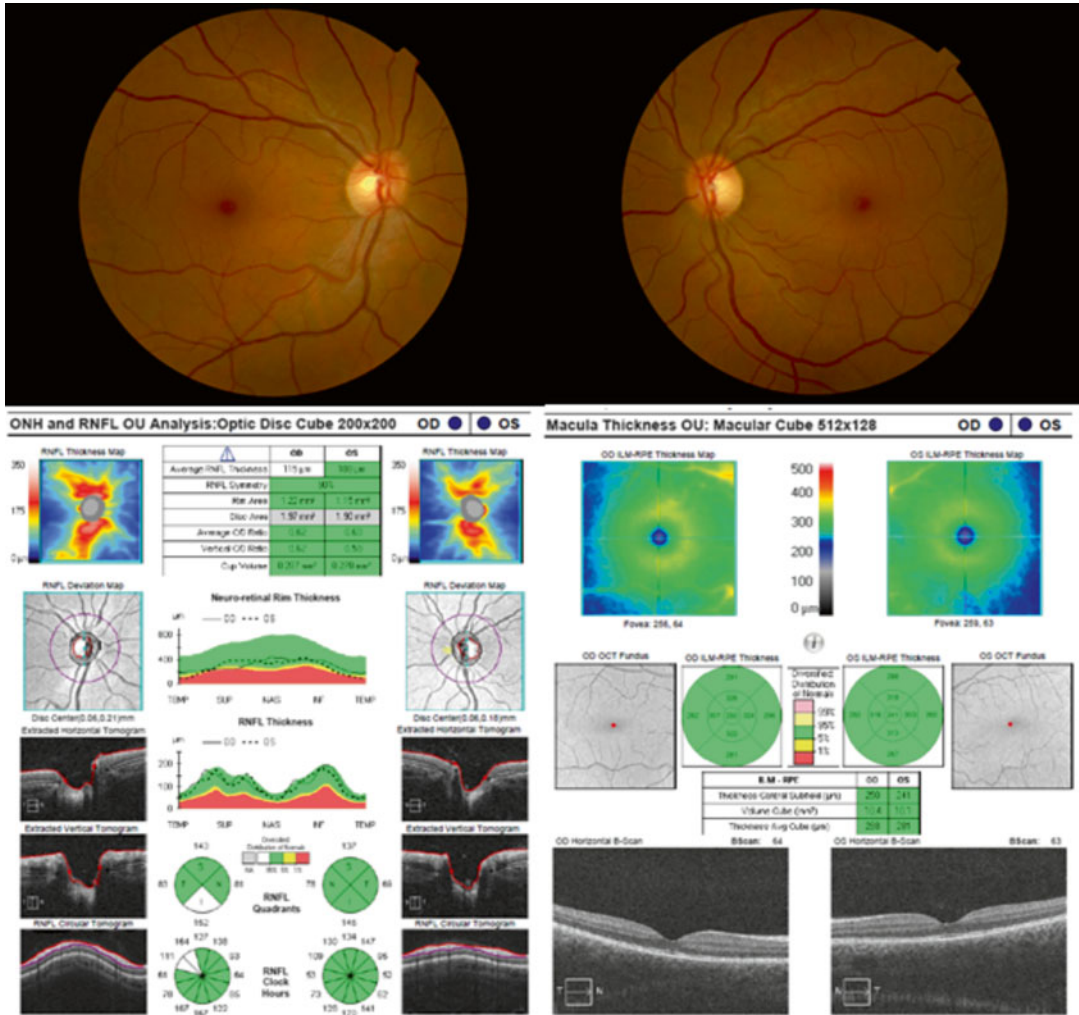


Fig. 4.3 Fundus photos (*top*). Peripapillary RNFL thickness (*bottom left*). Macular volume (*bottom right*)

References

1. Beck RW. The optic neuritis treatment trial. Arch Ophthalmol. 1988;106(8):1051–3.
2. Optic Neuritis Study Group. The clinical profile of optic neuritis. Experience of the Optic Neuritis Treatment Trial. Arch Ophthalmol. 1991;109(12):1673–8.
3. Beck RW, Cleary PA, Anderson Jr MM, Keltner JL, Shults WT, Kaufman DI, et al. A randomized, controlled trial of corticosteroids in the treatment of acute optic neuritis. The Optic Neuritis Study Group. N Engl J Med. 1992;326(9):581–8.
4. Beck RW, Kupersmith MJ, Cleary PA, Katz B. Fellow eye abnormalities in acute unilateral optic neuritis. Experience of the optic neuritis treatment trial. Ophthalmology. 1993;100(5):691–7; discussion 7–8.
5. Cleary PA, Beck RW, Bourque LB, Backlund JC, Miskala PH. Visual symptoms after optic neuritis. Results from the Optic Neuritis Treatment Trial. J Neuroophthalmol: Off J N Am Neuroophthalmol Soc. 1997;17(1):18–23; quiz 4–8.
6. Sorensen TL, Frederiksen JL, Bronnum-Hansen H, Petersen HC. Optic neuritis as onset manifestation of multiple sclerosis: a nationwide, long-term survey. Neurology. 1999;53(3):473–8.
7. Soderstrom M, Ya-Ping J, Hillert J, Link H. Optic neuritis: prognosis for multiple sclerosis from MRI, CSF, and HLA findings. Neurology. 1998;50(3):708–14.
8. Beck RW, Trobe JD, Moke PS, Gal RL, Xing D, Bhatti MT, et al. High- and low-risk profiles for the development of multiple sclerosis within 10 years after optic neuritis: experience of the optic neuritis treatment trial. Arch Ophthalmol. 2003;121(7):944–9.

9. Beck RW, Gal RL, Bhatti MT, Brodsky MC, Buckley EG, Chrousos GA, et al. Visual function more than 10 years after optic neuritis: experience of the optic neuritis treatment trial. *Am J Ophthalmol.* 2004;137(1):77–83.
10. Evangelou N, Konz D, Esiri MM, Smith S, Palace J, Matthews PM. Size-selective neuronal changes in the anterior optic pathways suggest a differential susceptibility to injury in multiple sclerosis. *Brain: J Neurol.* 2001;124(Pt 9):1813–20.
11. DeLuca GC, Williams K, Evangelou N, Ebers GC, Esiri MM. The contribution of demyelination to axonal loss in multiple sclerosis. *Brain: J Neurol.* 2006;129(Pt 6):1507–16.
12. Sisto D, Trojano M, Vetrugno M, Trabucco T, Iliceto G, Sborgia C. Subclinical visual involvement in multiple sclerosis: a study by MRI, VEPs, frequency-doubling perimetry, standard perimetry, and contrast sensitivity. *Invest Ophthalmol Vis Sci.* 2005;46(4):1264–8.
13. Lycke J, Tolleson PO, Frisen L. Asymptomatic visual loss in multiple sclerosis. *J Neurol.* 2001;248(12):1079–86.
14. Engell T, Trojaborg W, Raun NE. Subclinical optic neuropathy in multiple sclerosis. A neuro-ophthalmological investigation by means of visually evoked response, Farnworth-Munsell 100 Hue test and Ishihara test and their diagnostic value. *Acta Ophthalmol.* 1987;65(6):735–40.
15. Trobe JD, Beck RW, Moke PS, Cleary PA. Contrast sensitivity and other vision tests in the optic neuritis treatment trial. *Am J Ophthalmol.* 1996;121(5):547–53.
16. Balcer LJ, Baier ML, Cohen JA, Kooijmans MF, Sandrock AW, Nano-Schiavi ML, et al. Contrast letter acuity as a visual component for the multiple sclerosis functional composite. *Neurology.* 2003;61(10):1367–73.
17. Baier ML, Cutter GR, Rudick RA, Miller D, Cohen JA, Weinstock-Guttman B, et al. Low-contrast letter acuity testing captures visual dysfunction in patients with multiple sclerosis. *Neurology.* 2005;64(6):992–5.
18. Balcer LJ, Baier ML, Pelak VS, Fox RJ, Shuwairi S, Galetta SL, et al. New low-contrast vision charts: reliability and test characteristics in patients with multiple sclerosis. *Mult Scler.* 2000;6(3):163–71.
19. Ma SL, Shea JA, Galetta SL, Jacobs DA, Markowitz CE, Maguire MG, et al. Self-reported visual dysfunction in multiple sclerosis: new data from the VFQ-25 and development of an MS-specific vision questionnaire. *Am J Ophthalmol.* 2002;133(5):686–92.
20. Raphael BA, Galetta KM, Jacobs DA, Markowitz CE, Liu GT, Nano-Schiavi ML, et al. Validation and test characteristics of a 10-item neuro-ophthalmic supplement to the NEI-VFQ-25. *Am J Ophthalmol.* 2006;142(6):1026–35.
21. Mowry EM, Loguidice MJ, Daniels AB, Jacobs DA, Markowitz CE, Galetta SL, et al. Vision related quality of life in multiple sclerosis: correlation with new measures of low and high contrast letter acuity. *J Neurol Neurosurg Psychiatry.* 2009;80(7):767–72.
22. Sakai RE, Feller DJ, Galetta KM, Galetta SL, Balcer LJ. Vision in multiple sclerosis: the story, structure-function correlations, and models for neuroprotection. *J Neuroophthalmol: Off J N Am Neuroophthalmol Soc.* 2011;31(4):362–73.
23. Ikuta F, Zimmerman HM. Distribution of plaques in seventy autopsy cases of multiple sclerosis in the United States. *Neurology.* 1976;26(6 PT 2):26–8.
24. Toussaint D, Perier O, Verstappen A, Bervoets S. Clinicopathological study of the visual pathways, eyes, and cerebral hemispheres in 32 cases of disseminated sclerosis. *J Clin Neuroophthalmol.* 1983;3(3):211–20.
25. Parisi V, Manni G, Spadaro M, Colacino G, Restuccia R, Marchi S, et al. Correlation between morphological and functional retinal impairment in multiple sclerosis patients. *Invest Ophthalmol Vis Sci.* 1999;40(11):2520–7.
26. Trip SA, Schlottmann PG, Jones SJ, Altmann DR, Garway-Heath DF, Thompson AJ, et al. Retinal nerve fiber layer axonal loss and visual dysfunction in optic neuritis. *Ann Neurol.* 2005;58(3):383–91.
27. Petzold A, de Boer JF, Schippling S, Vermersch P, Kardon R, Green A, et al. Optical coherence tomography in multiple sclerosis: a systematic review and meta-analysis. *Lancet Neurol.* 2010;9(9):921–32.
28. Kanamori A, Escano MF, Eno A, Nakamura M, Maeda H, Seya R, et al. Evaluation of the effect of aging on retinal nerve fiber layer thickness measured by optical coherence tomography. *Ophthalmol J Int D'ophtalmol: Int J Ophthalmol Zeitschrift fur Augenheilkunde.* 2003;217(4):273–8.
29. Costello F, Coupland S, Hodge W, Lorello GR, Koroluk J, Pan YI, et al. Quantifying axonal loss after optic neuritis with optical coherence tomography. *Ann Neurol.* 2006;59(6):963–9.
30. Pro MJ, Pons ME, Liebmann JM, Ritch R, Zafar S, Lefton D, et al. Imaging of the optic disc and retinal nerve fiber layer in acute optic neuritis. *J Neurol Sci.* 2006;250(1–2):114–9.
31. Henderson AP, Altmann DR, Trip AS, Kallis C, Jones SJ, Schlottmann PG, et al. A serial study of retinal changes following optic neuritis with sample size estimates for acute neuroprotection trials. *Brain: J Neurol.* 2010;133(9):2592–602.
32. Costello F, Hodge W, Pan YI, Eggenberger E, Freedman MS. Using retinal architecture to help characterize multiple sclerosis patients. *Can J Ophthalmol J Can D'ophtalmol.* 2010;45(5):520–6.
33. Galetta KM, Graves J, Talman LS, Lile DJ, Frohman EM, Calabresi PA, et al. Visual pathway axonal loss in benign multiple sclerosis: a longitudinal study. *J Neuroophthalmol: Off J N Am Neuroophthalmol Soc.* 2012;32(2):116–23.
34. Fisher JB, Jacobs DA, Markowitz CE, Galetta SL, Volpe NJ, Nano-Schiavi ML, et al. Relation of visual

- function to retinal nerve fiber layer thickness in multiple sclerosis. *Ophthalmology*. 2006;113(2):324–32.
35. Henderson AP, Trip SA, Schlottmann PG, Altmann DR, Garway-Heath DF, Plant GT, et al. An investigation of the retinal nerve fibre layer in progressive multiple sclerosis using optical coherence tomography. *Brain: J Neurol*. 2008;131(Pt 1):277–87.
 36. Jeanjean L, Castelnovo G, Carlander B, Villain M, Mura F, Dupeyron G, et al. Retinal atrophy using optical coherence tomography (OCT) in 15 patients with multiple sclerosis and comparison with healthy subjects. *Rev Neurol*. 2008;164(11):927–34.
 37. Pueyo V, Martin J, Fernandez J, Almarcegui C, Ara J, Egea C, et al. Axonal loss in the retinal nerve fiber layer in patients with multiple sclerosis. *Mult Scler*. 2008;14(5):609–14.
 38. Pulicken M, Gordon-Lipkin E, Balcer LJ, Frohman E, Cutter G, Calabresi PA. Optical coherence tomography and disease subtype in multiple sclerosis. *Neurology*. 2007;69(22):2085–92.
 39. Sepulcre J, Murie-Fernandez M, Salinas-Alaman A, Garcia-Layana A, Bejarano B, Villoslada P. Diagnostic accuracy of retinal abnormalities in predicting disease activity in MS. *Neurology*. 2007;68(18):1488–94.
 40. Galetta KM, Calabresi PA, Frohman EM, Balcer LJ. Optical coherence tomography (OCT): imaging the visual pathway as a model for neurodegeneration. *Neurotherapeutics: J Am Soc Exp Neuro Ther*. 2011;8(1):117–32.
 41. Bock M, Brandt AU, Kuchenbecker J, Dorr J, Pfueller CF, Weinges-Evers N, et al. Impairment of contrast visual acuity as a functional correlate of retinal nerve fiber layer thinning and total macular volume reduction in multiple sclerosis. *Br J Ophthalmol*. 2012;96(1):62–7.
 42. Merle H, Olindo S, Donnio A, Beral L, Richer R, Smadja D, et al. Retinal nerve fiber layer thickness and spatial and temporal contrast sensitivity in multiple sclerosis. *Eur J Ophthalmol*. 2010;20(1):158–66.
 43. Cheng H, Laron M, Schiffman JS, Tang RA, Frishman LJ. The relationship between visual field and retinal nerve fiber layer measurements in patients with multiple sclerosis. *Invest Ophthalmol Vis Sci*. 2007;48(12):5798–805.
 44. Costello F, Hodge W, Pan YI, Metz L, Kardon RH. Retinal nerve fiber layer and future risk of multiple sclerosis. *Can J Neurol Sci: Le Journal Canadien Des sciences Neurologiques*. 2008;35(4):482–7.
 45. Siger M, Dziegielewska K, Jasek L, Bieniek M, Nicpan A, Nawrocki J, et al. Optical coherence tomography in multiple sclerosis: thickness of the retinal nerve fiber layer as a potential measure of axonal loss and brain atrophy. *J Neurol*. 2008;255(10):1555–60.
 46. Talman LS, Bisker ER, Sackel DJ, Long Jr DA, Galetta KM, Ratchford JN, et al. Longitudinal study of vision and retinal nerve fiber layer thickness in multiple sclerosis. *Ann Neurol*. 2010;67(6):749–60.
 47. Walter SD, Ishikawa H, Galetta KM, Sakai RE, Feller DJ, Henderson SB, et al. Ganglion cell loss in relation to visual disability in multiple sclerosis. *Ophthalmology*. 2012;119(6):1250–7.
 48. Gabilondo I, Martínez-Lapiscina EH, Fraga-Pumar E, Ortiz-Perez S, Torres-Torres R, Andorra M, Llufríu S, Zubizarreta I, Saiz A, Sanchez-Dalmau B, Villoslada P. Dynamics of retinal injury after acute optic neuritis. *Ann Neurol*. 2015;77:517–28.
 49. Kimbrough DJ, Sotirchos ES, Wilson JA, Al-Louzi O, Conger A, Conger D, Frohman TC, Saidha S, Green AJ, Frohman EM, Balcer LJ, Calabresi PA. Retinal damage and vision loss in African American multiple sclerosis patients. *Ann Neurol*. 2015;77:228–36. doi:10.1002/ana.24308.
 50. Moss HE, Gao W, Balcer LJ, Joslin CE. Association of race/ethnicity with visual outcomes following acute optic neuritis: an analysis of the Optic Neuritis Treatment Trial. *JAMA Ophthalmol*. 2014;132(4):421–7.
 51. Price MJ, Feldman RG, Adelberg D, Kayne H. Abnormalities in color vision and contrast sensitivity in Parkinson's disease. *Neurology*. 1992;42:887–90.
 52. Lynch DR, Farmer JM, Rochestie J, Balcer LJ. Contrast letter acuity as a measure of visual dysfunction in patients with Friedreich ataxia. *J Neuroophthalmol*. 2002;22:270–4.
 53. Henderson AP, Altmann DR, Trip SA, Miszkial KA, Schlottmann PG, Jones SJ, Garway-Heath DF, Plant GT, Miller DH. Early factors associated with axonal loss after optic neuritis. *Ann Neurol*. 2011;70(6):955–63.
 54. Villoslada P, Cuneo A, Gelfand J, Hauser SL, Green A. Color vision is strongly associated with retinal thinning in multiple sclerosis. *Mult Scler*. 2012;18(7):991–9.

Axel Petzold and Gordon T. Plant

Introduction

One clinically useful feature of retinal optical coherence tomography (OCT) is to help with the differential diagnosis of multiple sclerosis-associated optic neuritis (MSON) mimics. Early recognition of MSON mimics is relevant for patient management [1, 2]. An overview of the clinical differential diagnosis is shown in Table 5.1.

In this chapter, examples will be shown for the main differential diagnosis. For didactic reasons OCT examples are also provided for other pathologies. Together the cases presented will provide the reader with a broad impression of OCT findings as they are likely to be encountered in a clinical setting.

A. Petzold, MD, PhD (✉)
Department of Neuro-ophthalmology,
Moorfields Eye Hospital & National Hospital
of Neurology and Neurosurgery, London, UK

Department of Neuroimmunology,
UCL Institute of Neurology, London, UK

Dutch Expertise Center Neuro-Ophthalmology,
Departments of Neurology and Ophthalmology,
VU Medical Center, Amsterdam, The Netherlands
e-mail: a.petzold@ucl.ac.uk

G.T. Plant, MA, MD, FRCP, FRCOphth
Department of Neuro-ophthalmology,
Moorfields Eye Hospital, St. Thomas' Hospital,
National Hospital for Neurology and Neurosurgery,
London, UK

OCT Case Examples

Multiple Sclerosis-Associated Optic Neuritis (MSON)

A 22-year-old male presents with 4 episodes (2 on the right, 2 on the left) of visual loss associated with pain on eye movements. Now he mainly has problems with the Uhthoff phenomenon and visual fading. The unaided high-contrast visual acuity (VA) 6/6 (US notation 20/20) on the right (RE, OD), 6/24 (20/80) on the left (LE, OS); color vision RE Ishihara 17/17, LE 1/17; and superior nasal VF defect on the left to confrontation.

The confocal scanning laser ophthalmoscopy (cSLO) and OCT scans are shown in Fig. 5.1. The green circle in the cLSO image represents the peripapillary ring scan taken. The corresponding OCT B-scan is shown to the right. Note that the scale of the x- and y-axis is proportional in the cSLO scan, but stretched for the y-axis for the OCT scan (200 μm marker in bottom-left corner).

The innermost retinal layer imaged on the OCT B-scan is the retinal nerve fiber layer (RNFL). This layer is of strong reflectivity and can almost always be well distinguished from the other layers. Next, there are the ganglion cell layer (GCL), inner plexiform layer (IPL), and inner nuclear layer (INL). Typically, the image contrast between the GCL and IPL is poor. The INL can be well recognized as a darker gray band in the middle of the retina. Then there are the

Table 5.1 The differential diagnosis of optic neuritis mimics

Differential diagnosis	Clinical features
MSON	Mostly good recovery within 2 months
ION	Isolated ON
RION	Isolated ON with spontaneous relapses
CRION	Relapses on steroid withdrawal, poor recovery
NMO-ON	Relapses, poor recovery
Infectious	
HIV	Subacute or progressive visual loss
Syphilis	Exposure to infectious agent
Tuberculosis	Frequently with broader cellular
Lyme disease	Reaction in the eye
Viral	
Sinusitis	Sinus pain
Reactive	
Postinfectious	Bilateral and simultaneous
Postvaccination	Better prognosis in childhood compared to adult onset
ADEM	
Neuroretinitis	Mostly good prognosis
Vascular	
AION	Sudden onset visual loss
PION	Mostly painless (except GCA)
PAMM	Paracentral scotoma
GCA	Acutely swollen optic disk (except PION) Cardiovascular risk factors
Retinal vasospasm	Frequent episodes, migraine
SUSAC	Hearing loss, encephalitis
Diabetic papillopathy	Hyperemic, sometimes bilateral disc swelling
CCF	Proptosis, chemosis, orbital venous congestion, diplopia
Vascular malformations	(Intermittent) proptosis, seizures, neurological signs
Nutritional and toxic	
Vitamins B ₁₂ deficiency	Bilateral, painless
Tobacco-alcohol	Progressive
Endemic	Pale disks
Methanol	Poor prognosis
Ethambutol	Test for vitamin B ₁₂ , MMA
Compressive	
Primary tumors	Painless, progressive
Metastases	Pale disk at presentation
Tuberculoma	Cilioretinal shunt vessels, history of cancer
Graves' disease	History of thyroid disease
Sinus mucoceles	
Systemic disease	
Sarcoidosis	Painful, progressive, and often bilateral
Behçet disease	More frequent in non-Caucasians
SLE	
Cancer, paraneoplastic	Subacute visual loss
Persistent visual aura	History of migraine

Table 5.1 (continued)

Differential diagnosis	Clinical features
Ocular	
Posterior scleritis	Pain
Maculopathies	Painless, metamorphopsia
Retinopathies	Preserved color vision
Big blind spot syndromes	VF loss, photopsias
AZOOR	Preserved color vision
Hereditary	
LHON	Family history, test for OPA1&3
DOA	Bilateral painless

ADEM acute disseminated encephalomyelitis, *AION* anterior ischemic optic neuropathy, *AVM* arteriovenous malformation, *AZOOR* acute zonal occult outer retinopathy, *CCF* carotid cavernous sinus fistula, *DOA* dominant optic atrophy, *GCA* giant cell arteritis, *HIV* human immunodeficiency virus, *LHON* Leber’s hereditary optic neuropathy, *OPO* mutations present in patients with autosomal dominant optic atrophy, *PAMM* paracentral acute middle maculopathy, *PION* posterior ischemic optic neuropathy, *SLE* systemic lupus erythematosus

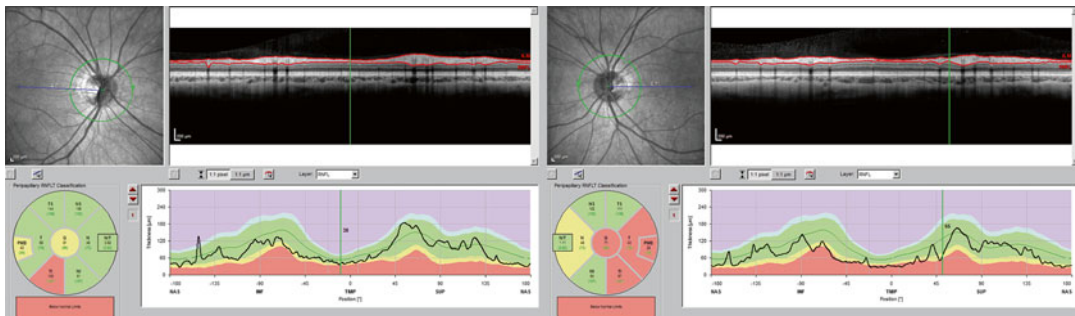


Fig. 5.1 Multiple sclerosis-associated optic neuritis (MSON) in the left eye of a 22-year-old male. His present diagnosis is clinically isolated syndrome (CIS). There is a high risk for him to convert to clinical definite MS [4]

outer plexiform layer (OPL) of lighter gray and the outer nuclear layer (ONL), which takes a darker gray shade (see also Figure 2.1 for consensus nomenclature in the chapter by Evangelou and Alrawashdeh). The four outer hyper-reflective bands are best seen in macular scans and typically referred to as the external limiting membrane (ELM), the boundary between the inner and outer photoreceptor segments, the Verhoeff membrane, and the retinal pigment epithelium (RPE) [3].

In this case there is bilateral RNFL loss. These data are represented in the summary graph to the bottom left of the figure. The global average is the most frequently reported value, in the *right eye* for this case 81 μm (yellow circle in the middle in Fig. 5.1 [4]). The corresponding normal value is 99 μm (given in green letters). Next there is a breakdown of data for individual sectors, nasal superior (NS), nasal (N), nasal inferior (NI), temporal inferior (TI), temporal (T), and

temporal superior (TS). Finally a small fraction of the temporal sector is singled out as the papillomacular bundle (PMB). This area is most frequently affected in MSON. Here a value of 43 μm is less than the reported normal value of 59 μm (green letters). The nasal to temporal ratio (N/T) is also reported.

In clinical routine, the thickness diagram to the right is also useful. The color-shaded areas are based on thickness data from a normal population. The bold green line represents the median and the green-shaded area the reference range. Borderline data are shown as blue or yellow, RNFL thickening as purple, and RNFL thinning as red.

In this case there is peripapillary RNFL loss for the PMB on the right and both temporally and nasally on the left.

In this case magnetic resonance imaging (MRI) confirmed inflammation of the optic nerve but also showed more than four lesions elsewhere

in the central nervous system (CNS). These lesions fulfilled the radiological criteria for dissemination in time and space for multiple sclerosis. The patient has a clinical diagnosis of a clinically isolated syndrome (CIS) with a high chance of having a relapse in the future and then being diagnosed as clinically definite MS [4].

Isolated Optic Neuritis (ION)

A 33-year-old female was referred with blurred vision and dyschromatopsia in her left temporal field, which was associated with left facial pain and headaches (VAS 10/10). The symptoms had fully recovered within 1 week. She now suffers from the Uhthoff phenomenon, the Pulfrich phenomenon, and daytime glare disability. At the time MRI, magnetic resonance angiography (MRA), and computed tomography (CT) imaging performed elsewhere were reported as normal.

The OCT scan taken about 14 days after onset is shown in Fig. 5.2. As in the previous case, the peripapillary ring scan is shown at the top for the right eye (to the left in Fig. 5.2) and left eye (to the right in Fig. 5.2). In the left eye there is a swollen peripapillary RNFL. The cSLO image also shows

looping of the blood vessels over the swollen RNFL at the optic disk margin. Compared to the right eye, veins appear to be more distended on the left. This can be seen both in the cSLO image and the OCT scan. There is also some thickening of the outer retinal layers suggestive of fluid shifts or possibly cytotoxic or vasogenic edema. This is interesting because hitherto disk edema was attributed to swollen axons as a consequence of stasis of axonal flow only.

In addition to the previous case, here the macular volume scan is also shown at the bottom of Fig. 5.2. The composite image of the macular volume scan contains three images. The large image consists of a semi-transparent retinal thickness map overlaying the cSLO image. The superimposed blue segmented circles are the 1 mm, 3 mm, and 6 mm ETDRS grid (a frequently used measurement grid). Summary thickness data for individual sectors of the ETDRS grid are presented to the right as absolute numbers and as a color-coded thickness map. Numeric data refer to averaged thickness in micrometers (black letters) and averaged volume data in mm^3 (red letters). In this case the total averaged ETDRS grid volume data are 9.43 mm^3 for the right eye and 9.40 mm^3 for the left eye. This shows that macular volume

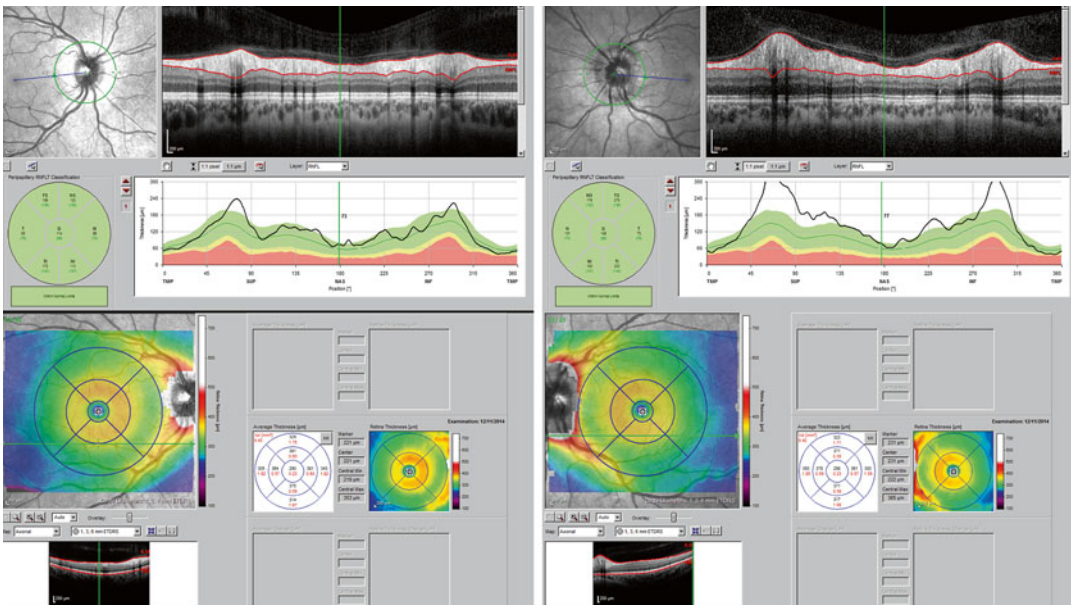


Fig. 5.2 Acute isolated optic neuritis (ION) in the left eye of a 33-year-old female

data are not much affected by disk swelling in optic neuritis. For illustration, the segmentation on which the thickness data are based is given at the very bottom of the graph. The two red lines in the OCT B-scan (taken at the location of the green horizontal reference line in the macular cSLO scan) reveal that all thickness map data were based on the total retinal thickness—a very robust and well-validated measure.

In conclusion the OCT showed optic disk swelling on the left. Brain and spinal cord imaging were normal. This patient has a diagnosis of an isolated left optic neuritis (ION) [1, 5].

Relapsing Isolated Optic Neuritis (RION)

A 26-year-old female experienced 2 episodes of blurred vision in her left eye over the past 2 years. Both were associated with pain on eye movements and recovered within only a few days. There was VA 6/9 (US notation 20/30) with full color vision. There was a left RAPD.

The reader should now be familiar with the OCT data presented in Fig. 5.3. The OCT scan reveals temporal loss of RNFL on the left. Brain and spinal cord imaging were normal. She has a diagnosis of relapsing isolated optic neuritis (RION) [5, 1].

CRION

A 24-year-old female experienced 10 episodes of relapsing optic neuritis over a 4-year period. Each episode was associated with pain on eye move-

ments. Her BCVA is poor OD (right eye) HM and OS (left eye) 6/30 (20/100). She has lost color vision. Repeated MRI brain and spinal cord imaging showed inflamed optic nerves, but no sign of CNS inflammation elsewhere. She does not have anti-AQP4 autoantibodies. Relapses always occur on tapering off steroids. She has a clinical diagnosis of chronic relapsing inflammatory optic neuropathy (CRION) [6]. Upon each relapse she receives hyperacute treatment with steroids [7].

The OCT scan is shown in Fig. 5.4. There is severe binocular RNFL atrophy. The peripapillary RNFL atrophy seen here is much more severe than what is seen at first presentation with typical MSON.

A new measure shown in this figure is the use of longitudinal data. The first scan was taken at baseline (thin black line in thickness diagram) and the second scan at 2-year follow-up (bold black line in thickness diagram). Despite the frequent episodes, the RNFL layer thickness remained essentially unchanged over the 2-year period.

NMO-OD

A 25-year-old female presented with NPL in her right eye following 1 severe episode of optic neuritis. There was BCVA OS 6/4.8 (20/16). She tested positive for anti-AQP4 autoantibodies. Under treatment with azathioprine, she experienced another episode of optic neuritis that affected the remaining good, left eye. Hyperacute treatment with steroids was initiated [7]. In total, 4 further episodes occurred and it was possible to preserve a BCVA OS of 6/6 (20/20).

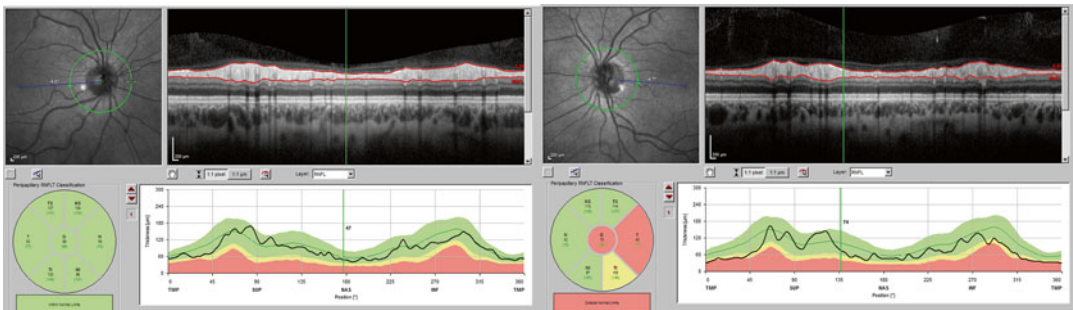


Fig. 5.3 Relapsing isolated optic neuritis (RION) in a 26-year-old female

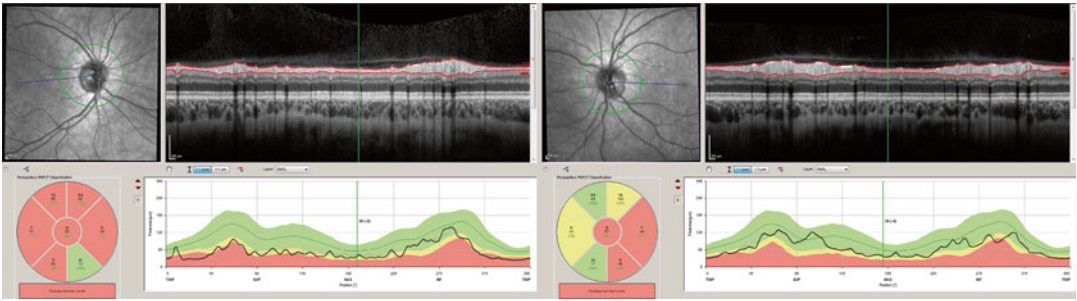


Fig. 5.4 Chronic relapsing optic neuropathy (CRION), 10 relapses, in a 24-year-old female

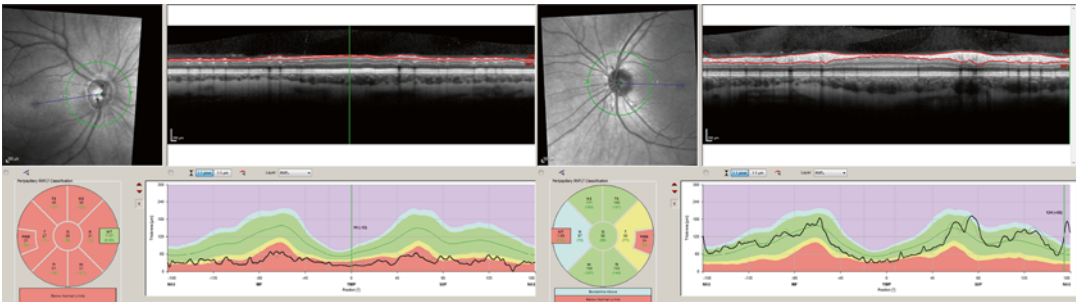


Fig. 5.5 NMO-ON, 5 relapses, in a 25-year-old female

The OCT scan is shown in Fig. 5.5. Severe loss of RNFL can be seen on the right. Despite a number of relapses, the RNFL remained relatively preserved on the left. As in the case before, the thick black line in the thickness diagram represents the baseline data and the bold line the last follow-up 2 years later. She has a diagnosis of neuromyelitis optica optic neuritis (NMO-ON) [8].

ION on PAOG

A 54-year-old male patient was diagnosed 5 years ago with primary open-angle glaucoma (PAOG). At the time his IOP spiked to 38 mmHg on the right and 34 mmHg on the left. About a year ago, he noticed 1 episode of scintillations in his left eye. He cannot remember if there was any pain on eye movements. His current problem is trying to judge the driving trajectories of other cars in busy traffic. There was BCVA 6/5 (20/16) bilaterally with mild dyschromatopsia on the left eye and a left RAPD.

The OCT scan is shown in Fig. 5.6. The OCT demonstrates a glaucomatous disk on the right, but

more severe RNFL loss than expected alone from glaucoma on the left. The bold black line in the thickness diagram refers to the OCT scan shown in Fig. 5.6 and the thin black line in the thickness diagram to the OCT taken 5 months earlier.

These findings are suggestive of an episode of an isolated optic neuritis on the left. As expected from longitudinal OCT data in ON [9], RNFL atrophy has now plateaued.

Chiasmitis

A 45-year-old female was referred with unexplained visual loss. On the 1st of January, she developed severe headaches, nausea, and vomiting. She was bedbound for 8 days, following which she noticed that her vision had gone blurred. There was a left RAPD, BCVA RE 6/6 (20/20), LE 6/36 (20/120). She did miss 5 Ishihara plates on the left.

The OCT scan is shown in Fig. 5.7. The OCT demonstrated severe bilateral nasal RNFL thinning as seen following chiasmitis. In addition there is more prominent loss of the PMB on the

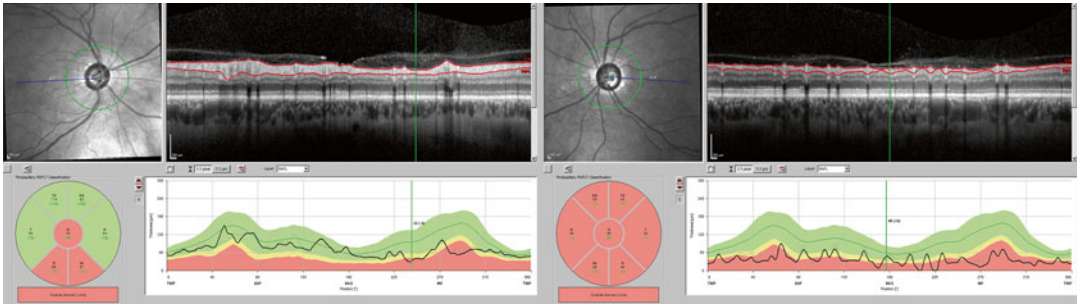


Fig. 5.6 ION in a 54-year-old male patient with PAOG

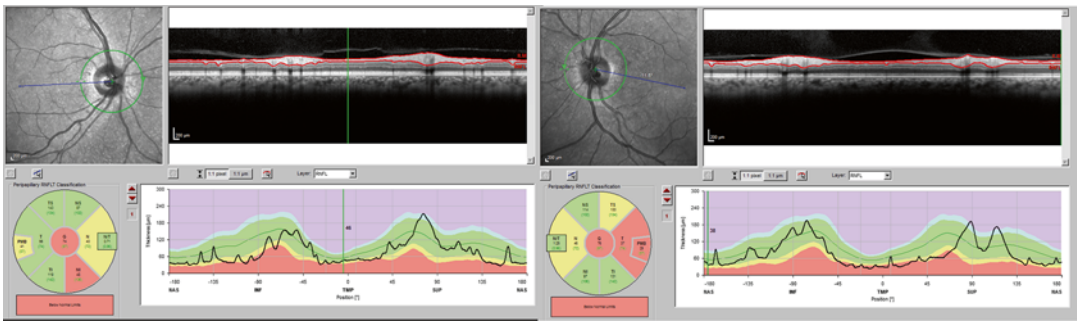


Fig. 5.7 Chiasmitis in a 45-year-old female

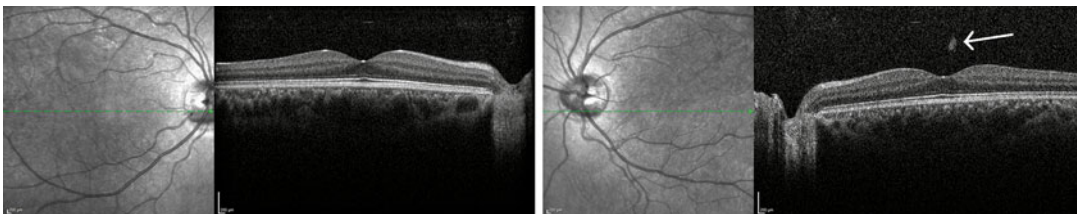


Fig. 5.8 Achiasma and left pre-foveal floater in a 27-year-old male

right explaining the poorer VA and color vision. She had a diagnosis of chiasmitis, which is clinically associated with severe headaches, nausea, vomiting, and binocular loss of vision. Chiasmitis is usually not associated with MS but can be occasionally. It is associated with NMO [1, 2, 10, 11].

Achiasma

A 27-year-old male patient with a lifelong history of a pendular seesaw nystagmus noticed a shadow obscuring a very small part of his central visual field on the left. There were BCVA OD 6/12 (20/40),

LE 6/24 (20/80), N4.5 bilaterally, and normal color vision. The nystagmus made funduscopy challenging. It was, therefore, not possible to be sufficiently certain that macular pathology was excluded.

The OCT line scan revealed a small pre-foveal floater on the left (arrow in Fig. 5.8). This small floater also casts a shadow, which is just visible to the right of the foveola, explaining his new symptoms. Note that because of the nystagmus, this OCT scan was only possible with 1 single horizontal line (dashed green horizontal reference line in cSLO image).

Electrodiagnostic testing was consistent with achiasma and the well-defined foveola, seen in

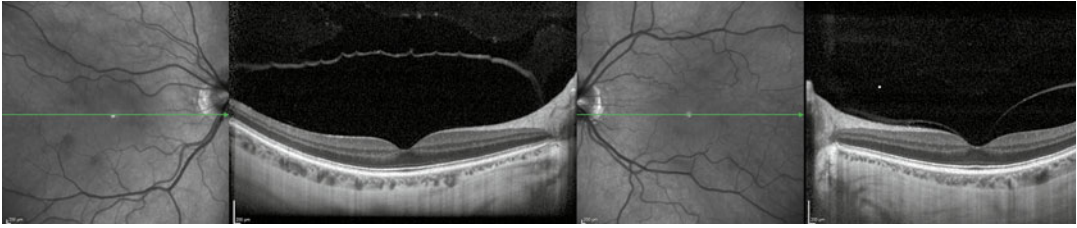


Fig. 5.9 Posterior vitreous detachment (PVD) in a 42-year-old female with visual snow

the OCT, explains his relatively good vision. He has a diagnosis of achiasma [12].

Visual Snow

A 42-year-old female presents with a 2-year history of binocular visual snow and an area of blurred vision clearly depicted on the Amsler chart. She has an overlap diagnosis between entoptic phenomena due to her PVD and visual snow [13].

The OCT scan is shown in Fig. 5.9. The OCT shows minimal central PVD in the left eye in the area corresponding to the central VF defect on the Amsler chart. In the right eye, it can be seen that the vitreous has already retracted completely from the entire macular area.

Nonorganic Visual Loss

Nonorganic visual loss occurred in a 23-year-old male. Visual acuity (VA) had decreased on the right from 6/6 (20/20) to count finger (CF), 9 months previously. Five months earlier VA decreased on the left from 6/6 to CF. He still can read Ishihara charts and walk freely between chairs in a dimmed examination room. The visual problems coincide with him being made redundant at work.

Figure 5.10 shows scans that the reader should already find familiar from the previous cases plus 1 additional new scan to the bottom: blue light autofluorescence (AF). The OCT scan was taken 9 months after subjective onset of visual loss in the right eye. The OCT scan, AF and electrophysiology were entirely normal. If this degree of visual loss would have been of an organic nature, inner

retinal layer atrophy should have been presented after about 3 months. He has a diagnosis of nonorganic visual loss.

Reactive

Postinfectious

A 72-year-old male patient experienced a febrile infection of unknown etiology abroad. Within 2 weeks he experienced painless loss of vision on the right, which was followed by the left eye within 7 days. On presentation there was perception of light bilaterally in a small area of superior and inferior peripheral vision. He did not respond to high-dose intravenous steroids given at presentation.

The OCT scan is shown in Fig. 5.11. In this example a 3D representation of the ONH volume scan was chosen. The scan to the top of Fig. 5.11 was taken at presentation and shows bilateral papilloedema. The cSLO image shows the blurred optic disk margin. Retinal folds, indicating severe optic disk swelling, are visible in the right eye (to the left of the optic disk) and in the left eye (right to optic disk). Veins are dilated. The earlier noted (Fig. 5.2) edematous swelling of the outer retinal layers is much more prominent in this case.

The inset to the colorized 3D image represents an OCT line scan from the optic disk to the macular at baseline and 6 months follow-up. The retinal folds are visible again. In addition there is central macular edema (CME) in the right foveola. Finally, hyper-reflective spots are visible in the OPL and INL close to the foveola on the right. These hyper-reflective spots represent an observation that is not yet fully understood. In our experience they are visible with more severe cases, can be adjacent to INL microcysts, and are

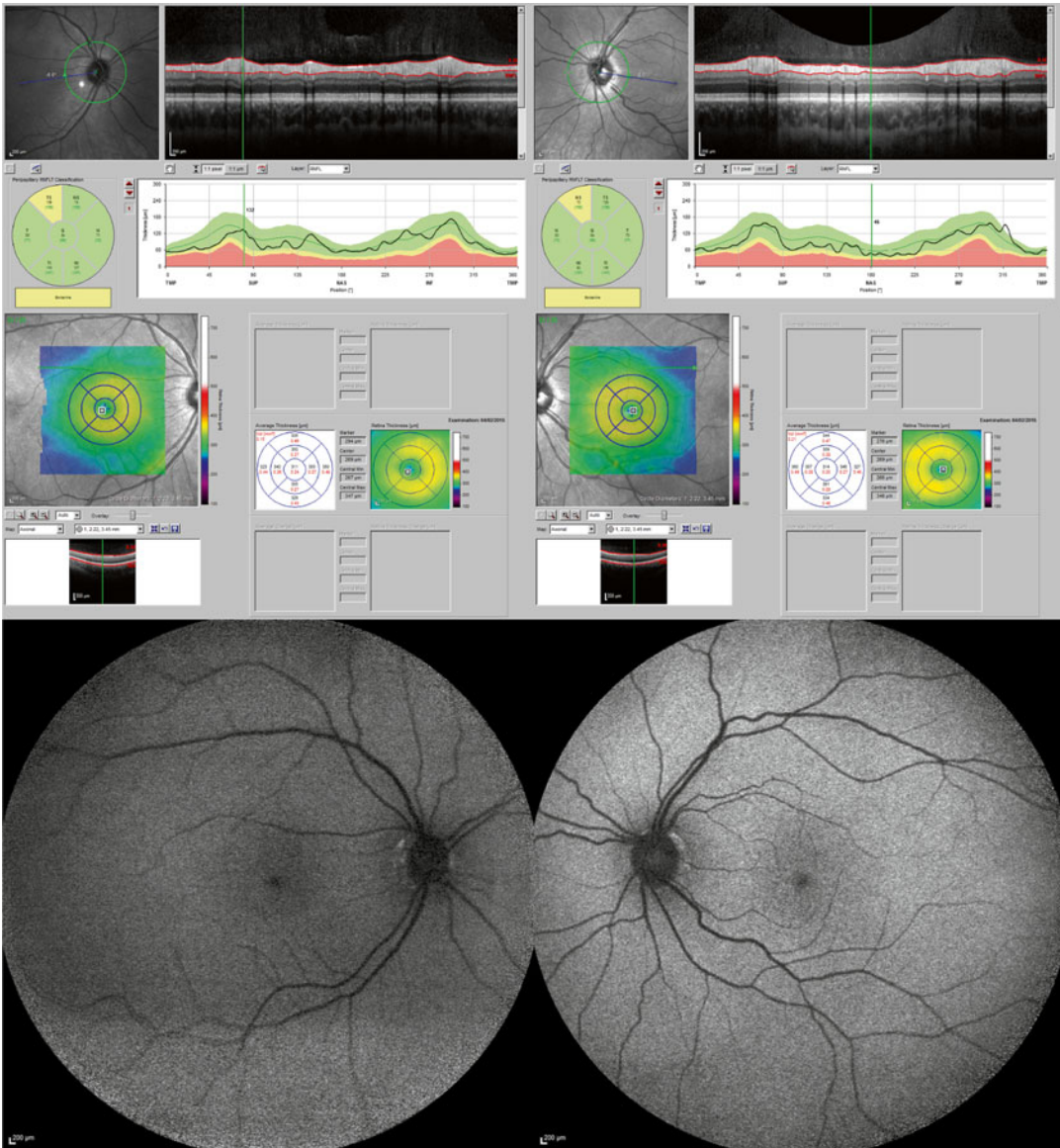


Fig. 5.10 OCT and AF from a 23-year-old male with nonorganic visual loss

not disease specific [14]. Could they be a sign of severe retinal inflammation?

The lower line scan shows resolution of optic disk swelling and loss of RNFL after 6 months. The degree of RNFL atrophy can be better appreciated on the ONH ring scan.

The extent of volume change from acute disk swelling to atrophy is better appreciated on the ONH volume maps at the bottom right in Fig. 5.11. The red-framed thickness map at the

top shows the GCL thickness map at presentation for both eyes. This is followed by the thickness map at 6 months. Finally, the difference between the 2 scans is shown in absolute numbers and as a thickness map where green represents areas with thinning. The color legends are shown to the right of the thickness map.

This patient had a diagnosis of severe, bilateral optic neuritis reactive to an infectious episode. Unlike in children where the prognosis is

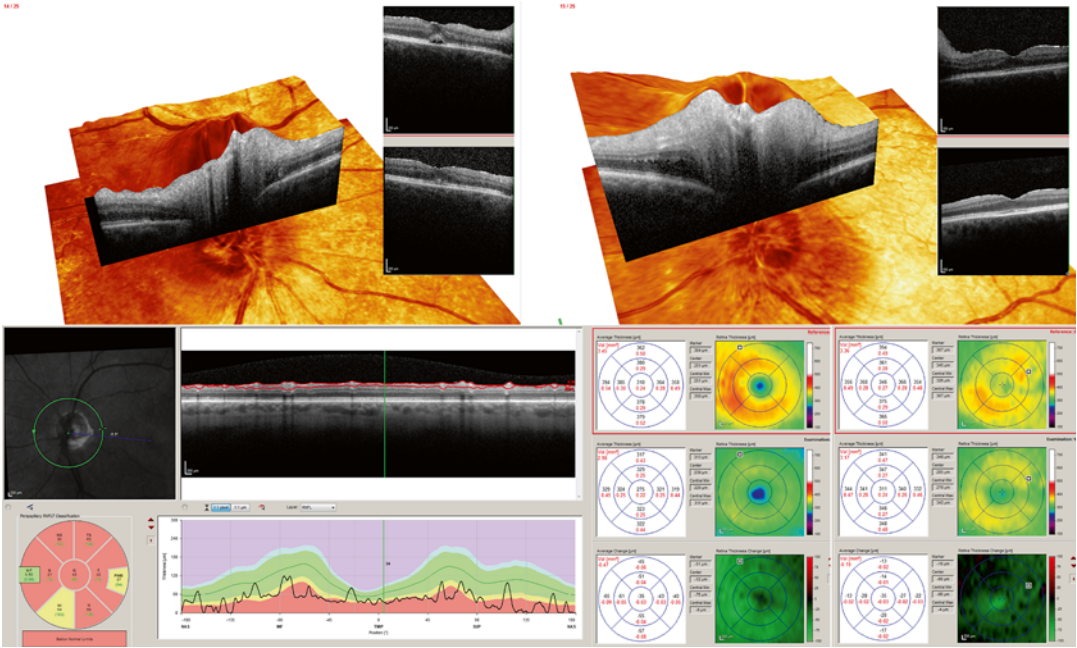


Fig. 5.11 Postinfectious optic neuritis in a 72-year-old male

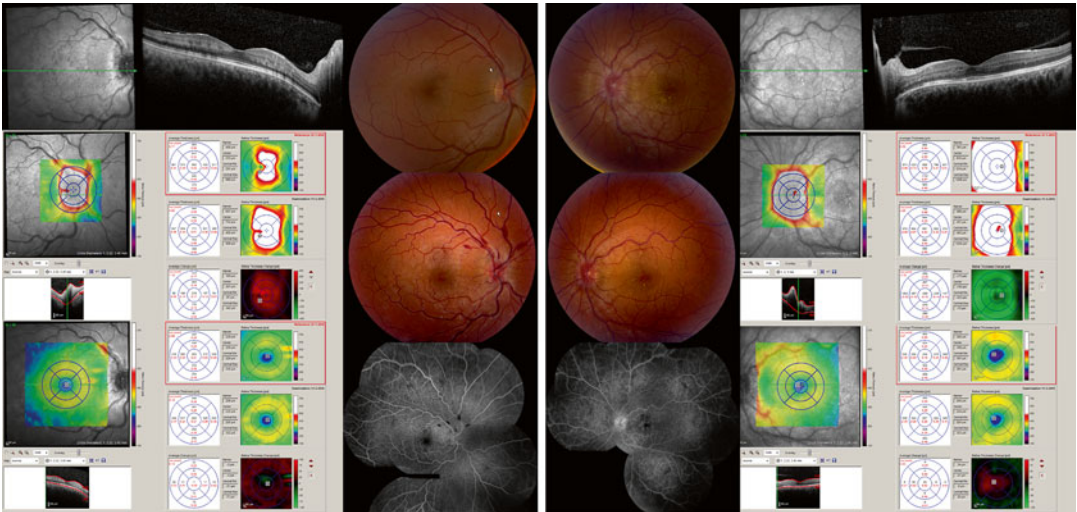


Fig. 5.12 Neuroretinitis in a 30-year-old female

frequently good, in this case the outcome was very poor, retinal atrophy severe and the patient was registered blind.

Neuroretinitis

A 30-year-old female returned from holidays in Mexico first with visual loss in the left eye. When

she presented in clinic, funduscopy showed the typical appearance of a left macular star as seen with neuroretinitis (fundus photographs in Fig. 5.12 top). There was optic disk swelling on the right. There was a mildly elevated titer for enterovirus, but this was not thought to be significant. OCT scans were taken. Subsequently she

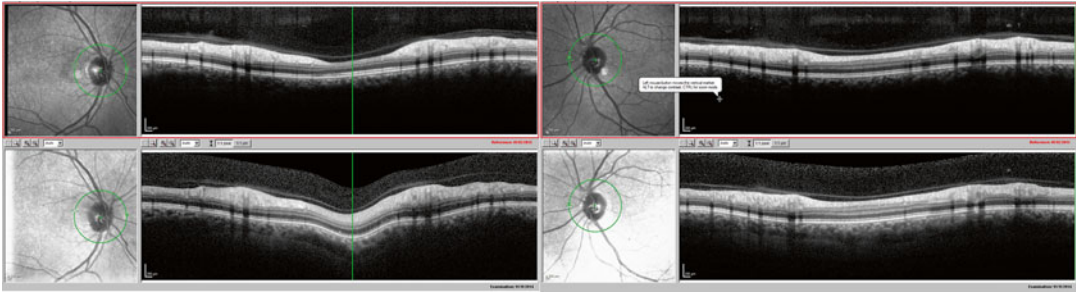


Fig. 5.13 Subacute NAION in the right eye of a 58-year-old male. Segmental atrophy of the RNFL is visible (*green reference line, top image*) 3 months after presentation (*bottom image*)

also developed visual loss on the right. Funduscopy showed severe optic disk swelling (fundus photographs in Fig. 5.12 middle). Fluorescein angiography showed some leakage on the right.

The OCT scans taken at the second visit are shown in Fig. 5.12. The OCT line scan for the right eye shows optic disk swelling and loss of contrast of the INL and OPL. Hypodense areas casting a shadow appear in the INL; 2 of these almost take the appearance of what has been described as MMO [15], but no clear microcysts could be identified. Thickness maps of the longitudinal OCT ONH volume scans revealed the extent of optic disk swelling (red area in thickness map). The macular volume scans make evident that there is also a small degree of swelling extending into the retina far beyond the optic disk.

For the left eye, the OCT line scan shows appearance of hyper-reflective spots in the INL close to the optic disk, as well as presence of microcysts in the INL/OPL. This association has been described previously [14]. The ONH volume scan on the right shows resolution of the optic disk swelling (green area in thickness map). The macular volume scan reveals 2 processes: peripheral thinning (green-shaded area) of presumed edema resolution and foveal/perimacular thickening (red-shaded area) of presumed microcyst formation.

Retinal microcysts are a nonspecific finding, seen with almost every pathology of either the inner or outer retinal layers [14].

This patient has a diagnosis of neuroretinitis of unknown etiology.

Vascular

NAION: Subacute

A 58-year-old man was referred with a scotoma. He noticed a shadow in front of his right central visual field. He has a past medical history of angina pectoris, requiring cardiac stent insertion. He is a recent ex-smoker, overweight, and hypercholesterolemic and has a family history of stroke in his father. His BCVA was 6/6 (20/20) bilaterally and there was an inferior scotoma on the right with a neat horizontal border extending to 8° of visual angle.

The longitudinal OCT ONH ring scans are shown in Fig. 5.13. Comparison of the baseline (bottom of Fig. 5.13) and 3-month follow-up OCTs (top of Fig. 5.13) gives an impression of the initial papilloedema in the right eye, which is followed by segmental RNFL loss (green vertical reference line). Note that again atrophy stops at level of the INL.

He has a diagnosis of a right NAION [16, 17].

NAION: Acute

A 45-year-old heavy smoker with a history of cocaine abuse: The OCT did show resolving optic disk swelling with ensuing segmental RNFL loss that corresponded to his central visual field scotoma (Fig. 5.14). Notwithstanding his young age, he has a diagnosis of NAION [16, 17]. Again there is substantial edematous swelling of the outer retinal layers suggesting that this observation is not specific for inflammatory or autoimmune optic neuropathies (Figs. 5.2 and 5.11).

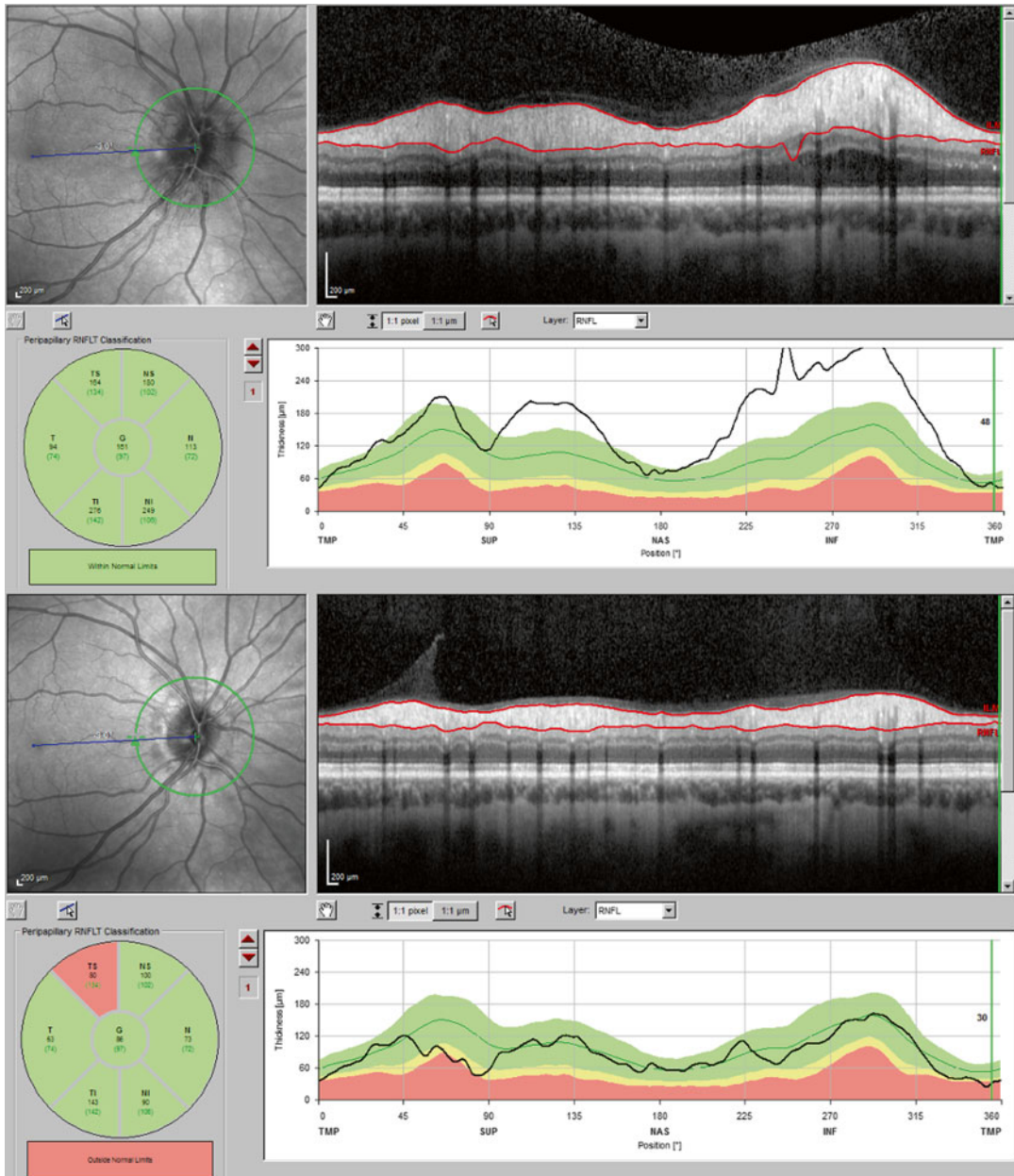


Fig. 5.14 Acute NAION in the right eye of a 45-year-old heavy smoker with cocaine abuse

BRAO: Small

A 49-year-old patient with a sudden onset central visual field scotoma respecting the horizontal meridian. He has a past medical history of hypertension. No embolus was seen.

The OCT scan is shown in Fig. 5.15. There is wedge-shaped loss of the RNFL in the temporal

superior sector of the optic disk. Inspection of the cSLO image shows that the first branch of the superior temporal retinal artery is attenuated (arrow in Fig. 5.15 top left).

Automated segmentation of individual retinal layers reveals that there is localized atrophy of the inner retinal layers corresponding to the area

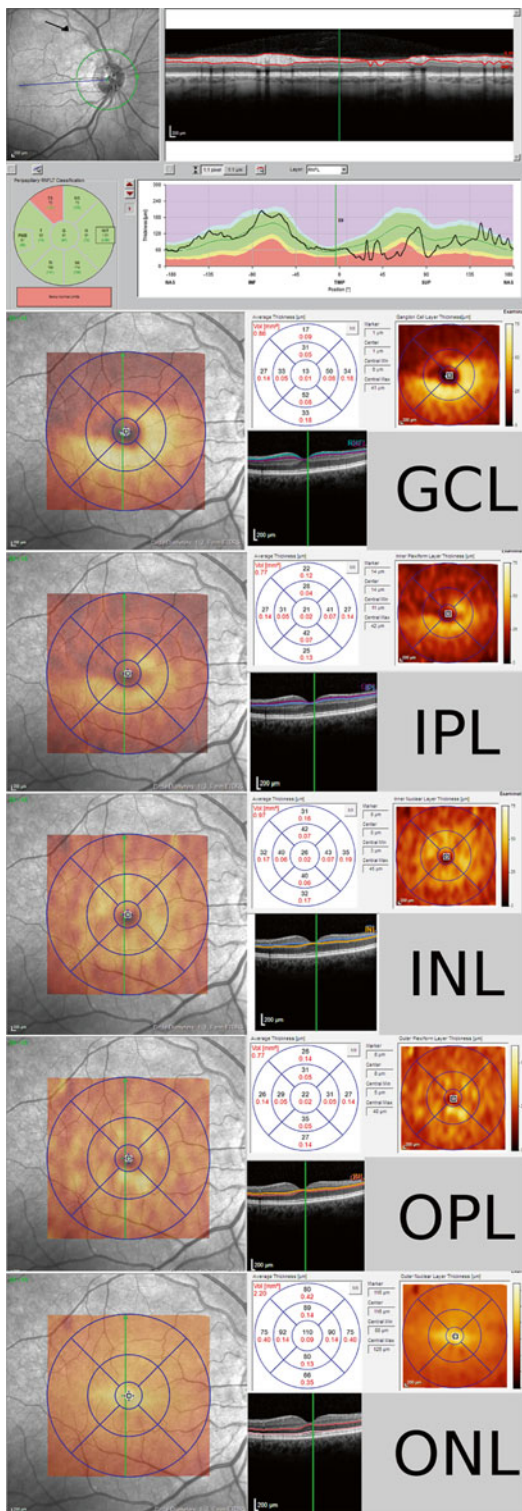


Fig. 5.15 BRAO (arrow) in a 49-year-old male

supplied by this branch retinal artery. To illustrate this relationship, layer-specific thickness maps were semi transparently overlaid on the cSLO image (to the left of Fig. 5.15). Summary thickness data and individual B-scan segmentation lines for the respective retinal layers are shown to the right in Fig. 5.15.

There are loss of GCL and IPL, but preservation of the INL, OPL, and ONL. He has a diagnosis of a small BRAO [18].

BRAO: Large Embolic

A branch retinal artery occlusion (BRAO) is seen in a 75-year-old male. He suffers from multiple vascular risk factors, smoking, overweight, diabetes mellitus, hypertension, hypercholesterolemia, and atrial fibrillation. There was BCVA 6/18 (20/60) binocularly. There are a right RAPD and a dense inferior visual field defect on the right.

The OCT scan is shown in Fig. 5.16. The OCT shows atrophy of all retinal layers from the RNFL to the ONL. Compared to the previous case, the atrophy is more extensive and profound and also affects the INL. This observation makes the point that the INL can only act as a physiological barrier to transsynaptic axonal degeneration to remote pathology. Direct injury to the INL, for example, by ischemia following a large thromboembolic event, will result in INL atrophy. This is a useful and clinically relevant OCT sign, not reported prior to the best of our knowledge.

A thrombus can be seen in inferior temporal retinal artery as revealed by a line scan orientated over the glistering reflection visible in the cSLO image. This thrombus appears to be located just outside the blood vessel wall. Thrombi occluding the microvasculature can be a blood clot, an atheromatous fragment, or other circulating debris. The mechanism thought to be responsible for a thrombus appearing adjacent to a blood vessel is called angiophagy [19].

This patient has a diagnosis of an embolic BRAO and was started on anticoagulation [18].

Hemiretinal Vein Occlusion

A 39-year-old male patient noticed dark spots in his superior visual field on the right. Within

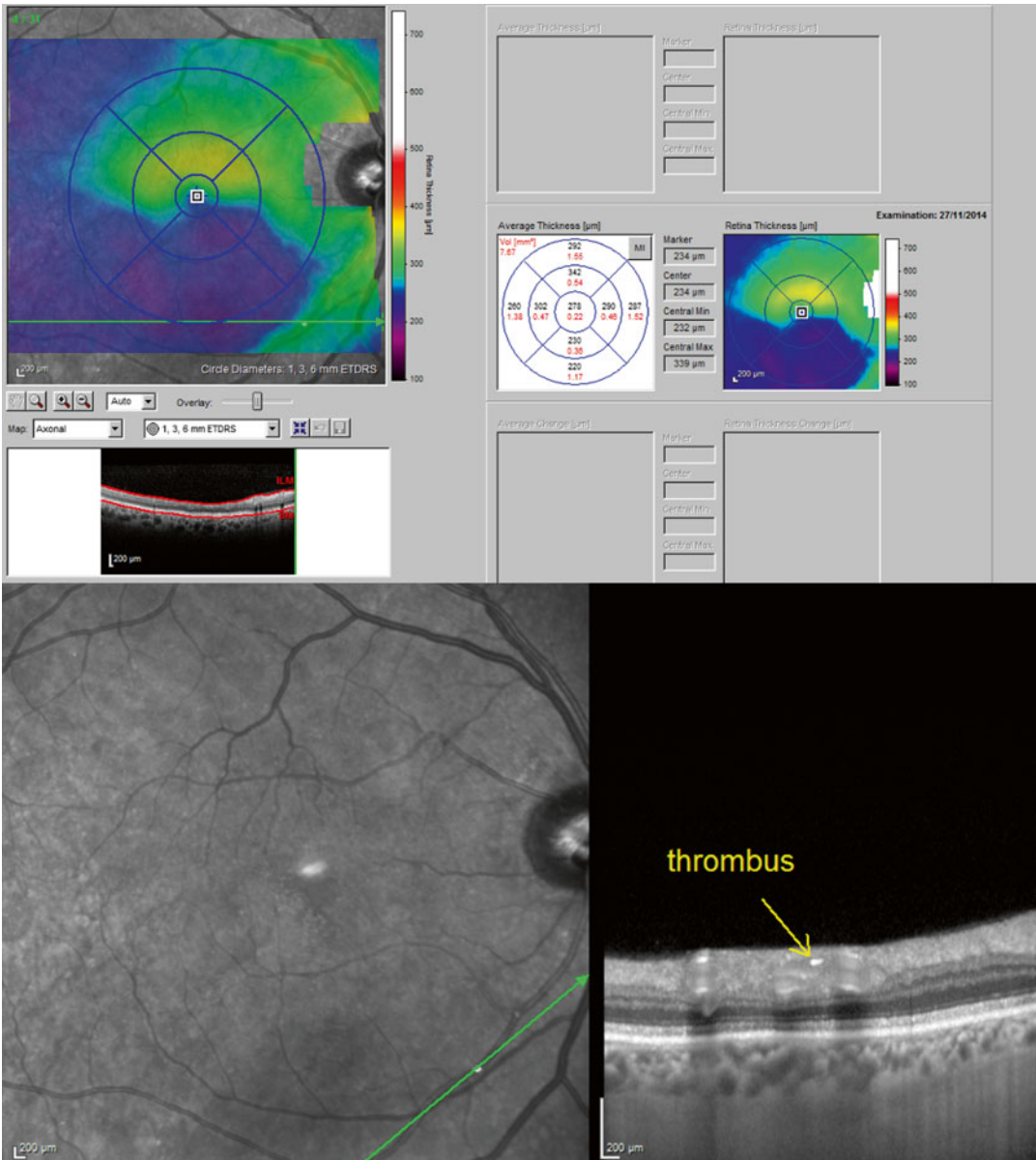


Fig. 5.16 Large embolic BRAO in a 75-year-old male. There is profound loss of retinal layers corresponding to the vascular territory of the inferior temporal retinal

artery. The thrombus (*arrow*) can still be seen in the cSLO image and OCT image

14 days his BCVA had decreased to 6/24 (20/80) on the right and there was periocular discomfort. On funduscopy there was a swollen optic disk on the right (Fig. 5.17). There are peripheral venous hemorrhages in the inferior retina on the right. There are optic disk splinter hemorrhages on the

right and a large cotton wool spot is seen at the site of the first bifurcation of the inferior retinal vein. The left eye was normal.

The corresponding OCT ONH volume scan demonstrates more severe optic disk swelling inferiorly. Inferior venous extension can also be



Fig. 5.17 Hemiretinal vein occlusion in a 39-year-old male

appreciated. The ring scan illustrates the distribution of optic disk swelling, which involves the superior disk to the venous outflow problem causing stasis of axonal flow. The longitudinal macular volume scans from the right eye finally show resolution of the inferior hemiretinal swelling within 1 month.

He has a diagnosis of a hemiretinal vein occlusion at level of the lamina cribrosa [20].

CVA

A 78-year-old male noticed a sudden onset shadow in his right visual field (Fig. 5.18). He has multiple vascular risk factors and a past medical history of triple bypass surgery and pulmonary embolism (PE). For the latter he was on macumar, which had been stopped. On examination there was a right homonymous hemianopia. The OCT demonstrates RNFL loss nasally on the right and temporally on the left. This is consistent with retrograde transsynaptic axonal degeneration following an ischemic cerebrovascular accident (CVA) [21, 22].

The OCT scan is shown in Fig. 5.16.

Systemic Disease

Sarcoidosis Optic Neuropathy

A 33-year-old male was referred with worsening visual symptoms following tapering out of prednisone treatment for an episode of optic neuritis on the right. He developed pain on eye movements (VAS 7/10), which was followed by dyschromatopsia within a day. On increase of steroids the pain stopped. There was no RAPD, and BCVA was 6/4 (20/13.3) bilaterally. He was able to read all Ishihara charts, but there was red desaturation on the right. Despite his good vision and only right-sided symptoms, OCT demonstrated severe bilateral optic atrophy, worse on the right (Fig. 5.19). Chest imaging suggested sarcoidosis, which was biopsy proven.

He has a diagnosis of bilateral sarcoidosis optic neuritis. About 5 % of patients with systemic sarcoidosis will have optic nerve involvement at some time [23, 24]. It is important to exclude that loss of vision is not due to uveitis [25, 26] or granuloma in the orbit or visual pathway [27, 28].

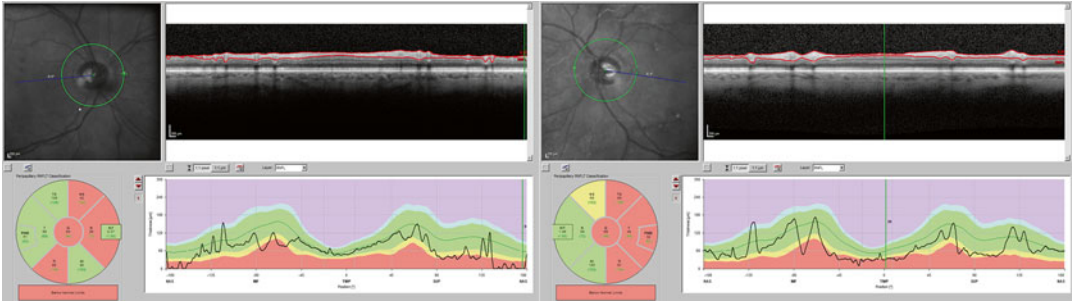


Fig. 5.18 Transsynaptic retrograde axonal degeneration in a 78-year-old male following a CVA

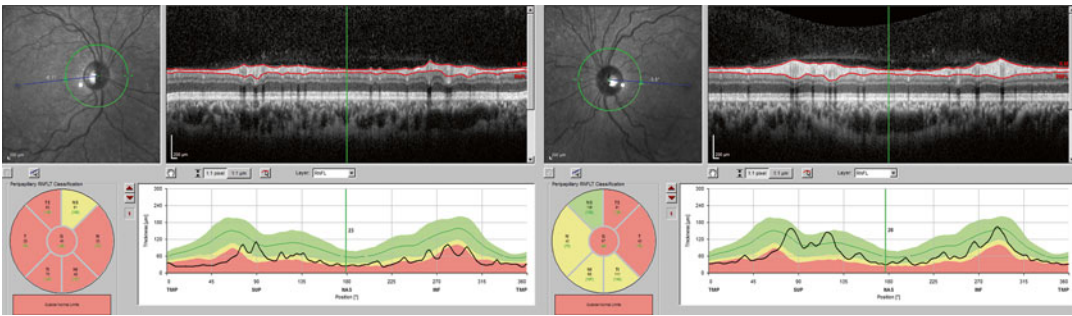


Fig. 5.19 Sarcoidosis ON in a 35-year-old male

In this patient the RAPD was absent because of bilateral pathology. Testing for red desaturation can be clinically more sensitive for recognizing an acquired optic neuropathy than using Ishihara charts, which have been designed to detect congenital color deficiencies. He is under immunosuppression with methotrexate 17.5 mg once weekly and a tapering regime with prednisone.

Ocular

Maculopathy

A 40-year-old male was referred for a suspected optic neuropathy on the right (Fig. 5.20). He describes an 11-month history of blurred vision and dyschromatopsia on the right. There was never pain on eye movements and the symptoms are progressive. VA was down to CF and he only managed to read the Ishihara control plate on the right. On funduscopy the optic disks looked healthy. But the OCT macular volume scan demonstrates pathology of the outer retinal layers,

which is not seen with neuropathies but with maculopathies (Fig. 5.20). Electrodiagnostic testing showed mild generalized cone and rod system involvement on the right causing secondary VEP abnormalities (VEP RE 125 ms 5 uV, LE 107 ms 7 uV).

Optic Neuropathy Following Diving

A 21-year-old male had been referred with unexplained progressive, painless visual loss 2 weeks following a 30-m deep dive. The BCVA were OD 6/60 (20/200), OS HM and bilateral dense central scotoma (Fig. 5.21).

The OCT demonstrates almost complete loss of the axons projecting to the macula bilaterally (Fig. 5.21). The inner nuclear layer and outer retinal layers remain preserved. Electrodiagnostic testing confirmed severe bilateral optic nerve and retinal ganglion cell dysfunction. He is currently under investigation for mitochondrial genetics. Taken together the combined OCT and electrodiagnostic investigation all point to an optic neuropathy.

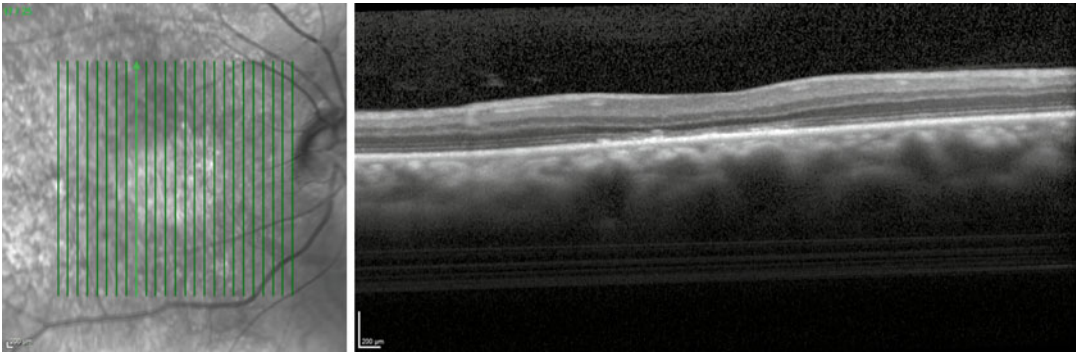


Fig. 5.20 Maculopathy in a 40-year-old male

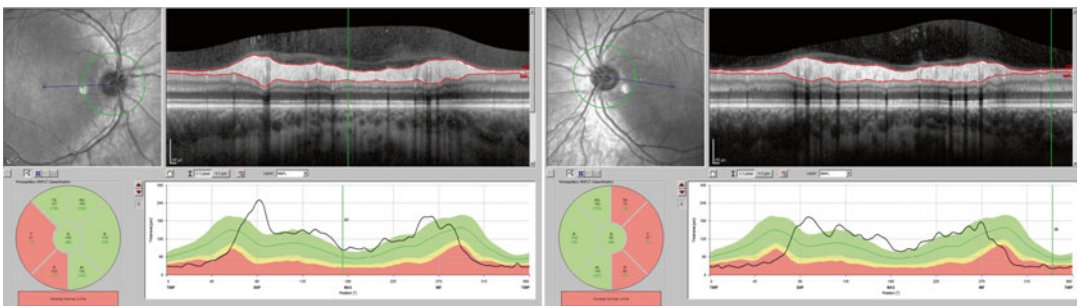


Fig. 5.21 Optic neuropathy in a 21-year-old male

Multiple Evanescent White-Dot Syndrome

A 53-year-old female developed photopsias and a gray-shaded, relative scotoma in the central visual field of her left eye. There was BCVA OD 6/6 (20/20), OS 6/12 (20/40). Optic disks were normal. The OCT showed a defect of the inner segment/outer segment (ISOS) in the left eye (Fig. 5.22). Corresponding fundus autofluorescence demonstrated hyper-reflective areas parafoveally (AF images to the far right in Fig. 5.22). These areas corresponded to a small degree of leakage on fluorescence angiography (not shown). Her vision recovered to BCVA OS 6/6 (20/20) within 5 months. Likewise, the OCT image normalized. She has a diagnosis of multiple evanescent white-dot syndrome (MEWDS) which belongs to the big blind spot syndromes listed in Table 5.1 [29].

Vitreomacular Traction

A 76-year-old male with a previous diagnosis of NAION developed a new “grayish curtain” in the

central visual right eye. His VA on the right is 6/9 (20/30) with N18. The Amsler chart shows a hazy central visual field defect extending 7° of visual angle vertically and 8° horizontally. He can still see the lines and describes metamorphosis.

The OCT is shown in Fig. 5.23. There is vitreomacular traction (VMT) in the right eye. His new symptoms are due to VMT. A possible association between NAION and traction at the vitreoretinal interface has recently been proposed [16].

Hereditary

LHON m. 1313G>A

This 14-year-old female developed acute, painless visual loss, first on the right (BCVA 6/9 (20/30)) and 5 months later on the left (6/60 (20/200)). Sequence analysis and mutation scanning detected a new mtDNA nucleotide variant (m. 1313G>A).

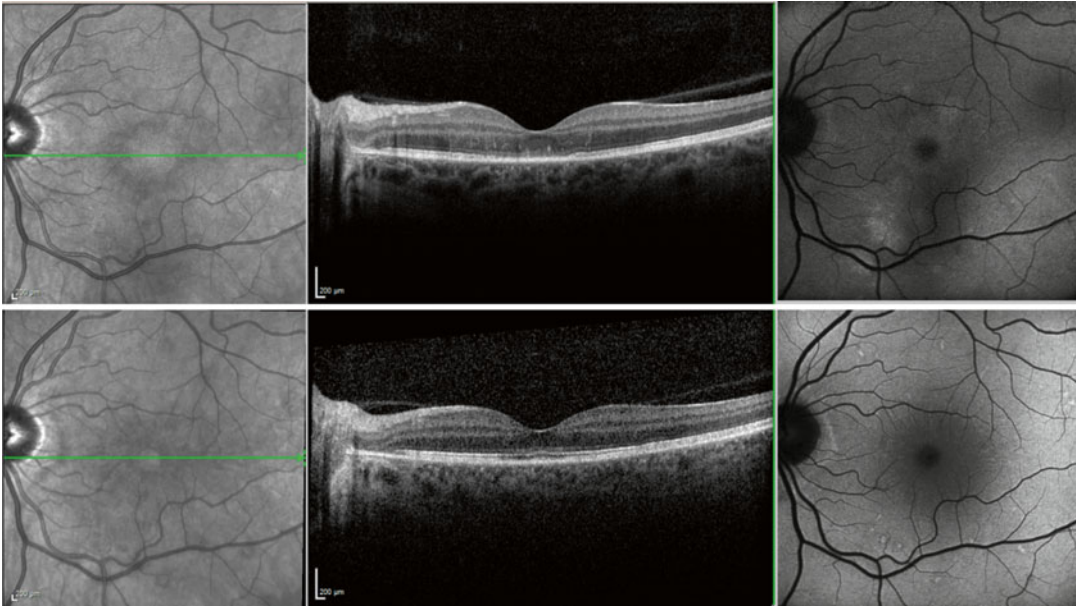


Fig. 5.22 Big blind spot syndrome (MEWDS) in a 53-year-old female

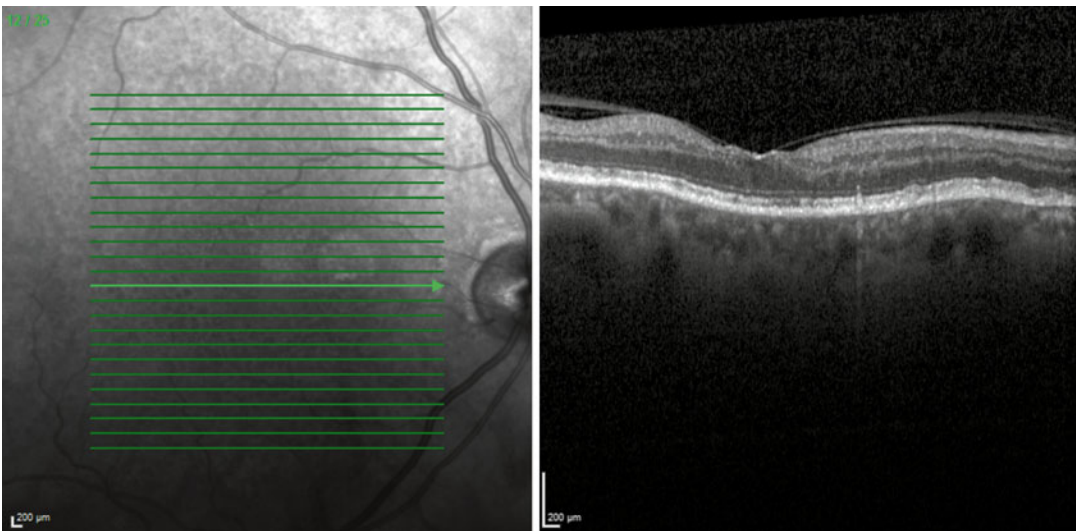


Fig. 5.23 Vitreomacular traction in a 76-year-old male with a past medical history of NAION

The OCT scan shown in Fig. 5.24 was taken when vision was lost on the left and compared to OCT scans taken 5 months earlier. The macular scans taken show inhomogeneity of the OPL, which appears like small axial columns. The longitudinal ONH ring scans show more severe peripapillary RNFL loss on the right compared to the left (area between bold and thin black lines in the thickness diagram). This is because there was

more time (5 months) for anterograde axonal degeneration to develop on the right.

Traumatic Optic Neuropathy

A 41-year-old man received a blunt hit to the right side of his head during a football match. His vision went immediately black and never

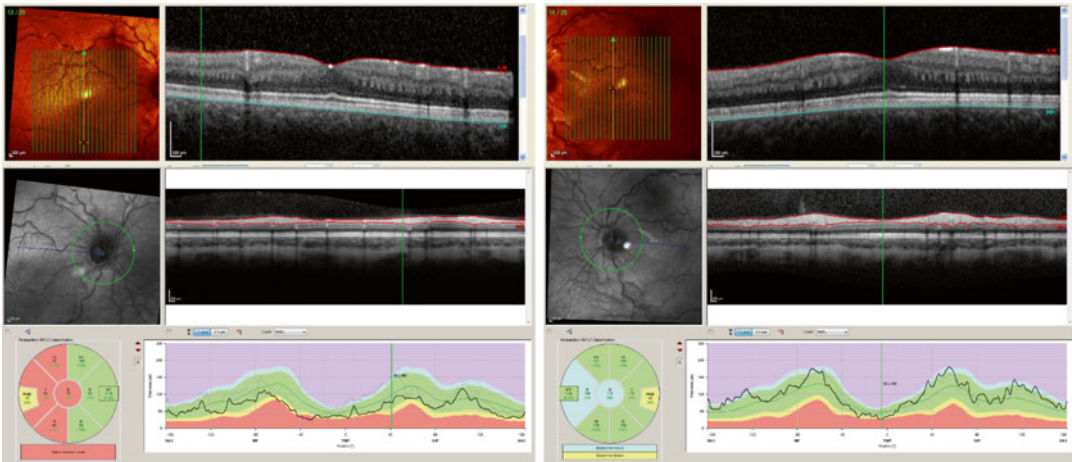


Fig. 5.24 Bilateral LHON in a 14-year-old female. The macular volume scans are shown at the top and the ring scans at the bottom of the image. The thickness diagram

to the bottom summarized the peripapillary RNFL data at first presentation (*thin black line*) and 5-month follow-up (*bold black line*)

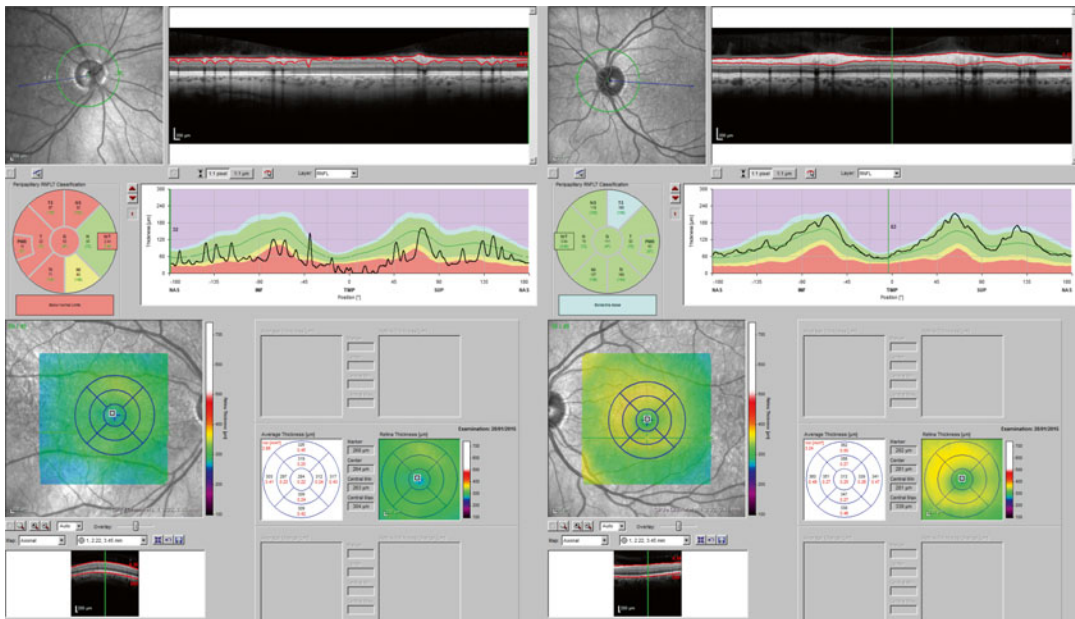


Fig. 5.25 Traumatic ON in a 41-year-old male

recovered. There was BCVA OD NPL, LE 6/6 (20/20). There was no pupil reaction on the right and the optic disk was pale.

The OCT is shown in Fig. 5.25. The OCT demonstrated presence of microcysts in the right perimacular rim. These microcysts are indicative of a retrograde maculopathy (see also Chap. 10 [30, 31].

Idiopathic Intracranial Hypertension

A 44-year-old lady presented with visual obscuration and headaches (VAS 7/10).

The OCT is shown in Fig. 5.26. The OCT shows bilaterally swollen disks. There is venous congestion, too. In addition, the angle of Bruch’s membrane opening is pushed

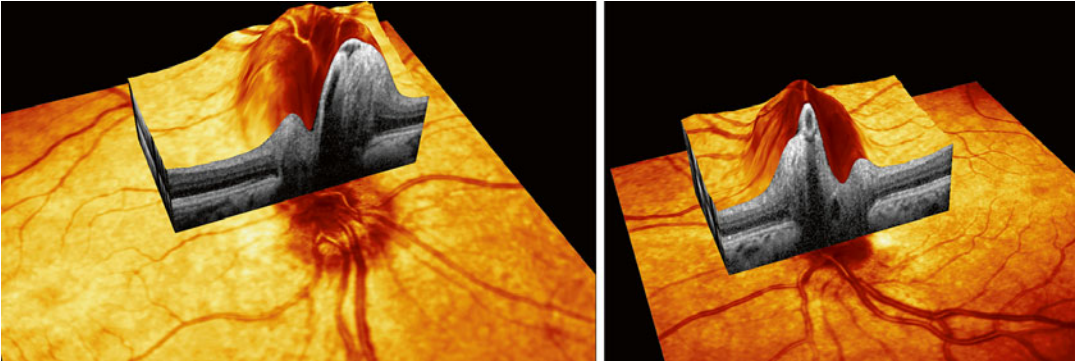


Fig. 5.26 IIH in a 44-year-old female

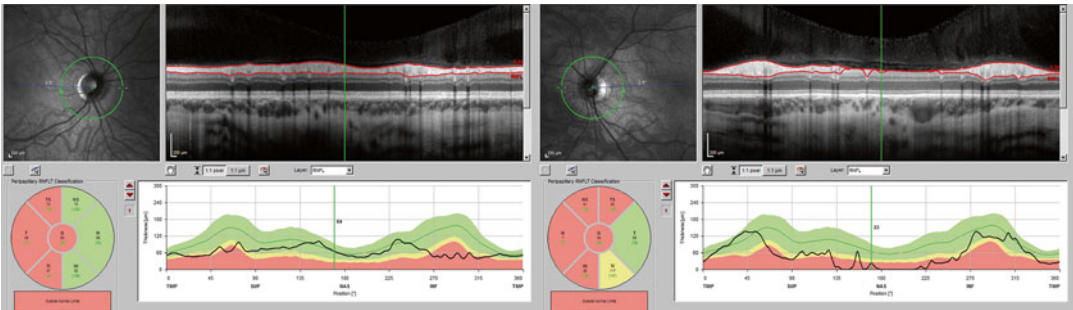


Fig. 5.27 Developmental CNS abnormality associated with inner retinal layer atrophy in a 27-year-old male

inward. For comparison see Fig. 5.11 where Bruch's membrane is angulated outward. She has a diagnosis of idiopathic intracranial hypertension (IIH).

Cerebral Cyst

A 27-year-old man presents with a left homonymous superior quadrantanopia. The OCT showed corresponding loss of the RNFL temporally on the right and nasally on the left. This was caused by a developmental malformation in the visual pathways in the right temporal lobe. The MRI showed a CSF-filled cyst with surrounding polymicrogyria. Note the virtual absence of the RNFL and GCL with preserved INL and ONL in the OCT (Fig. 5.27).

Choroidal Nevus

A 28-year-old female presented with visual snow following use of malaria prophylaxis with atovaquone and proguanil. The cSLO image revealed a choroidal nevus in the middle of the superior arcade on the left (Fig. 5.28). The nevus was flat, without orange pigment, and absence of subretinal fluid on OCT. She remains under observation.

Choroid Plexus Papilloma

Optic atrophy with preservation of the INL in a 21-year-old male who suffered extensive damage to his posterior visual pathways following complicated neurosurgery for a choroid plexus papilloma at the age of 5 years. There was VA OD HM, OS PL.

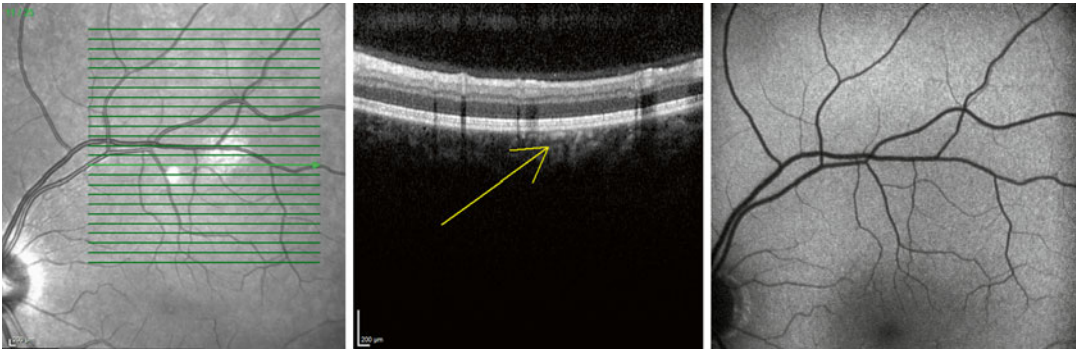


Fig. 5.28 Choroidal nevus (*arrow*) in a 28-year-old female with visual snow

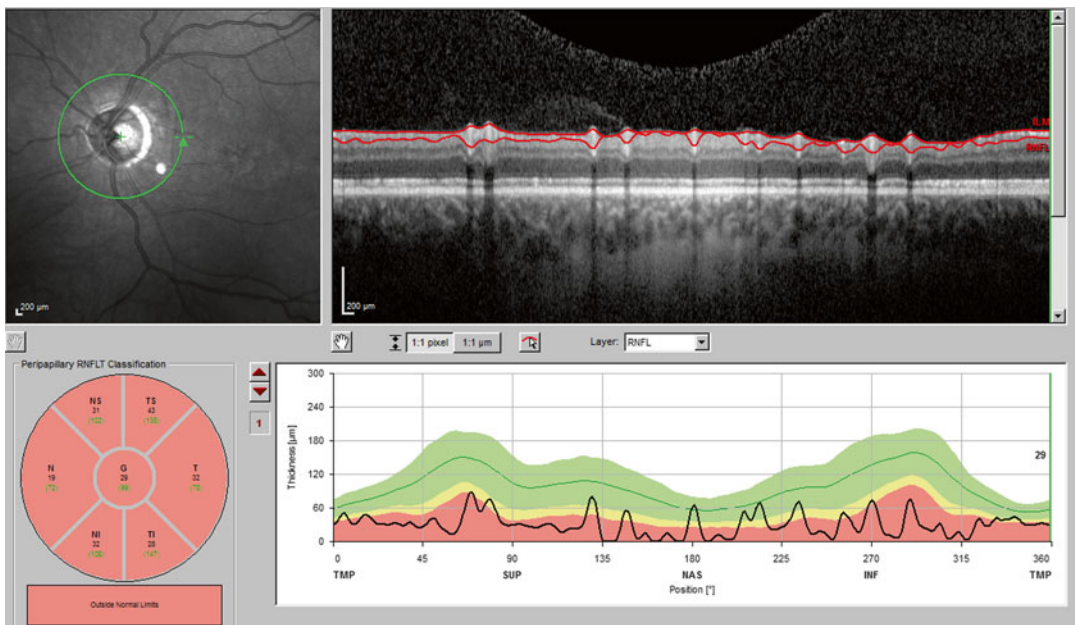


Fig. 5.29 Transsynaptic retrograde axonal degeneration stopping at the INL, in a 21-year-old male with a choroid plexus papilloma

The preservation of the INL in this blind patient strengthens the argument of the preservation of the INL as a physiological barrier to transsynaptic degeneration (Fig. 5.29). Originally described in MS and MSON [32], we have observed it in a larger range of pathologies—some of which are presented in this chapter.

Neurodegenerative Disease

Alzheimer’s Disease

A 67-year-old man was referred with progressive visual loss and cognitive problems.

The retinal OCT demonstrates severe bilateral optic atrophy (Fig. 5.30). There is also widespread loss of ganglion cells. In addition,

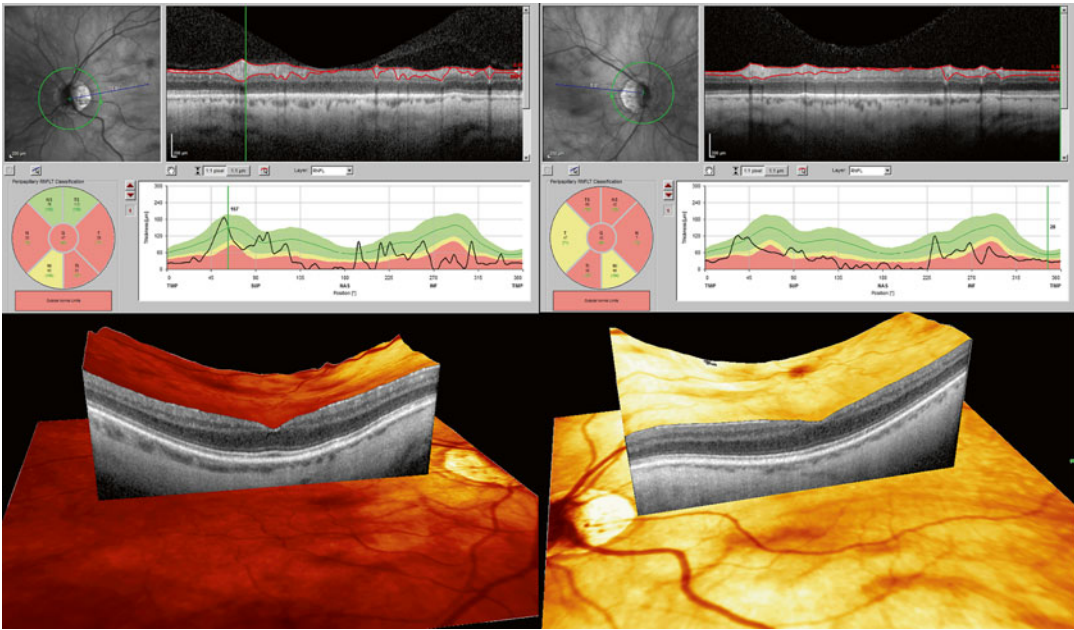


Fig. 5.30 Optic atrophy in a 67-year-old male with Alzheimer's disease

AF suggests reduced reflectivity, which has been discussed as a possible sign of retinal amyloid plaque deposition. Also the choroid was thin, another observation anecdotal ally associated with Alzheimer's disease (AD). Cognitive testing demonstrated reduced functioning in multiple cognitive domains on the CAMCOG psychometric and MRI brain scanning showed globally distributed atrophy. A diagnosis of AD was made and he was started on galantamine.

The OCT findings were seductive, but it appeared that he had visual problems since childhood and optic atrophy had been noted many years back. Taken together, the sequence of events does argue against a causal relationship of optic atrophy and AD in his case. More, the longstanding optic atrophy will mask any possible more subtle degree of retrograde transsynaptic axonal degeneration under current investigation in the scientific literature as a

potential surrogate for neurodegeneration in AD [33].

Corticobasal Degeneration

Optic atrophy is seen in a 58-year-old male with possible corticobasal degeneration (CBD). Rapid loss of praxic skills and cognitive abilities over a 2-year period coincided with progressive dyschromatopsia. The patient has stopped working. There were VA OD 6/6 (20/20), OS 6/12 (20/40) and Ishihara OD 17/17, OS 2/17. There was a left RAPD. Saccades were slow to initiate, hypo-metric, and substituted by head movements.

The OCT shows inner retinal layer atrophy in both eyes (Fig. 5.31). The extent of optic atrophy is suggestive of late-stage retrograde transsynaptic axonal degeneration in the context of more widespread CNS degeneration involving the visual pathways. The yellow arrows indicate the presence of microcysts in the INL indicative of a retrograde maculopathy [30, 31].

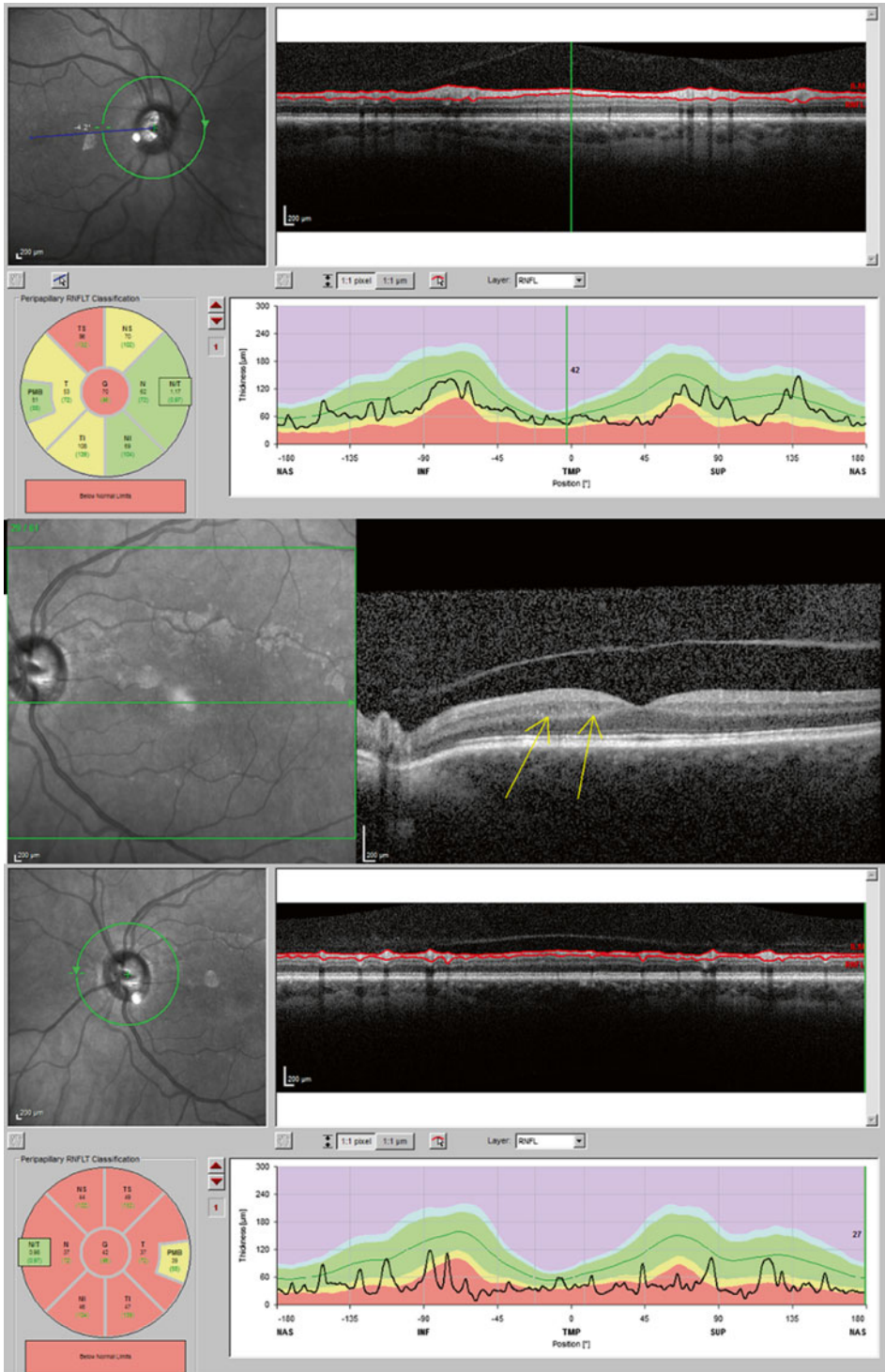


Fig. 5.31 Corticobasal degeneration in a 58-year-old male

Acknowledgment We are grateful for discussions with Dr. Willemien Vries-Knoppert and Professor Stevie Tan. We would like to thank Dr. Yvonne Yong-Heesen (MEWDS) and Dr. Stefan Elferink (neuroretinitis) for sharing their cases.

References

- Petzold A, Wattjes MP, Costello F, et al. The investigation of acute optic neuritis: a review and proposed protocol. *Nat Rev Neurol*. 2014;10:447–58.
- Plant G. Optic neuritis and multiple sclerosis. *Curr Opin Neurol*. 2008;21:16–21.
- Spaide RF, Curcio CA. Anatomical correlates to the bands seen in the outer retina by optical coherence tomography: literature review and model. *Retina (Philadelphia, Pa)*. 2011;31:1609–19.
- Brex P, Ciccarelli O, O’Riordan J, et al. A longitudinal study of abnormalities on MRI and disability from multiple sclerosis. *N Engl J Med*. 2002;346:158–64.
- Petzold A, Pittock S, Lennon V, et al. Neuromyelitis optica-IgG (aquaporin-4) autoantibodies in immune mediated optic neuritis. *J Neurol Neurosurg Psychiatry*. 2010;81:109–11.
- Petzold A, Plant GT. Chronic relapsing inflammatory optic neuropathy: a systematic review of 122 cases reported. *J Neurol*. 2014;261:17–26.
- Plant GT, Sibtain NA, Thomas D. Hyperacute corticosteroid treatment of optic neuritis at the onset of pain may prevent visual loss: a case series. *Mult Scler Int*. 2011;2011:815068.
- Wingerchuk DM, Lennon VA, Lucchinetti CF, et al. The spectrum of neuromyelitis optica. *Lancet Neurol*. 2007;6:805–15.
- Costello F, Hodge W, Pan YI, et al. Tracking retinal nerve fiber layer loss after optic neuritis: a prospective study using optical coherence tomography. *Mult Scler*. 2008;14:893–905.
- Kidd D. The optic chiasm. *Handb Clin Neurol*. 2011;102:185–203.
- Frohman L, Frieman B, Wolansky L. Reversible blindness resulting from optic chiasmitis secondary to systemic lupus erythematosus. *J Neuroophthalmol*. 2001;21:18–21.
- Apkarian P, Bour LJ, Barth PG, et al. Non-decussating retinal-fugal fibre syndrome. An inborn achiasmatic malformation associated with visuotopic misrouting, visual evoked potential ipsilateral asymmetry and nystagmus. *Brain*. 1995;118(Pt 5):1195–216.
- Bessero A-C, Plant GT. Should ‘visual snow’ and persistence of after-images be recognised as a new visual syndrome? *J Neurol Neurosurg Psychiatry*. 2014;85:1057–8.
- Burggraaff MC, Trieu J, de Vries-Knoppert WA, et al. The clinical spectrum of microcystic macular oedema. *Invest Ophthalmol Vis Sci*. 2014;55:952–61.
- Gelfand JM, Cree BA, Nolan R, et al. Microcystic inner nuclear layer abnormalities and neuromyelitis optica. *JAMA Neurol*. 2013;70:629–33.
- Parsa CF, Hoyt WF. Nonarteritic anterior ischemic optic neuropathy (NAION): a misnomer. Rearranging pieces of a puzzle to reveal a nonischemic papillopathy caused by vitreous separation. *Ophthalmology*. 2015;122:439–42.
- Kupersmith MJ, Anderson S, Durbin MK, Kardon RH. Scanning laser polarimetry, but not optical coherence tomography predicts permanent visual field loss in acute non-arteritic anterior ischemic optic neuropathy. *Invest Ophthalmol Vis Sci*. 2013;54:5514–9.
- Petzold A, Islam N, Hu H-H, Plant GT. Embolic and nonembolic transient monocular visual field loss: a clinicopathologic review. *Surv Ophthalmol*. 2013;58:42–62.
- Grutzendler J, Murikinati S, Hiner B, et al. Angiophagy prevents early embolus washout but recanalizes microvessels through embolus extravasation. *Sci Transl Med*. 2014;6:226ra31.
- Khan J, Chong V. Two retinal vein occlusions in a patient with venous tortuosity at the optic disc. *Graefes Arch Clin Exp Ophthalmol*. 2007;245:313–4.
- Jindahra P, Petrie A, Plant GT. Retrograde trans-synaptic retinal ganglion cell loss identified by optical coherence tomography. *Brain*. 2009;132:628–34.
- Jindahra P, Petrie A, Plant GT. The time course of retrograde trans-synaptic degeneration following occipital lobe damage in humans. *Brain*. 2012;135:534–41.
- Kidd D, Beynon HLC. The neurological complications of systemic sarcoidosis. *Sarcoidosis Vasc Diffuse Lung Dis*. 2003;20:85–94.
- Scott TF, Yandora K, Kunschner LJ, Schramke C. Neurosarcoidosis mimicry of multiple sclerosis: clinical, laboratory, and imaging characteristics. *Neurologist*. 2010;16:386–9.
- Bonfioli AA, Damico FM, Curi ALL, Orefice F. Intermediate uveitis. *Semin Ophthalmol*. 2005;20:147–54.
- Matsuoka M, Ogata N, Takahashi K, et al. Two cases of ocular sarcoidosis in which vitreous cytology was useful for supporting the diagnosis. *Clin Ophthalmol*. 2012;6:1207–9.
- Achiron L, Strominger M, Witkin N, Primo S. Sarcoid optic neuropathy: a case report. *J Am Optom Assoc*. 1995;66:646–51.
- Horwitz H, Friis T, Modvig S, et al. Differential diagnoses to MS: experiences from an optic neuritis clinic. *J Neurol*. 2014;261:98–105.
- Hamed L, Glaser J, Gass J, Schatz N. Protracted enlargement of the blind spot in multiple evanescent white dot syndrome. *Arch Ophthalmol*. 1989;107:194–8.
- Abegg M, Dysli M, Wolf S, et al. Microcystic macular edema: retrograde maculopathy caused by optic neuropathy. *Ophthalmology*. 2014;121:142–9.

31. Mahroo OA, Shalchi Z, Kisimbi J, et al. Re: Abegg et al.: Microcystic macular edema: retrograde maculopathy caused by optic neuropathy. *Ophthalmology*. 2014;121:142–9 (Ophthalmology 2014;121:e40).
32. Balk LJ, Twisk JWR, Steenwijk MD, et al. A dam for retrograde axonal degeneration in multiple sclerosis? *J Neurol Neurosurg Psychiatry*. 2014;85:782–9.
33. Marziani E, Pomati S, Ramolfo P, et al. Evaluation of retinal nerve fiber layer and ganglion cell layer thickness in Alzheimer's disease using spectral-domain optical coherence tomography. *Invest Ophthalmol Vis Sci*. 2013;54:5953–8.

Olivier Outteryck and Patrick Vermersch

Introduction

Neuromyelitis optica (NMO) is an inflammatory demyelinating autoimmune disease of the central nervous system (CNS), classically affecting optic nerve(s) uni- or bilaterally and the spinal cord with an extensive involvement. It can be monophasic, but most of the time relapsing. Progressive form seems very rare (<1 %) and questionable. For a long time, NMO has been thought to be a variant of multiple sclerosis (MS), but clinical, neuroimaging, immunological, and pathological findings enable us nowadays to strictly distinguish both of them [1]. NMO affects older people than MS (mean age of 40 years old)—most often female patients (sex ratio F/H=9). Clinical relapse of optic neuritis and myelitis is considered more severe than in MS because of usually incomplete recovery [2, 3]. All patients suffering from neuromyelitis optica (NMO) had a past history of clinical optic neuritis [4]. In the last decade, knowledge about NMO pathophysiology has much improved, notably with the discovery of an NMO-specific autoantibody directed against aquaporin 4 (AQP4) protein, which is the main channel regu-

lating water homeostasis in CNS [5, 6]. New rare phenotypes have also been described, involving the brain in an extensive manner [7, 8] or involving more specifically locations with high expression of AQP4 (periaqueductal, periventricular; [7, 9–11]). More sensitive tests for anti-AQP4 antibody (Ab) detection have been developed [12]. It has been demonstrated that patients presenting only 1 episode of transverse myelitis [13] or 2 or more episodes of isolated optic neuritis [14] being positive for anti-AQP4 Ab have a high risk to develop other severe relapses and NMO. In the same way, up to 5–6 % of patients suffering from chronic relapsing ON or single isolated ON or relapsing isolated ON presented anti-AQP4 Ab [15]. Thus, a concept of high-risk syndrome for clinical NMO conversion has emerged and allowed early therapeutic intervention in a disease where sequelae are the consequence of relapse and not the consequence of progressive lesion accumulation. For all these reasons, NMO criteria have to evolve, and recently the Mayo Clinic Research Group with other international experts proposed modified criteria for neuromyelitis optica spectrum disorders (NMOSD) [16]. This classification should replace the historical notion of Devic disease. In these new proposed criteria, anti-AQP4 Ab detection takes a major place. Thus, patients without ON can be diagnosed as NMOSD.

Except in Asian countries, NMOSD remains a rare disease and more rare than MS. While the

O. Outteryck, MD (✉) • P. Vermersch, MD, PhD
Department of Neurology, Université de Lille
(EA2686), Hôpital Roger Salengro, CHRU Lille,
Lille, France
e-mail: olivier_outteryck@hotmail.com

first optical coherence tomography study (OCT) in MS was published in 1999 [17], the first OCT studies in NMO were published a decade later [18, 19]. As NMOSD is not yet considered as a variant of MS, OCT findings in NMOSD are also quite different from MS. OCT may help to distinguish NMOSD patients from MS patients and appears as a wonderful outcome measure to evaluate retinal axonal loss and efficacy of potential aggressive therapies in NMOSD.

In this review, we will firstly focus on eyes with past history of optic neuritis (ON eyes) in NMOSD and then develop the arguments in favor or against a subclinical retinal axonal loss in non-ON eyes (NON eyes) of NMOSD patients. We will also consider the potential correlations between OCT values and disability and the added value of optic ways magnetic resonance imaging (MRI).

Optic Neuritis Eyes of NMOSD Patients

Most of the published NMOSD studies investigating anterior visual pathways damage by OCT in comparison to healthy controls (HC) or MS patients reported a severe retinal axonal loss versus HC [18–26] and a more severe retinal axonal loss in NMOSD than in MS [19–22, 24, 25, 27–31] as illustrated in Fig. 6.1. One study was interested only in NMOSD patients [32]. Up to now, all OCT studies in NMOSD involved adult patients. No study has been interested in OCT findings of pediatric NMOSD patients.

NMOSD Versus HC

All studies including NMOSD patients and HC demonstrated that peripapillary retinal nerve fiber layer (pRNFL) and total macular volume (TMV)/macular thickness were significantly reduced after 1 or more clinical episodes of ON versus HC. Ratchford et al. reported that a single episode of ON in NMOSD causes an estimated

decrease of 31 μm in pRNFL thickness compared to an estimated decrease of 10 μm in RRMS [20]. All studies reporting subanalysis of pRNFL quadrants reported significant atrophy in all quadrants for comparison of NMOSD and HC [18, 19, 24–26].

NMOSD Versus MS

Most of the studies including NMOSD and MS patients demonstrated that global pRNFL and TMV/macular thickness were significantly reduced after ON in both diseases but with a significant greater extent in NMOSD [19–22, 24, 25, 27, 29, 33], which is in agreement with consideration that ON is clinically more severe in NMOSD than in MS [2, 3]. Moreover visual disability of NMOSD-ON eyes is worse than in MSON eyes [3, 20, 24, 25, 27, 29, 31]. One additional study highlighted no significance but only a trend toward significance about a decreased VA in NMOSD-ON eyes versus MSON eyes [28]. Most of the previous OCT studies in NMOSD did not adjust for the number of clinical ON [19–22, 24, 25, 28, 29, 31] and/or did not perform statistical analysis with generalized estimation equation (GEE) models. The number of ON episodes increases the retinal axonal loss [29] and GEE is the best adapted statistical test for data with hierarchical structure including clusters of eyes on an individual level. Nevertheless, 1 study involving NMOSD and MS patients with only 1 MSON episode showed a greater pRNFL decrease in NMOSD [20] and another one with adjustment to the number of ON episodes showed more global pRNFL in NMOSD [27].

If post-ON retinal axonal loss seems to be higher in NMOSD than in MS, it seems not to involve all pRNFL quadrants with the same magnitude or as in MS. Compared to MS patients, NMOSD patients present frequently an inferior [19, 22, 24, 25, 27, 29] and a superior [22, 24, 27, 29] pRNFL atrophy after ON. Since temporal pRNFL atrophy is predominant in MSON eyes, comparison of NMOSD-ON eyes and MSON eyes rarely found more marked temporal pRNFL atrophy in NMOSD-ON eyes [19, 24, 25].

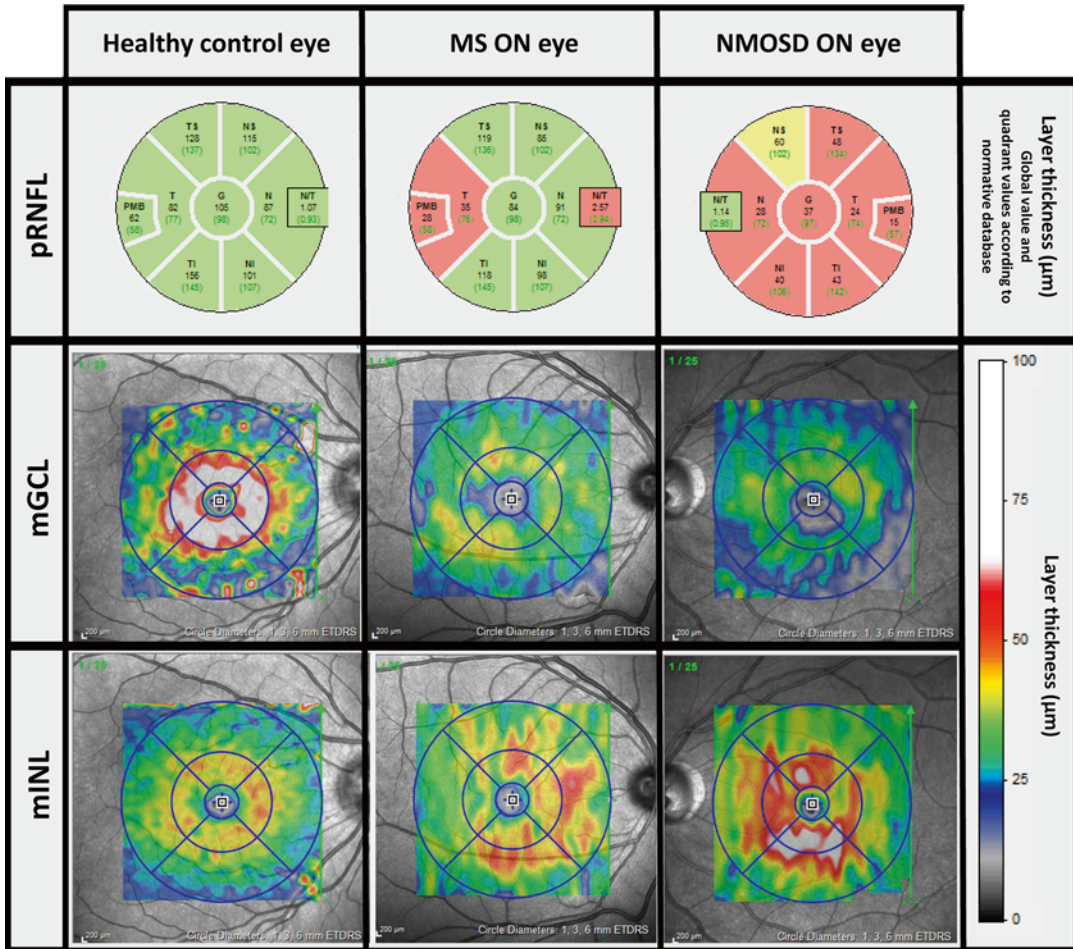


Fig. 6.1 Peripapillary and macular OCT scan from a healthy control (HC; female 30 years old), a multiple sclerosis associated optic neuritis eye (MSON eye; female 32 years old), and a neuromyelitis optica spectrum disorder associated optic neuritis eye (NMOSD-ON eye; 28 years old). MS and NMOSD-ON eyes suffered from 1 episode of clinical ON. Patients' ON eyes presented peripapillary

retinal nerve fiber layer (*pRNFL*), macular ganglion cells layer (*mGCL*) atrophy, and macular inner nuclear layer (*mINL*) thickening versus HC. In MSON eye, *pRNFL* atrophy predominates on temporal quadrant with an increased nasal/temporal (*N/T*) ratio. In NMOSD-ON eye, all *pRNFL* quadrants are involved by atrophic process and *N/T* ratio is normal

Merle et al. found temporal *pRNFL* atrophy in NMOSD eyes versus MS eyes but ON and NON eyes were mixed for both populations [19]. Interestingly nasal/temporal (*N/T*) *pRNFL* ratio in NMOSD remains in normal range [24, 26] arguing in favor of a more overall atrophy in NMOSD than in RRMS.

Only three studies did not show significant difference in retinal atrophy between NMOSD and MS [23, 26, 34]. In the first study, the authors compared ON eyes affected by only 1 episode of

ON between NMOSD and MS and showed no difference in macular RNFL and GCIP thicknesses. However, INL thickness of NMOSD population was significantly thicker than in the MS population, and the NMOSD population closed to that already published in another paper [22] presented significantly more *pRNFL* atrophy than MS. The second study [34] did not highlight significant *pRNFL* differences between ON eyes of NMOSD and MS ($p=0.46$). Indeed, it seems that patients with NMOSD presented more ON

episodes than MS patients. The third study [26] found pRNFL thinning in some nasal quadrants with a TMV decreasing in NMOSD versus MS, but after adjustment, notably including the number of ON episodes in GEE analysis, differences did not persist any longer.

It remains quite difficult to summarize all previously referenced NMOSD-OCT studies because all of them have not included MS patients or HC and because comparison sometimes included mixed MSON and NON eyes or specifically investigated MSON eyes or NON eyes or both.

Microcystic Macular Edema

For highlighting microcystic macular edema (MME), it is mandatory to perform OCT with a 4th-generation OCT (spectral-domain OCT). In MS, MME might occur in the absence of any clinical MSON episode [35–37]. However, these three studies did not report optic nerve imaging of the MME eye without MSON, and it is difficult to consider that MME and severe pRNFL thinning could be due to only retrograde transsynaptic degeneration. Five studies investigated specifically or reported MME in NMOSD. All these studies showed that NMOSD patients with MME have always presented at least 1 clinical episode of ON [24, 26, 30, 32, 36]. MME is most often located in the inner nuclear layer (INL) and sometimes the inner plexiform layer (IPL). It is not specific of neuroinflammatory diseases [38], but it is a marker of severe optic neuropathy as illustrated in an NMOSD patient in Fig. 6.2a–e.

The proportion of NMOSD patients presenting MME is ranged between 8.7 and 25.6 % and the proportion of NMOSD-ON eyes with MME between 6.3 and 29.8 % [24, 26, 30, 32, 36] (Table 6.1) [19, 21, 24, 26, 30, 32, 35–39]. MME seems more frequently observed in NMOSD than in MS [32, 36]. NMOSD patients with MME presented thinner pRNFL than NMOSD patients without MME [32]. In agreement with this last finding, it has been shown that patients with MME have presented more episodes of ON than those without, but these latter were younger [30]. All

pathologies included MS, CRION, and Whatever the cause of ON (MS, NMOSD, Chronic Relapsing Inflammatory Optic Neuropathy) is, MME is associated with a thinner pRNFL than the contralateral eye not affected by ON, but not with a lower total macular volume [36]—probably because of the slight INL thickening observed on ON eyes in this cohort. In MS, INL thickening is observed in MME eyes but also in MSON eyes without MME compared to contralateral NON eyes [35]. Fernandes et al. did not report MME in their cohort but interestingly reported the same INL thickening in NMOSD eyes with only 1 episode of ON versus HC but also versus MS patients with only 1 episode of MSON [23]. INL thickening seems to be of greater magnitude in NMOSD versus MS. MME is not always highlighted on an OCT scan, whereas ocular fundus may show macular changes (Fig. 6.2c–e). Inner nuclear layer thickening may be the ultimate step before microcyst formation.

In MS, the “outer” retinal layers (ORL; INL to photo receptor layer) seem not to be involved in the retinal atrophic process [21, 26, 40]. Balk and coworkers discussed a potential retinal neuroplasticity [40, 41]. In NMOSD, the same external retinal conservation has been found [26] whereas the thickness of ONL, which takes part of ORL, has been reported significantly increased in NMOSD-ON eyes presenting MME [24]. A recent study coupling OCT and optic nerve imaging in a MS/NMOSD/idiopathic ON cohort suggested that optic nerve with clinical or subclinical T2 lesion might be associated with an INL and ONL thickening whatever the presence of MME [42]. If ORL in NMOSD-ON eyes did not suffer from a retinal atrophic process, a thickening process may be discussed.

Non-optic Neuritis Eyes of NMOSD Patients: Is There Any Subclinical Retinal Involvement in NMOSD?

If a large majority of OCT studies considered that NMOSD patients affected by ON presented a more severe retinal atrophy than MS patients, subclinical retinal axonal loss in NMOSD is more

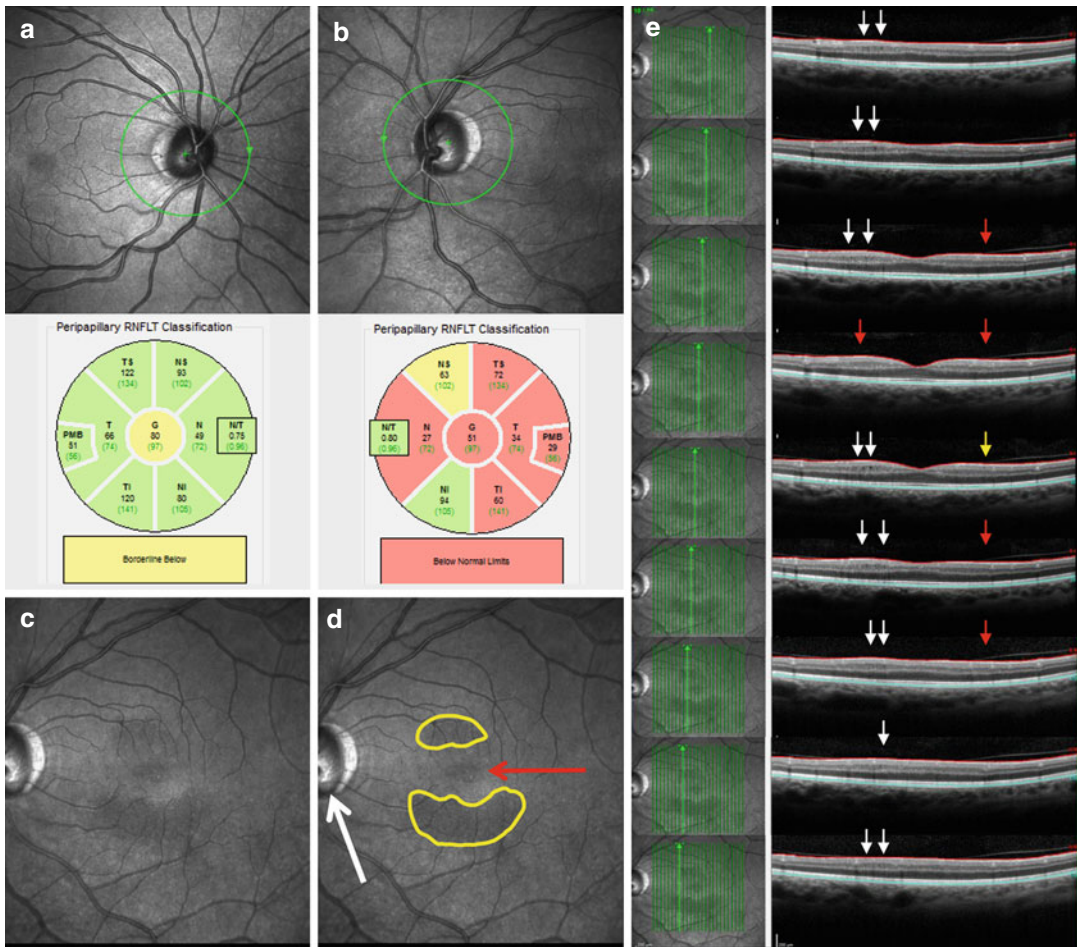


Fig. 6.2 Peripapillary and macular OCT scan from an NMOSD patient who alternatively experienced multiple optic neuritis on both sides. Clinical episodes were more severe on the left side. **(a)** Right peripapillary OCT scan showing slight pRNFL atrophy and normal N/T pRNFL ratio. **(b)** Left peripapillary OCT scan showing profound pRNFL atrophy and normal N/T pRNFL ratio. **(c)** Ocular fundus OCT image centered on fovea showing macular changes. **(d)** Ocular fundus OCT image centered on fovea

(red arrow) showing macular changes (circled in yellow) and papilla (white arrow). **(e)** Vertical OCT macular scans showing microcystic macular edema (MME) in the inner nuclear layer (white arrows) and in the inner plexiform layer (yellow arrow). Red arrows indicated areas without any individualized cystic lesions typical of MME at a location with macular changes on ocular fundus (possible INL thickening)

discussed. Only studies including HC [18–26] enable us to really discuss whether or not a sub-clinical retinal axonal loss in NMOSD exists. However, Park et al. [25] did not show interest in NMOSD-NON eyes, and in two other studies [22, 23], all NMOSD eyes presented past history of ON. Regardless of the very few patients without ON in the NMOSD group, the French collaborative work was not able to do a statistical comparison, but pRNFL values between HC and

NMOSD-NON eyes were very comparable [18]. Global peripapillary RNFL [24, 34] and total macular volume [24] of NMOSD-NON eyes appear in some studies similar to HC eyes. In other studies, macular involvement in NMOSD-NON eyes is highlighted [21, 26, 30]. GCIP [21, 30], average macular thicknesses/TMV [21, 30], and GCL volume [26] are reduced in NMOSD-NON eyes versus HC. Merle et al. [19] showed that global pRNFL value was significantly

Table 6.1 Clinical and OCT characteristics of eyes with or without optic neuritis in NMOSD and MS [19, 21, 24, 26, 30, 32, 35–39]

Disease	Optic neuritis eyes		Non-optic neuritis eyes	
	NMOSD ^a	MS ^b	NMOSD ^a	MS ^b
Visual disability	Moderate to severe	Slight to severe	Absent	Slight
pRNFL thickness	↘↘↘	↘↘ ^c	= ^d	↘ ^c
Nasal/temporal ratio	=	↗↗	=	↗
Total macular volume	↘↘↘	↘↘	= ^d	↘
Inner retinal layer volume	↘↘↘	↘↘	= ^d	↘
Outer retinal layer volume	↗	↗	=	=
Median proportion of eyes with microcystic macular edema ^e	20 % [6.3–29.8]	4.42 % [0–6.4]	0 % [0–0]	0.2 % [0–2.7]

Macular inner retinal layers (IRL) include retinal nerve fiber layer (RNFL), ganglion cell layer (GCL), and inner plexiform layer (IPL). Macular outer retinal layers (ORL) include inner nuclear layer (INL), outer plexiform layer (OPL), and outer nuclear layer (ONL)

NMOSD neuromyelitis optica spectrum disorder, MS multiple sclerosis, pRNFL peripapillary retinal nerve fiber layer

^aReferences for NMOSD: Gelfand et al. [32], Sortichos et al. [30], Schneider et al. [24], Kaufhold et al. [36], Outteryck et al. [26]

^bReferences for MS: Gelfand et al. [39], Saidha et al. [35], Kaufhold et al. [36], Burggraaff et al. [37], Schneider et al. [24], Abegg et al. [38]

^cPredominantly in temporal quadrant

^dFew papers reported subclinical retinal axonal loss in NMOSD on pRNFL (Merle et al. [19]) or macular parameters (Syc et al. [21], Sortichos et al. [30], Outteryck et al. [26]). Subclinical retinal axonal loss in NMOSD remains matter of debate but seems of lower extent than in MS

^eBy considering the patient as statistical unit, macrocystic macular edema is reported in 20 % (8.7–25.6) within NMOSD patients and in 3 % (2.7–6.1) within MS patients. These percentages depend in each cohort on the number of included MS patients without past history of optic neuritis and on the number of included NMOSD patients with only spinal cord involvement

reduced in NMOSD-NON eyes versus HC, and a recent work [26] only found significant atrophy in temporal and naso-inferior quadrants of pRNFL.

If subclinical retinal involvement may be discussed in NMOSD, it seems that it is probably of a lesser extent than in MS since it has been reported that there are lower global pRNFL [27] and temporal pRNFL [26] values in MS-NON eyes than in NMOSD-NON eyes.

Astroglial cells and Müller cells are AQP4-expressing cells. Müller cells are located inside the retina and astroglial cells inside the RNFL and the optic nerve [43, 44] but also in the chiasma, optic tract, and brain. Without any clinical ON episode, anti-AQP4 Ab may induce their pathological process directly on these cells inside the different retinal layers (astrocytes and Müller cells) and on the rest of the optic ways (astrocytes). Some NMOSD studies have already described extensive [8] or more located brain abnormalities [7, 10], particularly in the brainstem and near the lateral ventricles where the lateral geniculate nucleus and the posterior part

of optic radiations (OR) are located, respectively. As it has been demonstrated in MS [45], a retrograde transsynaptic degenerative process cannot be excluded in NMOSD.

How Could OCT Help to Distinguish NMOSD and MS?

Firstly, we propose to focus on ON eyes and what could be in favor of NMOSD (versus MS) is the presence of more severe pRNFL atrophy in global analysis but more particularly in another quadrant than temporal quadrant and a more frequent maculopathy (more atrophy, more MMO) associated with worse visual disability. Secondly, we propose to focus on NON eyes and an absence of temporal pRNFL atrophy would be in favor of NMOSD. In Table 6.1, the main results of OCT studies in NMOSD and MS are summarized.

Kim recently proposed that after a first episode of ON, global pRNFL less than 78.9 μm associ-

ated with a high-contrast visual acuity of less than 0.4 logMar leads to a specificity of 100 % in favor of NMOSD diagnostic [33].

Further multicentric collaborative studies with spectral-domain OCT and larger cohorts would be able to examine the question in more detail and to confirm or not the results of all previous exploratory OCT studies in NMOSD.

OCT and Magnetic Resonance Imaging in NMOSD

Another imaging biomarker that may help to distinguish these two diseases is optic nerve magnetic resonance imaging (MRI). In NMOSD, demyelinating lesion seen on MRI may involve more frequently the posterior part of the optic nerve and the chiasma [46, 47] with a greater extent [47] than in MS. To date no study has coupled optic nerve MRI and OCT assessments in NMOSD. One could expect that T2 lesion length in NMOSD may be higher in NMOSD than in MS, but these 2 latter studies with semiquantitative measurements remain contradictory. It was recently shown that 3D Double Inversion Recovery (DIR) sequence was superior to coronal 2D Short Tau Inversion Recovery - Fluid Attenuated Inversion Recovery (STIR-FLAIR) sequence in the detection of T2 optic nerve lesion [48]. This 3D sequence allows a direct T2 hyper-signal length measurement, strongly associated with retinal axonal loss in a MS/NMOSD/idiopathic ON cohort [42] as illustrated in an NMOSD patient in Fig. 6.3a–e.

If similar metabolic measurement by proton(H⁺)-magnetic resonance spectroscopy (H-MRS) in NMOSD and HC argued in favor of brain white matter (WM) sparing in NMOSD [49], many diffusion tensor imaging (DTI) studies [50] showed altered DTI parameters in NMOSD versus HC in many tracts and notably optic radiations [50–53]. In addition, voxel-based morphometry studies [50, 54–56] showed atrophic process in WM and grey matter of NMOSD patients. Recently, a Brazilian study group showed for the first time a high correlation between average pRNFL thickness and perical-

carine cortical thickness [56]. In this study, many other cortical areas were reduced in NMOSD versus HC. In MS associated ON, a relationship between retinal thicknesses and occipital cortex thickness seems to be weaker [40, 41].

Disability in NMOSD and OCT Correlations

In NMOSD, mild to very good correlations between retinal thicknesses (peripapillary RNFL and/or macular thicknesses) and visual disability, scored by high-contrast visual acuity or low-contrast visual acuity or visual field or P100 latency, have been found [18–22, 24, 26, 29]. These correlations were stronger and more likely to be observed specifically in the ON eye group.

Correlation studies between OCT values and EDSS remain contradictory. Very few studies investigated this issue [18, 19, 26, 34, 56]. No [19] or moderate correlations with trend toward significance (pRNFL in ON eyes [34]) or moderate significant correlations between EDSS (visual FS included) and few OCT parameters (TMV and GCC [26]) but also excellent correlation (global pRNFL/EDSS without visual FS [18], global pRNFL/EDSS [56]) have been reported. No correlations were observed by focusing on NON eyes [26, 34]. Furthermore, NMOSD patients with MME did not present higher clinical disability [30]. Since there are an obvious link between disease duration and the age of the patient but also the probability for the patient to present with an ON episode, lower RNFL values were reported significantly associated with longer disease duration [34]. Expanded disability status scale is a disability scale established for MS patients [57]. It includes visual, brainstem, pyramidal, sensory, cerebellar, bladder/bowel, and cognitive functional scores. It does not seem to be the best adapted disability scale for NMOSD, whereas it is the most widely used. Neurologists are used to performing EDSS scores during their consultation and other disability scales require more time to be performed. There is a need for the development of a more specific disability scale in NMOSD [58]. A more specific

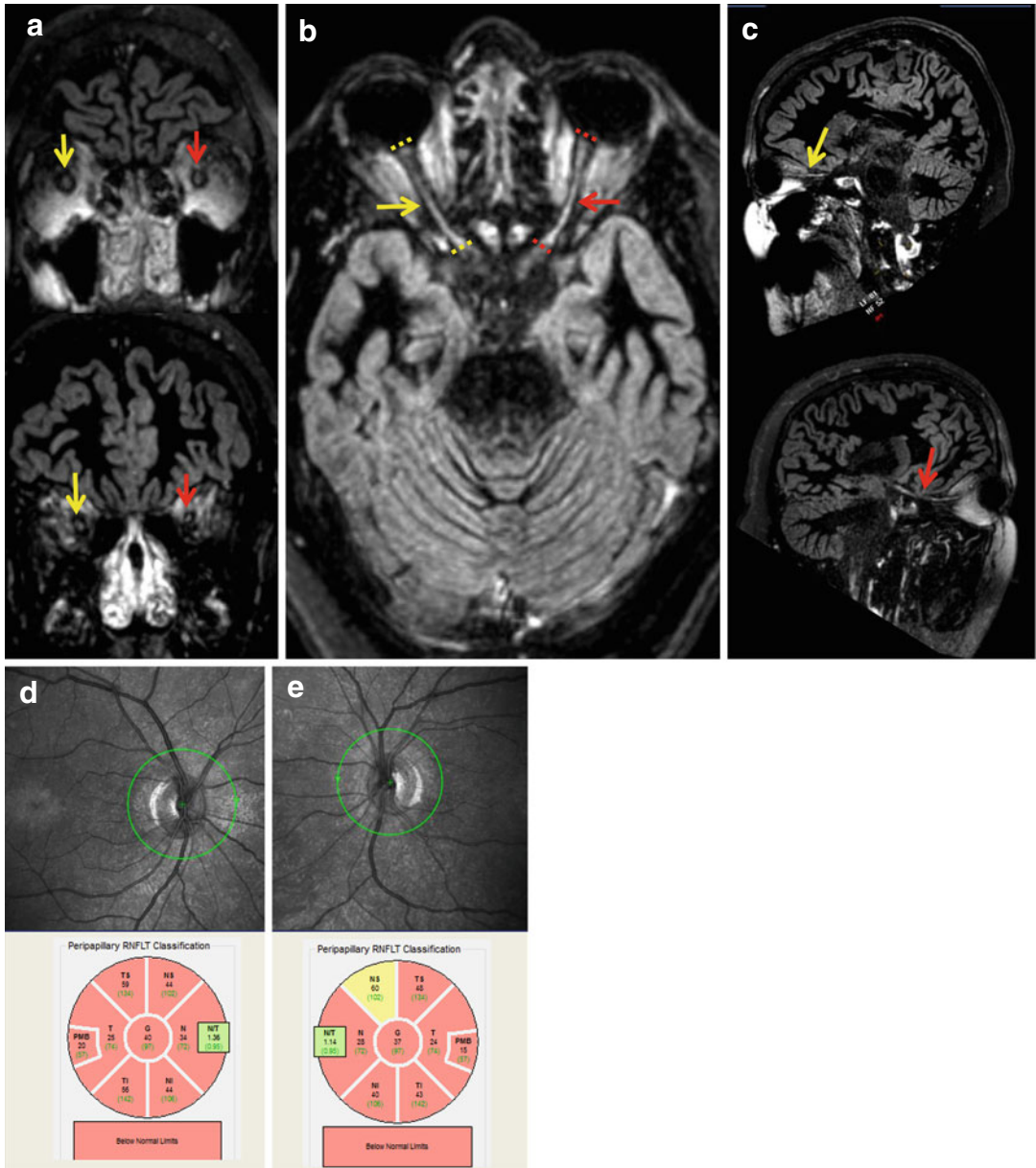


Fig. 6.3 Brain 3D double inversion recovery (DIR) MRI sequence and peripapillary OCT scans of an NMOSD patient with past history of severe bilateral optic neuritis. (a) Coronal reconstruction centered on optic nerves showing bilateral T2 hyperintensities (yellow and red arrows for the right and left optic nerves, respectively) in retrobulbar (top image) and orbital (bottom image) portions. (b) Axial reconstruction showing bilateral extended T2 hyperintensities on optic nerves. The length of T2 hyperintense lesion measured between both colored dotted lines

is 38 mm for both sides. (c) Oblique reconstruction along the right (yellow arrow) and the left (red arrow) optic nerves showing extended T2 hyperintensities. (d) Right profound global pRNFL atrophy (40 μ m) with nasal/temporal pRNFL ratio in normal ranges according to Heidelberg Spectralis Healthy Controls database. (e) Left profound global pRNFL atrophy (37 μ m) with nasal/temporal pRNFL ratio in normal ranges according to Heidelberg Spectralis Healthy Controls database

disability scale may be validated in the future but, OCT will probably remain a better biomarker of brain axonal loss in MS than in NMOSD.

Follow-Up Study of NMOSD Population

There is only one study reporting longitudinal OCT follow-up in NMOSD population [59]. With 3rd-generation OCT (time domain), the authors found significant retinal axonal loss in global pRNFL and all 4 classical pRNFL quadrants by comparing 2 different OCT assessments of a NMOSD cohort ($n=30$). The 2 OCT assessments were spaced 18 months in mean. Retinal axonal loss was only observed on eyes affected by ON previous to the first assessment and may occur independently of relapses (ON or not) during the follow-up. This pRNFL decreasing is difficult to explain but we can make different hypotheses. Peripapillary RNFL decreasing may be secondary to ON that occurred previous to the first assessment (<3 months after relapse) because pRNFL decrease in MSON eyes begins at the third month and seems maximal at 6 months, with some data in favor of a continuing axonal loss in the affected eye for at least 12 months [60, 61]. The authors argued also that new ON occurring in ON eyes have potentially been missed by both patient and neurologist and that few patients presented ON during the follow-up. Up to now, no OCT study with SD-OCT and longitudinal NMOSD follow-up has been published. Because of its higher definition (<5 μm) and higher reproducibility [62, 63], SD-OCT will be better than TD-OCT to appreciate retinal axonal loss in a follow-up study.

Difficulties of OCT Studies in NMOSD

Optical coherence tomography studies in NMOSD remain more difficult to perform than in MS. NMOSD is a rare disease and most of the monocentric studies already published included small-sized population ($n<30$). Multicentric OCT studies have to emerge in NMOSD in order

to increase the power of statistical analyses, but an additional difficulty in a multicenter study will be to perform OCT scans with the same 4th-generation OCT device. However, the Baltimore OCT study group recently showed a good concordance between CIRRUS (Zeiss) and Spectralis (Heidelberg) OCT scan for retinal segmentation using an open source segmentation algorithm [64].

Optic neuritis in NMOSD are more severe than MS and, in spite of aggressive therapeutic management, it is not unusual to observe severe sequelae and some cases of blindness. It has been previously reported that up to 54 % of NMOSD-ON eyes with monophasic disease course were totally blind [2] and that bilateral severe visual loss (<1/10) appeared in a median time of 13 years [3]. Weak residual visual function after ON leads to difficulty in the acquisition of OCT and to an OCT of lesser quality.

Another difficulty is to know if we have to consider anti-AQP4 Ab-negative and Ab-positive patients together or if they are two different types of NMOSD disease. Recently, it has been discussed that NMOSD patients negative for anti-AQP4 Ab could have anti-myelin-oligodendrocytes-glycoprotein Ab [65] or that NMOSD patients could have both anti-AQP4 and anti-KIR4.1 Ab [66]. Kir4.1 is a ubiquitous potassium channel notably coexpressed with AQP4 by Müller cells.

Indeed, NMOSD patients are older than MS patients. Older patients have greater chance to have other confounding ocular pathologies and naturally thinner retinal thickness [67]. Obviously, complete ophthalmological evaluations may exclude these confounding factors.

NMOSD is more frequent in Asian countries and Afro-Caribbean populations [1]. Peripapillary RNFL thickness and macular volume are known to vary according to ethnic origin [68–70]. As an example, Asian, Hispanic, and Indian people have thicker pRNFL than European people. Thus, cautiousness is required for comparing OCT studies with Caucasian patients and OCT studies with Asian patients. It has to be taken into account when matching to HC or MS patients is performed—notably for future multicentric studies.

Advantages of OCT Studies in NMOSD

Benign MS are very rare in NMOSD. Thus it seems unlikely to miss (physician) or to forget (the patient) any ON episode. It is very important in OCT study to know how many ON episodes occurred because the more ON episodes occur, the more atrophy you observed.

Subclinical retinal involvement (directly within the retina or as a result of optic ways involvement) remains discussed in NMOSD and very probably of a lesser extent in NMOSD than in MS. In MS, it is difficult to know if retinal atrophy occurring without any clinical episode of ON is due to subclinical MSON or to axonal retrograde transsynaptic degeneration. For testing potential neuroprotective drugs at the acute phase of ON, this could be an advantage of studies in NMOSD versus studies in MS.

Conclusion

OCT is a wonderful tool for evaluating retinal axonal secondary to ON in neuroinflammatory diseases affecting the optic nerve—notably NMOSD. OCT may help to differentiate NMOSD and MS. In future NMOSD therapeutic trials, OCT has to be an evaluation criterion. Multimodal studies (OCT, optic nerve and brain MRI, visual evoked potentials) are still lacking in NMOSD and are necessary to better understand the optic ways involvement in NMOSD. Multicentric follow-up studies will be able to clearly confirm or not a subclinical axonal loss in NMOSD, particularly in macula.

References

1. Wingerchuk DM, Lennon VA, Luchinetti CF, et al. The spectrum of neuromyelitis optica. *Lancet Neurol*. 2007;6:805–15.
2. Wingerchuk DM, Hogancamp WF, O'Brien PC, et al. The clinical course of neuromyelitis optica (Devic's syndrome). *Neurology*. 1999;53:1107–14.
3. Merle H, Olindo S, Bonnan M, et al. Natural history of the visual impairment of relapsing neuromyelitis optica. *Ophthalmology*. 2007;114:810–5.
4. Wingerchuk DM, Lennon VA, Pittock SJ. Revised diagnostic criteria for neuromyelitis optica. *Neurology*. 2006;66:1485–9.
5. Lennon VA, Wingerchuk DM, Kryzer TJ, et al. A serum autoantibody marker of neuromyelitis optica: distinction from multiple sclerosis. *Lancet*. 2004;364:2106–12.
6. Lennon VA, Kryzer TJ, Pittock SJ, et al. IgG marker of spinal multiple sclerosis binds to the aquaporin-4 water channel. *J Exp Med*. 2005;202:473–7.
7. Pittock SJ, Weinshenker BG, Luchinetti CF, et al. Neuromyelitis optica brain lesions localized at sites of high aquaporin 4 expression. *Arch Neurol*. 2006;63:964–8.
8. Ayrignac X, Daliere CC, Nerrant E, et al. Extensive cerebral white matter involvement in a patient with NMO spectrum disorder. *Mult Scler*. 2014;20:1401–3.
9. Nakashima I, Fujihara K, Miyazawa I, et al. Clinical and MRI features of Japanese patients with multiple sclerosis positive for NMO-IgG. *J Neurol Neurosurg Psychiatry*. 2006;77:1073–5.
10. Banker P, Sonni S, Kister I, et al. Pencil-thin ependymal enhancement in neuromyelitis optica spectrum disorders. *Mult Scler*. 2012;18:1050–3.
11. Appiwattanakul M, Popescu BF, Matiello M, et al. Intractable vomiting as the initial presentation of neuromyelitis optica. *Ann Neurol*. 2010;68:757–61.
12. Höfteberger R, Sabater L, Marignier R, et al. An optimized immunohistochemistry technique improves NMO-IgG detection: study comparison with cell-based assays. *PLoS One*. 2013;8, e79083.
13. Weinshenker BG, Wingerchuk DM, Vukusic S, et al. Neuromyelitis optica IgG predicts relapse after longitudinally extensive transverse myelitis. *Ann Neurol*. 2006;59:566–9.
14. Matiello M, Lennon VA, Jacob A, et al. NMO-IgG predicts the outcome of recurrent optic neuritis. *Neurology*. 2008;70:2197–200.
15. Petzold A, Pittock S, Lennon V, Maggiore C, Weinshenker BG, Plant GT. Neuromyelitis optica-IgG (aquaporin-4) autoantibodies in immune mediated optic neuritis. *J Neurol Neurosurg Psychiatry*. 2010;81:109–11.
16. Wingerchuk DM, Banwell B, Bennett JL, et al. International consensus diagnostic criteria for neuromyelitis optica spectrum disorders. *Neurology*. 2015 Jun 19. pii: 10.1212/WNL.0000000000001729. [Epub ahead of print].
17. Parisi V, Manni G, Spadaro M, Colacino G, Restuccia R, Marchi S, et al. Correlation between morphological and functional retinal impairment in multiple sclerosis patients. *Invest Ophthalmol Vis Sci*. 1999;40(11):2520–7.
18. de Seze J, Blanc F, Jeanjean L, Zéphir H, Labauge P, Bouyon M, et al. Optical coherence tomography in neuromyelitis optica. *Arch Neurol*. 2008;65(7):920–3.
19. Merle H, Olindo S, Donnio A, et al. Retinal nerve fiber layer thickness in neuromyelitis optica. *Invest Ophthalmol Vis Sci*. 2008;49:4412–7.

20. Ratchford JN, Quigg ME, Conger A, et al. Optical coherence tomography helps differentiate neuromyelitis optica and MS optic neuropathies. *Neurology*. 2009;73:302–8.
21. Syc SB, Saidha S, Newsome SD, et al. Optical coherence tomography segmentation reveals ganglion cell layer pathology after optic neuritis. *Brain*. 2012;135:521–33.
22. Monteiro ML, Fernandes DB, Apóstolos-Pereira SL, Callegaro D. Quantification of retinal neural loss in patients with neuromyelitis optica and multiple sclerosis with or without optic neuritis using Fourier-domain optical coherence tomography. *Invest Ophthalmol Vis Sci*. 2012;53(7):3959–66.
23. Fernandes DB, Raza AS, Nogueira RGF, et al. Evaluation of inner retinal layers in patients with multiple sclerosis of neuromyelitis optica using optical coherence tomography. *Ophthalmology*. 2013;120:387–94.
24. Schneider E, Zimmermann H, Oberwahrenbrock T, et al. Optical coherence tomography reveals distinct patterns of retinal damage in neuromyelitis optica and multiple sclerosis. *PLoS One*. 2013;8(6):e66151.
25. Park KA, Kim J, Oh YS. Analysis of spectral domain optical coherence tomography measurements in optic neuritis: differences in neuromyelitis optica, multiple sclerosis, isolated optic neuritis and normal healthy controls. *Acta Ophthalmol*. 2014;92:e57–65.
26. Outteryck O, Majed B, Defoort-Dhellemmes S, Vermersch P, Zéphir H. A comparative optical coherence tomography study in neuromyelitis optica spectrum disorder and multiple sclerosis. *Mult Scler*. 2015 Mar 31. pii: 1352458515578888. [Epub ahead of print]
27. Naismith RT, Tutlam NT, Xu J, et al. Optical coherence tomography differs in neuromyelitis optica compared with multiple sclerosis. *Neurology*. 2009;72:1077–82.
28. Green AJ, Cree BA. Distinctive retinal fibre layer and vascular changes in neuromyelitis optica following optic neuritis. *J Neurol Neurosurg Psychiatry*. 2009;80:1002–5.
29. Nakamura M, Nakazawa T, Doi H, et al. Early high dose intravenous methylprednisolone is effective in preserving retinal nerve fiber layer thickness in patients with neuromyelitis optica. *Graefes Arch Clin Exp Ophthalmol*. 2010;248:1777–85.
30. Sortichos ES, Saidha S, Byraiah G, et al. In vivo identification of morphologic retinal abnormalities in neuromyelitis optica. *Neurology*. 2013;80:1406–14.
31. Bichuetti DB, de Camargo AS, Falcao AB, et al. The retinal nerve fiber layer of patients with neuromyelitis optica and chronic relapsing optic neuritis is more severely damaged than patients with multiple sclerosis. *J Neuroophthalmol*. 2013;33:220–4.
32. Gelfand JM, Cree BA, Nolan R, et al. Microcystic inner nuclear layer abnormalities and neuromyelitis optica. *JAMA Neurol*. 2013;70:629–33.
33. Kim NH, Shin JY, Jeong KS, Cho JY and Kim HJ. Optical coherence tomography after first optic neuritis for the differentiation between neuromyelitis optica and multiple sclerosis. Poster 677, ECTRIMS/ACTRIMS 2014 at Boston.
34. Lange AP, Sadjadi R, Zhu F, et al. Spectral-domain optical coherence tomography of retinal nerve fiber layer thickness in NMO patients. *J Neuroophthalmol*. 2013;33:213–9.
35. Saidha S, Sortichos ES, Ibrahim MA, et al. Microcystic macular oedema, thickness of the inner nuclear layer of the retina, and disease characteristics in multiple sclerosis: a retrospective study. *Lancet Neurol*. 2012;11:963–72.
36. Kaufhold F, Zimmermann H, Schneider E, et al. Optic neuritis is associated with inner nuclear layer thickening and microcystic macular edema independently of multiple sclerosis. *PLoS One*. 2013;8, e71145.
37. Burggraaff MC, Trieu J, de Vries-Knopert WA, Balk L, Petzold A. The clinical spectrum of microcystic macular edema. *Invest Ophthalmol Vis Sci*. 2014;55:952–61.
38. Abegg M, Dysli M, Wolf S, et al. Microcystic macular edema. Retrograde maculopathy caused by optic neuropathy. *Ophthalmology*. 2014;121:142–9.
39. Gelfand JM, Nolan R, Schwartz DM, et al. Microcystic macular oedema in multiple sclerosis is associated with disease severity. *Brain*. 2012;135:1786–93.
40. Balk LJ, Steenwijk MD, Tewarie P, Daams M, Killestein J, Wattjes MP, Vrenkern H, Barkhof F, Polman CH, Uitdehaag BMJ, Petzold A. Bidirectional trans-synaptic axonal degeneration in the visual pathway in multiple sclerosis. *J Neurol Neurosurg Psychiatry*. 2015;86(4):419–24.
41. Balk LJ, Twisk JW, Steenwijk MD, Daams M, Tewarie P, Killestein J, et al. A dam for retrograde axonal degeneration in multiple sclerosis? *J Neurol Neurosurg Psychiatry*. 2014;85(7):782–9.
42. Hadhoum N, Hodel J, Defoort-Dhellemmes S, et al. Length of optic nerve double inversion recovery hypersignal: a new imaging biomarker for measuring axonal loss in neuroinflammatory diseases. *Mult Scler*. 2015. [Epub ahead of print].
43. Hamann S, Zeuthen T, La Cour M, et al. Aquaporins in complex tissues: distribution of aquaporins 1–5 in human and rat eye. *Am J Physiol*. 1998;274:1332–45.
44. Nagelhus EA, Veruki ML, Torp L, et al. Aquaporin 4 water channel protein in the rat retina and optic nerve: polarized expression in Müller cells and fibrous astrocytes. *J Neurosci*. 1998;18:2506–19.
45. Gabilondo I, Martinez-Lapiscina EH, Martinez-Heras E, et al. Trans-synaptic axonal degeneration in the visual pathway in multiple sclerosis. *Ann Neurol*. 2014;75:98–107.
46. Khanna S, Sharma A, Huecker J, Gordon M, Naismith RT, Van Stavern GP. Magnetic resonance imaging of optic neuritis in patients with neuromyelitis optica versus multiple sclerosis. *J Neuroophthalmol*. 2012;32:216–20.
47. Storoni M, Davagnanam I, Radon M, Siddiqui A, Plant GT. Distinguishing optic neuritis in neuromyelitis optica spectrum disease from multiple sclerosis: a

- novel magnetic resonance imaging scoring system. *J Neuroophthalmol.* 2013;33:123–7.
48. Hodel J, Outteryck O, Bocher AL, Zéphir H, Lambert O, Benadjaoud MA, Chechin D, Pruvo JP, Leclerc X. Comparison of 3D double inversion recovery and 2D STIR FLAIR MR sequences for the imaging of optic neuritis: pilot study. *Eur Radiol.* 2014;24(12):3069–75.
 49. de Seze J, Blanc F, Kremer S, Collongues N, Fleury M, Marcel C, Namer IJ. Magnetic resonances spectroscopy evaluation in patients with neuromyelitis optica. *J Neurol Neurosurg Psychiatry.* 2010;81:409–11.
 50. Pichiecchio A, Tavazzi E, Poloni G, Ponzio M, Palesi F, Pasin M, Piccolo L, Tosello D, Romani A, Bergamaschi R, Piccolo G, Bastianello S. Advanced magnetic resonance imaging of neuromyelitis optica: a multiparametric approach. *Mult Scler.* 2012;18:817–24.
 51. Rocca MA, Agosta F, Mezzapesa DM, Martinelli V, Salvi F, Ghezzi A, Bergamaschi R, Comi G, Filippi M. Magnetization transfer and diffusion tensor MRI show gray matter damage in neuromyelitis optica. *Neurology.* 2004;62:476–8.
 52. Yu C, Lin F, Li K, Jiang T, Qin W, Sun H, Chan P. Pathogenesis of normal-appearing white matter damage in neuromyelitis optica: diffusion-tensor MR imaging. *Radiology.* 2008;246:222–8.
 53. Liu Y, Duan Y, Yu C, Wang J, Huang J, Ye J, Butzkueven H, Li K, Shu N. A tract-based diffusion study of cerebral white matter in neuromyelitis optica reveals widespread pathological alterations. *Mult Scler.* 2012;18:1013–21.
 54. Rueda Lopes FC, Doring T, Martins C, Cabral FC, Malfetano FR, Pereira VCSR, Alves-Leon S, Gasparetto EL. The role of demyelination in neuromyelitis optica damage: diffusion-tensor MR imaging study. *Radiology.* 2012;263:235–42.
 55. Chanson JB, Lamy J, Rousseau F, et al. White matter volume is decreased in the brain of patients with neuromyelitis optica. *Eur J Neurol.* 2013;20:361–7.
 56. von Glehn F, Jarius S, Cavalcanti Lira RP, Alves Ferreira MC, von Glehn FH, Costa E, Castro SM, Beltramini GC, Bergo FP, Farias AS, et al. Structural brain abnormalities are related to retinal nerve fiber layer thinning and disease duration in neuromyelitis optica spectrum disorders. *Mult Scler.* 2014;20:1189–97.
 57. Kurtzke JF. Rating neurological impairment in multiple sclerosis: an expanded disability status scale (EDSS). *Neurology.* 1983;33:1444–52.
 58. Bennett JL, de Seze J, Lana-Peixoto M, et al. Neuromyelitis optica and multiple sclerosis: seeing differences through optical coherence tomography. *Mult Scler.* 2015;21:678–88.
 59. Bouyon M, Collongues N, Zéphir H, et al. Longitudinal follow-up of vision in a neuromyelitis optica cohort. *Mult Scler.* 2013;19:1320–2.
 60. Costello F, Coupland S, Hodge W, et al. Quantifying axonal loss after optic neuritis with optical coherence tomography. *Ann Neurol.* 2006;59:963–9.
 61. Costello F, Hodge W, Pan YI, et al. Tracking retinal nerve fiber layer loss after optic neuritis: a prospective study using optical coherence tomography. *Mult Scler.* 2008;14:893–905.
 62. Ho J, Sull AC, Vuong LN, Chen Y, Liu J, Fujimoto JG, Schuman JS, Duker JS. Assessment of artifacts and reproducibility across spectral- and time-domain optical coherence tomography. *Ophthalmology.* 2009;116:1960–70.
 63. Huang J, Liu X, Wu Z, Xiao H, Dustin L, Sadda S. Macular thickness measurements in normal eyes with time-domain and Fourier-domain optical coherence tomography. *Retina.* 2009;29:980–7.
 64. Bhargava P, Lang A, Al-Louzi O, et al. Applying an open source segmentation algorithm to different OCT devices in multiple sclerosis patients and healthy controls: Implications for clinical trials. *Mult Scler Int.* 2015 May 18. doi: 10.1155/2015/136295. [Epub ahead of print].
 65. Sato DK, Callegaro D, Lana-Peixoto MA, et al. Distinction between MOG antibody-positive and AQP4 antibody-positive NMO spectrum disorders. *Neurology.* 2014;82:474–81.
 66. Marignier R, Ruiz A, Cavagna S, Benetollo C, Durand-Dubief F, Vukusic S, Giraudon P. Potassium channel Kir4.1: a novel target for neuromyelitis optica autoantibodies ? Platform session PS7.6; ACTRIMSECTRIMS 2014 at Boston.
 67. Alamouti B, Funk J. Retinal thickness decreases with age: an OCT study. *Br J Ophthalmol.* 2003;87:899–901.
 68. Budenz DL, Anderson RA, Varma R, et al. Determinants of normal retinal nerve fiber layer thickness measured by Stratus OCT. *Ophthalmology.* 2007;114:1046–52.
 69. Girkin CA, McGwin G, Sinai MJ, et al. Variation in optic nerve and macular structure with age and race with spectral-domain optical coherence tomography. *Ophthalmology.* 2011;118:2403–8.
 70. Knight OJ, Girkin GA, Budenz DL, et al. Effect of race, age, and axial length on optic nerve head parameters and retinal nerve fiber layer thickness measured by Cirrus HD-OCT. *Arch Ophthalmol.* 2012;130:312–8.

Fiona Costello

Introduction

What Is “Early” Multiple Sclerosis?

Multiple sclerosis (MS) is an inflammatory disorder of the central nervous system (CNS) that causes progressive neurological disability over time [1, 2]. Affecting more than two million people worldwide, MS is recognized as the leading cause of nontraumatic neurological disability in young adults [2, 3]. For many patients, clinical manifestations involve the motor, sensory, visual, and autonomic systems, but less localizing symptoms and signs are also common, with fatigue being foremost among them [1, 2]. The diagnosis of MS can often be established on clinical grounds for patients who experience recurrent neurological events consistent with multifocal CNS inflammation [4, 5]. Since the publication of the original McDonald criteria and subsequent iterations [6–8], radiological endpoints have been used to confirm the diagnosis of MS in the absence of recurrent clinical events.

In truth, it is difficult to know when MS begins for any given patient, because many inflammatory CNS lesions cause no clinical symptoms.

F. Costello, MD, FRCP (✉)

Departments of Clinical Neurosciences and Surgery (Ophthalmology), University of Calgary, Foothills Medical Centre, Calgary, AB, Canada
e-mail: fiona.costello@albertahealthservices.ca,
fionacostello@rogers.com

Accordingly, it is challenging to define “early” MS, because onset of awareness that a problem exists is not synonymous with onset of the actual problem (Box 7.1). For 85 % of young adults, MS is heralded with a clinically isolated syndrome (CIS) of the optic nerves, brainstem, or spinal cord [9]. Thereafter, the majority (85 %) of MS patients manifest episodes of relapsing remitting neurological dysfunction [1, 2, 4–10], before transitioning to a secondary progressive course (SPMS) of the disease [1, 2, 9–11]. During this time, patients accumulate neurological disability with or without relapses.

Box 7.1

It is challenging to define “early MS” because onset of awareness that a problem exists is not synonymous with onset of the actual problem.

Approximately 15 % of MS patients experience a primary progressive course from onset (PPMS) [2]. While the acronyms RRMS, SPMS, and PPMS are embedded in the lexicon of neurologists, these labels are merely clinical descriptors and tell us nothing about underlying differences in pathobiology that distinguish MS phenotypes. At best, they represent our clinical perceptions of different ages and stages of the

disease [2, 10]. In reality, the driving force behind progression and the variables that affect transition from the relapsing remitting phase to the treatment-resistant progressive course in MS remain obscure. The context of this uncertainty has important implications because approved MS treatments act predominantly by targeting inflammation within the brain and spinal cord with an implicit assumption that recurrent, chronic inflammatory disease activity exacts a toll on the structural integrity and functional eloquence of the CNS over time.

Optic Neuritis: The Best Characterized Clinically Isolated Syndrome

Optic neuritis (ON) refers to an inflammatory injury of the optic nerve, which can manifest as a CIS or, in some cases, represent a harbinger for the diagnosis of MS. With an incidence of 1–5 per 100,000 per year [2, 11, 12], ON is a common cause of acquired vision loss in young adults and the best-characterized CIS [9]. In fact, 1 in every 5 MS patients presents with MS associated (MSON) as the first clinical manifestation of their disease [9]. Much of what we have come to understand in terms of the epidemiology and clinical presentation of typical MSON has been based on the initial experience and subsequent follow-up from the Optic Neuritis Treatment Trial (ONTT) [13, 14]. This randomized, multicenter study was initially designed to compare the benefits of treatment with either intravenous methylprednisolone (IVMP) (250 mg administered every 6 h for 3 days followed by oral prednisone [1 mg/kg/day] for 11 days), oral prednisone (1 mg/kg/day), or oral placebo in 457 patients with acute ON [2]. From the ONTT, we learned that most MSON patients are Caucasian (85 %) women (77 %), with a mean age of 32 years [2, 13, 14]. In adults, the majority of ON cases are unilateral, but occasionally bilateral simultaneous vision loss is observed. Yet, in this setting, ON mimics need to be considered including: neuromyelitis optica (NMO), toxic-metabolic optic neuropathies, and Leber's hereditary optic neuropathy (LHON).

From the point of view of their clinical presentation, MSON patients often report subacute onset vision loss that worsens over hours to days. Ninety-two percent of affected individuals experience pain within the 1st week of symptom onset, which is frequently provoked by eye movements [2]. Approximately one-third of individuals affected by MSON note flashes of light in the affected eye, known as photopsias or phosphenes [15, 16], albeit they may not divulge this information without prompting. When the diagnosis is suspected, there are several localizing features on initial examination, which are key to securing the diagnosis. Initially, the severity of vision loss in the affected eye (MSON eye) may range from mild (Snellen visual acuity equivalent of 20/20) to no light perception. In patients with unilateral optic nerve involvement, a relative afferent pupil defect (RAPD) will be apparent in the MSON eye. Visual field defects follow the topography of the retinal nerve fiber layer (RNFL). Cecocentral, altitudinal, and arcuate patterns of vision loss are often observed. Dyschromatopsia, or decreased color vision, is also common. This finding can be particularly helpful in localizing the diagnosis in patients with mild central vision loss and disproportionate deficits in color vision function [2]. In cases of retrobulbar MSON, the fundus examination is initially normal, whereas patients with anterior MSON (sometimes referred to as "papillitis") manifest mild to moderate optic disc swelling acutely. The ONTT demonstrated that severe optic disc edema, vitreous cell, and hemorrhage are relatively uncommon findings in MSON patients and may herald a mimic such as neuroretinitis. Not surprisingly, these atypical fundus features are associated with a reduced risk of developing MS, potentially because the patient does not in fact have MSON. The prognosis for recovery after MSON is generally favorable, with approximately 95 % of patients achieving a visual acuity of 20/40 vision in their affected eye a year after clinical presentation [2, 11, 17]. Despite regaining "normal" vision, however, many MSON patients report persistent

problems including fatigue and heat-induced (Uhthoff's phenomenon) vision loss, altered motion and depth perception (Pulfrich phenomenon), and decreased spatial vision at low-contrast levels [2]. There is therefore discordance between what patients report versus what is captured with standard ophthalmic testing in the setting of post-acute MSON, indicating a need for more sensitive measures of vision loss in this patient population.

The Afferent Visual Pathway: A Clinical Model of Multiple Sclerosis

As a putative model of MS, the afferent visual pathway (AVP), with MSON as its relapse "prototype," offers several potential advantages. First and foremost, there is the benefit of precise localization. In the setting of acute ON, the AVP model provides objective evidence of a symptomatic lesion in any optic nerve, which can be anatomically localized in the CNS [2]. As a second point of merit, more than 90 % of ON patients report pain at initial presentation. In light of the highly specialized nature of the afferent visual pathway, any perturbation in the system that interferes with visual perception, particularly central vision, will be noticed and reported by affected individuals. Functional recovery can therefore be monitored from a relatively precise point of onset in the AVP model of MS [2]. Thirdly, the afferent visual pathway is a functionally eloquent CNS system and deficits can be captured with reproducible measures of visual function including high- and low-contrast visual acuity, automated perimetry, and color vision testing. Furthermore, optical coherence tomography (OCT) provides structural measures of neuronal and axonal integrity. By pairing OCT measures with quantitative visual outcomes, it is possible to devise a structural–functional paradigm to elucidate the temporal evolution and relative contributions of inflammation, axonal loss, neuronal damage, and cortical compensation to post-MSON recovery in the

AVP model of MS [2]. Finally, previous pathological studies have shown that tissue-specific injury in the AVP mirrors global CNS effects in MS patients [2, 18]. Simply put, the back of the eye is the front of the brain. At the time of an acute MSON event, cytokine release induces transient conduction block, likely induced by nitric oxide [2, 19]. When myelination and axonal integrity are intact, recovery ensues with the removal of inflammatory mediators. During recovery from MSON, remyelination improves saltatory conduction through sodium channels, which are distributed along the demyelinated optic nerve segment [9]. Cortical plasticity is also believed to play a role in optimizing function in the more chronic phases of recovery, albeit the timeline and mechanisms involved therein are not well understood. The AVP model can therefore be interrogated to monitor tissue-specific factors that underpin CNS injury and repair in MS patients [2].

Optical Coherence Tomography: An In Vivo Optical Biopsy?

Optical coherence tomography (OCT) provides a noninvasive means of measuring neuroaxonal injury in the anterior visual pathway [20–22]. As the "optical analog" of ultrasound B-mode imaging, OCT facilitates in vivo imaging of retinal structures including the retinal nerve fiber layer (RNFL), ganglion cell layer (GCL), and inner nuclear layer (INL). Since the retina is typically devoid of myelin, OCT measures provide an ideal opportunity to capture the manifestations of CNS neurodegeneration, neuroprotection, and, potentially, neurorepair. Decrements in peripapillary RNFL thickness as measured by OCT have been interpreted to represent axonal damage [2]. Because the macula contains a large proportion of retinal ganglion cell neurons (about 34 % of total macular volume) [22], changes in macular volume and, more recently, GCL thickness have been interpreted to represent altered neuronal integrity in the afferent visual pathway. Widespread availability of spectral-domain OCT

has allowed us to obtain high-resolution imaging (5–7 μm) of retinal structures 50-fold faster than previous time-domain OCT models [21, 22]. As OCT continues to evolve, future studies will be able to employ novel techniques including longer wavelength and swept source technology, ultrahigh-resolution OCT, en face imaging, and polarization-sensitive OCT that will enhance our ability to diagnose, monitor, and treat MS patients [23].

Optical Coherence Tomography in Optic Neuritis

At the time of an acute MSON event, when vision loss is at its nadir, patients often manifest peripapillary RNFL measurements that are increased in their MSON eye relative to their non-MSON eye [2]. Correspondingly, the optic nerve in the MSON eye may be mildly edematous or hyperemic secondary to axoplasmic flow stasis. In contrast, at baseline OCT-measured macular volume and GCL measures are symmetric between MSON eyes and non-MSON eyes in the setting of acute ON [2]. Ganglion layer (GCL) thinning may be the first manifestation of retrograde neuronal loss detectable in the AVP model, because the ganglion layer “signal” is not obscured by superimposed edema [24]. In the ensuing 2–3 months, RNFL, GCL, and macular volume thinning evolve, with earliest signs of significant RNFL atrophy often manifesting in the temporal region [2]. These OCT-measured changes are commensurate with the evolution of optic disc pallor. Collectively the studies to date have shown that RNFL, GCL, and macular volume continue to decrease for 6–12 months after symptom onset, plateauing thereafter [2]. Yet, visual recovery 12 months after ON has not been linked to the extent of peripapillary RNFL swelling seen acutely but has instead been associated with the amount of RNFL, macular volume, and ganglion layer loss observed 6–12 months after symptom onset [2].

In the era of retinal segmentation with spectral-domain OCT, INL thickening and microcystic macular edema have been explored as

potential markers of inflammation in ON patients [25, 26]. In a study by Kaushik and colleagues [26], INL thickening was shown to correlate with lower RNFL values and reduced GCL thickness in ON eyes. Thus, more severe inflammation in the retina may be associated with more severe neuroaxonal injury in the afferent visual pathway of ON patients.

Prognosis for Recovery After MSON

As previously stated, the natural history of MSON is favorable, with the vast majority of patients achieving 20/20 or better Snellen acuity equivalent visual function in their MSON eyes a year after the acute event [11]. Kupersmith and colleagues [27] identified early functional and structural markers that may help predict recovery after MSON. Specifically, 1 month after presentation, high-contrast visual acuity values less than or equal to 20/50, contrast sensitivity measures less than 1.0 log units, and visual field mean deviation measures less than or equal to -15.0 dB (as determined by automated perimetry) predicted moderate to severe outcomes for each of these measures at 6 months. In a prospective study involving 25 MSON patients, Kupersmith [28] also demonstrated that early OCT-measured RNFL loss at 1 month was predictive of RNFL thinning at 6 months in MSON eyes [28]. Other studies have shown that a year after an isolated ON event, peripapillary RNFL measurements are reduced by approximately 20 % relative to the fellow eye [2]. In a meta-analysis of time-domain OCT studies [14 studies (2,063 eyes),] RNFL values were reduced from 5 to 40 μm (averaging 10–20 μm) in MSON eyes [29]. Furthermore, comparing MSON eyes with the eyes of healthy controls showed an estimated average RNFL loss of 20 μm [29]. Lower RNFL values have been shown to correlate with reduced visual acuity, visual field mean sensitivity, and color vision scores [2], reinforcing the notion that form and function are lightly linked in the AVP model of MS. For patients selected without recruitment bias, an OCT “cutoff” of 75 μm has been shown to represent a threshold of RNFL

integrity that can predict the extent of visual recovery after MSON [30]. The findings to date suggest that MSON may be the “relapse prototype” in the AVP model through which the acute consequences of an optic nerve injury can be tracked, and structural–functional correlations can be established over a defined time period. To this end, the impact of patient-related factors including age, gender, and ethnicity on recovery from a relapse event may also be explored in the AVP model. In a prospective study involving 39 men and 105 women with acute ON, men showed more apparent loss of RNFL thickness in their ON eyes from baseline to 6 months than women [31]. These findings raise interesting questions about the potential influence of gender in MS, which may be explored in future studies.

Optical Coherence Tomography: Other Clinically Isolated Syndromes

Optical coherence tomography studies have also revealed evidence of afferent visual pathway involvement in patients with nonvisual CIS, which raises interesting questions regarding mechanisms of subclinical neuroaxonal injury in the CNS of MS patients. Oberwahrenbrock and colleagues [32] used spectral-domain OCT to compare 45 CIS patients with age/sex-matched controls. Patients were stratified into categories based upon the presence or lack thereof of prior MSON by history. The subgroups in this study included CIS eyes with clinical MSON, CIS eyes with suspected subclinical MSON and CIS eyes unaffected by MSON. Interestingly, the eyes of CIS patients with no evidence of clinical or subclinical MSON showed significant reduction of GCL and INL layer thicknesses, with a topography similar to that of MSON eyes. Moreover, CIS eyes with suspected subclinical MSON showed significant RNFL thinning, albeit the most pronounced thinning was noted in CIS eyes with an established history of MSON. The observation that GCL damage is detectable in CIS eyes without clinical history of MSON, was interpreted to support the concept that neuroaxonal

loss can occur in the CNS of MS patients without preceding or concomitant demyelination. Thus, it is conceivable that OCT may be used to detect evidence of primary neurodegeneration in the AVP Model of MS. Finally, in this study, loss of GCL thickness in the eyes of nonvisual CIS patients also showed that neurodegeneration is not limited to advanced disease stages but a feature that occurs early in disease development [32]. Notably, the findings described by Oberwahrenbrock et al. [32] were in disagreement with prior reports, which have shown equivocal results perhaps owing to the limits of time-domain OCT technology [33, 34]. For example, in a time-domain OCT by Outteryck et al. [33], peripapillary RNFL values and macular volumes failed to distinguish CIS patients ($n=56$, including 18 patients with MSON and 38 patients without MSON) from control subjects.

Optical Coherence Tomography and Future Risk of Multiple Sclerosis

Few studies have explored the association between OCT measures in the afferent visual pathway at the time of an acute inflammatory relapse and future risk of MS. In a prospective study of 50 CIS patients with isolated MSON, there were no significant differences in RNFL thickness in either MSON eyes or non-MSON eyes observed between CIS patients who developed clinically definite MS (42 %) and those who did not develop MS (58 %) during the 2-year study period [35]. Moreover, a link between initial RNFL values and baseline evidence of CNS inflammation on magnetic resonance imaging (MRI) as future predictors for the development of MS in CIS patients has not been proven. In a previous study, 50 patients who experienced MSON as a CIS were followed for a mean period of 34 months with OCT testing [36]. RNFL values in MSON eyes and non-MSON eyes were compared between patients with MRI evidence of white matter lesions and patients with normal baseline MRI findings, over a 2-year period.

Twenty-one patients (42 %) developed clinically definite MS (CDMS) during the study. After 2 years, temporal RNFL values were thinner in MSON patients with MRI lesions at baseline, but the results were not significant. In a time-domain OCT study, Outteryck [33] evaluated 56 CIS patients and 32 control subjects to investigate whether OCT measures of RNFL thickness and macular volume revealed early axonal loss in the afferent visual pathway. In this prospective case series, there was no link between RNFL and MRI evidence of CNS inflammation at baseline, disseminated CNS inflammation according to the revised McDonald criteria, gadolinium enhancement on initial MRI, multifocal CIS presentation, altered visual-evoked potentials, or development of “McDonald”-proven MS at 6 months. These investigators concluded that OCT does not predict conversion to MS at 6 months in CIS patients [33]. Yet, in a more recent spectral-domain OCT study performed by Perez-Rico et al. [37] involving 29 CIS patients without MSON, OCT-measured RNFL thickness was found to be an independent predictor of clinically definitive MS diagnosis at 12 months. Based upon their findings, the authors concluded that retinal axonal loss measured by OCT is an important prognostic factor of conversion to MS in patients with CIS in the absence of symptomatic MSON [37]. Again, there may be discrepancies between published reports that reflect differences in the CIS patient population being evaluated, as well as disparity between the generations of OCT technology being used. As OCT continues to evolve, it may be possible to pair RNFL, GCL, INL and other paraclinical measures of CNS neuroaxonal integrity to identify which CIS patients manifest sub-clinical dissemination of lesions in space and time that portend a greater risk for developing MS.

Optical Coherence Tomography in Multiple Sclerosis

For most MS patients, the hallmark of the diagnosis is change, both in terms of neurological disability and the MRI-measured burden of disease over time. At this point, a role for OCT in complementing

conventional tools used to diagnose and monitor disease activity is beginning to emerge.

Using Optical Coherence Tomography to Detect Optic Neuritis in MS Patients

For all intents and purposes, RNFL changes after MSON in MS patients parallel those in patients with CIS because MSON has a deleterious impact on RNFL integrity that is directly proportional to the severity of the event and is less dependent on the diagnosis of MS or indeed MS subtype [20]. Therefore, a CIS patient with severe MSON and poor clinical recovery may manifest worse RNFL and GCL loss than an MS patient with a relatively mild MSON event. The key difference in distinguishing MS patients with MSON from CIS patients is that the former are more likely to have reduced RNFL and GCL findings in both their MSON and non-MSON eyes [20]. A meta-analysis of prior time-domain OCT studies (14 studies [2,063 eyes]) demonstrated that RNFL values are reduced from 5 to 40 μm (averaging 10–20 μm) in MSON eyes [29]. Furthermore, comparing MSON eyes with the eyes of healthy controls showed an estimated average RNFL loss of 20 μm (95 % confidence interval [CI], –23 to –18) [29]. In 27 studies comparing RNFL values in MSON eyes to the non-MSON eyes of the same patients (4,199 eyes), there was an estimated RNFL loss of 14.6 μm (95 % CI, –17 to –13) in MSON eyes compared to a 7.1 μm reduction in RNFL thickness in non-ON eyes relative to control eyes [29]. Thus, MS patients with MSON may manifest less inter-eye asymmetry with respect to RNFL and GCL thickness relative to CIS patients because changes in RNFL integrity are more likely to be bilateral in the former [20]. In light of the fact that neuroaxonal loss may manifest insidiously and perhaps independently of relapses in MS, the utility of OCT in detecting subclinical damage in the afferent visual pathway is paramount if the technology is to represent a structural marker of CNS integrity. In the current era, RNFL, GCL, and potentially INL values could eventually be used to capture clinically silent disease activity, providing there

is consensus regarding the amount of progressive RNFL thinning that constitutes paraclinical evidence of afferent visual pathway pathology and assurance that the increments of change in RNFL thickness can be distinguished from the test–retest variability of the OCT technology being used [20].

Optical Coherence Tomography in Benign Multiple Sclerosis

Benign MS is a term that has traditionally been used to describe MS patients with an Expanded Disability Status Score (EDSS) score measuring less than or equal to 3 (out of a total of 10) and disease duration equal to or greater than 15 years [38]. The benign variant of MS is thought to follow a milder course, yet recent spectral-domain OCT studies have shown that “benign” MS patients have the same RNFL loss, low-contrast letter acuity impairment, and decreased quality of life scores as MSON eyes, calling into question the moniker “benign” [38, 39]. Lange and colleagues [39] used spectral-domain OCT to follow 29 benign MS patients and 29 healthy controls. In this study, reduced RNFL thickness was associated with a history of MSON, but not with EDSS score or disease duration. Yet, RNFL values were lower in patients with benign MS than healthy controls, regardless of the previous history of MSON. Indeed, while overall neurologic impairment may be mild in benign MS patients, visual dysfunction (which is not well captured by the EDSS) accounts for a substantial degree of disability. The dichotomy between RNFL values and disability scores was highlighted in a cross-sectional, time-domain OCT study comparing different MS subtypes (63 patients with MSON as a CIS, 108 RRMS patients, 13 SPMS patients, and 9 PPMS patients) [40]. There were significant correlations between RNFL thickness and the extent of neurological disability for RRMS and CIS patients in this study, but this relationship did not hold true for progressive MS subtypes [40]. These data suggest that there may be concordance between the extent of axonal damage in the anterior visual pathway and measures of neurological impairment for MS patients with

mild to moderate neurological disability, but not for patients with either mild or advanced disease [40]. Patients with progressive MS may have more extensive axonal damage in a functionally eloquent region such as the spinal cord, with relative sparing of other CNS systems, including the afferent visual pathway. This is one possible explanation for the lack of correlation in structure and function between imaging modalities such as OCT and global measures of neurological disability in some MS patients.

Using Optical Coherence Tomography to Track Longitudinal Changes in MS

One of the major challenges in MS is to find a structural marker of progressive neuroaxonal damage that is sensitive to insidious changes over time, in which the “signal” of pathology can be distinguished from the inherent “noise” of the technology. In longitudinal time-domain OCT study, Talman and colleagues [41] followed 299 MS patients (84 % RRMS) and showed through pooled analysis that each year of follow-up was associated with a 2 μm decrease in RNFL integrity in MS eyes. In contrast, control subjects showed an average RNFL thinning of 0.5 % over the 3-year follow-up period [41]. The investigators concluded that RNFL thinning occurs as a consequence of subclinical axonal loss in the anterior visual pathway in MS and suggested that OCT could be used to potentially evaluate the effectiveness of neuroprotection protocols in MS [41]. Yet, caution should be employed when generalizing the time course of RNFL loss to a given individual from cross-sectional data [20, 29], particularly when the estimated yearly thinning of overall RNFL (2 μm) is below the detection limit of the time-domain OCT technology being used. Narayanan and colleagues [42] studied 133 RRMS patients (149 non-MSON eyes and 97 MSON eyes) (93 patients were scanned at 2 visits). Relations between RNFL and GCL thicknesses with MS duration and follow-up were assessed. Both RNFL and GCL values decreased with MS disease duration, and this observation was noted for both non-MSON eyes and MSON eyes. These findings were interpreted to indicate that in RRMS eyes without clinically

evident inflammation, progressive loss of RNFL and GCL thicknesses occurred [42]. Ideally, future longitudinal studies with spectral-domain OCT will incorporate associated hardware and software improvements that minimize repeat measurement variability. In this context, OCT may compliment emerging technologies and be used to capture reliable, reproducible evidence of neuroaxonal damage arising from clinical and subclinical disease activity in MS.

Ganglion Layer Analysis as a Marker of Neuronal Integrity in MS

In the era of retinal segmentation, spectral-domain OCT measures of GCL have emerged as a marker of neuronal integrity in the afferent visual pathway. Multiple sclerosis patients with evidence of active disease activity defined as relapses, new gadolinium-enhancing lesions, and new T2 lesions have shown faster rates of annualized GCL thinning [43]. Studies have also shown that annual GCL thinning occurs 37 % faster in MS patients with disability progression and 43 % faster in those with disease duration measuring less than 5 years versus greater than 5 years [43]. In patients with new gadolinium-enhancing lesions, new MRI-measured T2 lesions, and disease duration less than 5 years, GCL thinning was 70 % faster relative to patients who lacked these 3 cardinal characteristics [43]. Multiple sclerosis patients with clinical and/or radiologic non-ocular disease activity, particularly early in the disease course, exhibited accelerated ganglion layer thinning [43]. These findings indicated that retinal changes in MS reflect global CNS processes and that OCT-derived ganglion layer measurements may have utility as an outcome measure for assessing neuroprotective agents, particularly in early, active MS [43].

Transsynaptic Degeneration in Multiple Sclerosis

For any given MS patient, it is difficult to know whether inner and outer retinal damage arise as a

primary “neuronopathy” or whether damage to retinal ganglion cells and deeper neuronal elements occur as a dying back consequence of retrograde axonal degeneration from a retrobulbar optic nerve injury or a more posterior visual pathway lesion. The distinction has relevance, because evidence of primary neuronal loss in the retina would support the hypothesis that neurodegeneration can occur in the absence of demyelination in MS. In a previous pathological study of 82 eyes from MS patients, Green and colleagues [18] observed shrunken neurons, dropout of retinal ganglion cells (in 79 % of MS eyes), and INL atrophy (in 40 % of MS eyes). The finding of INL atrophy indicated that neuronal pathology in MS is not restricted to the retinal ganglion cell layer and that retinal injury is more widespread than previously appreciated [18]. In this study, the severity of retinal atrophy was significantly associated with postmortem brain weight, and there was an association with disease duration, suggesting that the retina pathology may reflect global changes occurring in the CNS of MS patients over time [18]. This study was instrumental in showing that with the exception of demyelination, virtually all manifestations of brain tissue injury in MS can be found in the retina. Thus, using OCT in the AVP model may help us decipher different types of retinal pathology and enhance our understanding of the factors that drive both inflammation and tissue atrophy in MS [2]. At this point, it is not known whether structural disruption occurs in retinal layers deeper than the inner nuclear layer in MS. If MS affects the outer retina directly, it could indicate that primary retinal neuronal pathology is a pathogenic feature of the disease [2]. Alternatively, loss of retinal neuronal constituents could arise from transsynaptic neuronal degeneration from more distal, retrogeniculate lesions in the afferent visual pathway [18]. Anterograde transsynaptic damage from an optic nerve injury leading to neuronal loss in the lateral geniculate nucleus has been described in MS, glaucoma, and after chemical injury to the optic nerve [2]. Recently retrograde transsynaptic degeneration has been interpreted from OCT manifestations of RNFL layer thinning in patients who suffered injury to

the posterior visual pathways [2]. Further investigations are needed to validate the phenomenon of bi-directional trans-synaptic axonal degeneration in the AVP, which could inform our understanding of mechanisms underpinning diffuse axonal loss in MS, which arise distal from remote or active sites of inflammation [2].

Microcystic Macular Edema and Inner Nuclear Layer Thickness

Interrogating the retina for evidence of MS-related pathology has prompted recent interest in microcystic macular edema located in the INL, which has been reported to occur in 5–6 % of MS patients [2]. First proposed by Gelfand and colleagues [44], retinal microcysts and associated thickening of the INL have been interpreted to be signs of inflammation in MS eyes. Subsequent work has shown that MS patients with microcystic macular edema and INL thickening have higher baseline multiple sclerosis severity scores and an increased predilection to develop MRI-measured contrast-enhancing lesions, new T2 lesions, relapses, and disability progression [45]. Thus, INL thickening may be a structure marker of retinal inflammation in MS eyes that can be correlated with global metrics of disease activity in these patients. This awaits further study.

Juvenile and Pediatric Multiple Sclerosis

Multifocal CNS demyelination has been reported to occur in approximately 0.4 per 100,000 of the pediatric patient population [46, 47]. Similar to adults, MSON is a relatively common occurrence in pediatric patients such that 22 % of children experience MSON as their first demyelinating event and 35 % of children who eventually develop MS experienced MSON during their first clinical episode [46]. In a pediatric ON study, Wilejto and colleagues [47] reported unilateral optic nerve involvement in the majority (58 %) of pediatric patients ($n=36$). Visual recovery after ON was considered complete in 39 of 47 affected

eyes (83 %) [47]. Cranial MRI scans demonstrated white matter lesions separate from the optic nerves in 54 % of children. In this study, the risk of MS was 36 % at 2 years, and bilateral ON was associated with a greater future risk of MS [47]. Clinical findings extrinsic to the visual system on baseline examination and MRI evidence of white matter lesions outside the optic nerves were strongly associated with a future diagnosis of MS [47]. Yeh and colleagues [48] used OCT in a cross-sectional study of 38 consecutive children (age <18 years) who had at least 1 documented clinical episode of an acquired demyelinating event and 2 control groups, including (1) 15 normal healthy children (30 eyes) with no history of neurological or other chronic disease and (2) 5 children (10 eyes) with other nondemyelinating disorders. In MS patients, RNFL thickness was 99 μm in non-MSON eyes and 83 μm in MSON eyes [48]. Children with acute disseminated encephalomyelitis and transverse myelitis had lower RNFL values in their ON eyes (67 μm) relative to non-ON eyes (102 μm) [48]. Macular volumes were markedly lower in ON eyes of children with acute disseminated encephalomyelitis/transverse myelitis and chronic relapsing inflammatory optic neuropathy, suggesting a more severe disease process in these clinical entities [48]. All subgroups with a clinical history of ON had lower average RNFL values than controls. On the basis of their findings, the investigators concluded that OCT may be a valuable tool for monitoring anterior optic pathway dysfunction in children with demyelinating disease. In a more recent spectral-domain OCT study, Yeh [49] compared GCL and RNFL values to other functional measures of afferent visual pathway integrity in a pediatric population with demyelinating disorders (37 children, aged 8–18 years, $n=74$ eyes) and 18 healthy controls ($n=36$ eyes). Mean RNFL thickness was 26 μm (25.6 %) lower in patients with demyelinating syndromes (76.2 μm [3.7]) compared to controls (102.4 μm [2.1]) ($p < 0.0001$). Mean GCL thickness was 20 % lower in patients as compared to controls ($p < 0.0001$). Mean GCL and RNFL thickness were strongly correlated, yet in contrast to RNFL thickness, no differences in GCL thickness were

noted between optic neuritis (ON) eyes and non-ON eyes of patients. These findings indicated that the retina may be a site of primary neuronal injury in pediatric demyelination.

Huhn and colleagues [50] evaluated the impact of neuroaxonal loss in the anterior visual pathway of patients with early-onset MS (defined as onset before the age of 18 years), with mean disease duration of 11.6 years using spectral-domain OCT. In comparison with controls, early-onset MS patients displayed significant reductions in RNFL thickness and macular volumes, which occurred independently of MSON history [50]. In a generalized estimating model, the early-onset MS group displayed a similar correlation between disease duration and RNFL compared to MS patients with later-onset disease. These data suggested that OCT may provide a structural basis for the observation that early-onset MS patients reach states of irreversible disability at a younger age than patients with later-onset disease.

Optical Coherence Tomography and Recurrent Optic Neuritis

It can be difficult to detect OCT-measured RNFL and GCL changes in the setting of recurrent ON, because the extent of cumulative retinal damage can be severe and the corresponding visual outcomes dire. In a recent time-domain OCT study of 193 MS patients, RNFL values were compared between 29 eyes affected by 2 or more MSON events, 125 eyes affected by a single MSON event, and 232 eyes without MSON. The mean RNFL values were significantly lower in recurrent MSON eyes (64.2 μm) relative to single MSON eyes (86.3 μm) ($P < .0001$) and eyes without MSON (100.1 μm) ($P < .0001$) [35]. In a time-domain OCT study of pediatric patients with demyelinating syndromes, the average RNFL thickness decreased with increasing number of ON episodes [48]. This observation supported the premise that recurrent inflammatory events have a cumulative impact in eroding axonal integrity in the anterior visual pathway. A more recent spectral-domain OCT pediatric study showed that when classified by number of

ON events (0, 1, 2, or more episodes), mean RNFL thickness declined by approximately 9 mm per ON episode [49]. Interestingly, no difference was seen in the mean GCL thickness between patients with 0, 1, or 2 or more episodes of ON [49], for reasons that were not entirely clear. It is possible that an isolated ON event in the pediatric population may be so profoundly detrimental to neuronal integrity in the afferent visual pathway that further episodes have a limited capacity to injure the limited residual tissue. Alternatively, there may be a floor effect with some OCT machines, such that detecting new damage to the ganglion layer may be difficult in the context of preexisting GCL thinning.

Optical Coherence Tomography and Other Paraclinical Measures

The AVP model with MSON as its relapse prototype has relevance to MS if the structure-function correlations therein can be captured with other testing modalities and reflect what is happening on a more global level of the CNS for these patients.

Visual-Evoked Potential Testing

The VEP is a response of the brain to repeated visual stimulation and has traditionally been recorded when visual field is stimulated with a single checkerboard pattern [2]. The VEP is generated at the level of striate cortex by the combined activity of postsynaptic potentials. The magnitude of the VEP reflects the number of functional afferent fibers reaching the striate cortex [2]. In MSON patients, diminished VEP amplitudes indicate inflammation-induced conduction block, axonal atrophy, or a combination of both [2]. Subsequently, VEP amplitudes increase due to resolution of inflammation and edema or possibly expansion of synaptic activity along the visual pathway up to the level of V1 in the visual cortex [2]. Delayed VEP conduction is recognized as one of the earliest features of acute MSON, with the subsequent shortening of latency thought to

represent the process of remyelination. Because it is a summation of a large number of neuronal elements, the full-field VEP is greatly dominated by the macular region due to its cortical overrepresentation [2]. Moreover, the waveform of the full-field VEP is prone to cancellation and distortion, which sometimes leads to apparent, rather than real, latency delay [2]. In contrast, the multifocal VEP (mfVEP) allows stimulation of small areas of the visual field. The result is a detailed topographical assessment of small groups of axons within the optic nerve and visual cortex, which is resistant to waveform distortion. Klistorner and colleagues [51] used mfVEP and OCT testing to prospectively study 25 subjects with acute unilateral MSON. While mfVEP amplitude asymmetry at baseline varied significantly among the patients, it was, on average, very high, indicating considerable reduction of amplitude in MSON eyes. The inter-eye asymmetry in mfVEP amplitude decreased over time indicating continuous functional recovery [51]. There was an insignificant correlation between the inter-eye asymmetry of OCT-measured RNFL thickness and that of mfVEP amplitude at 1 month. This was consistent with vasogenic edema in the acute phase, causing an increase in RNFL thickness, with a corresponding reduction in mfVEP amplitude [51]. Over the course of recovery, the correlation became more robust, indicating a diminishing role of optic nerve edema in measured RNFL thickness and unmasking the association between RNFL atrophy and low mfVEP amplitude [51]. The potential correlation between OCT-measured RNFL values and mfVEP measures of anterior visual pathway damage was demonstrated by the same group, who evaluated 32 patients with unilateral MSON and 25 control subjects [52]. The mean RNFL thickness in MSON eyes (85 μm) was reduced by 19 % compared with control eyes (104 μm), and there was a 40 % reduction in the amplitude of the mfVEP in MSON eyes relative to control eyes [52]. In addition to demonstrating the utility of mf VEP in tracking optic nerve injury in MSON patients, this study further confirmed the significant correlations between structural and functional measures of optic nerve integrity and showed that demyelination

contributes to axonal loss [52]. It may therefore be feasible to pair mfVEP measures with OCT testing to capture the synergistic effects of acute demyelination and axonal loss over time in ON/MS patients. Furthermore, the putative relationship between the VEP latency and axonal loss encourages the notion that therapeutic interventions aimed at reducing the effects of demyelination or enhancing remyelination may be trialed in the AVP model.

Magnetic Resonance Imaging

MRI studies have shown that OCT-measured RNFL atrophy correlates with worse disability and longer disease duration in MS patients. Sepulcre [53] studied 61 MS patients and 29 matched controls over a 2-year period and observed that temporal RNFL atrophy was associated with the presence of new relapses. Furthermore, RNFL thickness was correlated with white matter volume and gray matter brain volumes [53]. A more recent study aimed to determine the relationships between conventional and segmentation-derived RNFL measures with intracranial volume [54]. Among 84 MS patients and 24 controls, peripapillary RNFL and GCL thicknesses in MS eyes without a history of MSON were associated with cortical-gray matter and caudate volumes [54]. Inner nuclear layer thickness in MS eyes without a prior history of ON was associated with FLAIR-lesion volume and inversely associated with normal-appearing white matter volume in RRMS patients [54]. Thus, OCT measures may reflect global CNS pathology, which can be captured with MR imaging in MS patients.

Diffusion Tensor Imaging

Diffusion tensor imaging (DTI) is sensitive to water molecular diffusion in white matter and has been shown to be altered at the earliest stages of MSON [55, 56]. Optic neuritis eyes with increased radial diffusivity have greater degrees of RNFL thinning by OCT, which is in turn related to worse visual acuity outcomes [55]. In a

recent study of acute MSON, radial diffusivity of the optic nerve measured by DTI was associated with proportional decline in vision after MSON and was shown to distinguish controls' eyes from both MSON and non-MSON eyes of patients [55]. Van der Walt and colleagues [56] studied 37 patients with acute MSON at baseline, 1, 3, 6, and 12 months after symptom onset using optic nerve DTI to assess whether early measurements (axial and radial diffusivity) could predict axonal loss (defined as RNFL thinning or mfVEP amplitude loss) or clinical (defined as visual acuity and visual field loss) outcomes at 6 or 12 months. Reduced 1-month axial diffusivity measured with DTI correlated with RNFL thinning at 6 and 12 months and VEP amplitude loss at 6 and 12 months. Moreover, DTI-measured axial diffusivity reduction at 3 months correlated with high-contrast visual acuity at 6 and 12 months. The findings from this study showed that DTI-measured axial diffusivity was decreased during acute MSON. Furthermore, 1-month axial diffusivity reduction correlated with more extensive axonal loss, and DTI decrements at 3 months predicted poorer visual outcomes [56]. Thus, DTI measures can be paired with RNFL values to provide a composite marker of structural axonal integrity in the AVP model of MS and potentially be used to help define a structural–functional paradigm that can be used to study the impact of injury and repair in CNS inflammatory diseases.

Texture Analysis

Ideally, it would be possible to use MRI techniques to analyze the severity of tissue damage and clarify the interactions between structure and function in the afferent visual pathway over time. MRI texture analysis is a quantitative approach that evaluates inter-voxel relationships in an image and detects subtle structural changes following acute inflammation. Investigators have found that MRI texture analysis correlates with the type of pathological damage in postmortem MS brain. Furthermore, it differentiates *in vivo* acute lesions from chronic lesions and distinguishes acute lesions that persist from those that

recover [57]. Zhang and colleagues [57] evaluated 25 MSON patients with OCT, MRI (lesion length and enhancement; optic nerve area ratio) using multi-scale MRI texture analysis, as a measure of structural integrity, at baseline, and at 6 and 12 months. Eight healthy subjects were imaged for control. At baseline, time-domain OCT-measured RNFL values were 20 % thicker and lesion texture 14 % more heterogeneous in MSON eyes than in the non-MSON eyes of MSON patients. In the affected eyes, visual acuity recovered significantly over 6 and 12 months, while RNFL thickness and optic nerve area ratio decreased over time. Texture heterogeneity in the standard MRI of acute optic nerve lesions was the only measure that predicted functional recovery after MSON [57]. Thus, tissue heterogeneity as measured with texture analysis may be a potential measure of functional outcome in MSON patients, and the texture signal in standard MRI could provide insights into mechanisms of injury and recovery in patients with early MS.

Magnetic Transfer Imaging

Magnetization transfer imaging is used to measure the magnetic transfer ratio (MTR) and provide a marker of myelin content in multiple sclerosis. In fact, a significant association between optic nerve MTR and time-linked VEP latency following MSON has implicated a synergistic role for these techniques in detecting remyelination [58]. Thus, MTR could be used to track to what extent the amount of demyelinating injury predicts neuroaxonal loss in the AVP model of MS. Wang et al. [59] aimed to investigate changes in optic nerve MTR over 12 months following acute MSON to determine whether MTR measurements can predict clinical and paraclinical outcomes at 6 and 12 months. Thirty-seven patients with acute MSON were studied within 2 weeks of presentation and at 1, 3, 6, and 12 months. Assessments included optic nerve MTR, RNFL thickness, mfVEP amplitude and latency, and high-contrast (100 %) and low-contrast (2.5 %) letter acuity. Compared to the unaffected nerve, affected optic nerve MTR was

significantly reduced at 3 and 12 months. Greater reduction in MTR at 3 months was associated with subsequent loss of high-contrast letter acuity performance at 6 and 12 months, low-contrast letter acuity scores at 6 months, and RNFL thinning at 12 months. These findings indicate that MTR flux after acute MSON is predictive of axonal degeneration and visual disability outcomes.

Functional MRI

The link between functional recovery from optic neuritis and posterior visual pathway integrity and neuroplasticity has been the topic of recent functional MRI investigations. These studies have demonstrated that dynamic changes in functional connectivity occur within and outside the visual cortex following acute optic neuritis, suggesting compensatory neuroplasticity [60]. Gallo and colleagues [60] investigated functional connectivity of the visual resting-state network in normal-sighted RRMS patients with and without previous MSON. Compared to healthy controls, RRMS patients showed a reduced functional connectivity in the peristriate visual cortex bilaterally. Patients with prior MSON showed a region of stronger functional connectivity in the extrastriate cortex, at the level of right lateral middle occipital gyrus, as well as a region of reduced functional connectivity at the level of right inferior peristriate cortex relative to their counterparts with no prior MSON events. Thus, normal-sighted RRMS patients have demonstrated a significant functional disconnection in the visual resting-state network. Furthermore, RRMS patients recovered from previous MSON have shown a complex reorganization of the visual resting-state network, including an increased functional connectivity at the level of extrastriate visual areas. Conceivably, functional MRI could be used to assess what occurs at the cortical level to facilitate neurorepair in the AVP model of MS.

Conclusion

Using OCT in the AVP model offers an exciting opportunity to explore disease mechanisms that contribute to neurological disability in CIS

patients and those with early MS. Monitoring the acute and chronic consequences of clinically overt MSON may shed light on factors that govern injury and repair after an inflammatory relapse in the CNS. Furthermore, longitudinal studies of MS patients unaffected by clinical MSON events may help us determine whether neuroaxonal damage occurs independently of CNS inflammation in the afferent visual pathway. Because the AVP model is amenable to multiple interrogation techniques, it may be possible to identify neuroprotective, remyelinating, and regenerative effects of emerging therapies being trialed in MS patients. Sensitive and standardized tests of vision can be compared with high-resolution imaging measures of structural integrity in the AVP model to develop a structural–functional paradigm of CNS injury.

References

1. Compston A, Coles A. Multiple sclerosis. *Lancet*. 2008;372:1502–17.
2. Costello F. The afferent visual pathway: designing a structural-functional paradigm of multiple sclerosis. *ISRN Neurol*. 2013. doi:10.1155/2013/134858.
3. Racke MK. Disease mechanisms in ME: the potassium channel KIR4.1 a potential auto- antigen in MS. *Nat Rev Neurol*. 2012;8(11):595–6.
4. Poser CM, Paty DW, Scheinberg L. New diagnostic criteria for multiple sclerosis: guidelines for research protocols. *Ann Neurol*. 1983;13:227–31.
5. Lublin FD, Reingold SC. Defining the clinical course of multiple sclerosis: results of an international survey. *Neurology*. 1996;46(4):907–11.
6. McDonald WI, Compston A, Edan G, et al. Recommended diagnostic criteria for multiple sclerosis: guidelines from the International Panel on the Diagnosis of Multiple Sclerosis. *Ann Neurol*. 2001;50:121–7.
7. Polman CH, Reingold SC, Edan G, et al. Diagnostic criteria for multiple sclerosis: 2005 revisions to the McDonald criteria. *Ann Neurol*. 2005;58:840–6.
8. Polman CH, Reingold SC, Banwell B, et al. Diagnostic criteria for multiple sclerosis: 2010 revisions to the McDonald criteria. *Ann Neurol*. 2011;69:292–302.
9. Miller D, Barkhof F, Montalban X, Thompson A, Filippi M. Clinically isolated syndromes suggestive of multiple sclerosis, part 1: natural history, pathogenesis, diagnosis and prognosis. *Lancet Neurol*. 2005;4:281–8.
10. Confavreux C, Vukusic S. Natural history of multiple sclerosis: a unifying concept. *Brain*. 2006;129:606–16.

11. Costello F, Burton JM. An approach to optic neuritis: the initial presentation. *Expert Rev Ophthalmol.* 2013;8(6):539–51.
12. Hickman SJ, Dalton CM, Miller DH, Plant GT. Management of acute optic neuritis. *Lancet.* 2002; 360:1953–62.
13. Beck RW, Cleary PA, Anderson Jr MM, et al. A randomized, controlled trial of corticosteroids in the treatment of acute optic neuritis. The Optic Neuritis Study Group. *N Engl J Med.* 1992;326:581–8.
14. Optic Neuritis Study Group. The clinical profile of optic neuritis: experience of the Optic Neuritis Treatment Trial. *Arch Ophthalmol.* 1991;109:1673–8.
15. Beck RW. Optic neuritis. Chapter 12. In: Walsh & Hoyt's clinical neuro-ophthalmology, vol. 5. 5th ed. Baltimore: Williams & Wilkins; 1998. p. 599–647.
16. Costello F. Inflammatory optic neuropathies. *Continuum (Minneapolis).* 2014;20:816–37.
17. Shams PN, Plant GT. Optic neuritis: a review. *Int MS J.* 2009;16:82–9.
18. Green AJ, McQuaid S, Hauser SL, Allen IV, Lyness R. Ocular pathology in multiple sclerosis: retinal atrophy and inflammation irrespective of disease duration. *Brain.* 2010;133:1591–601.
19. Miller D, Barkhof F, Montalban X, Thompson A, Filippi M. Clinically isolated syndromes suggestive of multiple sclerosis, part 2: non-conventional MRI, recovery processes, and management. *Lancet Neurol.* 2005;4:341–8.
20. Costello FE, Klistorner A, Kardon R. Optical coherence tomography in the diagnosis and management of optic neuritis and multiple sclerosis. *Ophthalmic Surg Lasers Imaging.* 2011;42:S28–40.
21. Frohman EM, Fujimoto JG, Frohman TC, Calabresi PA, Cutter G, Balcer LJ. Optical coherence tomography: a window into the mechanisms of multiple sclerosis. *Nat Clin Pract Neurol.* 2008;4:664–5.
22. Sakai RE, Feller DJ, Galetta KM, et al. Vision in multiple sclerosis: the story, structure-function correlations, and models for neuroprotection. *J Neuroophthalmol.* 2011;31(4):362–73.
23. Costello FE. Optical coherence tomography: which machine do you want to own? *J Neuroophthalmol.* 2014;34(Suppl):S3–9.
24. Syc S, Saidha S, Newsome SD, et al. Optical coherence tomography segmentation reveals ganglion cell layer pathology after optic neuritis. *Brain.* 2012; 135:521–33.
25. Kaufhold F, Zimmermann H, Schneider E, et al. Optic neuritis is associated with inner nuclear layer thickening and microcystic macular edema independently of multiple sclerosis. *PLoS One.* 2013;8:e71145.
26. Kaushik M, Wang CY, Barnett MH. Inner nuclear layer thickening is inversely proportional to retinal ganglion cell loss in optic neuritis. *PLoS One.* 2013;8:e78341.
27. Kupersmith MJ, Gal RL, Beck RW, et al. Visual function at baseline and 1 month in acute optic neuritis: predictors of visual outcome. *Neurology.* 2007;69: 508–14.
28. Kupersmith MJ, Anderson S, Kardon R. Predictive value of 1 month retinal nerve fiber layer thinning for deficits at 6 months after acute optic neuritis. *Mult Scler.* 2013;19(13):1743–8.
29. Petzold A, de Boer JF, Schippling S, Vermersch P, Kardon R, Green A, et al. Optical coherence tomography in multiple sclerosis: a systematic review and meta-analysis. *Lancet Neurol.* 2010;9:921–32.
30. Costello F, Coupland S, Hodge W, Lorello GR, Koroluk J, Pan YI, et al. Quantifying axonal loss after optic neuritis with optical coherence tomography. *Ann Neurol.* 2006;59:963–9.
31. Costello F, Hodge W, Pan YI, Burton JM, Freedman MS, Stys PK, et al. Sex-specific differences in retinal nerve fiber layer thinning after acute optic neuritis. *Neurology.* 2012;79:1866–72.
32. Oberwahrenbrock T, Ringelstein M, Jentschke S, et al. Retinal ganglion cell and inner plexiform layer thinning in clinically isolated syndrome. *Mult Scler.* 2013;19(14):1887–95.
33. Outteryck O, Zephir H, Defoort S, et al. Optical coherence tomography in clinically isolated syndrome: no evidence of subclinical retinal axonal loss. *Arch Neurol.* 2009;66:1373–7.
34. Kallenbach K, Sander B, Tsakiri A, et al. Neither retinal nor brain atrophy can be shown in patients with isolated unilateral optic neuritis at the time of presentation. *Mult Scler.* 2011;17:89–95.
35. Costello F, Hodge W, Pan YI, Metz L, Kardon R. Retinal nerve fiber layer and future risk of multiple sclerosis. *Can J Neurol Sci.* 2008;35:482–7.
36. Costello F, Hodge W, Pan YI. Exploring the association between retinal nerve fiber layer thickness and initial magnetic resonance imaging findings in patients with acute optic neuritis. *Mult Scler Int.* 2011;2011:2899785.
37. Pérez-Rico C, Ayuso-Peralta L, Rubio-Pérez L. Evaluation of visual structural and functional factors that predict the development of multiple sclerosis in clinically isolated syndrome patients. *Invest Ophthalmol Vis Sci.* 2014;55:6127–31.
38. Galetta KM, Graves J, Talman LS. Visual pathway axonal loss in benign multiple sclerosis: a longitudinal study. *J Neuroophthalmol.* 2012;32:116–23.
39. Lange AP, Zhu F, Sayao AL, et al. Retinal nerve fiber layer thickness in benign multiple sclerosis. *Mult Scler.* 2013;10:1275–81.
40. Costello F, Hodge W, Pan YI, Eggenberger E, Freedman MS. Using retinal architecture to help characterize multiple sclerosis patients. *Can J Ophthalmol.* 2010;45(5):520–6.
41. Talman L, Bisker ER, Sackel DJ, et al. Longitudinal study of vision and retinal nerve fiber layer thickness in multiple sclerosis. *Ann Neurol.* 2010;67(6): 749–60.
42. Narayanan D, Cheng H, Bonem KN, Saenz R, Tang RA, Frishman LJ. Tracking changes over time in retinal nerve fiber layer and ganglion cell-inner plexiform layer thickness in multiple sclerosis. *Mult Scler.* 2014;20(10):1331–41.

43. Ratchford JN, Saidha S, Sotirchos ES, et al. Active MS is associated with accelerated retinal ganglion cell/inner plexiform layer thinning. *Neurology*. 2013;80:47–54.
44. Gelfand JM, Nolan R, Schwartz DM, Graves J, Green AJ. Microcystic macular oedema in multiple sclerosis is associated with disease severity. *Brain*. 2012;135:1786–93.
45. Saidha S, Sotirchos ES, Ibrahim MA, et al. Microcystic macular oedema, thickness of the inner nuclear layer of the retina, and disease characteristics in multiple sclerosis: a retrospective study. *Lancet Neurol*. 2012;11:963–72.
46. Costello F. Evaluating the use of optical coherence tomography in optic neuritis. *Mult Scler Int*. 2011(2011);148394: p. 9.
47. Wilejto M, Shroff M, Buncic JR, Kennedy J, Goia C, Banwell B. The clinical features, MRI findings, and outcome of optic neuritis in children. *Neurology*. 2006;67:258–62.
48. Yeh EA, Weinstock-Guttman B, Lincoff N, et al. Retinal nerve fiber thickness in inflammatory demyelinating diseases of childhood onset. *Mult Scler*. 2009;15:802–10.
49. Yeh EA, Marrie RA, Reginald YA. Functional-structural correlations in the afferent visual pathway in pediatric demyelination. *Neurology*. 2014;83(23):2147–52.
50. Huhn K, Lammer R, Oberwahrenbrock T, et al. Optical coherence tomography in patients with a history of juvenile multiple sclerosis reveals early retinal damage. *Eur J Neurol*. 2015;22(1):86–92.
51. Klistorner A, Arvind H, Garrick R, Graham SL, Paine M, Yiannikas C. Interrelationship of optical coherence tomography and multifocal visual-evoked potentials after optic neuritis. *Investig Ophthalmol Vis Sci*. 2010;51:2770–7.
52. Klistorner A, Arvind H, Nguyen T, et al. Axonal loss and myelin in early on loss in postacute optic neuritis. *Ann Neurol*. 2008;64:325–31.
53. Sepulcre J, Murie-Fernandez M, Salinas-ALaman A, et al. Diagnostic accuracy of retinal abnormalities in predicting disease activity in MS. *Neurology*. 2007;68(18):1488–94.
54. Saidha S, Sotirchos ES, Oh J, et al. Relationships between retinal axonal and neuronal measures and global central nervous system pathology in multiple sclerosis. *JAMA Neurol*. 2013;70(1):34–43.
55. Naismith RT, Xu J, Tutlam NT, Trinkaus K, Cross AH, Song SK. Radial diffusivity in remote optic neuritis discriminates visual outcomes. *Neurology*. 2007;74:1702–10.
56. Van der Walt A, Kolbe SC, Wang YE, et al. Optic nerve diffusion tensor imaging after acute optic neuritis predicts axonal and visual outcomes. *PLoS One*. 2013;8:e83825.
57. Zhang Y, Metz LM, Scott JN, Trufyn J, Fick GH, Costello F. MRI texture heterogeneity in the optic nerve predicts visual recovery after acute optic neuritis. *Neuroimage Clin*. 2014;4:302–7.
58. Hickman S, Toosy A, Jones S, Altmann D, Miszkiel K, et al. Serial magnetization transfer imaging in acute optic neuritis. *Brain*. 2004;127:692.
59. Wang Y, van der Walt A, Paine M. Optic nerve magnetisation transfer ratio after acute optic neuritis predicts axonal and visual outcomes. *PLoS One*. 2012;7:e52291.
60. Gallo A, Esposito F, Sacco R, et al. Visual resting-state network in relapsing remitting MS with and without previous optic neuritis. *Neurology*. 2012;79:1458–65.

Shiv Saidha and Peter A. Calabresi

Introduction

Multiple sclerosis (MS) is regarded as an autoimmune demyelinating disorder of the central nervous system (CNS) that is disseminated in time and space. The clinical relevance of MS is underpinned by its representation as the most common nontraumatic cause of neurologic disability in early to middle adulthood in the developed world [1]. MS is clinically classified according to a number of subtype designations: relapsing–remitting MS (RRMS), secondary progressive MS (SPMS), primary progressive MS (PPMS), and progressive relapsing MS [2].

RRMS accounts for approximately 85 % of all cases of MS at disease onset and is characterized by bouts or relapses during which new symptoms of CNS origin develop and then subsequently remit, either with complete or partial resolution of symptoms. Currently available disease-modifying therapies are licensed for the treat-

ment of RRMS and have not been shown to significantly alter the course of SPMS or PPMS in general [3]. Gradually progressive neurologic decline subsequently following more typical RRMS, which has often been ongoing for many years, is the hallmark of SPMS. On the other hand, PPMS is characterized by gradual progressive neurologic decline from the outset, while progressive relapsing MS represents a progressive subtype of the disease with superimposed relapses. By virtue of being the most common subtype of MS, as well as the subtype of MS shown to be most responsive to immunosuppressive and/or immunomodulatory therapies, RRMS represents the most extensively studied subtype of MS. The focus of this chapter will be on optical coherence tomography (OCT) in RRMS.

Optic Nerve Involvement in RRMS

Although the precise etiology and pathobiological features of RRMS remain to be completely elucidated, known pathologic hallmarks include alterations in the blood–brain barrier, inflammation, demyelination, axonal degeneration, neuronal loss, and gliosis [4, 5]. The anterior visual pathway provides a general window and an exciting opportunity to examine some of these hallmark processes underlying MS, as well as potentially remyelination of the retrobulbar optic nerve (beyond the lamina cribrosa at which point

S. Saidha, MBBCh, MD, MRCPI (✉)
Richard T. Johnson Division of Neuroimmunology
and Neuroinfectious Diseases, Department of
Neurology, Johns Hopkins Hospital,
Baltimore, MD, USA
e-mail: ssaidha2@jhmi.edu

P.A. Calabresi, MD
Richard T. Johnson Division of Neuroimmunology
and Neuroinfectious Diseases, Department of
Neurology, Multiple Sclerosis Center, Johns Hopkins
Hospital, Baltimore, MD, USA

the fibers of the optic nerves acquire myelin). Optic nerve lesions in MS display remarkable pathologic similarity to MS brain lesions in human and animal studies [6, 7]. The innermost layer of the retina is called the retinal nerve fiber layer (RNFL) and is principally composed of unmyelinated axons (Fig. 8.1) [8]. In fact, under normal circumstances, the retina constitutes an unmyelinated CNS structure, making it an ideal structure for investigating neurodegeneration in MS, since axonal and neuronal measures derived from the retina itself are not

confounded by myelin. This represents an advantage of examining neurodegeneration, as well as the impact of factors that may alter neurodegeneration (such as potentially neuroprotective and/or neurorestorative therapies), in the retina as opposed to the brain, where myelin is abundant, even in the gray matter. The axons of the RNFL (about 1.2 million per eye) are derived from ganglion cell neurons located in the ganglion cell layer (GCL) below the RNFL in the macula. These axons coalesce at the optic disks to form the optic nerves then exit the eye

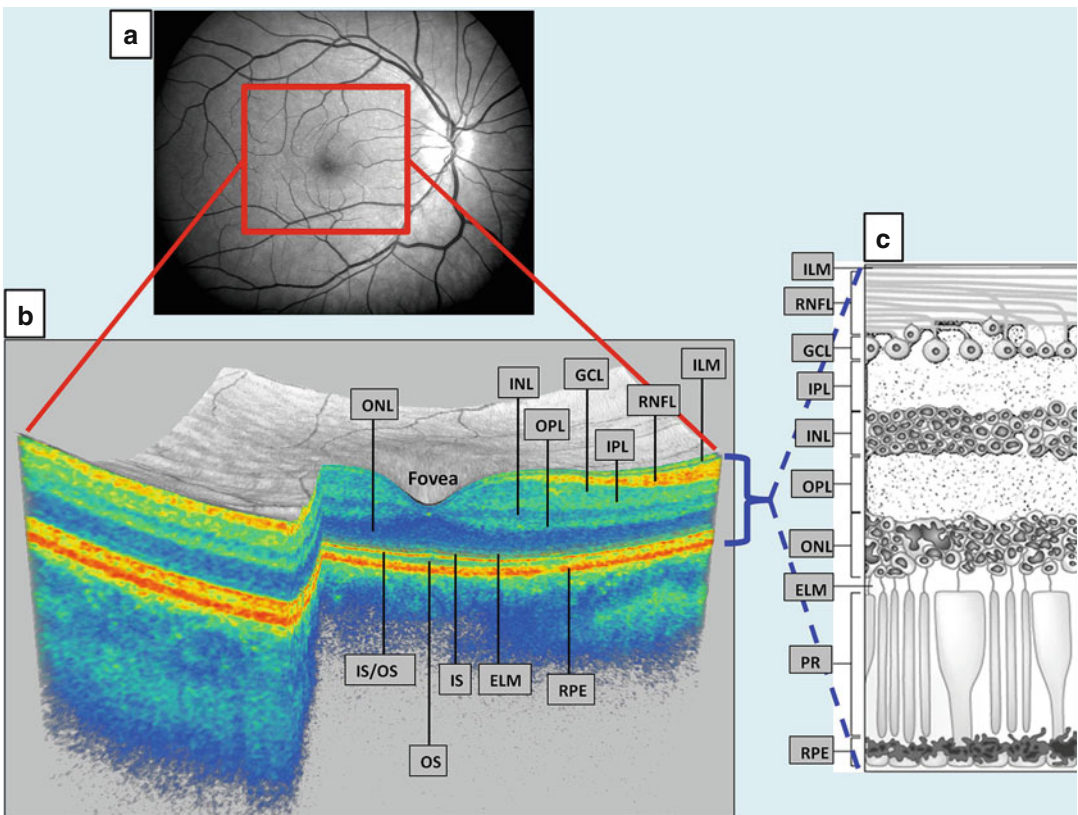


Fig. 8.1 Panel (a) represents a fundus photograph from a healthy control. Panel (b) is a 3D macular volume cube generated by Cirrus HD-OCT from the macular region denoted by the red box in panel (a) from the same healthy control. Note that the individual layers of the retina are readily discernible, except for the ganglion cell layer (GCL) and inner plexiform layer (IPL), which are difficult to distinguish. During segmentation of the OCT image, segmentation software identifies the outer boundaries of the macular retinal nerve fiber layer (RNFL), inner plexiform layer (IPL), and outer plexiform layer (OPL), as well as the inner boundary of the retinal pigment epithelium (RPE), which is identified by the conventional Cirrus

HD-OCT algorithm. The identification of these boundaries facilitates OCT segmentation, enabling determination of the thicknesses of the macular RNFL, GCL+IPL (GCIP), the inner nuclear layer (INL)+OPL, and the outer nuclear layer (ONL) including the inner and outer photoreceptor segments. Panel (c) illustrates the cellular composition of the retinal layers depicted in panel (b). *Abbreviations:* IS inner photoreceptor segments, OS outer photoreceptor segments, IS/OS IS/OS junction, PR photoreceptors, ILM inner limiting membrane, ELM external limiting membrane (Reproduced with permission from Saidha et al. [8])

posteriorly passing through the lamina cribrosa, beyond which oligodendrocyte-derived myelin is applied to them [9, 10].

Despite the conventional designation of RRMS as a primarily inflammatory demyelinating disorder of the CNS, earliest descriptions highlight prominent axonal and neuronal pathology [11, 12]. In recent years, axonal and neuronal pathology in RRMS has been the focus of considerable research. Investigation of neurodegeneration in RRMS has led to improvements in our understanding of the biological underpinnings of the disease. It is now widely recognized that axonal and neuronal degeneration, as opposed to inflammation itself, is the principal pathological substrates underlying permanent disability in RRMS and MS in general [13–19]. Although axonal and neuronal degeneration is primarily thought to occur as sequelae of inflammatory demyelination in RRMS [20–23], other contributory pathobiological processes operative as part of the disease process have been tentatively proposed.

There is a clear predilection for affliction of the optic nerves in MS. It is estimated that 25 % of RRMS patients suffer from acute multiple sclerosis associated optic neuritis (MSON) as their initial disease manifestation and that up to 70 % of MS patients experience acute MSON at least once during their disease course. In addition, subclinical or occult optic neuropathy is thought to be virtually ubiquitous in MS. In fact, 94–99 % of MS patients are found to have demyelinating lesions in their optic nerves on postmortem examination [24, 25]. Essentially all of the fundamental features of brain and spinal cord pathology in MS present themselves in the anterior visual pathway during the course of AON and subclinical optic neuropathy. Inflammation and demyelination occur simultaneously during acute MSON. Spatially, both processes may involve either the entire cross section of the nerve or a more limited portion of the nerve [26]. The inflammatory milieu in the optic nerves during acute MSON in RRMS, similar to that observed in other regions of the CNS in RRMS, is thought to play a central role in promoting demyelination and oligodendrocyte death [27, 28]. In fact, the identification of foamy macrophages (macrophages containing myelin degradation products)

is regarded as a histological feature of active MS lesions [29]. The result of these processes occurring during acute and possibly occult optic neuropathy is that axons constituent within the optic nerve are either partially or completely stripped of myelin. Evidence from experimental and pathologic studies in humans supports the notion that remyelination does occur in the adult CNS, albeit sparsely and incompletely. Although oligodendrocyte numbers may be reduced during active myelin destruction, demyelinating optic nerve injury is thought to trigger repair processes in inactive lesions including oligodendrocyte proliferation [30]. Based on animal data, the oligodendrocyte progenitor cell is currently regarded as the cell type with the greatest potential to possibly achieve differentiation in order to produce remyelination in the CNS, including within the optic nerves [31, 32]. Similar populations of oligodendrocyte progenitor cells are found in normal adult human white matter, as well as in acute and chronic lesions of MS patients [33]. Shadow plaques, composed of thinly myelinated axons, are thought to represent the outcome of remyelination. Endogenously remyelinated axons, however, tend to have thinner myelin sheaths, shorter internodal lengths, and suboptimal axonal conduction velocities, as compared to normal axons [34, 35]. Recurrent demyelinating optic nerve injury may further disrupt repair mechanisms, underlie failure of remyelination, and result in permanent demyelination [36]. Since myelin is thought to play an integral role in the maintenance of axonal health through the provision of a protective environment, demyelination and/or incomplete remyelination may result in axonal degeneration.

In addition to demyelination, inflammation in RRMS results in acute axonal transection and in turn retrograde neuronal degeneration, a dying-back phenomenon extending proximally from a point of injury along an axon, resulting in degeneration of the neuronal cell body of origin. Axonal degeneration may also proceed in an anterograde direction from a point of injury along an axon (Wallerian degeneration). Rodent models of retinal ganglion cell axotomy demonstrate concomitant anterograde and retrograde axonal degeneration [37]. Histopathologic studies

estimate that axonal densities are reduced by approximately 45 % in the optic nerves of MS patients when compared to healthy controls and with this reduction, not all explicitly linked to previous acute MSON, in part may be due to sub-clinical optic neuropathy [38]. Axonal degeneration following acute MSON may also extend anterogradely to the optic tract and retrogradely to the RNFL. Retinal ganglion cells are susceptible to the effects of retrograde axonal degeneration. This has been demonstrated in animal models showing marked ganglion cell apoptosis in response to axonal transection [39]. Postmortem human studies of MS patients have revealed significant retinal ganglion cell dropout and GCL atrophy in 73–79 % of MS eyes, of which the majority suffered from optic nerve atrophy and/or gliosis [40, 41].

Although Wallerian degeneration, retrograde axonal degeneration, and in turn neuronal degeneration following axonal injury are well described, whether these degenerative processes extend to the next cell in the chain of neuronal conduction (transsynaptic neurodegeneration) remains unclear. Dropout of neurons within the lateral geniculate nucleus (LGN) following lesions of the retina, optic nerve, and/or optic tract (anterograde transsynaptic degeneration) has been shown to occur [42]. It might also therefore be plausible for retrograde transsynaptic degeneration to occur following optic nerve injury. Early reports examining retrograde transsynaptic degeneration in the retina have described degeneration within the inner nuclear layer (INL) occurring synchronously with anterograde transsynaptic degeneration of the LGN following a lesion of the optic chiasm in a primate [43]. Curiously, the INL showed evidence of cystic changes that were irregularly rounded, the larger of which contained fine strands of tissue and debris (presumed to be the result of degeneration). These findings have been recapitulated in human eyes with lesions in the optic nerve and/or chiasm, further demonstrating a significant decrease in the cellularity of the INL [44]. Similarly, more refined histopathologic postmortem examinations have revealed prominent atrophy of the INL in 40 % of MS eyes [41].

Retinal Involvement in RRMS

As mentioned previously, dropout of ganglion cell axons located in the RNFL, as well as of ganglion cell neurons themselves (located in the GCL), is primarily felt to be the derivative of inflammatory axonal transection and chronic demyelination related to optic neuropathy. Moreover, neuronal dropout within the INL of MS eyes has also been demonstrated on post-mortem examination, although whether the etiology of this finding relates more to retrograde transsynaptic degeneration as opposed to primary neuronal mechanisms of retinal injury remains unclear. Additional evidence supporting the occurrence of deeper retinal pathology in MS is derived from a number of electroretinography (ERG) studies. In a study of 27 advanced MS patients, light-adapted and dark-adapted flicker ERG demonstrated a reduction of 2 or more standard deviations in some or all components of the ERG responses. ERG findings of eyes with chronic optic atrophy in MS patients were not found to be the same as ERG abnormalities in eyes with surgical section of the optic nerves, raising the possibility that detected ERG abnormalities in MS patients may not be the derivative of optic neuropathy and therefore not related to retrograde transsynaptic degeneration [45]. Another study compared ERG under photopic conditions to pattern reversal visual evoked potentials (PR-VEP) in MS patients with demyelinating optic neuropathy, and patients felt to have monocular demyelinating optic neuropathy. Although optic atrophy resulting from section or optic nerve compression has not been reliably found to result in diminution in amplitudes of flash ERG [46–48], patients with demyelinating optic neuropathy in this study demonstrated early and selective attenuation of the b wave (mostly thought to receive contributions from bipolar cells in the INL), which did not seem to correlate with PR-VEP results. Given the disconnect between PR-VEP (primarily thought of as reflecting the integrity of the optic nerve) and detected ERG abnormalities (predominantly thought to reflect retinal integrity) in this study, it was postulated that the derivative of the ERG

findings may be independent of optic nerve pathology [49]. ERG was also included as part of a study investigating MS patients for possible retinal autoantibodies [50]. Standard and bright flash ERG was performed in 34 MS patients. Bright flash a-wave, cone b-wave, and rod–cone b-wave implicit times were significantly delayed in MS patients, and the amplitude of the sums of photopic oscillatory potentials was also significantly reduced in MS patients. No correlation was detected between the ERG parameters and visual acuity, contrast sensitivity, color vision, or visual fields. Detected ERG abnormalities in this study implied dysfunction in several retinal layers but particularly so in the photoreceptor layer, and again, the study findings raised the possibility that the etiology of the ERG findings may not be related to optic neuropathy but instead primary retinal pathology.

The RNFL, GCL, and INL atrophy observed in ocular histological studies of MS patients has been based on qualitative assessment [40, 41]. Qualitative analyses of the plexiform layers (inner and outer plexiform layers), as well as deeper retinal structures such as the outer nuclear layer, photoreceptors, and retinal pigment epithelium in MS eyes, are lacking. Quantitative pathologic ultrastructural retinal analysis has not been previously performed in MS eyes and may relate to postmortem retinal detachment, rapid degradation of retinal tissue, difficulty with obtaining MS eyes for postmortem assessment, and challenges surrounding fixation of retinal tissue among other potential reasons. Similarly, clinicopathologic correlation of ultrastructural retinal changes from eyes of MS patients is lacking. The majority of retinal pathologic descriptions in MS are limited by being restricted to end-of-life analysis and as a result are not necessarily informative regarding the pathobiological mechanisms underlying observed findings or their temporal evolution.

The retina, although unmyelinated, appears to be a frequent site of inflammation, blood–retinal barrier disruption, and neuronal loss in MS. Retinal perivascular inflammation (periphlebitis), indicating blood–retinal barrier disruption, is estimated to occur in up to 20 % of MS patients [40, 51]. This ophthalmoscopic

finding refers to visible cuffs of inflammatory cells surrounding retinal veins analogous to cellular infiltrates seen around cerebral veins in prototypical MS lesions [52]. There may be a tendency for active retinal periphlebitis to occur simultaneously with blood–brain barrier disruption in MS [53], retinal periphlebitis may be related to overall MS severity, and may be a risk factor for the development of relapses and gadolinium-enhancing lesions, as well as an increase in T1 lesion volume during follow-up [54, 55]. Retinal periphlebitis may occur at the same time as acute MSON, and its presence in the setting of acute MSON may confer a greater risk for conversion to clinically definite MS in the future [56]. Intermediate uveitis, particularly of the pars planitis subtype, occurs in up to 16 % of MS patients [57]. Consistent with clinical observations, postmortem analyses reveal retinal inflammation with activated microglia in MS eyes [41]. Intriguingly, these collective findings raise the contentious possibility that myelin may not be necessary for instigating or propagating inflammation in MS and highlight the unmyelinated retina as an opportune site within which to study inflammation and neurodegeneration in MS.

Optical Coherence Tomography

First reported in 1991, optical coherence tomography (OCT) is a noninvasive imaging technology that uses near-infrared light to generate cross-sectional or 3-dimensional (3D) images of tissues such as the retina [58, 59]. This enables quantification of the thicknesses of retinal structures with very high resolution (<10 μm) [60]. Ophthalmologists have been using this technology for some time in the evaluation and management of a variety of disorders, including glaucoma and age-related macular degeneration among many more. In neurologic disorders, the most relevant structure conventionally imaged by OCT has been the peripapillary RNFL (RNFL located around the optic disk where the thickness of the RNFL is in general regarded as being at its greatest). In addition to providing a measurement of axonal integrity through the measurement of

RNFL thickness, the other conventional measure OCT has traditionally provided is total macular volume (TMV) or average macular thickness (AMT). Since the macula is thought to be relatively enriched by ganglion cell bodies, OCT-derived measures of TMV/AMT have been used in the past as estimates of neuronal integrity in the retina [61, 62]. However, it is worth noting that AMT/TMV is entirely nonspecific and simply represents composite measures of all of the intervening layers of the retina [10]. Except in situations where total retinal thickness is of interest, AMT and TMV have been largely superseded by specific measurements of discrete retinal layers within the macula, as generated by modern intraretinal layer segmentation techniques.

The cross-sectional or 3D images produced by OCT are generated through the measurement of magnitude and echo time delay of backscattered light from an optical beam scanned across tissue such as the retina [9]. OCT may be regarded as the optical analog of ultrasound B-mode imaging. Contemporary OCT devices were based on Michelson's principle of low-coherence interferometry [63, 64]. With this technique, measurements are performed by the use of a Michelson-type interferometer with a low-coherence-length, superluminescent diode light source. One arm of the interferometer directs light and collects the backscattered signal from the object of interest. A second reference arm with a reflecting mirror is mechanically controlled to vary the time delay and measure interference. The use of low-coherence-length light means that interference occurs when the distance traveled by the light in the sample and reference arms of the interferometer matches to within the coherence length. This allows echo delays of light from a tissue to be measured with a high degree of accuracy. The resulting data is a representation of optical backscattering in a cross section or volume of tissue.

Within the past decade, OCT technologies have dramatically evolved, leading to the generation of OCT technology known as "Fourier domain" or "spectral domain" OCT. In spectral domain OCT, light echoes are detected

by measuring the interference spectrum of infrared light by the use of an interferometer with a stationary reference arm [65]. This advanced OCT technology detects light echoes simultaneously, allowing high-speed scanning to be performed. Most current commercial spectral domain OCT devices achieve axial image resolution of approximately 5 μm , with dramatically faster imaging speeds than earlier generations of OCT technology [66–69]. Currently, the fastest commercially available spectral domain OCT (Spectralis OCT, Heidelberg Engineering, Heidelberg, Germany) has imaging speeds of approximately 40,000 axial scans per second—roughly 100 times faster than older time domain OCT.

OCT is inexpensive, reproducible, well tolerated, fast, painless, and easily repeatable. The high resolution of the images generated by OCT enables both quantitative and qualitative assessment of retinal structures. Typically OCT scan acquisition takes less than 5 min and can be performed by nonmedical personnel. Intervisit intraclass correlation (ICC) coefficients for average RNFL thickness using spectral domain OCT in healthy controls have been shown to be approximately 0.97 [70]. Modern high-speed, high-definition, spectral domain OCT is capable of rendering extremely high-resolution images, from which the individual retinal layers can be discriminated. This has led to the development of precise and fully automated segmentation algorithms allowing objective, reliable quantification of distinctive retinal layers in the macular region, in addition to conventional peripapillary RNFL thickness [9, 10, 71, 72]. Such techniques are now transitioning into clinical practice, enabling real-time quantification of the macular RNFL, combined GCL and inner plexiform layer (GCIP), combined INL and outer plexiform layer (INL), and ONL including the photoreceptor segments (ONL), in addition to peripapillary RNFL thickness [71]. Intervisit ICCs for average GCIP, INL, and ONL thickness using spectral domain OCT in healthy controls have been shown to be approximately 0.99 (0.99 in MS patients), 0.91 (0.94 in MS patients), and 0.93 (0.92 in MS patients), respectively [71].

OCT Assessment of the RNFL and GCIP in RRMS

The first study to report OCT findings in MS eyes was reported in 1999 [73]. In this pilot study using first-generation OCT technology, 14 MS patients with a history of acute MSON, with a complete recovery of visual acuity and 14 age-matched controls underwent OCT. In eyes previously affected by acute MSON, the RNFL thickness was reduced by an average of 46 % as compared to the eyes of healthy controls and by an average of 28 % when compared to the opposite “unaffected” eye of the same patient. In eyes without acute MSON history (“unaffected” eyes), the RNFL thickness was reduced by an average of 26 % relative to the eyes of healthy controls. While RNFL thickness was found to be associated with pattern ERG, no association with visual evoked potentials (VEPs) was detected. However, subsequent studies have found associations between OCT-derived measures and VEPs. In 2005, one of the earliest studies of OCT in RRMS patients with a history of acute MSON (as well as patients with a history of isolated acute MSON) to also assess macular volume was performed [74]. In eyes previously affected by acute MSON, the RNFL thickness was reduced by an average of 33 % when compared to the eyes of controls and by an average of 27 % when compared to the opposite “unaffected” eye of the same patient. Furthermore, TMV was reduced by an average of 11 % when compared to the eyes of controls and by 9 % when compared to the opposite “unaffected” eye of the same patient. In this same study, RNFL thinning correlated better with VEP P100 amplitude (thought to mainly reflect axonal integrity) rather than P100 latency (thought to mainly reflect myelin integrity), supporting the concept that reductions in RNFL thickness may be attributable to axonal degeneration. The literature is now replete with similar findings reproduced across a multitude of different studies, with many studies consistently showing that both RRMS eyes with and without a history of acute MSON have a reduced RNFL thickness as compared to healthy controls.

OCT-derived findings of reductions in RNFL thickness in RRMS confirm what is already known from postmortem studies: that subclinical optic neuropathy affects MS eyes and that similar but accelerated RNFL thinning occurs following acute MSON. Along these lines and since the advent of OCT retinal layer segmentation, there are now several studies showing reductions in GCIP thickness in MS eyes, both with and without a history of acute MSON, again with greater reductions in GCIP thickness similarly observed in eyes with acute MSON history [71, 75, 76]. RNFL thickness has been found to correlate cross-sectionally with visual function, visual quality of life, and expanded disability status scale (EDSS) scores [72]. Since the RNFL represents the axonal tracts of ganglion cell neurons, GCIP reduction is believed to be the result of retrograde axonal degeneration of the retinal nerve fibers. In other words, reduction in both RNFL and GCIP thicknesses is thought to be the derivative of the same pathologic processes—namely, optic neuropathy. Despite their similarity (the RNFL and GCIP may be regarded as biological extensions of one another), OCT-derived measures of GCIP thickness seem to have superior structure–function relationships to those of RNFL thickness [76]. This appears to be the case with high-contrast (100 %) and low-contrast (2.5 and 1.25 %) visual acuity, as well as EDSS scores. This may relate to (1) better reproducibility, (2) astrogliosis within the RNFL confounding RNFL measurements, and (3) reduced susceptibility of the GCIP to edema during optic nerve inflammation [70, 71, 75]. In a study of 132 MS patients, of which the majority had RRMS (73 %), the correlation coefficient between OCT-derived RNFL thickness and 2.5 % low-contrast letter acuity scores was 0.38, and with 1.25 % low-contrast letter acuity scores, it was 0.39 [76]. In this same study, the correlation coefficient between OCT-derived GCIP thickness and 2.5 % low-contrast letter acuity scores was 0.49, and with 1.25 % low-contrast letter acuity scores, it was 0.52. GCIP thickness also correlated better with EDSS than RNFL thickness in this same study.

Although cross-sectional findings of OCT-derived RNFL thickness and indeed

GCIP thickness in RRMS have been relatively consistent across studies, longitudinal findings have been less consistent. Although baseline RNFL thicknesses in a recent longitudinal study (consisting of 164 MS patients, of which 116 had RRMS) were consistent with thicknesses observed in previous studies [72–74, 77, 78], the rate of RNFL thinning ($-0.21 \mu\text{m}/\text{year}$) was lower than that observed in other longitudinal studies and was not significantly different from healthy controls. In one study of more than 1000 MS patients (83 % had RRMS), the rate of RNFL thinning in MS eyes was $-2.0 \mu\text{m}/\text{year}$ [79], and in another study of 166 MS patients (94 % RRMS), it was $-2.7 \mu\text{m}/\text{year}$ [80]. In the latter study, RRMS patients with disease durations <10 years, as well as those experiencing non-ocular relapses, were interestingly found to have faster rates of RNFL thinning. However, in addition to the more recent study, two other studies similarly failed to demonstrate a significant decrease in RNFL thickness during follow-up of MS patients. This being said, in one of these studies, the cohort was primarily composed of PPMS patients, and in the other study, only 37 MS patients (of which 27 had RRMS) were investigated [81, 82]. Discrepancies in RNFL change across studies may relate to differences in cohort characteristics, statistical analyses employed, and differences in the use of disease-modifying therapies between patients in studies. Although these longitudinal studies excluded patients who developed acute MSON during follow-up, failure to capture and exclude all patients that developed acute MSON, as well as the possible effects of subclinical and/or subradiological inflammation of the optic nerves, may also be a contributor to these discrepancies.

There is a paucity of studies examining longitudinal change in GCIP thickness in RRMS and MS in general. In the recent longitudinal study mentioned previously in which significant RNFL thinning was not observed during follow-up, it is interesting that significant GCIP thinning was observed during the course of follow-up [83]. Moreover, GCIP thinning was found to be accelerated in patients exhibiting non-ocular relapses, new T2 lesions, and new gadolinium-enhancing lesions during the course of study follow-up. Patients exhibiting disability progression were

also found to have faster rates of GCIP thinning. Furthermore, rates of GCIP thinning were faster in patients with disease duration <5 years, which may reflect a greater availability of retinal ganglion cells for neurodegeneration earlier in the course of the disease, or alternatively a greater tendency for inflammatory disease activity to occur earlier in the disease process. Rates of GCIP thinning were augmented when these independent factors were present in combination. For example, patients with new T2 lesions, new enhancing lesions, and disease durations <5 years exhibited 70 % faster rates of GCIP thinning. The association between faster rates of GCIP thinning and disease activity outside of the visual pathway may raise the possibility that microscopic (subclinical and subradiological) inflammation occurs in the optic nerves. This could be a reflection of more diffuse opening of the blood–brain barrier (than can be appreciated clinically or radiologically), including in the optic nerves, during disease activity in RRMS. In this context, it is interesting to consider that RNFL thickness increases during acute MSON, the basis of which is thought to be related to a combination of interstitial edema and axonal swelling related to impaired transport mechanisms [9]. On the other hand, at least compared to fellow eyes, GCIP thickness is not thought to be increased during acute MSON (Fig. 8.2) [75]. Since optic nerve inflammation is associated with RNFL swelling, but not GCIP swelling [75], subclinical inflammation within the optic nerves (which may not be detectable by MRI) could theoretically result in the pseudo-normalization or swelling of RNFL thicknesses, thereby underestimating true rates of RNFL thinning. The absence of GCIP swelling during optic nerve inflammation, as well as minimal astroglial influence on GCIP thickness measures (the retinal astrocytes are predominantly located in the RNFL), may contribute toward the better reproducibility and lower variance of GCIP over RNFL thickness measures and help explain the discrepancy in RNFL and GCIP findings observed in this longitudinal study. In keeping with evidence-based characterizations of postmortem visual system analysis in MS [40, 41], OCT has provided replete in vivo evidence of RNFL and GCIP thinning in RRMS eyes, irrespective of a history of acute MSON.

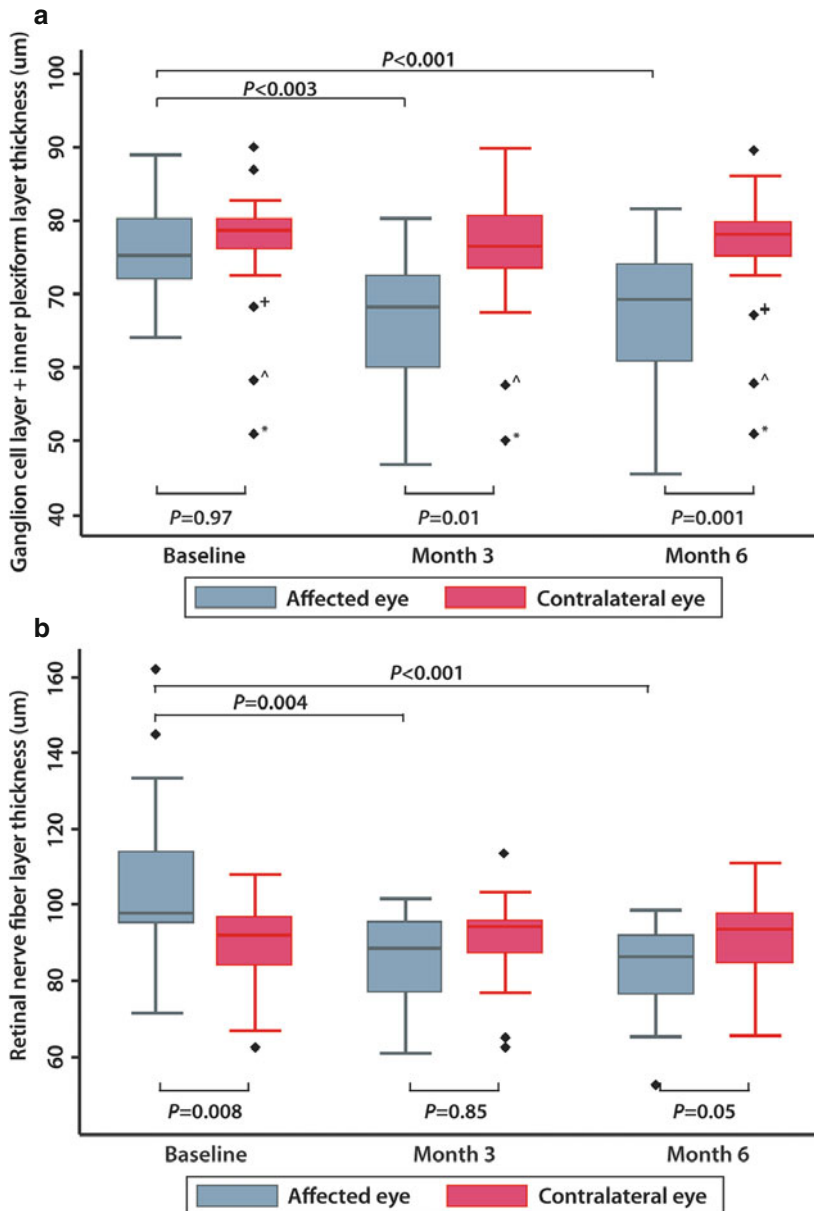


Fig. 8.2 Ganglion cell layer+inner plexiform layer (GCIP, **a**) and retinal nerve fiber layer (RNFL, **b**) thicknesses are significantly reduced following acute optic neuritis at 3 and 6 months as compared to baseline in affected eyes. Note the significant swelling of the RNFL, but not of the GCIP, within eyes affected by acute optic neuritis as compared to contralateral unaffected eyes at baseline. No significant longitudinal changes were seen in contralateral eyes for either GCIP or RNFL thicknesses. Twenty study participants were included in the baseline and month 6 data, while 17 participants were included in month 3 data. The p -values presented at month 3 represent the significant change in optical coherence tomography measures from those 17 individuals from baseline to

month 3. The p -values presented at month 6 represent the significant change from the entire cohort at baseline to the entire cohort at month 6. The error bars represent the 5th and 95th percentiles of the measure. Asterisk indicates a 45-year-old female, relapsing–remitting multiple sclerosis patient with multiple sclerosis for 10 years and two remote episodes of optic neuritis in the contralateral eye; wedge symbol indicates a 35-year-old female, relapsing–remitting multiple sclerosis patient with a duration of 7 years and one remote episode of optic neuritis in the contralateral eye; plus symbol indicates a 24-year-old female with clinically isolated syndrome and no prior history of optic neuritis. (Reproduced by permission of Oxford University Press from Syc et al. [75])

OCT Assessment of the INL and ONL in RRMS

Consistent with ERG and postmortem findings [41, 45, 49, 50, 84], OCT segmentation demonstrates quantitative INL and ONL abnormalities in MS. Although the basis for INL and potentially ONL involvement (the latter of which has not been confirmed to occur in MS eyes pathologically, although is suggested on the basis of ERG and OCT studies in MS *in vivo*) remains to be determined, highly conspicuous observations raise the possibility that a primary retinal neuronal mechanism of pathology may be operative in the anterior visual system in a limited, but not necessarily insignificant, proportion of MS patients. OCT identification of INL and ONL thinning in MS eyes without a prior history of optic neuritis, in which there is relative preservation of the RNFL and GCIP, has been referred to as the macular thinning predominant (MTP) phenotype of MS and may occur in up to 10 % of MS patients, of which the vast majority appear to have RRMS (Fig. 8.3) [71]. The MTP phenotype may be associated with more rapid accumulation of sustained disability in MS, as evidenced by higher multiple sclerosis severity scale (MSSS) scores, as well as unique visual symptoms not typical of optic neuropathy including excessive glare and photopsia [71]. The thinning of INL and ONL that is a characteristic of the MTP phenotype may be pathobiologically distinct from those that characterize tissue injury within the RNFL and GCIP related to optic neuropathy—although this and indeed even the existence of an MTP MS phenotype remain the subject of debate.

Although ocular histopathological examination reveals dropout of INL neurons in up to 40 % of MS eyes [41], qualitative assessment of OCT scans derived from MS patients *in vivo* reveals macular microcystoid changes in a small proportion (approximately 5 % of patients), which are predominantly localized to the INL (Fig. 8.4) [85, 86]. Macular microcystoid changes appear to mainly occur in the eyes of patients with RRMS and seem to occur more commonly in eyes with a prior history of acute MSON. The etiology and significance of macular microcystoid

changes in RRMS eyes have been the source of lively scientific debate. Some proponents have raised the possibility that macular microcystoid changes may represent sites of primary retinal inflammation, on the basis that 25 % of patients with macular edema demonstrating fluorescein leakage examined in an ophthalmological study exhibited similar appearing macular microcystoid changes [87], that macular microcystoid changes in MS eyes may be dynamic in nature over time, and that they may be a harbinger of more aggressive MS. Given that macular microcystoid changes may be dynamic in nature, some authors have suggested that increased INL thickness in the absence of visible macular microcystoid changes may enable capturing of the same process. As such, a longitudinal study of 164 MS patients (123 RRMS) found that increased INL thickness at baseline predicted disease activity (non-ocular relapses, formation of new T2 and/or contrast-enhancing lesions) and disability progression during follow-up, suggesting that processes within the INL might somehow be relevant or related to global disease activity in RRMS and more specifically inflammation [86]. On the other hand, some investigators have proposed that macular microcystoid changes in MS eyes are of little significance, since they may be seen in other neuroinflammatory disorders (including neuromyelitis optica and chronic relapsing inflammatory optic neuropathy) as well as noninflammatory disorders such as neurofibromatosis, Leber's hereditary optic neuropathy, and glaucoma [88–91]. Given the array of conditions in which macular microcystoid changes have been described, some consider them a final common pathway of retrograde degeneration, especially since there are histopathological descriptions of cavitation occurring within the INL following optic nerve transection dating back to the 1960s [44]. Moreover, some investigators feel these macular microcystoid changes may simply represent mechanical changes resulting from vitreomacular traction [90]. This being said, a recent study utilizing a mechanical model to examine for the presence of vitreomacular traction in OCT scans demonstrating macular microcystoid changes did not find support in favor of this hypothesis [92].

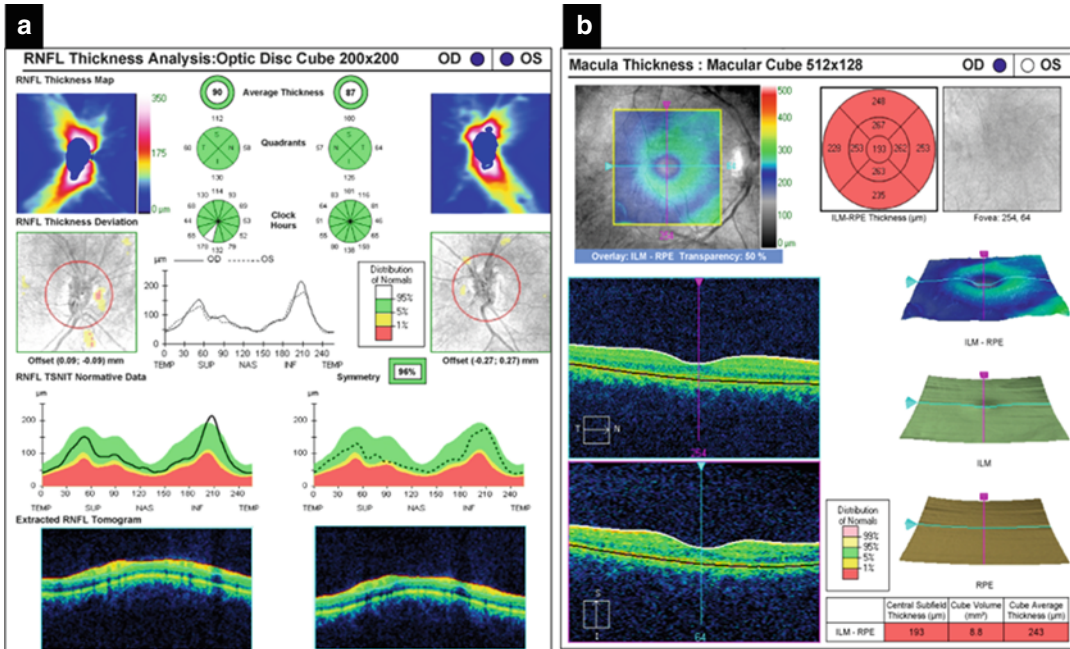


Fig. 8.3 An optical coherence tomography (OCT) peripapillary retinal nerve fiber layer (RNFL; panel a) and macular (panel b) report generated by Cirrus HD-OCT (Carl Zeiss Meditec, Dublin, California) in a patient with multiple sclerosis without a history of optic neuritis. The upper middle section of panel a displays the average RNFL thickness for the right eye (OD) and the left eye (OS), as well as the quadrant and clock hour measures of RNFL thickness for each eye. Note that the average RNFL thickness, as well as the quadrant and clock hour measures, is represented in colors that correspond to the normal distribution of RNFL thickness values. The average RNFL thickness (as well as quadrants and sectors) in each eye is represented in green (indicating values within normal range defined as being between the 5th and 95th percentiles relative to an age- and sex-matched reference population). The top right section of panel (b) displays quadrant measurements of retinal thickness. Again, these are represented in colors that correspond to the normal distribution of macular thickness values. The central mac-

ula represents the foveola, with the four quadrants immediately surrounding this (inner macula) representing the parafovea. Note that the average macular thickness (cube average thickness) indicated in the bottom right chart (as well as all of the macular quadrant thicknesses) is represented in red indicating values less than 1 % of what would be expected compared to an age- and sex-matched reference population. The macular scan of the left eye in the same patient (not shown) is similar to that of the right eye in panel (b). The combination of OCT findings described in this figure fulfills proposed criteria for a macular thinning predominant (MTP) patient. While this figure depicts OCT findings from an MS patient in whom average macular thickness was <1st percentile, MS patients with a normal average RNFL thickness together with an average macular thickness between the 1st and 5th percentiles also fulfill criteria proposed for defining the MTP MS phenotype (Reproduced with by permission of the Oxford University Press from Saidha et al. [71])

Relationships Between OCT and Magnetic Resonance Imaging in RRMS

Although magnetic resonance imaging (MRI) of the neuraxis is regarded as the gold standard imaging modality for monitoring RRMS, the association between parameters reflecting inflammatory activity (new and enlarging T2 lesions and contrast-enhancing lesions) and disability

progression in MS is modest [93]. MRI estimates of neurodegeneration, however, seem to correlate better with disability progression in MS [94, 95], which may not be unsurprising since neurodegeneration as opposed to inflammation itself has been shown across numerous studies to be the principal pathological substrate underlying disability in RRMS, and indeed in MS in general. Non-conventional MRI techniques including brain substructure volumetrics reveal that gray

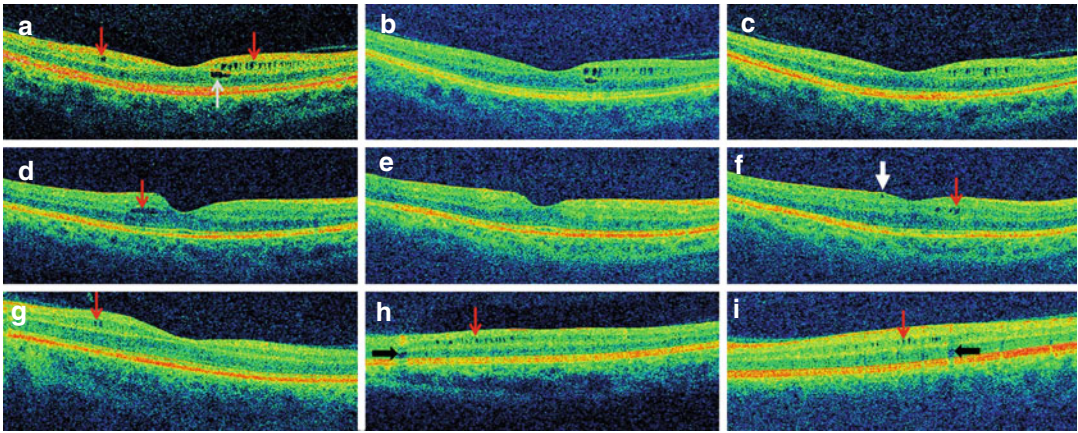


Fig. 8.4 (a–c) All images are from the same patient in chronological order over a 3-year period. (a) Microcystoid macular changes of the inner nuclear layer (INL) (red arrows) were present at baseline, as well as a foveal microcystoid macular change of the outer nuclear layer (ONL). (b–c) The foveal ONL microcystoid macular change progressively resolved during the follow-up period. (d–f) All images are from the same patient in chronological order over a 2-year period. (d) A single INL microcystoid macular change (red arrow) was present at

baseline. (e) The microcystoid macular change spontaneously resolved after 1 year. (f) Following fingolimod treatment (initiated after scan e), the patient developed new microcystoid macular changes of the INL (red arrow). An epiretinal membrane is noted (white arrow) that had been present on previous scans as well. (g–i) Three different patients with microcystoid macular changes of the INL (red arrows). Vessel artifacts (black arrows) are demonstrated for comparison. (Reproduced with permission from *Lancet Neurology* from Saidha et al. [86])

matter (GM) atrophy is a common, early feature of MS and may be better associated with disability than white matter (WM) atrophy [18, 19, 96, 97]. Despite these findings, measures derived from existing non-conventional MRI techniques may not be sufficiently sensitive to assess progression at the individual patient level or indeed in small numbers of patients. The development of novel techniques for objectively quantifying neurodegeneration in vivo in MS has therefore been an ongoing goal. For the reasons outlined previously, OCT has been proposed as an ideal candidate for this purpose [98].

To date, 13 studies have been performed assessing the relationships between OCT and MRI in MS, with the vast majority of included participants across studies mainly having RRMS. Of these studies, seven utilized older third-generation time domain OCT [54, 99–104], and six utilized newer fourth-generation spectral domain OCT [8, 83, 86, 105–107]. None of the studies using time domain OCT included OCT segmentation, while four of the spectral domain OCT studies did include OCT segmentation [8, 83, 86, 106].

All seven studies assessing relationships between time domain OCT and brain MRI in MS were cross-sectional. Six of these studies assessed the relationships between OCT-derived RNFL thickness and brain volumetrics. A consistent significant relationship between RNFL thickness and whole brain volume was observed across studies, with the exception of one study in which whole brain volume was not assessed [54] but rather just brain substructure volumes. On the other hand, whole brain volume alone, without brain substructure volumes, was assessed in two of the studies [102, 103]. In the four studies that included brain substructure volumetrics [54, 99–101], relationships between RNFL thickness and GM, WM, T1 lesion, and T2 lesion volumes were inconsistent across studies. Only one of these studies assessed differences in the relationships of brain volume with RNFL thickness between eyes with and without a history of acute MSON [101]. In this study, RNFL thickness, only from eyes without acute MSON history, correlated with whole brain and GM volumes, raising the possibility that MSON may mask underlying retinal–brain relationships in MS due to

disproportionate retinal injury following acute MSON. One of the OCT volumetric studies also included magnetic resonance spectroscopy [103]. This study found that reduced RNFL thickness was independently associated with whole brain volume and reduced N-acetyl-aspartate (NAA) concentrations in the visual cortex in MS. Whole brain volume and visual cortex NAA concentrations were not associated. These findings suggest RNFL thickness in MS may reflect global, as well as visual pathway-specific neurodegeneration. The study, which did not include brain volumetrics, assessed the relationship between OCT measures and diffusion tensor imaging (DTI) indices along the optic radiation [104]. RNFL thickness and DTI indices along the optic radiation in the MS cohort studied were associated, suggesting anterior and posterior visual pathway neurodegeneration in MS is related.

Six studies assessed relationships between spectral domain OCT and brain MRI in MS. Of these, four studies included brain volumetrics and were cross-sectional [8, 105–107], although in one of these studies, analysis of relationships was repeated after 1 year [107], without direct comparison to baseline. This latter study, which did not include OCT segmentation, investigated relationships between anterior visual pathway OCT-derived measures and posterior visual pathway measures (assessed by 3T MRI-derived volumetry and spectroscopy). At baseline, visual cortex volume, visual cortex NAA, and optic radiation volume were associated with RNFL thickness. Repeating the same analyses after 1 year, visual cortex and optic radiation volumes remained associated with RNFL thickness, highlighting anterior–posterior visual pathway relationships in MS. One other study, which also did not include OCT segmentation, found a relationship between RNFL thickness and whole brain volume, as well as WM volume [105]. Limited OCT segmentation was included in one study, which found that RNFL and GCIP thicknesses were both associated with whole brain volume, GM volume, and WM volume [106]. Interestingly, the relationships between RNFL and GCIP thicknesses with GM volume were abolished in eyes with MSON history, again raising the possibility that

excessive tissue injury following MSON may mask retinal–brain relationships in MS. A more detailed assessment of associations between OCT segmentation measures and 3T brain volumetrics in MS was performed in a single study (Fig. 8.5) [8]. This study included 84 subjects of which 58 had RRMS and demonstrated that RNFL and GCIP thicknesses, only from eyes without MSON history, were associated with GM volume. Increased INL thickness, only in RRMS eyes without acute MSON history, was found to be associated with increased FLAIR lesion volume, while reduced ONL thickness (curiously only in eyes with acute MSON history) tended toward being associated with most of the brain substructure volumes. The results of this study raise the possibility that pathology within the INL and ONL might reflect different aspects of the MS disease process than those reflected by the RNFL and GCIP. It remains to be clarified whether potential alterations in the INL and ONL of MS patients are the result of glial cell (including Müller cell) activation, possibly in response to ganglion cell death, or alternatively aberrations in their capacity to process interstitial retinal fluid, changes in extracellular matrix, hypertrophy of cell bodies within these predominantly neuronal layers, or a combination of such factors.

The remaining two spectral domain studies assessing the relationships between OCT and brain MRI in MS did not include brain volumetrics. Both of these studies were described in greater detail earlier. In one study, MS patients exhibiting clinical and/or radiological evidence of disease activity (non-ocular relapses, formation of new T2, and/or contrast-enhancing lesions) or disability progression during follow-up were found to have accelerated rates of GCIP thinning [83]. Results of this study suggest that disease activity in MS results in an increased rate of GCIP thinning, possibly related to either trans-synaptic effects, or the occurrence of subclinical and subradiological concomitant inflammation within the optic nerves. In the final study, increased INL thickness at baseline was found to be predictive of disease activity (non-ocular relapses, formation of new T2, and/or contrast-enhancing lesions) and disability progression

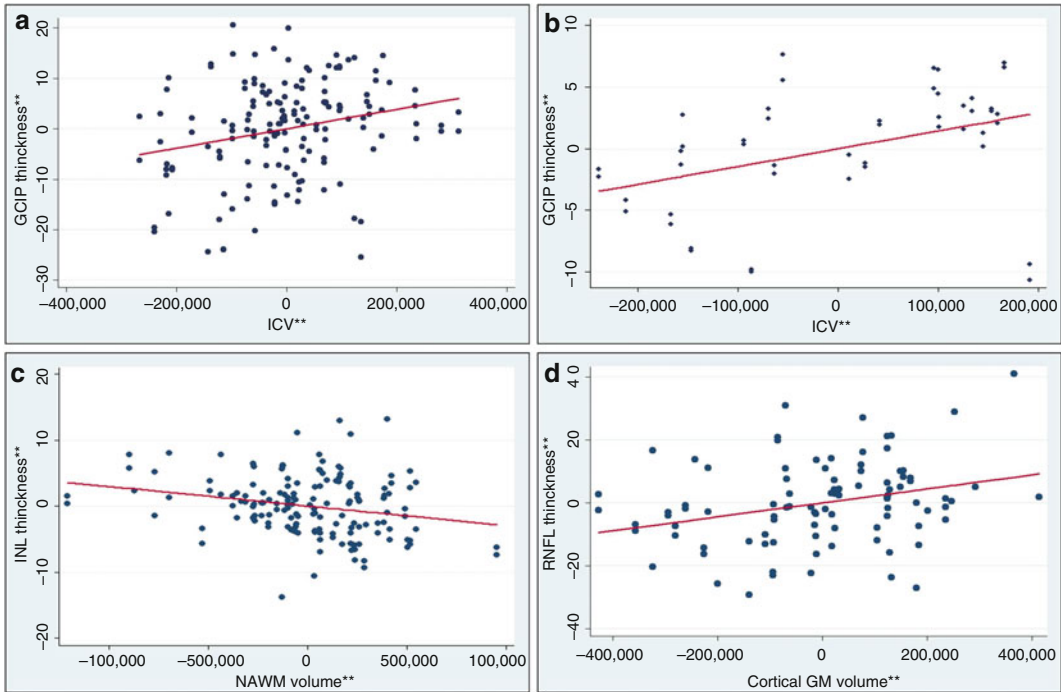


Fig. 8.5 Panel (a) represents an adjusted variable plot of ganglion cell layer+inner plexiform layer (*GCIP*) thickness and intracranial volume (*ICV*) in multiple sclerosis (*MS*), adjusted for age, sex, and disease duration. The *solid red line* illustrates the independent relationship between *GCIP* thickness and *ICV* in *MS*. Note that as *ICV* increases, *GCIP* thickness similarly increases, consistent with the detection of significant associations between *GCIP* thickness and *ICV* in *MS* ($p=0.008$). Panel (b) represents an adjusted variables plot of *GCIP* thickness and *ICV* in healthy controls (*HCS*), adjusted for age and sex. The *solid red line* graphically illustrates the independent relationship between *GCIP* thickness and *ICV* in *HCS*. As *ICV* increases, *GCIP* thickness similarly increases. Panel (c)

represents an adjusted variables plot of inner nuclear layer (*INL*) thickness and normal appearing white matter (*NAWM*) volume in *MS*, adjusted for age, sex, disease duration, and *ICV*. The *solid red line* shows the independent relationship between *INL* thickness and *NAWM* volume in *MS*. Note that as *INL* thickness increases, *NAWM* volume decreases. Panel (d) depicts an adjusted variable plot of peripapillary retinal nerve fiber layer (*RNFL*) thickness and cortical gray matter (*GM*) volume in *RRMS*, adjusted for age, sex, disease duration, and *ICV*. The *solid red line* graphically illustrates the independent relationship between *RNFL* thickness and cortical *GM* volume in *RRMS*. **Residual values from multivariate regression models (Reproduced with permission from Saidha et al. [8])

during follow-up, suggesting that processes within the *INL* of the eye might somehow be relevant or related to global disease activity and more specifically inflammation in *MS* [86].

None of the aforementioned 13 studies assessed concomitant changes in either conventional OCT or OCT segmentation-derived retinal measures and whole brain (or brain substructure) volumetrics over time in *MS*. Although results of some of the above investigations assessing the relationships between OCT-derived measures and brain substructure volumes in *MS* were conflicting, the consistently observed relationship between *RNFL* thickness and whole brain

volume is encouraging, providing evidence that at least to an extent *RNFL* thickness measures reflect global CNS processes in *MS*. Given the biological similarity of the *RNFL* and *GCIP*, it is not surprising that relationships between *RNFL* thickness and *GCIP* thickness with brain MRI volumes have been found to be largely similar in *MS*. Moreover, OCT-derived *INL* and *ONL* thicknesses may impart information regarding different processes operative within different compartments of the *MS* brain, as compared to *RNFL* and *GCIP* thicknesses. This could relate to different disease mechanisms underlying changes in the *INL* and *ONL*, from *RNFL* and

GCIP changes in MS. At the same time, it must be acknowledged that there is need for further study of the relationships between OCT-derived measures and brain MRI in MS, since this overall remains an understudied area. Specifically, there is a need for longitudinal assessments of OCT and MRI in MS, which are currently lacking [108].

OCT as an Outcome Measure in RRMS Clinical Trials

OCT has several important characteristics that make it a good potential clinical trial outcome for evaluating axonal (RNFL) and neuronal (GCIP) damage, neuroprotection, and remyelination (of the retrolaminar optic nerve). These include pathologic specificity, strong structure–function relationships, good reproducibility and reliability, practicality, the potential to identify change over time, and lack of confounding of OCT-derived measures of axonal and neuronal structures within the retina due to myelin.

OCT measurements of RNFL and GCIP thickness are thought to predominantly reflect axonal and neuronal integrity, respectively. The prevailing hypothesis is that degeneration of these structures in MS is primarily the result of a retrograde process stemming from axonal transection and/or demyelination of axons within the optic nerve. Although this process of neurodegeneration ensues rapidly and in a more marked fashion immediately following acute MSON, significant neurodegeneration of these structures also occurs in the absence of acute MSON in RRMS eyes and MS eyes in general and is more than likely related to subclinical optic neuropathy. Therefore, OCT may not only have a role in assessing neurodegeneration, neuroprotection, and remyelination in the setting of acute MSON but also in MS patients not experiencing acute MSON. In terms of assessing neurodegeneration, OCT-derived GCIP thickness measures may have several advantages over RNFL thickness measures, including better reproducibility, lower variance, and absence of swelling during optic nerve inflammation, as well as a limited influence of

astroglia on GCIP thickness measures. Since RRMS patients exhibiting inflammatory disease activity (clinically, radiographically, or both), as well as those with shorter disease durations, may have faster rates of GCIP thinning, potentially, targeting early active RRMS patients for recruitment may help enrich clinical trials using OCT as an outcome measure. Collectively, the findings outlined previously support the use of OCT measures to monitor subclinical and clinical disease progression in RRMS, as well as treatments primarily targeting neurodegenerative processes. From a pathophysiological perspective, demyelinated axons are not always destined to degenerate, although this may obviously occur. A demyelinated but intact axon may potentially be remyelinated (either partially or completely) by local viable adult oligodendrocytes or differentiating oligodendrocyte cells, possibly protecting against degeneration. On these grounds, OCT is being utilized as an outcome measure in a number of studies of putatively remyelinating therapies. For example, OCT has been incorporated as an outcome measure in two phase 2 studies of the potentially remyelinating compound anti-LINGO-1. In one of these studies (called RENEW), the compound was tested in the setting of acute MSON (the study is now complete and finalized results from the study are still awaited), while in the other study, which is ongoing (SYNERGY), predominantly RRMS patients are being investigated. Remyelination of the retrolaminar optic nerve may protect demyelinated nerve fibers from degeneration. Along these lines, neuroprotective therapies or therapies that prevent or protect damaged axons/neurons from degenerating might also produce effects on the RNFL and GCIP that may be measurable by OCT. For these reasons, OCT is also being used as an outcome measure in trials of putatively neuroprotective therapies. For example, OCT was incorporated as an outcome measure assessing the neuroprotective effects of erythropoietin in AON [109] and is currently being used as an outcome measure to assess the potential neuroprotective effects of phenytoin in AON, among many other studies assessing neuroprotective strategies in acute MSON and non-MSON RRMS.

Conclusion

OCT fulfills the unmet need of an imaging modality allowing highly reproducible quantification of axonal and neuronal measures in RRMS and MS in general. Moreover, OCT is noninvasive, inexpensive, well tolerated, and easily repeatable/performed. In recent years, the advent of OCT segmentation allowing the assessment of discrete retinal layers has significantly added to the potential utility of OCT. In particular, OCT-derived measures of GCIP thickness may be superior to conventionally derived OCT measures of peripapillary RNFL thickness. Since optic neuropathy is virtually ubiquitous as part of the MS disease process, OCT-derived measures of RNFL and GCIP thickness in particular essentially reflect neurodegenerative processes operative within the optic nerves of MS patients. In addition to demonstrating utility for tracking neurodegeneration related to acute MSON in RRMS, OCT also demonstrates utility for the purpose of tracking subclinical optic neuropathy in RRMS, as well as in the progressive subtypes of the disease. By allowing highly sensitive and reproducible quantification of the RNFL and GCIP, OCT also affords the potential capability to assess the effects of remyelination of the retrolaminar optic nerve fibers, as well as neuroprotection of optic nerve fibers on the integrity of the RNFL and neuronal cell predominant GCIP. Although OCT-derived RNFL and GCIP thicknesses are functionally related to visual function and in particular to low-contrast visual function in RRMS, one of the most attractive features of these OCT measures is the insight they provide regarding the global disease process in RRMS. While related to EDSS, they are also associated with whole brain volumes and therefore the more global state of neurodegeneration in RRMS. By extension, utilizing OCT to assess remyelination and/or neuroprotection in the anterior visual pathway of RRMS patients may reflect ongoing similar processes elsewhere in the CNS. This premise is critical and central to the inclusion of OCT as an outcome measure of putatively remyelinating and neuroprotective therapies.

In addition to a role for OCT in monitoring neurodegeneration and the effect of potential therapeutics on the process of neurodegeneration in RRMS, OCT has also helped shed light on the pathobiology of RRMS. OCT segmentation has been particularly beneficial in this respect. Although the etiology of INL and potential ONL changes in RRMS remain to be elucidated, their relationships with global disability, as well as inflammatory disease activity and disability progression, do raise the possibility that they may be biologically significant. RRMS patients harboring the MTP phenotype appear to have higher MSSS scores, as well as unique visual symptoms not typically attributable to optic neuropathy. The identification of macular microcystoid changes in the INL of RRMS eyes, particularly with a prior history of acute MSON, represents one of the most contentious findings in recent times related to OCT in MS. Similar findings have been observed in other inflammatory and noninflammatory disorders, and given the demonstration of cavitory changes in the INL following optic nerve injury in the past, collectively these factors call into question the significance and etiology of microcystoid macular changes. This, being said, increased INL thickness at baseline (regardless of visible microcystoid changes or not) has been shown to predict inflammatory disease activity and disability progression in RRMS. Moreover, increased INL thickness in RRMS has been shown cross-sectionally to correlate with T2 lesion volume.

While OCT and advances in OCT, such as OCT retinal layer segmentation, have undeniably led to the development of potential new measures for tracking neurodegeneration and potentially assessing neuroprotection and remyelination in RRMS and MS in general, as well as led to an improved understanding of the MS disease process, much further work is required. Although there is an abundance of data available for OCT in RRMS, the majority of such studies also included small numbers of progressive MS patients and, on occasion, patients with clinically isolated syndromes.

In addition, studies vary in terms of the OCT devices utilized, as well as the segmentation techniques employed. OCT segmentation across studies to date has varied in terms of being manual, semiautomatic, or fully automatic, and even within these different types of segmentation techniques, there has been a great degree of variability in terms of the software employed, as well as the retinal layers assessed. This also similarly applies to the MRI devices and MRI volumetric techniques employed across studies assessing retinal–brain relationships. Statistical analysis across studies also varies widely. Collectively, these factors challenge the generalizability of findings from individual studies and contribute to difficulty in comparing results across studies. Future studies need to be more homogenous in terms of their patient inclusion, OCT and MRI devices utilized, and OCT and MRI segmentation techniques employed, as well as their approach to analyses, in order to make the results of studies more comparable. There is also a paucity of longitudinal studies of OCT in RRMS. While cross-sectional studies suggest relationships between RNFL and GCIP thicknesses and whole brain volume, as well as INL thickness with lesion volume, a critical yet unanswered question is whether atrophy within specific retinal layers concomitantly mirrors global neurodegeneration over time in MS. Similarly, in terms of establishing a biological relevance for the INL in MS, it needs to be determined whether INL thickness changes over time mirror global inflammation. In order to answer these questions, a longitudinal study of OCT and MRI in RRMS is required.

Although much further work is needed, results to date of OCT in RRMS are exciting. Through the use of OCT, physicians may be able to gain deeper insight into ongoing processes within the brains of their MS patients at the bedside. Moreover, OCT may be critical for the definitive identification and monitoring of neuroprotection and remyelination due to novel therapeutics, thereby playing a central role in shaping the future of novel therapeutic avenues in MS.

Disclosures SS has received consulting fees from Medical Logix for the development of CME programs in neurology, consulting fees from Axon Advisors LLC, educational grant support from Novartis and Teva Neurosciences, and speaking honoraria from the National Association of Managed Care Physicians, Advanced Studies in Medicine, and the Family Medicine Foundation of West Virginia. He has also served on a scientific advisory boards for Biogen-Idec and Genzyme.

PAC has received personal compensation for consulting and serving on scientific advisory boards from Vertex, Vaccinex, Merck, and Abbvie and has received research funding from Biogen IDEC, MedImmune, and Novartis.

References

1. Anderson DW, Ellenberg JH, Leventhal CM, Reingold SC, Rodriguez M, Silberberg DH. Revised estimate of the prevalence of multiple sclerosis in the United States. *Ann Neurol*. 1992;31(3):333–6.
2. Lublin FD, Reingold SC. Defining the clinical course of multiple sclerosis: results of an international survey. National Multiple Sclerosis Society (USA) Advisory Committee on Clinical Trials of New Agents in Multiple Sclerosis. *Neurology*. 1996;46(4):907–11.
3. Saidha S, Eckstein C, Calabresi PA. New and emerging disease modifying therapies for multiple sclerosis. *Ann N Y Acad Sci*. 2012;1247:117–37.
4. Prineas J. Pathology of multiple sclerosis. In: Cook S, editor. *Handbook of multiple sclerosis*. New York: Marcel Dekker; 2001. p. 289–324.
5. Frohman EM, Racke MK, Raine CS. Multiple sclerosis – the plaque and its pathogenesis. *N Engl J Med*. 2006;354(9):942–55.
6. Allen IV. The pathology of multiple sclerosis – fact, fiction and hypothesis. *Neuropathol Appl Neurobiol*. 1981;7(3):169–82.
7. Guy J, Fitzsimmons J, Ellis EA, Beck B, Mancuso A. Intraorbital optic nerve and experimental optic neuritis. Correlation of fat suppression magnetic resonance imaging and electron microscopy. *Ophthalmology*. 1992;99(5):720–5.
8. Saidha S, Sotirchos ES, Oh J, et al. Relationships between retinal axonal and neuronal measures and global central nervous system pathology in multiple sclerosis. *JAMA Neurol*. 2013;70(1):34–43.
9. Frohman EM, Fujimoto JG, Frohman TC, Calabresi PA, Cutter G, Balcer LJ. Optical coherence tomography: a window into the mechanisms of multiple sclerosis. *Nat Clin Pract Neurol*. 2008;4(12):664–75.
10. Saidha S, Eckstein C, Ratchford JN. Optical coherence tomography as a marker of axonal damage in multiple sclerosis. *CML – Mult Scler*. 2010;2(2):33–43.
11. Marburg O. Die sogennate akute multiple sklerose. *Jahrb Psychiatrie*. 1906;27:211–312.
12. Putnam T. Studies in multiple sclerosis. *Arch Neurol Psychol*. 1936;35:1289–308.

13. van Waesberghe JH, Kamphorst W, De Groot CJ, et al. Axonal loss in multiple sclerosis lesions: magnetic resonance imaging insights into substrates of disability. *Ann Neurol*. 1999;46(5):747–54.
14. De Stefano N, Narayanan S, Francis GS, et al. Evidence of axonal damage in the early stages of multiple sclerosis and its relevance to disability. *Arch Neurol*. 2001;58(1):65–70.
15. Compston A, Coles A. Multiple sclerosis. *Lancet*. 2002;359(9313):1221–31.
16. Miller DH. Biomarkers and surrogate outcomes in neurodegenerative disease: lessons from multiple sclerosis. *NeuroRx*. 2004;1(2):284–94.
17. Minneboo A, Uitdehaag BM, Jongen P, et al. Association between MRI parameters and the MS severity scale: a 12 year follow-up study. *Mult Scler*. 2009;15(5):632–7.
18. Calabrese M, Atzori M, Bernardi V, et al. Cortical atrophy is relevant in multiple sclerosis at clinical onset. *J Neurol*. 2007;254(9):1212–20.
19. Calabrese M, Agosta F, Rinaldi F, et al. Cortical lesions and atrophy associated with cognitive impairment in relapsing-remitting multiple sclerosis. *Arch Neurol*. 2009;66(9):1144–50.
20. Rawes JA, Calabrese VP, Khan OA, DeVries GH. Antibodies to the axolemma-enriched fraction in the cerebrospinal fluid and serum of patients with multiple sclerosis and other neurological diseases. *Mult Scler*. 1997;3(6):363–9.
21. Madigan MC, Rao NS, Tenhula WN, Sadun AA. Preliminary morphometric study of tumor necrosis factor- α (TNF α)-induced rabbit optic neuropathy. *Neurol Res*. 1996;18(3):233–6.
22. Shindler KS, Ventura E, Dutt M, Rostami A. Inflammatory demyelination induces axonal injury and retinal ganglion cell apoptosis in experimental optic neuritis. *Exp Eye Res*. 2008;87(3):208–13.
23. Frischer JM, Bramow S, Dal-Bianco A, et al. The relation between inflammation and neurodegeneration in multiple sclerosis brains. *Brain*. 2009;132(Pt 5):1175–89.
24. Toussaint D, Perier O, Verstappen A, Bervoets S. Clinicopathological study of the visual pathways, eyes, and cerebral hemispheres in 32 cases of disseminated sclerosis. *J Clin Neuroophthalmol*. 1983;3(3):211–20.
25. Ikuta F, Zimmerman HM. Distribution of plaques in seventy autopsy cases of multiple sclerosis in the united states. *Neurology*. 1976;26(6 PT 2):26–8.
26. Burton EV, Greenberg BM, Frohman EM. Optic neuritis: a mechanistic view. *Pathophysiology*. 2011;18(1):81–92.
27. di Penta A, Moreno B, Reix S, et al. Oxidative stress and proinflammatory cytokines contribute to demyelination and axonal damage in a cerebellar culture model of neuroinflammation. *PLoS One*. 2013;8(2), e54722.
28. Smith KJ, Lassmann H. The role of nitric oxide in multiple sclerosis. *Lancet Neurol*. 2002;1(4):232–41.
29. Noseworthy JH, Lucchinetti C, Rodriguez M, Weinschenker BG. Multiple sclerosis. *N Engl J Med*. 2000;343(13):938–52.
30. Lucchinetti C, Bruck W, Parisi J, Scheithauer B, Rodriguez M, Lassmann H. A quantitative analysis of oligodendrocytes in multiple sclerosis lesions. A study of 113 cases. *Brain*. 1999;122(Pt 12):2279–95.
31. Carroll WM, Jennings AR, Mastaglia FL. The origin of remyelinating oligodendrocytes in antiserum-mediated demyelinating optic neuropathy. *Brain*. 1990;113(Pt 4):953–73.
32. Reynolds R, Wilkin GP. Cellular reaction to an acute demyelinating/remyelinating lesion of the rat brain stem: localisation of GD3 ganglioside immunoreactivity. *J Neurosci Res*. 1993;36(4):405–22.
33. Scolding N, Franklin R, Stevens S, Heldin CH, Compston A, Newcombe J. Oligodendrocyte progenitors are present in the normal adult human CNS and in the lesions of multiple sclerosis. *Brain*. 1998;121(Pt 12):2221–8.
34. Hanafy KA, Sloane JA. Regulation of remyelination in multiple sclerosis. *FEBS Lett*. 2011;585(23):3821–8.
35. Wu LM, Williams A, Delaney A, Sherman DL, Brophy PJ. Increasing internodal distance in myelinated nerves accelerates nerve conduction to a flat maximum. *Curr Biol*. 2012;22(20):1957–61.
36. Prineas JW, Barnard RO, Revesz T, Kwon EE, Sharer L, Cho ES. Multiple sclerosis. Pathology of recurrent lesions. *Brain*. 1993;116(Pt 3):681–93.
37. Kanamori A, Catrinescu MM, Belisle JM, Costantino S, Levin LA. Retrograde and wallerian axonal degeneration occur synchronously after retinal ganglion cell axotomy. *Am J Pathol*. 2012;181(1):62–73.
38. Evangelou N, Konz D, Esiri MM, Smith S, Palace J, Matthews PM. Size-selective neuronal changes in the anterior optic pathways suggest a differential susceptibility to injury in multiple sclerosis. *Brain*. 2001;124(Pt 9):1813–20.
39. Fairless R, Williams SK, Hoffmann DB, et al. Preclinical retinal neurodegeneration in a model of multiple sclerosis: the journal of neuroscience 2012; 32(16):5585–5597. *Ann Neurosci*. 2012;19(3):121–2.
40. Kerrison JB, Flynn T, Green WR. Retinal pathologic changes in multiple sclerosis. *Retina*. 1994;14(5):445–51.
41. Green AJ, McQuaid S, Hauser SL, Allen IV, Lyness R. Ocular pathology in multiple sclerosis: retinal atrophy and inflammation irrespective of disease duration. *Brain*. 2010;133(6):1591–601.
42. Goldby F. A note on transneuronal atrophy in the human lateral geniculate body. *J Neurol Neurosurg Psychiatry*. 1957;20(3):202–7.
43. VanBuren JM. Trans-synaptic retrograde degeneration in the visual system of primates. *J Neurol Neurosurg Psychiatry*. 1963;26:402–9.
44. Gills Jr JP, Wadsworth JA. Degeneration of the inner nuclear layer of the retina following lesions of the

- optic nerve. *Trans Am Ophthalmol Soc.* 1966;64:66–88.
45. Gills Jr JP. Electroretinographic abnormalities and advanced multiple sclerosis. *Invest Ophthalmol.* 1966;5(6):555–9.
 46. Dawson WW, Maida TM, Rubin ML. Human pattern-evoked retinal responses are altered by optic atrophy. *Invest Ophthalmol Vis Sci.* 1982;22(6):796–803.
 47. Seiple W, Price MJ, Kupersmith M, Siegel IM, Carr RE. The pattern electroretinogram in optic nerve disease. *Ophthalmology.* 1983;90(9):1127–32.
 48. Kaufman D, Celesia GG. Simultaneous recording of pattern electroretinogram and visual evoked responses in neuro-ophthalmologic disorders. *Neurology.* 1985;35(5):644–51.
 49. Papakostopoulos D, Fotiou F, Hart JC, Banerji NK. The electroretinogram in multiple sclerosis and demyelinating optic neuritis. *Electroencephalogr Clin Neurophysiol.* 1989;74(1):1–10.
 50. Forooghian F, Sproule M, Westall C, et al. Electroretinographic abnormalities in multiple sclerosis: possible role for retinal autoantibodies. *Doc Ophthalmol.* 2006;113(2):123–32.
 51. Rucker CW. Sheathing of the retinal veins in multiple sclerosis. Review of pertinent literature. *Mayo Clin Proc.* 1972;47(5):335–40.
 52. Engell T, Jensen OA, Klinken L. Periphlebitis retinae in multiple sclerosis. A histopathological study of two cases. *Acta Ophthalmol (Copenh).* 1985;63(1):83–8.
 53. Engell T, Hvidberg A, Uhrenholdt A. Multiple sclerosis: periphlebitis retinalis et cerebro-spinalis. A correlation between periphlebitis retinalis and abnormal technetium brain scintigraphy. *Acta Neurol Scand.* 1984;69(5):293–7.
 54. Sepulcre J, Murie-Fernandez M, Salinas-Alaman A, Garcia-Layana A, Bejarano B, Villoslada P. Diagnostic accuracy of retinal abnormalities in predicting disease activity in MS. *Neurology.* 2007;68(18):1488–94.
 55. Ortiz-Perez S, Martinez-Lapiscina EH, Gabilondo I, et al. Retinal periphlebitis is associated with multiple sclerosis severity. *Neurology.* 2013;81(10):877–81.
 56. Lightman S, McDonald WI, Bird AC, et al. Retinal venous sheathing in optic neuritis. Its significance for the pathogenesis of multiple sclerosis. *Brain.* 1987;110(Pt 2):405–14.
 57. Donaldson MJ, Pulido JS, Herman DC, Diehl N, Hodge D. Pars planitis: a 20-year study of incidence, clinical features, and outcomes. *Am J Ophthalmol.* 2007;144(6):812–7.
 58. Huang D, Swanson EA, Lin CP, et al. Optical coherence tomography. *Science.* 1991;254(5035):1178–81.
 59. Hrynchak P, Simpson T. Optical coherence tomography: an introduction to the technique and its use. *Optom Vis Sci.* 2000;77(7):347–56.
 60. Hsu JJ, Sun CW, Lu CW, Yang CC, Chiang CP, Lin CW. Resolution improvement with dispersion manipulation and a retrieval algorithm in optical coherence tomography. *Appl Optics.* 2003;42(2):227–34.
 61. Moura FC, Medeiros FA, Monteiro ML. Evaluation of macular thickness measurements for detection of band atrophy of the optic nerve using optical coherence tomography. *Ophthalmology.* 2007;114(1):175–81.
 62. Burkholder BM, Osborne B, Loguidice MJ, et al. Macular volume determined by optical coherence tomography as a measure of neuronal loss in multiple sclerosis. *Arch Neurol.* 2009;66(11):1366–72.
 63. Fercher AF, Mengedocht K, Werner W. Eye-length measurement by interferometry with partially coherent light. *Opt Lett.* 1988;13(3):186–8.
 64. Hitzengerber CK. Optical measurement of the axial eye length by laser Doppler interferometry. *Invest Ophthalmol Vis Sci.* 1991;32(3):616–24.
 65. Forte R, Cennamo GL, Finelli ML, de Crecchio G. Comparison of time domain stratus OCT and spectral domain SLO/OCT for assessment of macular thickness and volume. *Eye (Lond).* 2009;23(11):2071–8.
 66. de Boer JF, Cense B, Park BH, Pierce MC, Tearney GJ, Bouma BE. Improved signal-to-noise ratio in spectral-domain compared with time-domain optical coherence tomography. *Opt Lett.* 2003;28(21):2067–9.
 67. Wojtkowski M, Srinivasan V, Ko T, Fujimoto J, Kowalczyk A, Duker J. Ultrahigh-resolution, high-speed, Fourier domain optical coherence tomography and methods for dispersion compensation. *Opt Express.* 2004;12(11):2404–22.
 68. Nassif N, Cense B, Park BH, et al. In vivo human retinal imaging by ultrahigh-speed spectral domain optical coherence tomography. *Opt Lett.* 2004;29(5):480–2.
 69. Leitgeb R, Hitzengerber C, Fercher A. Performance of fourier domain vs. time domain optical coherence tomography. *Opt Express.* 2003;11(8):889–94.
 70. Syc SB, Warner CV, Hiremath GS, et al. Reproducibility of high-resolution optical coherence tomography in multiple sclerosis. *Mult Scler.* 2010;16(7):829–39.
 71. Saidha S, Syc SB, Ibrahim MA, et al. Primary retinal pathology in multiple sclerosis as detected by optical coherence tomography. *Brain.* 2011;134(Pt 2):518–33.
 72. Petzold A, de Boer JF, Schippling S, et al. Optical coherence tomography in multiple sclerosis: a systematic review and meta-analysis. *Lancet Neurol.* 2010;9(9):921–32.
 73. Parisi V, Manni G, Spadaro M, et al. Correlation between morphological and functional retinal impairment in multiple sclerosis patients. *Invest Ophthalmol Vis Sci.* 1999;40(11):2520–7.
 74. Trip SA, Schlottmann PG, Jones SJ, et al. Retinal nerve fiber layer axonal loss and visual dysfunction in optic neuritis. *Ann Neurol.* 2005;58(3):383–91.
 75. Syc SB, Saidha S, Newsome SD, et al. Optical coherence tomography segmentation reveals ganglion cell layer pathology after optic neuritis. *Brain.* 2012;135(Pt 2):521–33.

76. Saidha S, Syc SB, Durbin MK, et al. Visual dysfunction in multiple sclerosis correlates better with optical coherence tomography derived estimates of macular ganglion cell layer thickness than peripapillary retinal nerve fiber layer thickness. *Mult Scler*. 2011;17(12):1449–63.
77. Costello F, Coupland S, Hodge W, et al. Quantifying axonal loss after optic neuritis with optical coherence tomography. *Ann Neurol*. 2006;59(6):963–9.
78. Fisher JB, Jacobs DA, Markowitz CE, et al. Relation of visual function to retinal nerve fiber layer thickness in multiple sclerosis. *Ophthalmology*. 2006;113(2):324–32.
79. Talman LS, Bisker ER, Sackel DJ, et al. Longitudinal study of vision and retinal nerve fiber layer thickness in multiple sclerosis. *Ann Neurol*. 2010;67(6):749–60.
80. Garcia-Martin E, Pueyo V, Almarcegui C, et al. Risk factors for progressive axonal degeneration of the retinal nerve fibre layer in multiple sclerosis patients. *Br J Ophthalmol*. 2011;95(11):1577–82.
81. Henderson AP, Trip SA, Schlottmann PG, et al. A preliminary longitudinal study of the retinal nerve fiber layer in progressive multiple sclerosis. *J Neurol*. 2010;257(7):1083–91.
82. Serbecic N, Aboul-Enein F, Beutelspacher SC, et al. High resolution spectral domain optical coherence tomography (SD-OCT) in multiple sclerosis: the first follow up study over two years. *PLoS One*. 2011;6(5), e19843.
83. Ratchford JN, Saidha S, Sotirchos ES, et al. Active MS is associated with accelerated retinal ganglion cell/inner plexiform layer thinning. *Neurology*. 2013;80(1):47–54.
84. Gundogan FC, Demirkaya S, Sobaci G. Is optical coherence tomography really a new biomarker candidate in multiple sclerosis? – A structural and functional evaluation. *Invest Ophthalmol Vis Sci*. 2007;48(12):5773–81.
85. Gelfand JM, Nolan R, Schwartz DM, Graves J, Green AJ. Microcystic macular oedema in multiple sclerosis is associated with disease severity. *Brain*. 2012;135(Pt 6):1786–93.
86. Saidha S, Sotirchos ES, Ibrahim MA, et al. Microcystic macular oedema, thickness of the inner nuclear layer of the retina, and disease characteristics in multiple sclerosis: a retrospective study. *Lancet Neurol*. 2012;11(11):963–72.
87. Brar M, Yuson R, Kozak I, et al. Correlation between morphologic features on spectral-domain optical coherence tomography and angiographic leakage patterns in macular edema. *Retina*. 2010;30(3):383–9.
88. Sotirchos ES, Saidha S, Byraiah G, et al. In vivo identification of morphologic retinal abnormalities in neuromyelitis optica. *Neurology*. 2013;80(15):1406–14.
89. Kaufhold F, Zimmermann H, Schneider E, et al. Optic neuritis is associated with inner nuclear layer thickening and microcystic macular edema independently of multiple sclerosis. *PLoS One*. 2013;8(8), e71145.
90. Barboni P, Carelli V, Savini G, Carbonelli M, La Morgia C, Sadun AA. Microcystic macular degeneration from optic neuropathy: not inflammatory, not trans-synaptic degeneration. *Brain*. 2013;136(Pt 7), e239.
91. Wolff B, Basdekidou C, Vasseur V, Mauget-Faysse M, Sahel JA, Vignal C. Retinal inner nuclear layer microcystic changes in optic nerve atrophy: a novel spectral-domain OCT finding. *Retina*. 2013;33(10):2133–8.
92. Brandt AU, Oberwahrenbrock T, Kadas EM, Lagreze WA, Paul F. Dynamic formation of macular microcysts independent of vitreous traction changes. *Neurology*. 2014;83(1):73–7.
93. Kappos L, Moeri D, Radue EW, et al. Predictive value of gadolinium-enhanced magnetic resonance imaging for relapse rate and changes in disability or impairment in multiple sclerosis: a meta-analysis. *Gadolinium MRI Meta-Analysis Group. Lancet*. 1999;353(9157):964–9.
94. Fisher E, Rudick RA, Simon JH, et al. Eight-year follow-up study of brain atrophy in patients with MS. *Neurology*. 2002;59(9):1412–20.
95. Sormani MP, Arnold DL, De Stefano N. Treatment effect on brain atrophy correlates with treatment effect on disability in multiple sclerosis. *Ann Neurol*. 2014;75(1):43–9.
96. Simon JH. Brain atrophy in multiple sclerosis: what we know and would like to know. *Mult Scler*. 2006;12(6):679–87.
97. Inglese M, Oesingmann N, Casaccia P, Fleysher L. Progressive multiple sclerosis and gray matter pathology: an MRI perspective. *Mt Sinai J Med*. 2011;78(2):258–67.
98. Saidha S, Calabresi PA. Optical coherence tomography should be part of the routine monitoring of patients with multiple sclerosis: yes. *Mult Scler*. 2014;20(10):1296–8.
99. Gordon-Lipkin E, Chodkowski B, Reich DS, et al. Retinal nerve fiber layer is associated with brain atrophy in multiple sclerosis. *Neurology*. 2007;69(16):1603–9.
100. Grazioli E, Zivadinov R, Weinstock-Guttman B, et al. Retinal nerve fiber layer thickness is associated with brain MRI outcomes in multiple sclerosis. *J Neurol Sci*. 2008;268(1–2):12–7.
101. Siger M, Dziegielewska K, Jasek L, et al. Optical coherence tomography in multiple sclerosis: thickness of the retinal nerve fiber layer as a potential measure of axonal loss and brain atrophy. *J Neurol*. 2008;255(10):1555–60.

102. Dorr J, Wernecke KD, Bock M, et al. Association of retinal and macular damage with brain atrophy in multiple sclerosis. *PLoS One*. 2011;6(4), e18132.
103. Pfueller CF, Brandt AU, Schubert F, et al. Metabolic changes in the visual cortex are linked to retinal nerve fiber layer thinning in multiple sclerosis. *PLoS One*. 2011;6(4), e18019.
104. Reich DS, Smith SA, Gordon-Lipkin EM, et al. Damage to the optic radiation in multiple sclerosis is associated with retinal injury and visual disability. *Arch Neurol*. 2009;66(8):998–1006.
105. Young KL, Brandt AU, Petzold A, et al. Loss of retinal nerve fibre layer axons indicates white but not grey matter damage in early multiple sclerosis. *Eur J Neurol*. 2013;20(5):803–11.
106. Zimmermann H, Freing A, Kaufhold F, et al. Optic neuritis interferes with optical coherence tomography and magnetic resonance imaging correlations. *Mult Scler*. 2013;19(4):443–50.
107. Gabilondo I, Martinez-Lapiscina EH, Martinez-Heras E, et al. Trans-synaptic axonal degeneration in the visual pathway in multiple sclerosis. *Ann Neurol*. 2014;75(1):98–107.
108. Hutchinson M. Optical coherence tomography should be part of the routine monitoring of patients with multiple sclerosis: commentary. *Mult Scler*. 2014;20(10):1302–3.
109. Suhs KW, Hein K, Sattler MB, et al. A randomized, double-blind, phase 2 study of erythropoietin in optic neuritis. *Ann Neurol*. 2012;72(2):199–210.

Friedemann Paul and Alexander U. Brandt

Approximately half of all multiple sclerosis (MS) patients show a progressive phenotype [1]. In these patients, accumulation of clinical impairment follows a progressive course rather than being relapse associated. Depending on whether the patient experienced relapses prior to the progressive phase, the disease course is then either classified as *primary progressive MS* (PPMS, without prior relapses, 10–20 % of patients) or *secondary progressive MS* (SPMS, with prior relapses) (Fig. 9.1) [2]. SPMS with or without superimposed relapses evolves from relapsing-remitting MS (RRMS). The rate at which this occurs varies greatly; however, according to natural history data, approximately 50 % of patients progress to SPMS within 14–20 years from disease onset [3]. In terms of age, conversion from RRMS to progressive MS tends to occur in a time window of 35–50 years, which is also the typical age of disease onset in PPMS [1, 4].

Prior to the 2013 MS disease course revision, the phenotype of a patient with primary progressive disease course, who concurrently experiences relapses, was classified as *progressive relapsing MS* (PRMS) [5]. However, according to current nomenclature, descriptors for *disease activity* (relapses or MRI activity) and

progression (clinical worsening or progression of brain atrophy) are appended to primary and secondary progressive disease courses (Fig. 9.1) [2].

Pathological and imaging studies suggest that relapsing and progressive MS are a single disease entity with distinct clinical phenotypes [4, 6]. However, in contrast to RRMS, the mechanisms underlying progressive MS are poorly understood, and therapeutic options available in RRMS are usually not effective. As a consequence, therapeutic options in progressive MS are limited to fairly unspecific immunosuppressive agents, such as azathioprine, mitoxantrone, or cyclophosphamide, which all carry the risk of serious side effects [7–9], and symptomatic treatments. When a certain disability landmark or a progressive course has been reached, the disease tends to progress relentlessly and largely independently of the preceding course and relapse number and severity [10, 11]. This is presumably related to the fact that the efficiency of remyelination declines with increasing age and disease duration [12, 13]. In progressive MS, neurodegeneration is thought to occur independently of the initial inflammatory response [4], although inflammation is present at all MS stages [14]. Neuropathological studies suggest that inflammatory processes in progressive MS brains at least partially evolve independently of damage to the blood-brain barrier, which may explain why potent anti-inflammatory disease-modifying drugs given in the periphery are inefficacious in

F. Paul, MD (✉) • A.U. Brandt, MD
Department of Neurology, NeuroCure Clinical
Research Center, Charité University Medicine Berlin,
Berlin, Germany
e-mail: friedmann.paul@charite.de

2013 revised multiple sclerosis progressive phenotypes

<u>Course</u>	<u>Modifiers</u>	
<p>Primary Progressive (PP)</p> <p style="text-align: center;">Progressive accumulation of disability from onset</p>	<p>Activity</p> <p>yes / no</p>	<p>Progression</p> <p>yes / no</p>
<p>Secondary Progressive (SP)</p> <p style="text-align: center;">Progressive accumulation of disability after initial relapsing course</p>	<p>Activity</p> <p>yes / no</p>	<p>Progression</p> <p>yes / no</p>

Fig. 9.1 Progressive multiple sclerosis nomenclature. Progressive MS nomenclature according to the current criteria [2]

progressive MS [4]. A key feature of progressive MS is pronounced cortical demyelination including cortical lesions and, more broadly, diffuse and widespread damage to the normal-appearing white and gray matter. Several mechanisms underlying disease progression have been proposed, including axonal demise in focal white matter lesions and loss of remyelination, which may cause ongoing accrual of neurological disability when functional compensation is exhausted. Microglial activation, altered axonal ion homeostasis, mitochondrial injury, oxidative stress, and iron accumulation are—although not unique to progressive MS—considered relevant contributing factors to irreversible tissue damage [4, 12, 15].

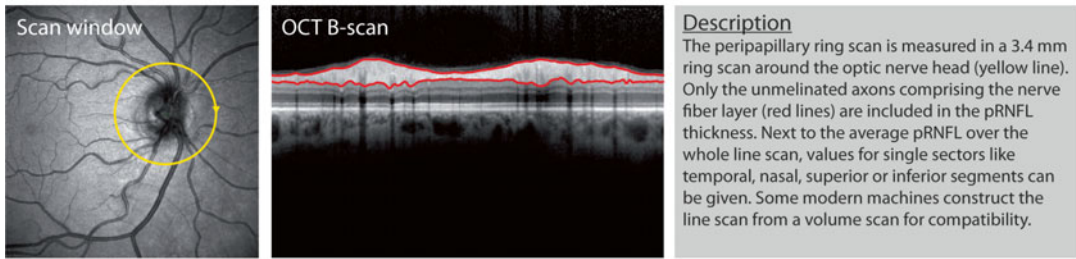
Optical Coherence Tomography in Progressive Multiple Sclerosis

An overview of current optical coherence tomography (OCT) measurement protocols used in progressive multiple sclerosis is given

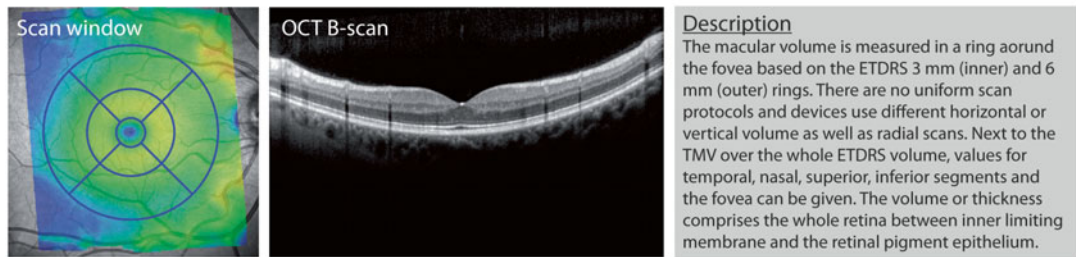
in Fig. 9.2. The peripapillary retinal nerve fiber layer (RNFL or the more specific abbreviation pRNFL) is the most established parameter and features in almost all studies to date. Measurement of total macular volume (TMV) is less common and has been recently superseded by intraretinal layer segmentation in macular volume scans.

Investigation of progressive MS using OCT is far rarer than in relapsing-remitting MS [16]. The few studies that include OCT findings specifically in progressive MS have had cohorts of such a few patients each and have used different generations of OCT technology (time domain and spectral domain OCT, whose measurements are not directly comparable) [17, 18]. Some studies (e.g., [19]) combine relapsing-remitting and progressive MS patients in one analysis and are therefore not discussed here in detail. An overview of relevant studies, including key findings, is given in Table 9.1 [20–32]. The key findings of all studies are summarized below.

Peripapillary retinal nerve fiber layer thickness (pRNFL)



Total Macular Volume (TMV)



Intraretinal Layer Thickness or Volume

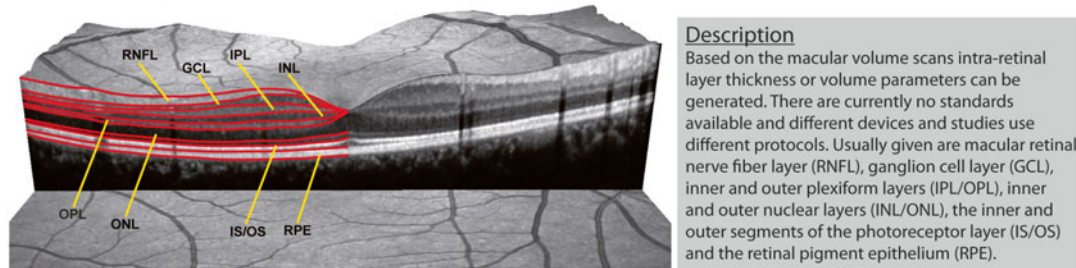


Fig. 9.2 Optical coherence tomography measurements. Common optical coherence tomography protocols and derived parameters useful in diagnosing and monitoring patients with progressive MS

Retinal Nerve Fiber Layer Thickness and Total Macular Volume

Scans of patients with progressive MS show reduced RNFL thickness in the peripapillary ring compared to healthy controls and also relapsing-remitting MS patients. An overview plot from [30] is given in Fig. 9.3, and a sample report is shown in Fig. 9.4.

Two potential explanations for the pronounced RNFL thinning in progressive patients exist: first, these patients may show more pronounced loss based on a more severe or also different disease pathology than relapsing-remitting patients [27]; and second, the investigated patients may simply have experienced longer

disease duration, giving time for a greater damage accumulation [29, 30]. Data from studies published to date are not sufficient to answer this question. An additional confounder is a patient history of MS-associated optic neuritis (MSON). It is universally accepted that MSON additionally damages the retina, quantified by increased RNFL thinning, and such episodes may often be subclinical or unrecognized, leading to an accumulation of damage the longer the disease lasts. Nonetheless, it is conspicuous that PPMS patients, who by definition do not suffer from relapsing MSON, show a similar RNFL reduction as SPMS patients without previous optic neuritis, suggesting that non-relapse-associated neuro-axonal degeneration in the

Table 9.1 Cross-sectional studies investigating progressive MS patients using OCT [20–32]

First author	Year	OCT	PPMS	SPMS	Key finding ^a	Ref.
Pulicken	2007	TD	12	16	This study did not differentiate between eyes with and without previous optic neuritis but included this information as covariate RNFL thickness in eyes from SPMS ($81.8 \pm 15.6 \mu\text{m}$) and PPMS patients ($88.9 \pm 13.3 \mu\text{m}$) was significantly lower than in HC ($102.7 \pm 11.5 \mu\text{m}$) and showed a marked decrease compared to RRMS patients ($94.4 \pm 14.6 \mu\text{m}$) TMV was not different between HC ($6.6 \pm 0.5 \text{mm}^3$), RRMS ($6.5 \pm 0.5 \text{mm}^3$), and PPMS patients ($6.5 \pm 0.6 \text{mm}^3$). SPMS patients showed decreased TMV ($6.2 \pm 0.4 \text{mm}^3$)	[20]
Henderson	2008	TD	23	27	This study specifically investigated eyes without previous optic neuritis In comparison to HC ($98.8 \pm 10.5 \mu\text{m}$), RNFL thickness from SPMS patients' eyes ($88.4 \pm 10.9 \mu\text{m}$) was significantly lower and RNFL thickness from PPMS patients' eyes nonsignificantly lower ($93.9 \pm 13.9 \mu\text{m}$) The same was true for TMV with HC ($6.81 \pm 0.31 \text{mm}^3$), SPMS ($6.46 \pm 0.41 \text{mm}^3$), and PPMS ($6.64 \pm 0.42 \text{mm}^3$)	[21]
Costello	2009 2010	TD TD	0 9	7 13	This study separated between eyes with and without previous MSON In eyes without history of MSON, RNFL thickness was reduced in PPMS ($94.3 \pm 8.3 \mu\text{m}$), RRMS ($99.6 \pm 14.3 \mu\text{m}$), and SPMS eyes ($84.7 \pm 11.7 \mu\text{m}$), compared to CIS eyes ($105.7 \pm 12.3 \mu\text{m}$)	[22] [23]
Siepmann	2010	TD	29	(34) ^b	This study found no difference in RNFL thickness in eyes of PPMS patients with eyes of (data not published)	[24]
Serbecic	2010 2014	SD SD	0 0	17 17	SPMS patients with or without previous MSON showed significantly reduced RNFL thickness compared to healthy controls. In patients with previous optic neuritis, even greater RNFL reduction was found	[25] [26]
Saidha	2011	SD	16	20	GCL+IPL was significantly thinner in RRMS patients ($71.6 \pm 9.8 \mu\text{m}$), SPMS ($66.4 \pm 10.2 \mu\text{m}$), and PPMS ($74.1 \pm 7.1 \mu\text{m}$) than in healthy controls ($81.8 \pm 6.3 \mu\text{m}$). GCL+IPL thickness was most decreased in SPMS. GCL+IPL thickness correlated significantly with EDSS, high-contrast, 2.5 % low-contrast, and 1.25 % low-contrast letter acuity in MS. A subset of patients showed thinning of the outer retinal layers	[27]
Albrecht	2012	SD	12	41	PPMS and SPMS patients showed significant thinning of peripapillary RNFL and GCL+IPL in both patients with and without previous MSON. The INL was only reduced in PPMS in comparison to HC in both patients with and without previous optic neuritis	[28]

Table 9.1 (continued)

First author	Year	OCT	PPMS	SPMS	Key finding ^a	Ref.
Gelfand	2012	SD	33	60	This study focused on CIS and compared damage to later disease stages Retinal axonal loss was increasingly prominent in more advanced disease stages with proportionally greater thinning in eyes previously affected by optic neuritis. In the absence of clinically evident optic neuritis, RNFL thinning was similar between progressive MS subtypes	[29]
Oberwahrenbrock	2012	SD	41	65	RNFL thickness was reduced in SPMS eyes compared to RRMS eyes, and TMV was reduced in SPMS and PPMS eyes compared to RRMS eyes, regardless of MSON history. Independent of MS subtype, more pronounced RNFL thinning and TMV reduction were found in eyes with previous MSON	[30]
Balk	2014	SD	29	61	PPMS patients showed more intact inner retinal layers (RNFL to INL) compared to relapsing onset MS patients. Only in MS eyes without previous MSON did patients with typical MS show more severe thinning of the inner retinal layers compared to patients with a benign disease course, even after an average disease course of 20 years	[31, 32]

Abbreviations: OCT optical coherence tomography, PPMS primary progressive multiple sclerosis, SPMS secondary progressive multiple sclerosis, Ref reference, SD spectral domain OCT, TD temporal domain OCT, HC healthy controls, RNFL retinal nerve fiber layer, GCL ganglion cell layer, IPL inner plexiform layer, INL inner nuclear layer, TMV total macular volume, MSON MS related optic neuritis

^aMeasurement values are only provided if available and are limited to parameters of interest

^bThis study combines RRMS and SPMS patients in a group called “relapse onset”

retina and optic nerve also occurs in other MS disease courses.

Current data does not allow any solid conclusions regarding the spatial distribution of RNFL reduction in progressive MS. MSON-associated damage leads to pronounced effect of the temporal quadrant in relapsing-remitting MS [33, 34], but whether this is also the case in progressive MS patients without previous MSON has not been investigated sufficiently. Likewise, the few applicable longitudinal studies to date do not show how RNFL reduction develops over time (see later).

Data on total macular volume (TMV) or thickness changes is scarce. Only a few studies have investigated TMV together with RNFL, because TMV is generally considered less specific than RNFL as it measures the whole retinal thickness instead of solely the main region of interest. [35] Published data supports this notion with similar

but less specific findings in comparison to RNFL (see Fig. 9.4 for an example).

Intraretinal Layers

Since the introduction of spectral domain OCT, different intraretinal layer thicknesses can be derived from macular volume scans. This allows the potential investigation of distinct pathologies in the retina of patients with MS, which affect other layers than the RNFL. Evidence for intraretinal changes in MS is shown in histopathology studies, in which, for example, neuronal loss in the inner nuclear layer has been reported [36]. So far, the few studies applying intraretinal segmentation have detected changes—as expected—mainly in the ganglion cell layer (GCL) and inner plexiform layer (IPL) thickness (often combined as ganglion cell and inner plexiform layer [GCIPL] for increased

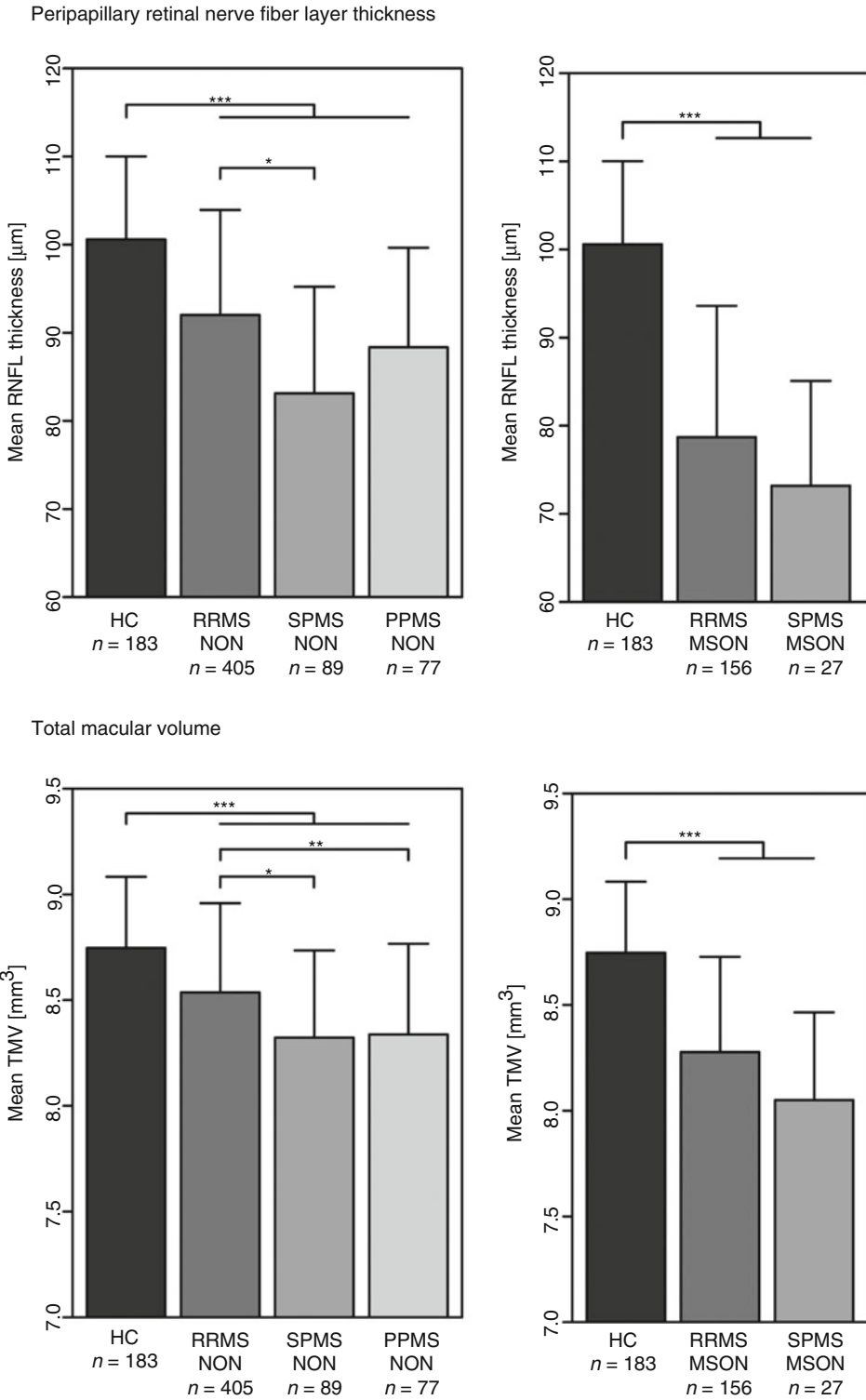
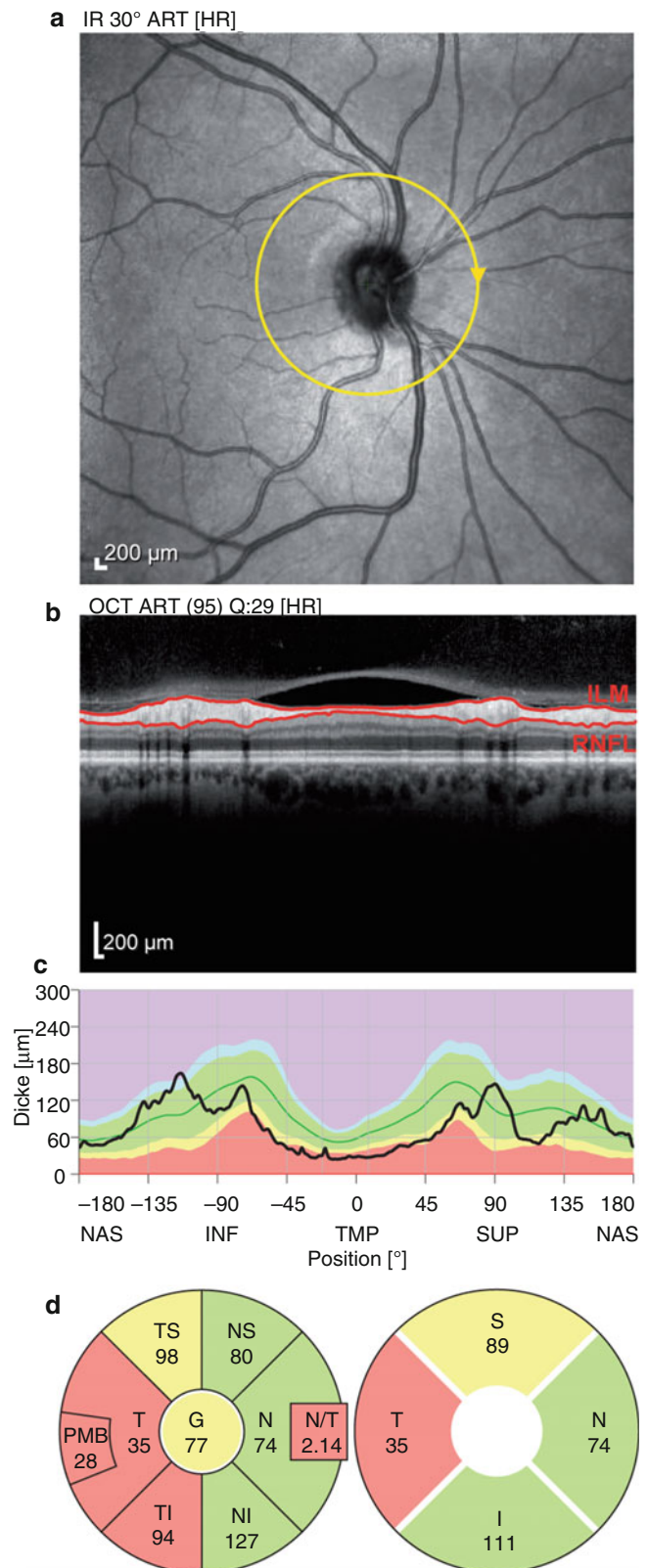


Fig.9.3 RNFL and TMV in progressive MS. Peripapillary RNFL and TMV from patients with relapsing-remitting and progressive MS (Adapted from Oberwahrenbrock et al. [30]). Eyes with a previous history of MSON on the left, eyes without history of MSON (*NON*) on the right

Fig. 9.4 OCT imaging in secondary progressive MS. Shown are sample findings from an eye from an SPMS patient with a history of optic neuritis. **(a)** Normal scanning laser ophthalmoscopy image showing the peripapillary ring scan area. **(b)** Peripapillary OCT ring scan showing reduced RNFL thickness (*red lines*). Note that the coincidental vitreous detachment is of no pathologic relevance. **(c)** Height profile in comparison to normative data in the nasal (*NAS*), inferior (*INF*), temporal (*TMP*), and superior (*SUP*) areas of the ring scan. Colors indicate RNFL thickness within the 95th percentile (*green*), between the 95th and 99th percentile (*yellow*), below the 99th percentile (*red*), and with regard to thicker RNFL higher than 1st percentile (*purple*) and between the 1st and 5th percentile (*blue*). **(d)** Profile data from **c** visualized in a typical sectorial circle with color indicators derived from **c**. On the left, a detailed view on the temporal-superior (*TS*), nasal-superior (*NS*), nasal (*N*), nasal-inferior (*NI*), temporal-inferior (*TI*), and temporal (*T*) sectors. Additionally, the figure shows average RNFL thickness (*G*) and RNFL thickness in the papillomacular bundle (*PMB*) as well as the N/T ratio. The right-hand image focuses on superior, nasal, inferior, and temporal quadrants exclusively. The temporally accented RNFL thickness reduction is typical for eyes after optic neuritis both in relapsing-remitting and secondary progressive MS. The nasal sectors are also affected, but here thickness reduction is often mild and is within normal physiology, as is the case for this patient



reliability). Data for outer retinal layers is less consistent. Of interest is the inner nuclear layer (INL), for which both thickening and thinning have been reported. One study suggested that INL thickness increases with disease severity [37]. Another study showed that an increased INL thickness correlates with worsened brain atrophy, specifically in progressive MS. However, several studies also showed INL thinning in progressive MS (e.g., [28]), and it is currently unclear exactly how INL thinning and thickening occur in relation to MSON, disease duration, and disease severity.

Microcystic Macular Edema, and Retrograde Maculopathy

One form of INL thickening is microcystic macular edema (MME), initially described in less than 10 % of MS patients [38]. MME can also occur in progressive MS, as the example in Fig. 9.5 shows. However, MME is not specific to MS and has since been reported in several different ocular pathologies [39]. It is now established that MME is associated with acute optic nerve damage [40] and most likely reflects unspecific reactive processes in the inner nuclear layer to acute ganglion cell degeneration, as also discussed in the chapter by Mathias Abegg in this book [41]. The terms *retrograde maculopathy* or

macular microcystoids have been suggested as more appropriate than MMO for this OCT sign [42, 43].

Primary Macular Phenotype

On the other hand, Saidha et al. have reported macular thinning spanning all intraretinal layers of a subgroup of MS patients with comparably intact RNFL [44]. The study showed that this macular thinning predominant (MTP) phenotype occurred more frequently in progressive MS patients than in relapsing-remitting MS patients and could represent an extreme form of a primary macular pathology in MS patients. The MTP phenotype was potentially recently confirmed in a different US cohort [45]. However, its exact characteristics and significance are currently unclear. We and others (personal communication) have not been able to identify any patients showing this phenotype, and this potentially interesting finding requires further investigation [46].

Association of OCT Findings with MRI Measures of Brain Damage

Several studies have shown an association of retinal damage as measured by OCT with brain atrophy (brain parenchymal fraction [BPF], gray and

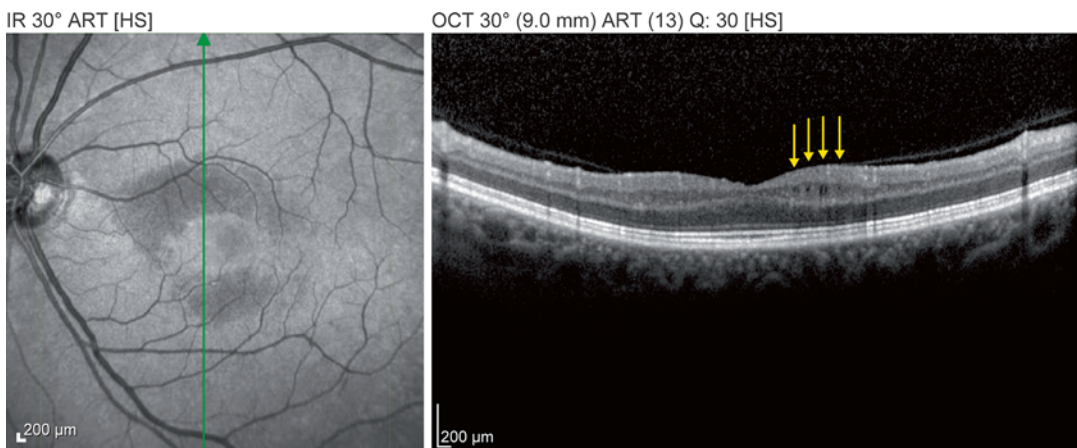


Fig. 9.5 Microcystic macular edema can occur in eyes from patients with MS, including progressive MS. On the left, a scanning laser ophthalmoscopy image shows typical darker areas around the macula with accentuation of

the optic nerve head-facing side. The green line indicates the B-scan position on the right. On the right a B-scan of the affected area shows few cystoid structures, marked with yellow arrows, in the inner nuclear layer

white matter volume) on magnetic resonance imaging (MRI) (Fig. 9.6) [37, 40, 47–52]. However, only a few of these studies described or investigated patients with progressive MS separately. A key finding in a study of 61 MS patients by Sepulcre et al., comprising 5 SPMS, 6 PPMS,

and 29 healthy controls [19], showed significant correlation of whole gray matter and whole white matter volumes with average RNFL thickness in MS patients; however, separated analyses for the few progressive patients were not provided. Gordon-Lipkin et al. were the first to show that

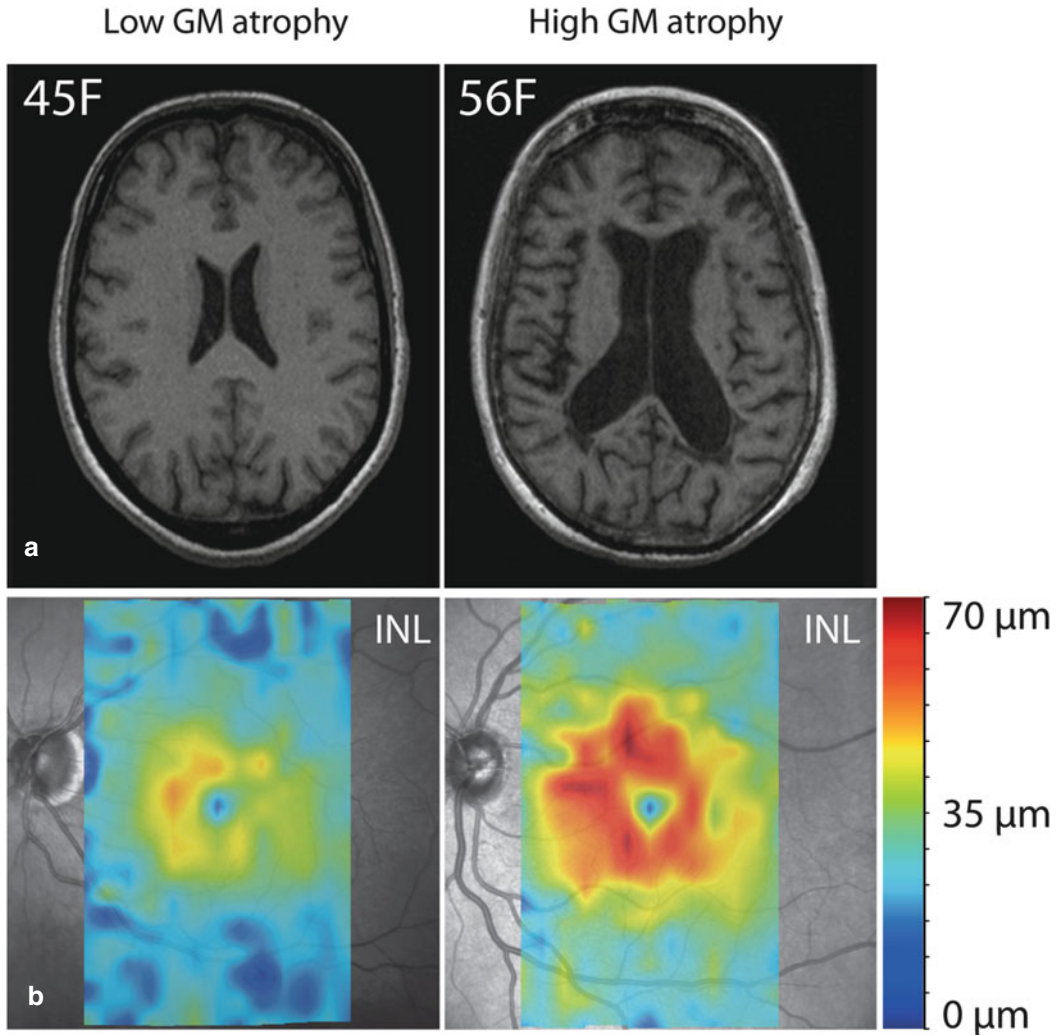


Fig. 9.6 OCT and brain atrophy. Retinal layer thickness correlates with brain atrophy and also disease severity in progressive MS. Shown are 2 cases: one patient with low disease activity and low gray matter (GM) atrophy on the left, and one patient with high disease activity and severe GM atrophy on the right. (a) T1 MRI scans from these patients showing a periventricular slice. (b) Inner nuclear layer (INL) changes. Some patients with high disease activity show increased INL thickness, which might correspond to higher neuroinflammatory activity in these patients [37, 40]. INL can also appear unchanged or thinned in severely affected patients, and the relevance, if any, of either occur-

rence still needs to be determined. Factors leading to either development still need to be determined. (c) Ganglion cell and inner plexiform layer (GCIPL) thickness correlates with brain and GM atrophy similarly to retinal nerve fiber layer thickness (RNFL). Neuronal loss in the brain coincides with neuronal loss in the ganglion cell complex (GCC), consisting of inner plexiform, ganglion cell, and retinal nerve fiber layers. Retinal ganglion cell dendrites reside in the inner plexiform layer, cell bodies in the ganglion cell layer, and projecting axons in the retinal nerve fiber layer. However, neurodegeneration does not seem to spread beyond the INL [47]

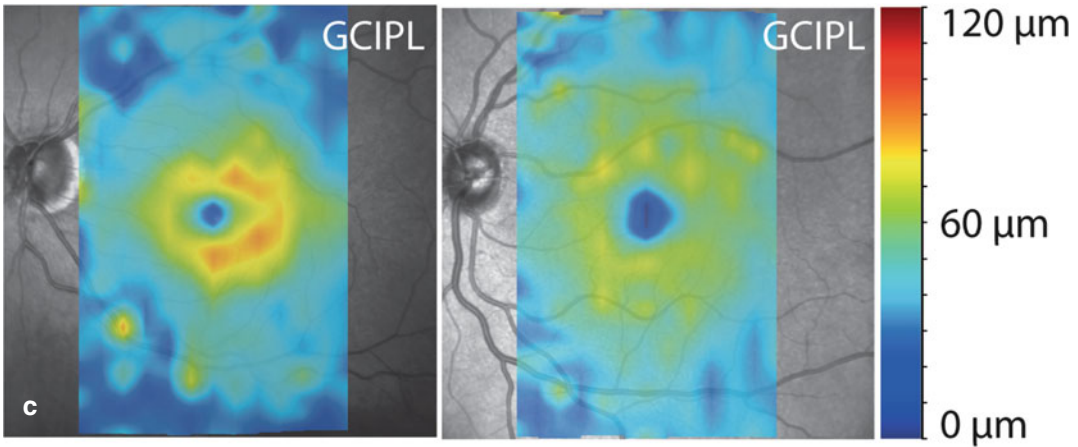


Fig. 9.6 (continued)

lower RNFL thicknesses were associated with reduced BPF and cerebrospinal fluid (CSF) volume in a cohort of 40 MS patients, but not in 15 healthy controls [48]. The MS cohort comprised 20 RRMS, 15 SPMS, and 5 PPMS patients; however, OCT results (RNFL, TMV) were only given for the MS group as a whole, instead of per subgroup. Subgroup analyses on correlation between OCT measurements and brain atrophy were only run on RRMS and SPMS patients and revealed that RNFL thickness was significantly related to BPF and CSF volume in RRMS, but not SPMS. The authors discussed two possible explanations: (1) a possible basement effect in progressive patients, in which either RNFL or brain volume bottom out with minimal further decline, or (2) primary involvement of the spinal cord, but less cerebral involvement in SPMS. Both these intriguing hypotheses will require longitudinal studies. However, using OCT as an outcome tool in trials with potentially neuroprotective agents in patients with progressive disease carries an important caveat: when substantial retinal loss has already occurred at the time of study inclusion, it may be too late to detect slowing of further tissue loss by experimental treatment versus placebo or active comparator when measuring RNFL or TMV.

Another cross-sectional study on the relationship between retinal neuro-axonal measures and brain volume measurements comprised 84 MS patients (58, relapsing-remitting disease course;

18, secondary progressive; 8, primary progressive) [52]. SPMS and PPMS patients were older than RRMS patients (mean 58.3 and 55.0, respectively, vs. 37.4 years) and had longer disease duration (mean 21.7 and 15.8, respectively, vs. 7.5 years), whereas the proportion of eyes with a history of optic neuritis was comparable between RRMS and SPMS patients (26 % and 28 %, respectively). In contrast to Gordon-Lipkin et al., this study used advanced spectral domain OCT technology, which enables segmentation of individual intraretinal layers (see previous). Intracranial volume was significantly positively associated with the combined measure (GCIPL) of ganglion cell layer (GCL) and inner plexiform layer (IPL) in both healthy controls and the entire MS cohort. Inner nuclear layer (INL) thickness was inversely associated with the volume of the normal-appearing white matter (NAWM) in the entire MS cohort, and peripapillary RNFL (pRNFL) thickness positively correlated with cortical gray matter volume in RRMS. Subgroup analyses revealed a positive association of outer nuclear layer (ONL) thickness with cortical gray matter (GM) volume in SPMS patients and in PPMS patients, positive correlations of ONL thickness with brainstem volume and of pRNFL thickness with NAWM and cortical GM volume. However, the significance of these findings—as the authors acknowledge—is limited by the low number of patients in the progressive disease course groups and the high number of statistical

tests without correction for multiple comparisons, giving rise to the possibility that the identified correlations occurred by chance alone.

The aforementioned study did not compare OCT measures between disease subtype groups; however, mean and standard deviations show only minute differences between the RNFL, GCIPL, and INL measures [52]. Consequently, the study is too preliminary to allow for generalizable conclusions on the association of retinal thinning with global or regional brain volume measurements in patients with progressive disease.

Longitudinal Studies

As the previous discussion shows, longitudinal studies are indispensable to describe temporal dynamics of retinal thinning in relation to clinical disease progression and other surrogate markers of disease activity such as MRI. They are also vital to assessing whether OCT is an appropriate investigative tool. Only longitudinal studies can show whether retinal tissue loss is exhibiting a basement effect, which would render OCT ineffective in monitoring disease progression and efficacy of neuroprotective compounds. To date, only a few studies have investigated temporal changes in retinal measures with OCT (Table 9.2) [19, 22, 26, 37, 53–55]. The first longitudinal study that included a subgroup of progressive patients was performed with time domain OCT

technology by Sepulcre et al. [19]. Five SPMS and 6 PPMS patients were recruited into a total cohort of 61 MS patients. In the entire patient group, average RNFL thickness decreased significantly by 4.8 μm versus a mean change of $-2.2 \mu\text{m}$ in 29 healthy controls over a follow-up period of 2 years, and the thickness of the temporal quadrant RNFL correlated with the number of relapses. However, separated data from the few progressive patients were not reported. In another 2-year longitudinal study, Costello et al. reported a subgroup of 7 SPMS patients in a cohort of 84 MS and CIS patients analyzed with time domain OCT in a longitudinal study [23]. Neither MSON-affected eyes nor non-affected eyes exhibited a significant decrease in RNFL values at year 2 compared to year 1; however, comparative data from healthy controls were not reported. Henderson et al. investigated 18 SPMS and 16 PPMS patients at 2 different time points versus 18 age-matched healthy controls. Median (range) follow-up was 579 (453–895), 592 (411–762), and 656 (398–890) days in SPMS, PPMS, and controls, respectively [53]. The study followed up a larger cross-sectional cohort comprising 50 subjects with progressive MS and 20 healthy controls [21]. While there was significant reduction in some RNFL measures in progressive MS versus controls (see above and Table 9.1 [20–32]), none of the 3 groups showed a significant decrease in mean RNFL thickness when compared to baseline, although PPMS patients tended to show reduced RNFL (annual change in mean RNFL thickness $-0.99 \mu\text{m}$, $p=0.075$, 95 % CI $-2.09, 0.10$). When analyzing PPMS and SPMS groups as a whole, the mean annual change from baseline in RNFL thickness was $-0.70 \mu\text{m}$ ($p=0.067$, 95 % CI $-1.44, 0.05$) versus $-0.5 \mu\text{m}$ in controls ($p=0.340$, 95 % CI $-1.52, 0.53$). This mean difference of $0.2 \mu\text{m}$ (95 % CI $-1.47, 1.07$) between all progressive patients and controls was not significant ($p=0.750$). The changes in both the latter parameters were small enough to be classified as physiological variation. When analyzing RNFL thickness in the 4 quadrants (temporal, superior, nasal, inferior), only the inferior quadrant RNFL thickness in all progressive patients and in the PPMS group showed a

Table 9.2 Longitudinal studies of progressive MS patients using OCT [19, 22, 26, 37, 53–55]

First author	Year	OCT	PPMS	SPMS	Ref.
Sepulcre	2007	TD	6	5	[19]
Costello	2009	TD	0	7	[22]
Henderson	2010	TD	16	18	[53]
Serbecic	2011	SD	0	10	[54]
Saidha	2012	SD	25	16	[37]
Ratchford	2013	SD	16	24	[55]
Serbecic	2014	SD	0	10	[26]

Abbreviations: OCT optical coherence tomography, PPMS primary progressive multiple sclerosis, SPMS secondary progressive multiple sclerosis, Ref reference, SD spectral domain OCT, TD temporal domain OCT

significant reduction from baseline (all patients $-2.07 \mu\text{m}$, 95 % CI $-3.56, -0.59$, $p=0.007$; PPMS $-2.99 \mu\text{m}$, 95 % CI $-5.15, -0.83$, $p=0.008$). However, the control group also showed a mean decrease in inferior quadrant RNFL thickness of $-1.71 \mu\text{m}$ (95 % CI $-3.74, 0.33$, $p=0.098$) resulting in a nonsignificant difference in annual change between patients and controls.

In contrast, both groups showed a significant and similar reduction in macular volume (controls: annual change -0.083 mm^3 , $p=0.013$, 95 % CI $-0.067, -0.008$; progressive MS -0.031 mm^3 , $p=0.005$, 95 % CI $-0.052, -0.009$). Annual reduction in macular volume was significant in PPMS ($p=0.003$) and showed a trend toward reduction in SPMS ($p=0.059$). In a separate analysis in the same study, the affected and unaffected eyes of individual MSON patients were compared in terms of serial changes in OCT measures. No significant differences between changes in RNFL thickness, macular volume changes, or any individual quadrant RNFL thickness were found.

Some measures of visual function (logMAR visual acuity on ETDRS charts, Sloan low-contrast acuity, 25 %) showed significant reductions over time in the progressive MS group, while others did not (Sloan low-contrast acuity, 5 and 1.25 %). Compared to controls, the annual change in logMAR acuity and Sloan 25 % low-contrast acuity was significant for the progressive MS (PPMS and SPMS patients combined) and for the SPMS group alone, while the PPMS group only showed a trend in deterioration in the logMAR acuity, but not the Sloan low-contrast acuity. Except for macular volume and Sloan 25 % contrast acuity in the SPMS group, none of retinal changes was significantly related to changes in visual acuity and low-contrast acuity measures. As macular volume and Sloan 25 % correlations in SPMS were not verified by adjustment for multiple comparisons, the authors presumed the initial findings were an aberration. It is noteworthy that there was no significant EDSS change in either MS group over the follow-up period. In summary, this study does not seem to support the assumption that ongoing axonal retinal loss

occurs in progressive MS. However, the failure to detect longitudinal changes in progressive patients may be due to the study design:

1. Median follow-up was at less than 2 years, before that it may not be possible to detect meaningful changes by time domain OCT technology, which was used in this study and is prone to substantial test-retest variability of up to several μm .
2. Progressive patients in this study were arguably not representative of the progressive MS population as a whole, because they were relatively stable and exhibited no clinically detectable disease activity. As retinal thinning has been reported as associated with disease activity (e.g., [19, 55]), OCT may have shown more pronounced retinal thinning over time in a progressive cohort of patients with clinical evidence of disease activity.
3. Statistical analysis was based on the assumption of a linear decline of retinal changes over time, which is unlikely to truly reflect the biology and pathology underlying progressive retinal thinning. In fact, a nonlinear or nonuniform temporal pattern with a more rapid RNFL loss in earlier stages of MS has recently been suggested [56].
4. A basement effect may have masked previous, significant retinal loss. If RNFL damage is already advanced at study entry, current technology may not be sensitive enough to detect any further deterioration. The significant reduction in macular volume over time in healthy controls in this study is in line with previous findings and suggests that the macula, which contains a high proportion of ganglion cells, may be a more sensitive region for measuring age-related retinal changes compared to the RNFL [57, 58]. The very similar decrease in macular volume in progressive MS suggests an age-related phenomenon in patients and healthy aging subjects alike and argues against disease-related effects.

The first longitudinal study using spectral domain OCT technology that included progressive MS patients was published by Serbecic et al.

[54]. The study monitored 27 RRMS and 10 SPMS patients over a median interval of 22.4 months (19 months to 27 months). Overall, the changes over time were minor ($\pm 2 \mu\text{m}$) and were within the test-retest variability and physiological variation of spectral domain OCT. In fact, the RNFL appeared to have increased in thickness in some patients. Moreover, functional tests (ETDRS, low-contrast Sloan charts) showed no difference to baseline results.

In a large retrospective study (123 RRMS, 25 SPMS, 16 PPMS patients, 60 controls), Saidha et al. analyzed INL thickness in relation to clinical and radiological measures of disease activity [37]. Higher baseline INL thickness was associated with the occurrence of contrast-enhancing lesions, new T2 lesions, and EDSS progression and relapses (in the RRMS group only) during a mean follow-up of 25.8 months. The authors suggested that INL thickness could be a predictor of disease progression when this finding should be confirmed in prospective studies. However, no separate subgroup analyses for SPMS and PPMS were reported, and the data awaits independent confirmation.

Another large, recent longitudinal study by Ratchford et al. comprised 24 SPMS and 16 PPMS patients in a cohort of 164 MS patients and 59 healthy controls. Here, spectral domain OCT scans were performed every 6 months. Differences from controls for baseline RNFL and GCIPL thickness were most pronounced in SPMS patients (RNFL $-9.05 \mu\text{m}$ [$p=0.01$], GCIPL $-12.82 \mu\text{m}$ [$p<0.001$]), while differences were smaller in the entire MS group and the other MS subgroups (all MS: RNFL $-7.26 \mu\text{m}$ [$p<0.001$], GCIP $-9.97 \mu\text{m}$ [$p<0.001$]; RRMS: RNFL $-7.50 \mu\text{m}$ [$p<0.001$], GCIP $-9.90 \mu\text{m}$ [$p<0.001$]; PPMS: RNFL $-2.16 \mu\text{m}$ [$p=0.58$], GCIP $-7.05 \mu\text{m}$ [$p=0.006$]) [55]. Interestingly, baseline differences in RNFL and GCIPL thicknesses between disease subtypes were not significant after adjusting for disease duration. At last follow-up at a mean of 21.1 months, differences in RNFL from baseline were significant for all MS ($-0.43 \mu\text{m}$, $p=0.02$) and RRMS ($-0.49 \mu\text{m}$, $p=0.03$), but not SPMS ($-0.23 \mu\text{m}$, $p=0.60$), PPMS

($-0.61 \mu\text{m}$, $p=0.15$), CIS ($0.33 \mu\text{m}$, $p=0.076$), and healthy controls ($-0.39 \mu\text{m}$, $p=0.12$). In contrast, GCIPL differences between baseline and last follow-up were significant for all MS ($-0.66 \mu\text{m}$, $p<0.001$), RRMS ($-0.66 \mu\text{m}$, $p<0.001$), SPMS ($-0.51 \mu\text{m}$, $p=0.01$), and controls ($-0.39 \mu\text{m}$, $p<0.001$), while differences were not significant in PPMS ($-0.61 \mu\text{m}$, $p=0.07$) and CIS ($-0.58 \mu\text{m}$, $p=0.12$). RNFL and GCIPL were adjusted for age, sex, and within-subject inter-eye correlations, and MS and CIS analyses were also adjusted for disease duration. Taken together, GCIPL thinning was 46 % faster in patients with MS/CIS than in controls ($p=0.008$), whereas RNFL thinning was similar in MS/CIS and controls. In terms of the study's statistical analysis, the order of magnitude of GCIP thinning was similar across MS subgroups (ranging from $-0.51 \mu\text{m}$ in SPMS to $-0.66 \mu\text{m}$ in RRMS and the whole MS group). However, these findings have to be interpreted with caution, as the subgroup sample sizes differed considerably. In particular, the SPMS ($n=24$) and PPMS ($n=16$) groups were much smaller than the RRMS group ($n=116$). Thus, at this stage, the data support neither a more rapid ganglion cell loss in progressive MS compared to early/relapsing forms nor a linear loss of retinal tissue as the disease advances. Interestingly, in mixed-effects linear regression models adjusted for age and sex, rates of GCIPL thinning in the MS groups as a whole were faster in patients with disability progression (≥ 1 -point increase in EDSS score at follow-up) than in those without ($-0.52 \mu\text{m}/\text{year}$ vs. $-0.33 \mu\text{m}/\text{year}$, $p=0.01$) and in patients with disease duration < 5 years versus > 5 years ($-0.54 \mu\text{m}$ vs. $-0.31 \mu\text{m}$, $p=0.003$). GCIPL thinning was highest in patients with combinations of new gadolinium-enhancing lesions, new T2 lesions, and disease duration < 5 years. These statistical models were not used to compare individual progressive subgroups, presumably due to insufficient statistical power of the low sample size. In contrast, other variables were not associated with accelerated GCIPL thinning (e.g., disease duration $<$ or > 10 years, MS subtype, baseline EDSS score, MSFC

progression, prior history of MSON, and high-contrast or low-contrast visual loss). The data on the association of faster GCIPL loss in patients with short versus longer (<5 and >5 years) disease duration seem to support the suggestion that GCIPL reduces at a faster rate in early compared to later stages of MS; however, given the numerous possible influencing factors (such as unknown disease activity prior to the MS diagnosis, presumed treatment effects of disease-modifying drugs, etc.) and a mean follow-up time of just 21.1 months, firm conclusions cannot be drawn. In contrast to GCIPL, RNFL thinning was not associated with any of the clinical and radiological markers of disease activity; only in eyes with a prior MSON there was a trend toward a faster rate of RNFL thinning compared to eyes without prior MSON (78 % faster, -0.41 vs. -0.09 $\mu\text{m}/\text{year}$, $p=0.07$). In summary, the Ratchford et al. study suggests that active MS is associated with GCIPL thinning, which could render this OCT measure useful as an outcome parameter in clinical trials.

In 2014, Serbecic et al. reported macular volume data from their previously published longitudinal cohort of 27 RRMS and 10 SPMS patients [26, 54]. Both longitudinal studies were follow-up investigations from a larger cross-sectional study published in 2010 [24] that comprised 42 RRMS, 17 SPMS patients, and 59 healthy controls matched for age and sex (Table 9.1 [20–32]). In the longitudinal macular volume study, a median follow-up period of 22.4 months (19 months to 27 months), TMV values remained within the test-retest variability of the spectral domain OCT device. Moreover, the healthy control subjects from the initial cross-sectional study were not followed longitudinally so that specific disease-related retinal changes could not be assessed.

In short, while longitudinal OCT studies are indispensable in MS, the sample sizes and duration of follow-up of investigations to date have been inadequate to allow meaningful conclusions regarding the temporal dynamics of neuro-axonal retinal damage and its association with clinical and radiographic markers of disease activity in this patient population.

Conclusion

Although several studies have shown that retinal thinning (of both the retinal nerve fiber layer and the ganglion cell layer) occurs in progressive MS, key questions remain unanswered: (1) Is the mechanism underlying retinal damage in progressive MS primarily age or disease course related? (2) Do basement effects occur, and if so, how may they impede the assessment of longitudinal retinal changes? (3) How does retinal thinning relate to clinical progression of MS?

Answers to these questions are needed to show that OCT is a useful technique for monitoring MS disease progression and the therapeutic effect of neuroprotective treatment on disease course. Prospective studies with sufficient sample sizes of progressive patients and follow-up periods of ideally at least 3 years or more are urgently needed to shed light on the association of retinal thinning measured by OCT and disease course in progressive MS.

References

1. Confavreux C, Vukusic S. Natural history of multiple sclerosis: a unifying concept. *Brain*. 2006;129(Pt 3): 606–16.
2. Lublin FD, Reingold SC, Cohen JA, Cutter GR, Sørensen PS, Thompson AJ, et al. Defining the clinical course of multiple sclerosis: the 2013 revisions. *Neurology*. 2014;83(3):278–86.
3. Tremlett H, Zhao Y, Rieckmann P, Hutchinson M. New perspectives in the natural history of multiple sclerosis. *Neurology*. 2010;74(24):2004–15.
4. Lassmann H, van Horssen J, Mahad D. Progressive multiple sclerosis: pathology and pathogenesis. *Nat Rev Neurol*. 2012;8(11):647–56.
5. Lublin FD, Reingold SC. Defining the clinical course of multiple sclerosis: results of an international survey. National Multiple Sclerosis Society (USA) Advisory Committee on Clinical Trials of New Agents in Multiple Sclerosis. *Neurology*. 1996;46(4):907–11.
6. Kuchling J, Ramien C, Bozin I, Dörr J, Harms L, Rosche B, et al. Identical lesion morphology in primary progressive and relapsing-remitting MS – an ultrahigh field MRI study. *Mult Scler*. 2014; 20(14):1866–71.
7. Paul F, Dörr J, Würfel J, Vogel H-P, Zipp F. Early mitoxantrone-induced cardiotoxicity in secondary progressive multiple sclerosis. *J Neurol Neurosurg Psychiatry*. 2007;78(2):198–200.

8. Dörr J, Bitsch A, Schmailzl KJG, Chan A, von Ahnen N, Hummel M, et al. Severe cardiac failure in a patient with multiple sclerosis following low-dose mitoxantrone treatment. *Neurology*. 2009;73(12):991–3.
9. Stroet A, Hemmelmann C, Starck M, Zettl U, Dörr J, Friedemann P, et al. Incidence of therapy-related acute leukaemia in mitoxantrone-treated multiple sclerosis patients in Germany. *Ther Adv Neurol Disord*. 2012;5(2):75–9.
10. Confavreux C, Vukusic S, Adeleine P. Early clinical predictors and progression of irreversible disability in multiple sclerosis: an amnesic process. *Brain*. 2003;126(Pt 4):770–82.
11. Leray E, Yaouanq J, Le Page E, Coustans M, Laplaud D, Oger J, et al. Evidence for a two-stage disability progression in multiple sclerosis. *Brain*. 2010;133(7):1900–13.
12. Franklin RJM, Ffrench-Constant C, Edgar JM, Smith KJ. Neuroprotection and repair in multiple sclerosis. *Nat Rev Neurol*. 2012;8(11):624–34.
13. Goldschmidt T, Antel J, König FB, Brück W, Kuhlmann T. Remyelination capacity of the MS brain decreases with disease chronicity. *Neurology*. 2009;72(22):1914–21.
14. Frischer JM, Bramow S, Dal-Bianco A, Lucchinetti CF, Rauschka H, Schmidbauer M, et al. The relation between inflammation and neurodegeneration in multiple sclerosis brains. *Brain*. 2009;132(Pt 5):1175–89.
15. Kremer D, Küry P, Dutta R. Promoting remyelination in multiple sclerosis: current drugs and future prospects. *Mult Scler*. 2015;26:1352458514566419.
16. Petzold A, de Boer JF, Schippling S, Vermersch P, Kardon R, Green A, et al. Optical coherence tomography in multiple sclerosis: a systematic review and meta-analysis. *Lancet Neurol*. 2010;9(9):921–32.
17. Bock M, Brandt AU, Dörr J, Pfueller CF, Ohlraun S, Zipp F, et al. Time domain and spectral domain optical coherence tomography in multiple sclerosis: a comparative cross-sectional study. *Mult Scler*. 2010;16(7):893–6.
18. Zimmermann H, Oberwahrenbrock T, Brandt AU, Paul F, Dörr J-M. Optical coherence tomography for retinal imaging in multiple sclerosis. *Degener Neurol Neuromuscul Dis*. 2014;4:153–162.
19. Sepulcre J, Murie-Fernandez M, Salinas-Alaman A, García-Layana A, Bejarano B, Villoslada P. Diagnostic accuracy of retinal abnormalities in predicting disease activity in MS. *Neurology*. 2007;68(18):1488–94.
20. Pulicken M, Gordon-Lipkin E, Balcer LJ, Frohman E, Cutter G, Calabresi PA. Optical coherence tomography and disease subtype in multiple sclerosis. *Neurology*. 2007;69(22):2085–92.
21. Henderson APD, Trip SA, Schlottmann PG, Altmann DR, Garway-Heath DF, Plant GT, et al. An investigation of the retinal nerve fibre layer in progressive multiple sclerosis using optical coherence tomography. *Brain*. 2008;131(Pt 1):277–87.
22. Costello F, Hodge W, Pan YI, Freedman M, DeMeulemeester C. Differences in retinal nerve fiber layer atrophy between multiple sclerosis subtypes. *J Neurol Sci*. 2009;281(1–2):74–9.
23. Costello F, Hodge W, Pan YI, Eggenberger E, Freedman MS. Using retinal architecture to help characterize multiple sclerosis patients. *Can J Ophthalmol*. 2010;45(5):520–6.
24. Siepmann TAM, Bettink-Remeijer MW, Hintzen RQ. Retinal nerve fiber layer thickness in subgroups of multiple sclerosis, measured by optical coherence tomography and scanning laser polarimetry. *J Neurol*. 2010;257(10):1654–60.
25. Serbecic N, Aboul-Enein F, Beutelspacher SC, Graf M, Kircher K, Geitzenauer W, et al. Heterogeneous pattern of retinal nerve fiber layer in multiple sclerosis. High resolution optical coherence tomography: potential and limitations. *PLoS One*. 2010;5(11), e13877.
26. Serbecic N, Aboul-Enein F, Beutelspacher SC, Khan A, Vass C, Kristoferitsch W, et al. High-resolution spectral domain-optical coherence tomography in multiple sclerosis, part II – the total macular volume. The first follow-up study over 2 years. *Front Neurol*. 2014;5:20.
27. Saidha S, Syc SB, Durbin MK, Eckstein C, Oakley JD, Meyer SA, et al. Visual dysfunction in multiple sclerosis correlates better with optical coherence tomography derived estimates of macular ganglion cell layer thickness than peripapillary retinal nerve fiber layer thickness. *Mult Scler*. 2011;17(12):1449–63.
28. Albrecht P, Ringelstein M, Mueller A, Keser N, Dietlein T, Lappas A, et al. Degeneration of retinal layers in multiple sclerosis subtypes quantified by optical coherence tomography. *Multiple sclerosis (Houndmills, Basingstoke, England)* [Internet]. 2 Mar 2012 [cited 2 Aug 2012]; Available from: <http://www.ncbi.nlm.nih.gov/pubmed/22389411>
29. Gelfand JM, Goodin DS, Boscardin WJ, Nolan R, Cuneo A, Green AJ. Retinal axonal loss begins early in the course of multiple sclerosis and is similar between progressive phenotypes. *PLoS One*. 2012;7(5), e36847.
30. Oberwahrenbrock T, Schippling S, Ringelstein M, Kaufhold F, Zimmermann H, Keser N, et al. Retinal damage in multiple sclerosis disease subtypes measured by high-resolution optical coherence tomography. *Mult Scler Int*. 2012;2012:530305.
31. Balk L, Tewarie P, Killestein J, Polman C, Uitdehaag B, Petzold A. Disease course heterogeneity and OCT in multiple sclerosis. *Mult Scler*. 2014;20(9):1198–206.
32. Balk LJ, Steenwijk MD, Tewarie P, Daams M, Killestein J, Wattjes MP, et al. Bidirectional trans-synaptic axonal degeneration in the visual pathway in multiple sclerosis. *J Neurol Neurosurg Psychiatry*. 2015;86:419–424.
33. Bock M, Brandt AU, Dörr J, Kraft H, Weinges-Evers N, Gaede G, et al. Patterns of retinal nerve fiber layer loss in multiple sclerosis patients with or without

- optic neuritis and glaucoma patients. *Clin Neurol Neurosurg.* 2010;112(8):647–52.
34. Costello F, Coupland S, Hodge W, Lorello GR, Koroluk J, Pan YI, et al. Quantifying axonal loss after optic neuritis with optical coherence tomography. *Ann Neurol.* 2006;59(6):963–9.
 35. Burkholder BM, Osborne B, Loguidice MJ, Bisker E, Frohman TC, Conger A, et al. Macular volume determined by optical coherence tomography as a measure of neuronal loss in multiple sclerosis. *Arch Neurol.* 2009;66(11):1366–72.
 36. Green AJ, McQuaid S, Hauser SL, Allen IV, Lyness R. Ocular pathology in multiple sclerosis: retinal atrophy and inflammation irrespective of disease duration. *Brain.* 2010;133(Pt 6):1591–601.
 37. Saidha S, Sotirchos ES, Ibrahim MA, Crainiceanu CM, Gelfand JM, Sepah YJ, et al. Microcystic macular oedema, thickness of the inner nuclear layer of the retina, and disease characteristics in multiple sclerosis: a retrospective study. *Lancet Neurol.* 2012;11(11):963–72.
 38. Gelfand JM, Nolan R, Schwartz DM, Graves J, Green AJ. Microcystic macular oedema in multiple sclerosis is associated with disease severity. *Brain.* 2012;135(Pt 6):1786–93.
 39. Burggraaff MC, Trieu J, de Vries-Knoppert WA, Balk L, Petzold A. The clinical spectrum of microcystic macular oedema. *Invest Ophthalmol Vis Sci.* 2014;55:952–961.
 40. Kaufhold F, Zimmermann H, Schneider E, Ruprecht K, Paul F, Oberwahrenbrock T, et al. Optic neuritis is associated with inner nuclear layer thickening and microcystic macular edema independently of multiple sclerosis. *PLoS One.* 2013;8(8), e71145.
 41. Brandt AU, Oberwahrenbrock T, Kadas EM, Lagrèze WA, Paul F. Dynamic formation of macular microcysts independent of vitreous traction changes. *Neurology.* 2014. doi: [10.1212/WNL.0000000000000545](https://doi.org/10.1212/WNL.0000000000000545).
 42. Abegg M, Zinkernagel M, Wolf S. Microcystic macular degeneration from optic neuropathy. *Brain.* 2012;135(Pt 12), e225.
 43. Ziemssen F, Ziemssen T, Brandt AU, Lagrèze WA. Dynamic formation of macular microcysts independent of vitreous traction changes. *Neurology.* 2015;84(4):436–7.
 44. Saidha S, Syc SB, Ibrahim MA, Eckstein C, Warner CV, Farrell SK, et al. Primary retinal pathology in multiple sclerosis as detected by optical coherence tomography. *Brain.* 2011;134(Pt 2):518–33.
 45. Wings KM, Werner JS, Harvey DJ, Cello KE, Durbin MK, Balcer LJ, et al. Baseline retinal nerve fiber layer thickness and macular volume quantified by OCT in the North American phase 3 fingolimod trial for relapsing-remitting multiple sclerosis. *J Neuroophthalmol.* 2013;33(4):341–8.
 46. Brandt AU, Oberwahrenbrock T, Ringelstein M, Young KL, Tiede M, Hartung HP, et al. Primary retinal pathology in multiple sclerosis as detected by optical coherence tomography. *Brain [Internet].* 19 May 2011 [cited 25 Aug 2011]; Available from: <http://www.ncbi.nlm.nih.gov/pubmed/21596763>
 47. Balk LJ, Twisk JWR, Steenwijk MD, Daams M, Tewarie P, Killestein J, et al. A dam for retrograde axonal degeneration in multiple sclerosis? *J Neurol Neurosurg Psychiatry.* 2014;85(7):782–9.
 48. Gordon-Lipkin E, Chodkowski B, Reich DS, Smith SA, Pulicken M, Balcer LJ, et al. Retinal nerve fiber layer is associated with brain atrophy in multiple sclerosis. *Neurology.* 2007;69(16):1603–9.
 49. Dörr J, Wernecke KD, Bock M, Gaede G, Wuerfel JT, Pfueller CF, et al. Association of retinal and macular damage with brain atrophy in multiple sclerosis. *PLoS One.* 2011;6(4), e18132.
 50. Zimmermann H, Freing A, Kaufhold F, Gaede G, Bohn E, Bock M, et al. Optic neuritis interferes with optical coherence tomography and magnetic resonance imaging correlations. *Mult Scler [Internet].* 30 Aug 2012 [cited 6 Sep 2012]; Available from: <http://www.ncbi.nlm.nih.gov/pubmed/22936335>
 51. Young KL, Brandt AU, Petzold A, Reitz LY, Lintze F, Paul F, et al. Loss of retinal nerve fibre layer axons indicates white but not grey matter damage in early multiple sclerosis. *Eur J Neurol.* 2013;20(5):803–11.
 52. Saidha S, Sotirchos ES, Oh J, Syc SB, Seigo MA, Shiee N, et al. Relationships between retinal axonal and neuronal measures and global central nervous system pathology in multiple sclerosis. *JAMA Neurol.* 2013;70(1):34–43.
 53. Henderson APD, Trip SA, Schlottmann PG, Altmann DR, Garway-Heath DF, Plant GT, et al. A preliminary longitudinal study of the retinal nerve fiber layer in progressive multiple sclerosis. *J Neurol.* 2010;257(7):1083–91.
 54. Serbecic N, Aboul-Enein F, Beutelspacher SC, Vass C, Kristoferitsch W, Lassmann H, et al. High resolution spectral domain optical coherence tomography (SD-OCT) in multiple sclerosis: the first follow up study over two years. *PLoS One.* 2011;6(5), e19843.
 55. Ratchford JN, Saidha S, Sotirchos ES, Oh JA, Seigo MA, Eckstein C, et al. Active MS is associated with accelerated retinal ganglion cell/inner plexiform layer thinning. *Neurology.* 2013;80(1):47–54.
 56. Gabilondo I, Gelfand JM, Boscardin WJ, Villoslada P, Nolan R, Calabresi PA, et al. Retinal nerve fibre layer loss in multiple sclerosis is nonlinear and most rapid early in disease. *Mult Scler J.* 2013;19(11):537–8.
 57. Budenz DL, Anderson DR, Varma R, Schuman J, Cantor L, Savell J, et al. Determinants of normal retinal nerve fiber layer thickness measured by Stratus OCT. *Ophthalmology.* 2007;114(6):1046–52.
 58. Eriksson U, Alm A. Macular thickness decreases with age in normal eyes: a study on the macular thickness map protocol in the Stratus OCT. *Br J Ophthalmol.* 2009;93(11):1448–52.

Mathias Abegg

Introduction

Optical coherence tomography (OCT) provides a fast, cheap, and noninvasive high-resolution optical access to a part of the human brain: the optic nerve head and the retina. This new diagnostic tool fueled hope of using OCT to monitor neurodegenerative diseases such as multiple sclerosis (MS). A recent climax of this yearning was reached when “microcystic macular edema,” an unprecedented retinal lesion in patients suffering from multiple sclerosis, was discovered. As is often with true novelties, it took a detour until that finding found its clinical significance. This process is still in plain progress.

Rise and Fall of Microcystic Macular Edema in Multiple Sclerosis

In 2012, Gelfand et al. described small vacuoles in the inner nuclear layer (INL) of the macula in 4.7 % of patients with MS [1]. For this observation, they coined the term “microcystic macular

edema” (MMO). This acronym was later changed to MME (microcystic macular edema) in order to comply with the American spelling. The authors found MME to be associated with a history of optic neuritis; i.e., the eyes with optic neuritis were more prone to develop MME. It was also associated with lower visual acuity and a thinning of the retinal nerve fiber layer (Fig. 10.1). Importantly, patients with MME had greater disease severity as measured with the Multiple Sclerosis Severity Score. These findings led to the concept that presence of MME might be used as an additional parameter in judging disease severity and disease progression. This idea was tested by Saidha et al., who analyzed 164 patients with MS and 60 control patients [2]. As with the initial report of Gelfand et al., they too found MME to be associated with disease severity and visual loss. Additionally, they found that inner nuclear layer (INL) thickness was significantly higher in patients with MME, whereas the combined ganglion cell and inner plexiform layer was thinner. Of note, the authors used the combined thickness of inner nuclear layer and outer plexiform layer as surrogate for inner nuclear layer thickness. Importantly, they found that INL thickness correlated with the development of contrast-enhancing lesions, new T2 lesions, with progression of the “expanded disability status scale” (EDSS) and with relapses in patients with relapsing remitting MS. Thus, they found that increased thickness of INL is associated with

M. Abegg, MD, PhD
Universitätsklinik für Augenheilkunde, Universität
Bern, Inselspital, CH-3010 Bern, Switzerland
e-mail: mathias.abegg@insel.ch

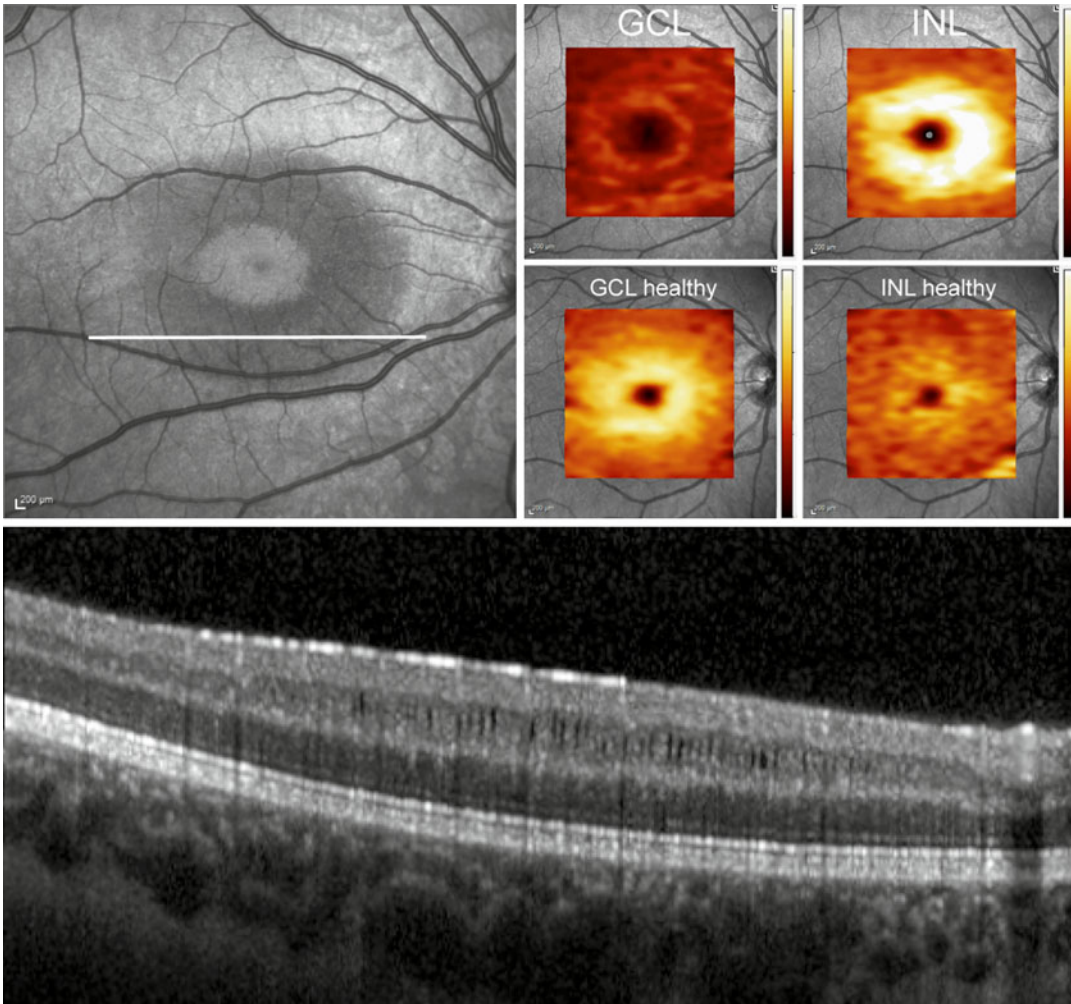


Fig. 10.1 Typical example of a microcystic macular edema (MME) in a patient with a compressive optic neuropathy. Thickness maps of ganglion cell layer (*GCL*) and inner nuclear layer (*INL*) are shown. For comparison, the author's *GCL* and *INL* are shown at the same scale below.

Areas affected from ganglion cell loss display a darkening in infrared imaging in a C-shaped perifoveal distribution pattern. The edema is characterized by vertical vacuolar spaces and thickening of the inner nuclear layer in OCT sections (localization indicated with *white bar*)

disease activity and, if confirmed, serves as a predictor for disease progression [2]. Together, these reports stirred hope that MME might be a novel “T2 lesion” and possibly be useful as a surrogate outcome marker for interventional treatment trials [3]. Similar as for patients suffering from MS, MME was found in patients suffering from neuromyelitis optica (NMO). The prevalence of MME in NMO was found to be between 20 % [4] and 26 % [5], thus about five times higher than in MS. In comparison with the MS cohort, the NMO

patients had a more profound visual loss from a more severe optic neuropathy.

Shortly after the first report of MME, the specificity of MME for demyelinating disease was questioned by two concurrent letters to the editor: (1) Balk et al. described presence of MME in a patient with relapsing isolated optic neuritis and severe optic neuropathy [6], and (2) Abegg et al. found MME in a patient with a chiasmal glioma, thus a lesion far from the affected retina [7]. Later, MME was also described in patients with

Leber's hereditary optic neuropathy [8], autosomal dominant optic neuropathy [9, 10], glaucoma, and more; none of those cases were associated with MS. This led to the conclusion that MME in multiple sclerosis is caused indirectly by MS-associated optic neuropathy, and thus severity of optic neuropathy might be a better marker for MS.

Even though MME is clearly not exclusively present in MS, the use of MME in MS might still be valid. To date, there is no evidence against the role of MME as a predictor of disease progression. However, further research is required to investigate whether INL thickness is a predictor that is independent of ganglion cell layer thickness. This could possibly be achieved by a reanalysis of the existing data of Saidha et al. [2].

Microcystic Macular Edema in Optic Neuropathy

With the exception of Burggraaff et al. [11], all reports on MME showed presence of optic atrophy. One possible reason was segmentation algorithm failure in the Burggraaff study due to severe retinal pathology. Our finding of a case with MME from a chiasmal glioma raised the possibility that MME might be a sign of optic neu-

ropathy rather than retinal inflammation as hypothesized in the initial reports. The retinal lesion in a patient without ocular disease indicated that MME might originate from a retrograde degeneration. Soon it became clear that pathologies at the level of the optic disk or along the optic nerve, thus outside the macula, were sufficient to cause MME.

Several case reports and case series showed that optic neuropathy of any etiology may lead to MME: These include compressive optic neuropathy [7, 12], anterior ischemic optic neuropathy [12], autosomal dominant optic neuropathy [9], glaucoma [13], Leber's hereditary optic neuropathy [8], MS-associated optic neuropathy [1, 2], NMO-associated optic neuropathy [4, 5], relapsing isolated optic neuritis [6], Tanzanian endemic optic neuropathy [14], etc. (Table 10.1 [1, 2, 4–6, 8, 10–15]).

The temporal relation of MME appearance and onset of optic neuropathy is still unclear. In one reported case of a new-onset anterior ischemic optic neuropathy, we found that MME was present 4 months after onset but not 10 days after disease onset [13] (Fig. 10.2). This indicates a delayed development of the edema. Also disease without progression or extremely slow progression, such as autosomal dominant optic atrophy (ADOA), may be associated with MME [9, 10].

Table 10.1 Etiologies and prevalence of MME. A selection of case series is listed [1, 2, 4–6, 8, 10–15]

Pathology	Prevalence of MME	Atrophy	References
Multiple sclerosis	15/318 patients (4.7 %) 10/164 patients (6 %) 1/129 patients (1 %)	Mild	[1] [2] [6]
Neuromyelitis optica	5/25 patients (20 %) 10/39 patients (26 %)	Severe	[4] [5]
Compressive optic neuropathy	9/53 eyes (17 %)	Severe	[12]
Glaucoma	6/160 patients (4 %) 15/85 eyes (17 %)	Moderate	[13] [15]
Tanzanian endemic optic neuropathy	16/113 patients (14 %)	Severe	[14]
Ischemic optic neuropathy	3/36 eyes (8 %)	Moderate	[12]
Hereditary optic atrophy	2/14 eyes (14 %) 2/49 patients (4 %) 30/40 eyes (75 %) 10/“several hundred” patients	Severe	[12] [10] [15] [8]
Primary retinal disease (MS and optic neuropathy excluded)	128/1045 patients (12 %)	Severe	[11]
MS	26/611 (4 %)	Mild	[1, 2, 6]

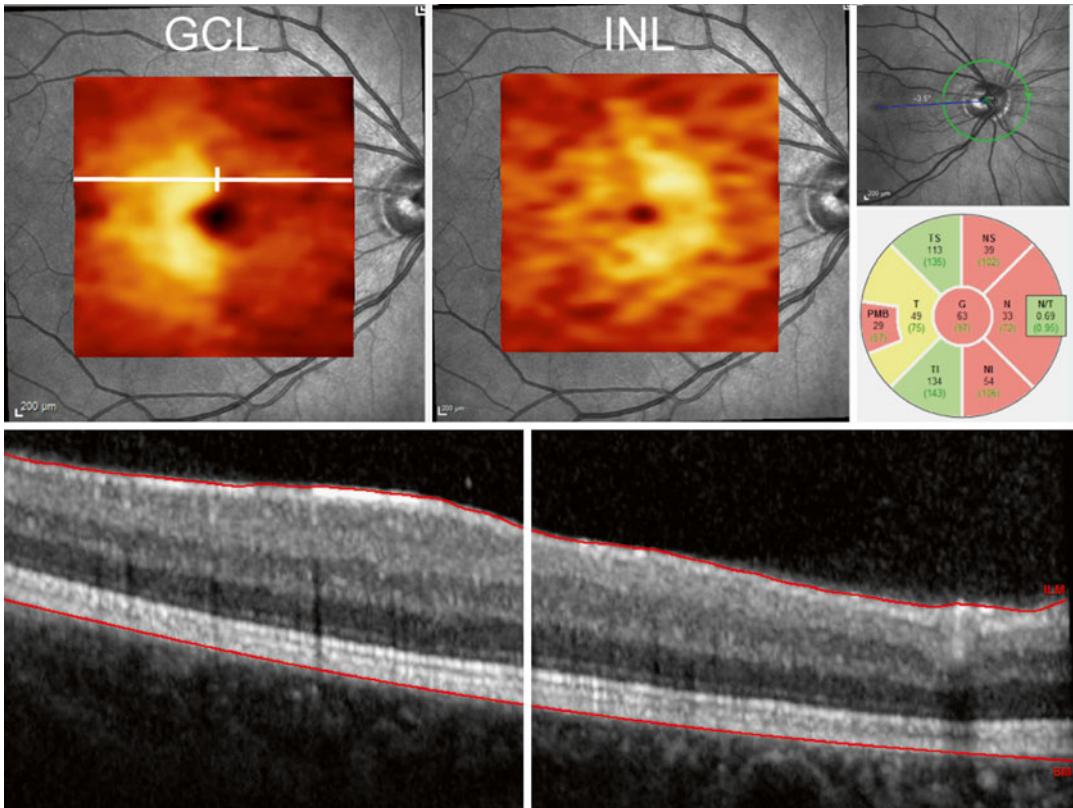


Fig. 10.2 Example of a case with retrograde maculopathy without microcystic macular edema. A patient with an optic tract lesion on the left from bleeding of a cavernous hemangioma. Thickness map of inner nuclear layer (INL) shows relative nasal thickening. Top right panels show location of OCT with the corresponding thickness values of the peripapillary nerve fiber layer

by ganglion cell loss and yet increased inner nuclear layer thickness on the right side of the area indicated with a white bar. Thickness map of inner nuclear layer (INL) shows relative nasal thickening. Top right panels show location of OCT with the corresponding thickness values of the peripapillary nerve fiber layer

These observations suggest that MME gradually develops a few weeks after onset of optic neuropathy and then remains stable for months, possibly for a lifetime.

The anatomy of MME is well described: It is restricted to the inner nuclear layer and forms a C shape around the fovea, thus not affecting the fovea and the temporal raphe. It is associated with a loss of retinal nerve fibers and ganglion cell loss [12]. The overall retinal thickness may not change, as thickening of INL may counter-balance ganglion cell layer thinning (Fig. 10.1).

We found that youth is a risk factor for the development of MME [12]. This finding awaits confirmation. Also it is not clear whether youth truly is an independent risk factor, or rather MME

has a higher prevalence in diseases that affect the young more commonly.

Microcystic Macular Edema in Primary Retinal Disease

Up until the report of Burggraaff et al., MME was strictly associated with optic neuropathy and the associated ganglion cell loss. Burggraaff et al. defined MME as “lacunar areas of hyporeflectivity with clear boundaries in the INL” in at least two adjacent scans. Based on that definition, they identified MME in patients with age-related macular degeneration, epiretinal membranes, postoperative lesions, diabetic retinopathy, vascular

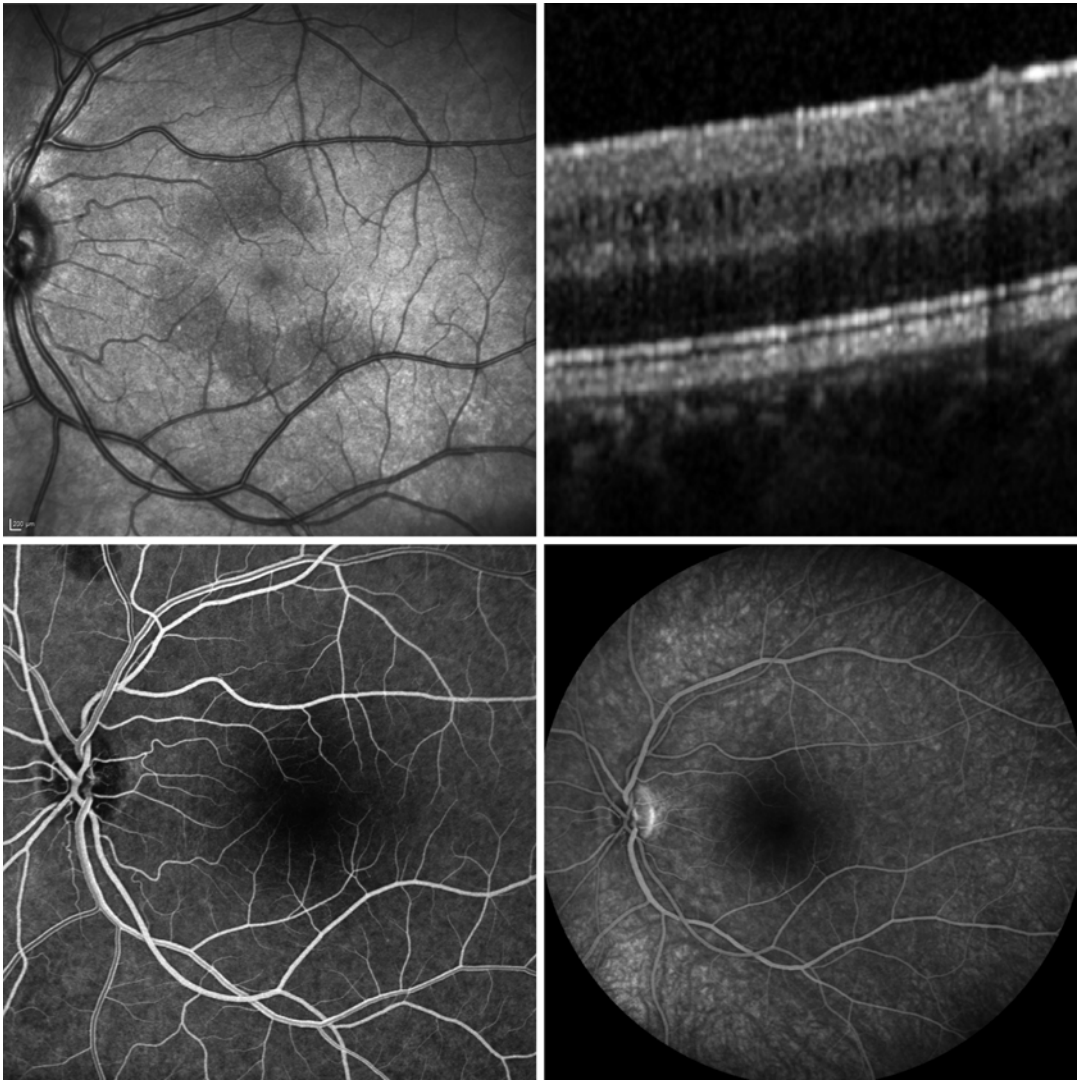


Fig. 10.3 MME is a nonvascular edema. *Top left*, dark areas in infrared imaging show distribution of MME around the fovea. *Top right*, OCT section through the affected areas shows thickening of the inner nuclear layer

and presence of vertical vacuoles. Early (*bottom left*) and late phase (*bottom right*) of fluorescein angiography shows normal vasculature and absent leakage

occlusion, MS (with/without optic neuritis), optic neuropathy, central serous chorioretinopathy, and other causes. This observation raises the possibility that MME may not be limited to optic neuropathy but may be present in other conditions too. Given the fact that the authors included cases with a clearly vascular cause of the edema, such as diabetes, this shows that MME may be a morphological special case of cystoid macular edema [16]. However, several reports have shown the

absence of leakage in fluorescein angiography in MME associated to optic neuropathy (Fig. 10.3). Thus, the lack of leakage in fluorescein angiography might be a good possibility to separate MME from cystoid macular edema. On this background, the observation of Singer et al. is of interest: They showed macular changes that match the description of MME, including normal fluorescein angiography, in patients with epiretinal membranes. Even though Sigler et al. doubted altogether that

MME is a separate clinical entity [16], they showed convincing evidence of MME in a primary retinal disease without a vascular origin [9].

Pathomechanism of Microcystic Macular Edema

The mechanism underlying MME is not clear and subject to an active debate. Initially, based on the association with multiple sclerosis, an inflammatory process with an associated breakdown of the blood-retina barrier was suspected to cause the edema. Even though this was plausible at the time, it later became clear that MME has an anatomy that differs from cystoid macular edema, which has a well-accepted vascular origin, while MME failed to show leakage on fluorescein angiography [8, 17, 18] (Fig. 10.3).

Barboni et al. speculated that vitreoretinal traction might be at the origin of MME. Possibly mechanical traction leads to an extension of INL. As can be seen from patients with juvenile X-linked retinoschisis, INL may indeed be the point of least resistance: Those patients also show disruption at the level of INL [19]. Lujan et al. showed a case with a partially detached vitreous with MME only present at the location of vitreoretinal adherence but not outside [20]. In an informal analysis of our own cases, however, we found that of 19 eyes with MME, 11 eyes had a completely attached vitreous, five eyes had a completely detached vitreous, and only three eyes showed a partially detached vitreous, similar to the case published by Lujan et al. (data not published). The fact that MME is present in children without any retinopathy and in patients without a vitreous indicates that traction is not a sufficient explanation for the great majority of the published cases. A study dedicated to the investigation of traction on the development of MME came to the same conclusion [21]. Vitreoretinal traction might be a causal factor, however, in those cases of MME that are associated with primary retinal disease such as epiretinal membranes [17].

Thus, today we know that MME is not of vascular origin and traction is not necessary for its development. And yet it is an edema, associated with increased tissue volume and not just a degen-

erative process. This edema thus has none of the known possible causes of retinal edema, and a new hypothesis for its generation is required.

An interesting idea was proposed by Balk et al. and later developed by others: Ganglion cell loss may cause a retrograde Muller cell dysfunction, which in turn impairs the water pumping function of those cells. Interestingly, Muller cells express the water channel aquaporin 4, and antibodies against aquaporin 4 are a key finding in patients with NMO. Thus, the high incidence of MME in NMO patients (up to 30 %) might be explained by a retrograde Muller cell dysfunction and an additional impairment of aquaporin 4-mediated water transport due to blockade with antibodies. This mechanism was also thought relevant by several other groups (e.g., [4, 5, 14, 18, 22]); it is however speculative and awaits experimental evidence.

Retrograde Maculopathy Versus Microcystic Macular Edema

The so-called microcysts are the most obvious and prominent feature of retrograde maculopathy. However, the detection of small vacuoles is not always obvious. Image quality of single sections may raise doubts about the presence of vertical microcysts, which have a resolution of barely more than a pixel. Averaging of sections, on the other hand, may improve image quality but also bears the risk of averaging out small vacuolar spaces. Thus, INL thickness alone, possibly combined with INL reflectivity, might be better suited to describe the changes. Indeed, INL thickening without “microcysts” have been predicted in the past [2] (see an example in Fig. 10.3). Another problem of today’s terminology of MME is that cysts are defined by an endothelial lining of a cavity. An endothelium on the tiny vacuolar spaces of MME is most unlikely to be present, and thus the term “microcysts” is a misnomer. “Microcystoid” might better describe the finding, only the word is ugly. In order to describe the macular changes in deeper retinal layers of patients with optic neuropathy, we had suggested the term “retrograde maculopathy” [12]. This term has received support [23].

Treatment of Retrograde Maculopathy

Currently, there is no treatment available for MME. And even if there were, the benefit would be uncertain because it is unclear whether MME

affects visual function. Given that presence of MME is associated with ganglion cell loss, there is a certain loss of function in the areas displaying MME. Possibly the intraretinal fluid leads to an additional functional loss. Anecdotal evidence

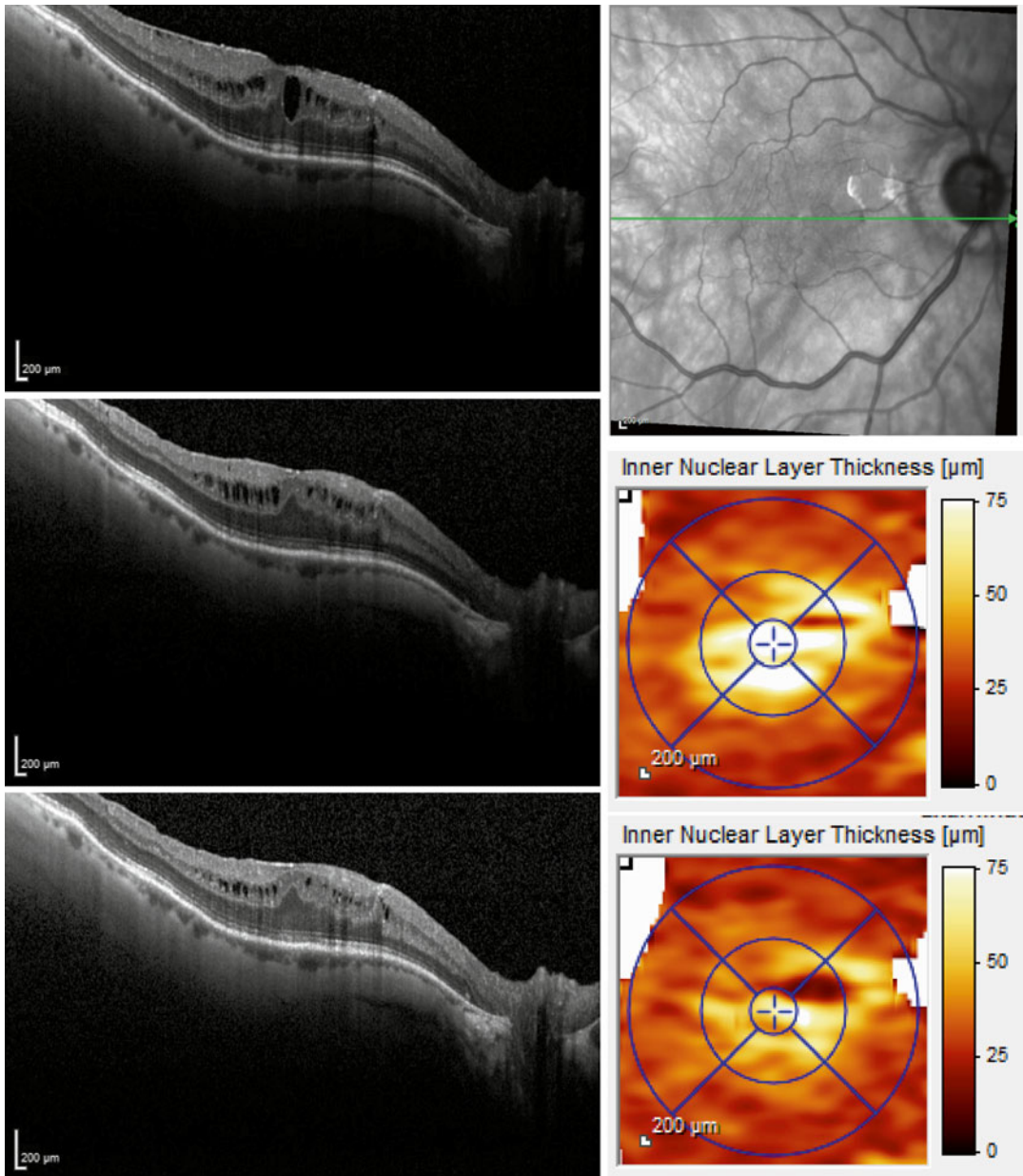


Fig. 10.4 Microcystic macular edema in a patient with macular pucker. OCT scans show retina before peeling (*top*), after peeling (*middle*), and after treatment with acetazolamide (*bottom*). The inner nuclear layer thickening did not change after membrane peeling while the tractive

edema was considerably improved. Treatment of the edema with acetazolamide led to a rapid and reduction of INL thickness. Thickness maps show INL thickness before (*top*) and after (*bottom*) treatment with acetazolamide

comes from a patient with hereditary optic neuropathy with long-standing stable vision and visual fields. She noticed a new-onset “shadow” in her visual field in the area affected by MME (Abegg, unpublished observation). This indicates that some additional functional loss might indeed be caused by the edema. Nevertheless, a more interesting treatment target than MME associated with optic neuropathy would be MME from primary retinal disease. Those patients might benefit better from a possible treatment.

Given the nonvascular nature of MME, the use of anti-VEGF or steroids would be counterintuitive. More logical on the background of the hypothesized pathomechanism would be to improve the water pumping function of the Muller cells. As these cells express carbonic anhydrase, the use of acetazolamide, which inhibits carbonic anhydrase, might be a good candidate. We have treated some patients suffering from MME with acetazolamide (Borruat and Abegg, unpublished observation) and found a significant reduction of INL thickness after treatment (see Fig. 10.4). There was, however, no corresponding improvement of visual function.

Conclusion

MME and retrograde maculopathy are recent findings. Both the clinical significance and possible treatment options remain to be determined. The high prevalence rate and the fact that it is easily detectable with a standard technique promote a clinical significance, the precise nature of which remains to be determined.

Acknowledgments The author received financial support from the Swiss National Science Foundation.

References

1. Gelfand JM, Nolan R, Schwartz DM, Graves J, Green AJ. Microcystic macular oedema in multiple sclerosis is associated with disease severity. *Brain*. 2012;135(Pt 6):1786–93.
2. Saidha S, Sotirchos ES, Ibrahim MA, Crainiceanu CM, Gelfand JM, Sepah YJ, u. a. Microcystic macular oedema, thickness of the inner nuclear layer of the

retina, and disease characteristics in multiple sclerosis: a retrospective study. *Lancet Neurol*. 2012;11(11):963–72.

3. Petzold A. Microcystic macular oedema in MS: T2 lesion or black hole? *Lancet Neurol*. 2012;11(11):933–4.
4. Gelfand JM, Cree BA, Nolan R, Arnow S, Green AJ. Microcystic inner nuclear layer abnormalities and neuromyelitis optica. *JAMA Neurol*. 2013;70(5):629–33.
5. Sotirchos ES, Saidha S, Byraiah G, Mealy MA, Ibrahim MA, Sepah YJ, u. a. In vivo identification of morphologic retinal abnormalities in neuromyelitis optica. *Neurology*. 2013;80(15):1406–14.
6. Balk LJ, Killestein J, Polman CH, Uitdehaag BMJ, Petzold A. Microcystic macular oedema confirmed, but not specific for multiple sclerosis. *Brain*. 2012;135(12):e226.
7. Abegg M, Zinkernagel M, Wolf S. Microcystic macular degeneration from optic neuropathy. *Brain*. 2012;135(Pt 12), e225.
8. Barboni P, Carelli V, Savini G, Carbonelli M, La Morgia C, Sadun AA. Microcystic macular degeneration from optic neuropathy: not inflammatory, not trans-synaptic degeneration. *Brain*. 2013;136(Pt 7), e239.
9. Abegg M, Zinkernagel M, Wolf S. Re: Rönnbäck et al.: Imaging of the macula indicates early completion of structural deficit in autosomal-dominant optic atrophy (*Ophthalmology* 2013;120:2672–7). *Ophthalmology*. 2014;121(6):e29–30.
10. Rönnbäck C, Milea D, Larsen M. Author reply: to *Ophthalmology*. 2014;121(6):e30–1.
11. Burggraaff MC, Trieu J, de Vries-Knoppert WAEJ, Balk L, Petzold A. The clinical spectrum of microcystic macular edema. *Invest Ophthalmol Vis Sci*. 2014;55(2):952–61.
12. Abegg M, Dysli M, Wolf S, Kowal J, Dufour P, Zinkernagel M. Microcystic macular edema: retrograde maculopathy caused by optic neuropathy. *Ophthalmology*. 2014;121(1):142–9.
13. Wen JC, Freedman SF, El-Dairi MA, Asrani S. Microcystic macular changes in primary open-angle glaucoma. *J Glaucoma*. 2014: Epub.
14. Kisimbi J, Shalchi Z, Mahroo OA, Mhina C, Sanyiwa AJ, Mabey D, u. a. Macular spectral domain optical coherence tomography findings in Tanzanian endemic optic neuropathy. *Brain*. 2013;136(11):3418–26.
15. Wolff B, Azar G, Vasseur V, Sahel J-A, Vignal C, Mauget-Fâysse M. Microcystic changes in the retinal internal nuclear layer associated with optic atrophy: a prospective study. *J Ophthalmol*. 2014;2014:1–5.
16. Sigler EJ. Microcysts in the inner nuclear layer, a non-specific SD-OCT sign of cystoid macular edema. *Invest Ophthalmol Vis Sci*. 2014;55(5):3282–4.
17. Sigler EJ, Randolph JC, Charles S. Delayed onset inner nuclear layer cystic changes following internal limiting membrane removal for epimacular membrane. *Graefes Arch Clin Exp Ophthalmol*. 2013;251(7):1679–85.

18. Wolff B, Basdekidou C, Vasseur V, Mauget-Faÿsse M, Sahel J-A, Vignal C. Retinal inner nuclear layer microcystic changes in optic nerve atrophy: a novel spectral-domain OCT finding. *Retina*. 2013;33(10):2133–8.
19. Menke MN, Feke GT, Hirose T. Effect of aging on macular features of X-linked retinoschisis assessed with optical coherence tomography. *Retina*. 2011;31(6):1186–92.
20. Lujan BJ, Horton JC. Microcysts in the inner nuclear layer from optic atrophy are caused by retrograde trans-synaptic degeneration combined with vitreous traction on the retinal surface. *Brain*. 2013;136(11):e260.
21. Brandt AU, Oberwahrenbrock T, Kadas EM, Lagrèze WA, Paul F. Dynamic formation of macular microcysts independent of vitreous traction changes. *Neurology*. 2014;83(1):73–7.
22. Bhargava P, Calabresi PA. The expanding spectrum of aetiologies causing retinal microcystic macular change. *Brain*. 2013;136(Pt 11):3212–4.
23. Mahroo OA, Shalchi Z, Kisimbi J, Sanyiwa AJ, Mohamed MD, Plant GT. Re: Abegg et al.: Microcystic macular edema: retrograde maculopathy caused by optic neuropathy. *Ophthalmology*. 2014; 121:142–9. *Ophthalmology*. 13. Mai 2014.

Shin C. Beh, Teresa C. Frohman,
and Elliot M. Frohman

Approximately 20 % of patients with multiple sclerosis (MS) develop acute MS associated optic neuritis (MSON) as the initial symptom of their disease, and half of MS patients suffer acute MSON during the course of their disease [1]. Even so, almost all MS patients have evidence of optic nerve demyelination at autopsy [2–4], indicating that occult, subclinical optic nerve demyelination occurs in virtually all MS patients. In agreement with these neuropathologic findings, the Optic Neuritis Treatment Trial (ONTT) showed evidence that subclinical or asymptomatic optic neuropathy was present in a significant proportion of fellow “unaffected” eyes at the time of enrolment in the ONTT and at 10 years follow-up [5].

Since the first study of optical coherence tomography (OCT) in MS [6], the interest and

number of publications on its application in MS has risen exponentially. Advancements in the application of OCT permit an objective, reproducible, office-based, noninvasive, in vivo method of visualizing and measuring the retinal layers. OCT has proven to be a sensitive, precise, and reproducible method of quantifying and tracking axonal loss in MS, an important cause of sustained disability [7]. OCT technology has evolved from the time domain OCT to the current higher-bandwidth spectral domain OCT. In fact, in vivo retinal nerve fiber layer (RNFL) thickness assessed by high-precision, high-resolution, fourth-generation, spectral domain OCT accurately correlates with ex vivo histological measurements and can even be considered an “optical biopsy” [7–9]. Figure 11.1 demonstrates the findings that can be found in MS-related optic neuropathy.

All OCT studies have shown that mean peripapillary RNFL thickness is decreased in MS patients compared to normal subjects. Greater RNFL thinning occurs in MS patients who are not treated with immunomodulatory agents [11]; this is unsurprising, since disease-modifying agents reduce the number of MS relapses and, therefore, would be expected to reduce axonal damage. The magnitude of RNFL atrophy is greater in the eyes with a history of prior acute MSON; on average, the RNFL thins by about 20 % following an attack of acute MSON; additional episodes of MSON result in more severe RNFL loss [12, 13].

S.C. Beh, MD (✉)
Neuroimmunology & Multiple Sclerosis
Program, Department of Neurology,
University of Texas Southwestern Medical Center,
Dallas, TX, USA
e-mail: shin.beh@utsouthwestern.edu

T.C. Frohman, PA-C
Department of Neurology, University of Texas
Southwestern Medical Center at Dallas,
Dallas, TX, USA

E.M. Frohman, MD, PhD, FAAN
Departments of Neurology and Ophthalmology,
Multiple Sclerosis and Neuroimmunology Program
and Clinical Center for Multiple Sclerosis,
University of Texas Southwestern School
of Medicine, Dallas, TX, USA

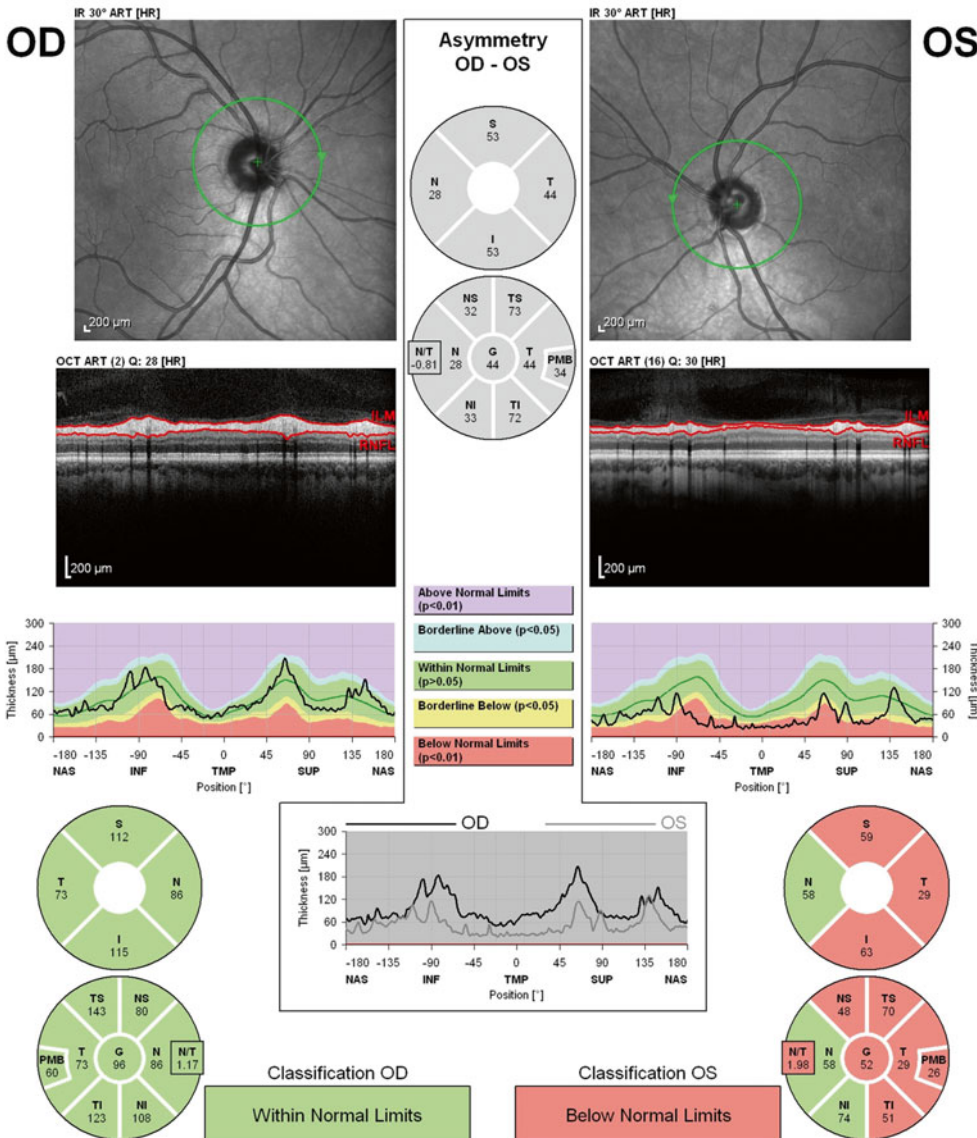
Axonal Single Exam Report OU with FoDi™
SPECTRALIS® Tracking Laser Tomography



Patient:
Patient ID:
Diagnosis: ---

DOB:
Exam.:
Comment: ---

Sex:



Notes:
Date: 5/1/2014 Signature:

Fig. 11.1 This is a spectral domain OCT analysis of peripapillary retinal nerve fiber layer (RNFL) thickness in a multiple sclerosis patient with prior left MSON. The RNFL thickness in the right eye (OD) is normal with the typical “double-hump” appearance (corresponding with the normal increased thickness of the superior and inferior

arcuate fibers). However, the RNFL thickness in the left eye (OS) is atrophied in almost all quadrants (especially the temporal; TMP). Also note the absence of the normal “double-hump” appearance in the left eye due to RNFL loss in the superior (S) and inferior (I) quadrants

In the immediate aftermath of acute MSON, the RNFL appears thicker due to inflammatory edema; this swelling normally resolves within about 6 weeks [14, 15]. This early reduction in RNFL thickness may be mistaken for atrophy and has therefore been termed “pseudoatrophy”; current technology does not permit differentiation between axonal loss (i.e., true atrophy) and inflammation-related pseudoatrophy. The majority of patients experience significant RNFL loss within 1 year after an attack of acute MSON; most of this loss occurs within 3–6 months following the event and stabilizes at between 6 and 12 months depending on the area analyzed [15, 16].

Consistent with neuropathological studies that demonstrate optic nerve demyelination in virtually all MS patients, the RNFL atrophies by approximately 2- μ m per year in most patients, regardless of history of prior acute MSON [17]. The earliest and most prominent RNFL loss occurs in the temporal quadrant [18–20], corresponding with the fibers of the papillomacular bundle, which mediates central vision. RNFL loss is the result of retrograde retinal ganglion cell axon degeneration following inflammatory demyelination of the optic nerve [21]. Alternately, damage to the retrochiasmatic visual pathways can also cause RNFL thinning as a consequence of retrograde transsynaptic degeneration of the retinal ganglion cells and their axons [22–27].

A robust relationship between RNFL atrophy and visual function is well established. RNFL loss correlates with reduced Snellen (high contrast) visual acuity in most studies [14, 16, 28–34], but not all [35, 36]. Reduced visual acuity logMAR scores are also associated with RNFL atrophy [18, 37–40]. Interestingly, RNFL atrophy may be present despite 20/20 Snellen visual acuity, suggesting that RNFL thickness is a more sensitive marker of MS disease activity, compared to high-contrast visual acuity. Alternately, low-contrast letter acuity (a more sensitive marker of visual dysfunction than high-contrast visual acuity) correlates better with RNFL loss [33–35, 38, 39, 41]—for every one line of low-contrast letter acuity lost, the mean RNFL thickness decreased by 4 μ m [35].

Additionally, loss of RNFL correlates with other measures of visual function, including impaired color vision [42] and visual field loss [14, 16, 27, 32, 38, 40]. Once the RNFL thickness falls below 75 μ m, every 10 μ m drop in RNFL is associated with a 6.46 dB decrease in visual field mean deviation (a value that gives the average of differences from normal expected value for the patient’s age) [16]. However, visual fields may be normal despite the presence of RNFL atrophy [28], confirming that visual field testing may not be sensitive enough to detect retinal ganglion cell damage until it is at an advanced stage. Furthermore, from the glaucoma literature, it is well known that about 25–35 % of retinal ganglion cells need to be lost prior to detection of visual field loss [76–78].

RNFL loss correlates with perturbations in visual electrophysiology as well. Visual evoked potential (VEP) amplitudes are reduced in patients with RNFL atrophy, the consequence of axonal loss in MS [32, 37, 43–46]. Several studies have also demonstrated an association between prolonged VEP latencies (the electrophysiologic hallmark of visual pathway demyelination) and RNFL loss [6, 32, 45, 47]. Similar findings have been found using multifocal VEP [45, 48]. Furthermore, RNFL atrophy correlates with abnormalities of the pattern electroretinography P50 latency as well as P50–P95 amplitude [6], the likely consequence of inner retinal degeneration resulting from optic nerve demyelination. However, electrophysiologic dysfunction may precede any detectable RNFL atrophy [31, 49]. Therefore, it remains possible that early pathologic changes that begin at a cellular level may escape the detection of even the most sensitive, high-resolution, technologically advanced OCT.

MS-related changes in the visual pathway mirror the pathological damage sustained by other anatomically distinct neural structures; as such, RNFL atrophy has been shown to correlate with a host of other markers of neurological impairment in MS and provides a window into disease processes. For instance, RNFL thinning correlates with the severity of neurologic disability and loss of quality of life in MS patients [18–20, 36–38, 50–53]. In the clinically isolated

syndrome, RNFL atrophy correlates with cognitive impairment [54]. In addition, RNFL loss correlates with changes in other radiologic markers of disease in MS, particularly those related to brain atrophy [36, 51, 52]. Specifically, RNFL loss has been correlated with T1 lesion volume [51], T2 lesion volume [20, 50, 51], normalized brain volume [20, 50], brain parenchymal fraction [51, 52], gray matter volume [20, 51], white matter volume [20], magnetization transfer ratio [50, 55], bicaudate ratio [56], fractional anisotropy, and diffusion tensor imaging [30, 50], as well as an increase in CSF volume [52]. The correlation between RNFL atrophy and radiologic markers of the disease is tantalizing; for monitoring disease progression, it is possible that OCT metrics may one day be used in the place of many of these time-consuming, technically demanding, and costly radiologic studies in the clinical setting.

While RNFL loss represents axonal damage, total macular volume (TMV) loss indicates neuronal death since retinal ganglion cells constitute a large population of the macula. TMV loss correlates with RNFL thinning in MS patients; when compared to healthy controls, TMV is reduced in MS patients, especially in the eyes affected by prior acute MSON [37]. A 10- μm difference in RNFL thickness corresponds to a 0.20- mm^3 reduction in TMV [57]. TMV loss has been correlated with impaired ambulatory capabilities in MS patients, as measured by the timed 25-ft and the 6-min walk [58]. On the other hand, a subset of MS patients with more severe disease demonstrate evidence of primary retinal neuronopathy (termed “macular thinning predominant phenotype”), evidenced by loss of TMV that predominantly affects the outer retina instead of the inner retina [59, 60]. This fascinating observation suggests that the inflammatory changes associated with MS optic neuropathy may begin in the retina in some patients; similar findings have been shown in murine models of MS [61].

Advancements in segmentation technology have improved the resolution of OCT devices and enabled measurements of each layer of the retina, in addition to the RNFL. This has led to the discovery that ganglion cell–inner plexiform layer (GCIPL) thickness correlates better with visual

function and radiologic markers of MS disease activity, compared to RNFL thinning [62–67]. Indeed, GCIPL atrophy may be a more accurate measurement of the damage sustained from attacks of acute MSON, since unlike the RNFL, GCIPL thickness is unaffected by inflammatory edema in the acute stages of acute MSON [65]. Furthermore, GCIPL atrophy occurs rapidly following acute MSON (even in a matter of days) and is marked at 1 month following the ictus; in fact, GCIPL atrophy precedes macular volume and macular RNFL loss [80]. Indeed, GCIPL loss in the first month following acute MSON is a good predictor of short-term visual dysfunction. A loss of less than 4.5 μm predicts low-contrast acuity recovery; if the loss does not exceed 7 μm , good visual field and color vision recovery will usually take place [80]. Additionally, improved OCT resolution has enabled the identification of small vacuolar inclusions in the inner nuclear layer, the so-called macular microcysts, which appear to be confined to regions with corresponding RNFL and GCIPL atrophy and are associated with a characteristic perifoveal crescent of punctuate changes that spares the fovea centralis on fundoscopic scanning laser ophthalmoscopy [68, 69]. These changes were first reported in MS patients and neuromyelitis optica (NMO) patients with prior acute MSON [70, 71] and attributed to retinal inflammation. Since then, however, macular microcysts have been identified in optic neuropathies from many other etiologies, including ischemia, compression, glaucoma, trauma, hereditary causes (dominant optic atrophy, Leber’s hereditary optic neuropathy), non-demyelinating inflammation (chronic relapsing inflammatory optic neuropathy), toxic–metabolic etiologies, and hydrocephalus [68, 69, 72–74], as well as in optic tract lesions [68]. Therefore, macular microcysts are not specific for inflammatory pathologies but may occur in conditions that result in retrograde degeneration of the retinal ganglion cells.

The OCT may be used as a clinical tool for evaluating suspected ocular pathology in MS patients with visual complaints. We have found OCT to be very useful in monitoring patients on fingolimod for evidence of macular edema—an infrequent but serious adverse effect of the drug.

Alternatively, OCT is very useful for evaluating for non-MS-related ocular or retinal disorders that may affect patients (e.g., epiretinal membranes, posterior vitreous detachment, neuroretinitis). We have also detected incidental ocular diseases in MS patients, including a few cases of ocular bartonellosis. The ability to detect such conditions in the MS clinic would allow timely ophthalmologic referral and institution of interventions or therapies that could potentially save the patient from serious visual loss.

As discussed in the preceding text, there is a robust correlation between OCT metrics and visual function in MS both cross-sectionally and longitudinally; OCT is a promising tool for screening and studying neuroprotective and repair-promoting therapies [79]. Furthermore, sample sizes needed to demonstrate the neuroprotective effects of novel therapies may be smaller if OCT metrics were used as outcome measures. Using serial RNFL measurements from their study, Henderson et al. [15] generated sample sizes for putative clinical trials of acute neuroprotective agents for acute MSON and suggested that such trials could be limited to 6 months since RNFL thinning appears to stabilize beyond this point. Overall sample sizes for detecting a moderate 50 % neuroprotective effect at 6 months—inferred from a 50 % reduction in the amount of RNFL loss compared to the fellow eye in a trial comparing active and placebo arms—are ~35 per arm (95 % CI ~20, 70) with 80 % power and ~50 per arm (CI ~30, 110) with 90 % power. The equivalent sample sizes for a lesser 30 % neuroprotective effect at 6 months are ~100 (CI ~55, 200) and ~130 (CI ~70, 300) per arm [15]. For neuroprotective trials using GCIPL thickness as an outcome (based on an end point and optimal power as a loss of GCIPL thickness of less than 4.5 μm 1 month following an attack of optic neuritis), Gabilondo et al. [80] calculated that 25 patients with acute MSON per group would suffice to detect differences between the groups.

Indeed, OCT is beginning to be used as the primary or secondary outcome measure for several therapeutic trials related to MS. For example, anti-IL-17 antibodies were shown to prevent RNFL and GCIPL loss in experimental

autoimmune encephalomyelitis mouse studies [81]. In MS clinical trials, OCT metrics are currently being used as preclinical outcomes for ongoing studies of erythropoietin in optic neuritis, as well as two potential neuroprotective agents (phenytoin and amiloride) [82]. A randomized placebo-controlled phase II trial of autologous mesenchymal stem cell use in MS demonstrated a trend toward fewer gadolinium-enhancing lesions but failed to show any significant changes in OCT data (peripapillary RNFL thickness and macular volume) [83].

Conclusion

Undoubtedly, we are only scratching the surface of the role of OCT in MS clinical trials; as OCT technology advances and as our understanding of MS-related retinal pathology increases, its utility as a marker of disease activity and progression will continue to expand.

Nevertheless, despite the future promise of OCT as a biomarker of MS, more longitudinal studies are needed before recommendations can be made for using OCT as a tool to monitor the efficacy of disease-modifying therapies in the clinical setting. Although OCT has been shown to detect axonal loss (i.e., the hallmark of neurodegeneration), it remains unclear how this information would impact clinical practice. The utility of OCT in trials of neurorestorative therapies that could potentially halt axonal degeneration is exciting; however, currently, there are no agents available to the clinician to remedy neurodegeneration. Furthermore, the pathobiological underpinnings of neurodegeneration in MS are not well understood. As such, even though OCT can detect neurodegeneration, the next course of action for the clinician is vague. Would a clinician be compelled to escalate immune-modulating therapy (and expose the patient to the risk such treatment entails) if there is evidence of RNFL or GCIPL loss, in the absence of evidence of radiologic or clinical worsening?

Standardized and uniform methods for interpreting and reporting OCT results, like the recent OSCAR-IB proposals [75], and similar to the visual electrophysiology protocols

established by the International Society for Clinical Electrophysiology of Vision (ISCEV) would also be very useful in streamlining and promoting the use of OCT as a tool for monitoring treatment in MS. With more clinical trials utilizing OCT metrics as an outcome measure, its role in monitoring treatment in MS will become clearer in the near future, and OCT may very well be a routine part of the clinical evaluation of MS patients (and may even be considered as an “extension” of the clinical examination).

References

- Balcer LJ. Optic neuritis. *N Engl J Med*. 2006;354:1273–80.
- Ulrich J, Groebke-Lorenz W. The optic nerve in multiple sclerosis. A morphological study with retrospective clinic-pathological correlations. *Neuroophthalmol*. 1983;3:149–59.
- Lumsden CE. Chapter 7: The neuropathology of multiple sclerosis. In: Vinken PJ, Bruyn GW, editors. *Handbook of clinical neurology*, vol. 9. Amsterdam/New York: North Holland Publishing Company/American Elsevier Publ. Co. Inc; 1970. p. 161–216.
- Ikuta F, Zimmerman HM. Distribution of plaques in seventy autopsy cases of multiple sclerosis in the United States. *Neurology*. 1976;26:26–8.
- Optic Neuritis Study Group. Visual function more than 10 years after optic neuritis: experience of the optic neuritis treatment trial. *Am J Ophthalmol*. 2004;137:77–83.
- Parisi V, Manni G, Spadaro M, Colacino G, Restuccia R, Marchi S, et al. Correlation between morphological and functional retinal impairment in multiple sclerosis patients. *Invest Ophthalmol Vis Sci*. 1999;40:2520–7.
- Frohman EM, Costello O, Zivadinov R, Stuve O, Conger A, Winslow H, et al. Optical coherence tomography in multiple sclerosis. *Lancet Neurol*. 2006;5:853–63.
- Fischer MD, Huber G, Beck SC, Tanimoto N, Muehlfriedel R, Fahl E, et al. Noninvasive, in vivo assessment of mouse retinal structure using optical coherence tomography. *PLoS One*. 2009;4, e7507.
- Spaide RF, Curcio CA. Anatomical correlates to the bands seen in the outer retina by optical coherence tomography: literature review and model. *Retina*. 2011;31:1609–19.
- Ferguson LR, Grover S, Dominguez Ii JM, Balaiya S, Chalam KV. Retinal thickness measurement obtained with spectral domain optical coherence tomography assisted optical biopsy accurately correlates with ex vivo histology. *PLoS One*. 2014;9, e111203.
- Herrero R, Garcia-Martin E, Almarcequi C, Ara JR, Rodriguez-Mena D, Martin J, et al. Progressive degeneration of the retinal nerve fiber layer in patients with multiple sclerosis. *Invest Ophthalmol Vis Sci*. 2012;53:8344–9.
- Petzold A, de Boer JF, Schippling S, Vermersch P, Kardon R, Green A, et al. Optical coherence tomography in multiple sclerosis: a systematic review and meta-analysis. *Lancet Neurol*. 2010;9:921–32.
- Costello F. Evaluating the use of optical coherence tomography in optic neuritis. *Mult Scler Int*. 2011;2011:148394.
- Noval S, Contreras I, Rebolleda G, Muñoz-Negrete FJ. Optical coherence tomography versus automated perimetry for follow-up of optic neuritis. *Acta Ophthalmol Scand*. 2006;84:790–4.
- Henderson APD, Altmann DR, Trip AS, Kallis C, Jones SJ, Schlottmann PG, et al. A serial study of retinal changes following optic neuritis with sample size estimates for acute neuroprotection trials. *Brain*. 2010;133:2592–602.
- Costello F, Coupland S, Hodge W, Lorello GR, Koroluk J, Pan YI, et al. Quantifying axonal loss after optic neuritis with optical coherence tomography. *Ann Neurol*. 2006;59:963–9.
- Talman LS, Bisker ER, Sackel DJ, Long Jr DA, Galetta KM, Ratchford JN, et al. Longitudinal study of vision and retinal nerve fiber layer thickness in multiple sclerosis. *Ann Neurol*. 2010;67:749–60.
- Costello F, Hodge W, Pan YI, Eggenberger E, Coupland S, Kardon RH. Tracking retinal nerve fiber layer loss after optic neuritis: a prospective study using optical coherence tomography. *Mult Scler*. 2008;14:893–905.
- Bock M, Brandt AU, Dörr J, Kraft H, Weinges-Evers N, Gaede G, et al. Patterns of retinal nerve fiber layer loss in multiple sclerosis patients with or without optic neuritis and glaucoma patients. *Clin Neurol Neurosurg*. 2010;268:12–7.
- Sepulcre J, Murie-Fernandez M, Salinas-Alaman A, Garcia-Layana A, Bejarano B, Villoslada P. Diagnostic accuracy of retinal abnormalities in predicting disease activity in MS. *Neurology*. 2007;68:1488–94.
- Shindler KS, Ventura E, Dutt M, Rostami A. Inflammatory demyelination induces axonal injury and retinal ganglion cell apoptosis in experimental optic neuritis. *Exp Eye Res*. 2008;87:208–13.
- Reich DS, Smith SA, Gordon-Lipkin EM, Ozturk A, Caffo BS, Balcer LJ, Calabresi PA. Damage to the optic radiation in multiple sclerosis is associated with retinal injury and visual disability. *Arch Neurol*. 2009;66:998–1006.
- Mehta JS, Plant GT. Optical coherence tomography (OCT) findings in congenital/long-standing homonymous hemianopia. *Am J Ophthalmol*. 2005;140:727–9.
- Jindahra P, Petrie A, Plant GT. Retrograde trans-synaptic retinal ganglion cell loss identified by optical coherence tomography. *Brain*. 2009;132:628–34.

25. Gabilondo I, Martinez-Lapiscina EH, Martinez-Heras E, Fraga-Pumar E, Llufrui S, et al. Trans-synaptic axonal degeneration in the visual pathway in multiple sclerosis. *Ann Neurol*. 2014;75:98–107.
26. Klistorner A, Sriram Vootakuru N, Wang C, Barnett MH, Garrick R, et al. Axonal loss of retinal neurons in multiple sclerosis associated with optic radiation lesions. *Neurology*. 2014;82:2165–72.
27. Balk LJ, Steenwijk MD, Tewarie P, Daams M, Killestein J, Wattjes MP, et al. Bidirectional trans-synaptic axonal degeneration in the visual pathway in multiple sclerosis. *J Neurol Neurosurg Psychiatry*. 2015;86(4):419–24. doi:10.1136/jnnp-2014-308189.
28. Cheng H, Laron M, Schiffman JS, Tang RA, Frishman LJ. The relationship between visual field and retinal nerve fiber layer measurements in patients with multiple sclerosis. *Invest Ophthalmol Vis Sci*. 2007;48:5798–805.
29. Merle H, Olindo A, Donnio A, Richer R, Smadja D, Cabre P. Retinal peripapillary nerve fiber layer thickness in neuromyelitis optica. *Invest Ophthalmol Vis Sci*. 2008;49:4412–7.
30. Naismith RT, Xu J, Tutlam NT, Snyder A, Benzinger T, Shimony J, et al. Disability in optic neuritis correlates with diffusion tensor-derived directional diffusivities. *Neurology*. 2009;72:589–94.
31. Naismith RT, Tutlam NT, Xu J, Shepherd JB, Klawiter EC, Song SK, Cross AH. Optical coherence tomography is less sensitive than visual evoked potentials in optic neuritis. *Neurology*. 2009;73:46–52.
32. Pueyo V, Martin J, Fernandez J, Almarcequi C, Ara J, Egea C, et al. Axonal loss in the retinal nerve fiber layer in patients with multiple sclerosis. *Mult Scler*. 2008;14:609–14.
33. Pulicken M, Gordon-Lipkin E, Balcer LJ. Optical coherence tomography and disease subtype in multiple sclerosis. *Neurology*. 2007;69:2085–92.
34. Zaveri MS, Conger A, Salter A, Frohman TC, Galetta SL, Markowitz CE, et al. Retinal imaging by laser polarimetry and optical coherence tomography evidence of axonal degeneration in multiple sclerosis. *Arch Neurol*. 2008;65:924–8.
35. Fisher JB, Jacobs DA, Markowitz CE, Galetta SL, Volpe NJ, Nano-Schiavi ML, et al. Relation of visual function to retinal nerve fiber layer thickness in multiple sclerosis. *Ophthalmology*. 2006;113:324–32.
36. Grazioli F, Zivadinov R, Weinstock-Guttman B, Lincoff N, Baier M, Wong JR, et al. Retinal nerve fiber layer thickness is associated with brain MRI outcomes in multiple sclerosis. *J Neurol Sci*. 2008;268:12–7.
37. Trip SA, Schlottmann PG, Jones SJ, Altmann DR, Garway-Heath DF, Thompson AJ, et al. Retinal nerve fiber layer axonal loss and visual dysfunction in optic neuritis. *Ann Neurol*. 2005;58:383–91.
38. Henderson AP, Trip SA, Schlottmann PG, Altmann DR, Garway-Heath DF, Plant GT, et al. An investigation of the retinal nerve fiber layer in progressive multiple sclerosis using optical coherence tomography. *Brain*. 2008;131:277–87.
39. Spain RI, Maltenfort M, Sergott RC, Leist TP. Thickness of the retinal nerve fiber layer correlates with disease duration in parallel with corticospinal tract dysfunction in untreated multiple sclerosis. *J Rehabil Res Dev*. 2009;46:633–42.
40. Siepmann TAM, Bettink-Remeijer MW, Hintzen RQ. Retinal nerve fiber layer thickness in subgroups of multiple sclerosis, measured by optical coherence tomography and scanning laser polarimetry. *J Neurol*. 2010;257:1654–60.
41. Bock M, Brandt AU, Kuchenbecker J, Dorr J, Pfueller CF, Weinges-Evers N, et al. Impairment of contrast visual acuity as a functional correlate of retinal nerve fibre layer thinning and total macular volume reduction in multiple sclerosis. *Br J Ophthalmol*. 2012;96:62–7.
42. Villoslada P, Cuneo A, Gelfand J, Hauser SL, Green A. Color vision is strongly associated with retinal thinning in multiple sclerosis. *Mult Scler*. 2012;18:991–9.
43. Brusa A, Jones SJ, Plant GT. Long-term remyelination after optic neuritis: a 2-year visual evoked potential and psychophysical serial study. *Brain*. 2001;124:468–79.
44. Frohman AR, Schnurman Z, Conger A, Conger D, Beh S, et al. Multifocal visual evoked potentials are influenced by variable contrast stimulation in MS. *Neurology*. 2012;79:797–801.
45. Klistorner A, Arvind H, Nguyen T, Garrick R, Paine M, Graham S, et al. Axonal loss and myelin in early on loss in postacute optic neuritis. *Ann Neurol*. 2008;64:325–31.
46. Thurtell MJ, Bala E, Yaniglos SS, et al. Evaluation of optic neuropathy in multiple sclerosis using low-contrast visual evoked potentials. *Neurology*. 2009;73:1849–57.
47. Gundogan FC, Demirkaya S, Sobaci G. Is optical coherence tomography really a new biomarker candidate in multiple sclerosis? – a structural and functional evaluation. *Invest Ophthalmol Vis Sci*. 2007;48:5773–81.
48. Frohman EM, Fujimoto LG, Frohman TC, Calabresi PA, Cutter G, Balcer LJ. Optical coherence tomography: a window into the mechanisms of multiple sclerosis. *Nat Clin Pract Neurol*. 2008;4:664–75.
49. Di Maggio G, Santangelo R, Guerrieri S, Bianco M, Ferrari L, et al. Optical coherence tomography and visual evoked potentials: which is more sensitive in multiple sclerosis? *Mult Scler*. 2014;20:1342–7.
50. Frohman EM, Dwyer MG, Frohman T, Cox JL, Salter A, Greenberg BM, et al. Relationship of optic nerve and brain conventional and non-conventional MRI measures and retinal nerve fiber layer thickness, as assessed by OCT and GDx: a pilot study. *J Neurol Sci*. 2009;282:96–105.
51. Siger M, Dziegielewska K, Jasek L, Bieniek M, Nicpan A, Nawrocki J, Selmaj K. Optical coherence tomography in multiple sclerosis: thickness of the retinal nerve fiber layer as a potential measure of axonal loss and brain atrophy. *J Neurol*. 2008;255:1555–60.

52. Gordon-Lipkin E, Chodkowski B, Reich DS, Smith SA, Pulicken M, Balcer LJ, et al. Retinal nerve fiber layer is associated with brain atrophy in multiple sclerosis. *Neurology*. 2007;69:1603–9.
53. Garcia-Martin E, Rodriguez-Mena D, Herrero R, Almarcegui C, Dolz I, Martin J, et al. Neuro-ophthalmologic evaluation, quality of life, and functional disability in patients with MS. *Neurology*. 2013;81:76–83.
54. Anhoque CF, Biccás-Neto L, Dominques SC, Teixeira AL, Dominques RB. Cognitive impairment and optic nerve axonal loss in patients with clinically isolated syndrome. *Clin Neurol Neurosurg*. 2013;115:1032–5.
55. Trip SA, Schlottmann PG, Jones SJ, Li WY, Garway-Heath DF, Thompson AJ, et al. Optic nerve magnetization transfer imaging and measures of axonal loss and demyelination in optic neuritis. *Mult Scler*. 2007;13:875–9.
56. Abalo-Lajo JM, Limeres CC, Gomez MA, Baleato-Gonzalez S, Cadarso-Suarez C, Capeans-Tome C, Gonzalez F. Retinal nerve fiber layer thickness, brain atrophy, and disability in multiple sclerosis patients. *J Neuroophthalmol*. 2014;34:23–8.
57. Burkholder BM, Osborne B, Loguidice MJ, Bisker E, Frohman TC, Conger A, et al. Macular volume determined by optical coherence tomography as a measure of neuronal loss in multiple sclerosis. *Arch Neurol*. 2009;66:1366–72.
58. Balantrapu S, Sandroff BM, Pula JH, Motl RW. Integrity of the anterior visual pathway and its association with ambulatory performance in multiple sclerosis. *Mult Scler Int*. 2013;2013:481035.
59. Saidha S, Syc SB, Ibrahim MA, Warner CV, Farrell SK, Oakley JD, et al. Primary retinal pathology in multiple sclerosis as detected by optical coherence tomography. *Brain*. 2011;134:518–33.
60. Brandt AU, Oberwahrenbrock T, Ringelstein M, Young KL, Tiede M, Hartung HP, et al. Primary retinal pathology in multiple sclerosis as detected by optical coherence tomography. *Brain*. 2011;134:e193, author reply e194.
61. Fairless R, Williams SK, Hoffmann DB, Stojic A, Hochmeister S, Schmitz F, et al. Preclinical retinal neurodegeneration in a model of multiple sclerosis. *J Neurosci*. 2012;32:5585–97.
62. Oberwahrenbrock T, Ringelstein M, Jentschke S, Deuschle K, Klumbies K, Bellmann-Strobl J, Harmel J, et al. Retinal ganglion cell and inner plexiform layer thinning in clinically isolated syndrome. *Mult Scler*. 2013;19:1887–95.
63. Saidha S, Syc SB, Durbin MK, Eckstein C, Oakley JD, Meyer SA, et al. Visual dysfunction in multiple sclerosis correlates better with optical coherence tomography derived estimates of macular ganglion cell thickness than peripapillary retinal nerve fiber layer thickness. *Mult Scler*. 2011;17:1449–63.
64. Saidha S, Sotirchos ES, Oh J, Syc SB, Seigo MA, Shiee N, et al. Relationships between retinal axonal and neuronal measures and global central nervous system pathology in multiple sclerosis. *JAMA Neurol*. 2013;70:34–43.
65. Syc SB, Saidha S, Newsome S, Ratchford JN, Levy M, Ford E, et al. Optical coherence tomography segmentation reveals ganglion cell layer pathology after optic neuritis. *Brain*. 2012;135:521–33.
66. Ratchford JN, Saidha S, Sotirchos ES, Oh JA, Seigo MA, Eckstein C, et al. Active MS is associated with accelerated retinal ganglion cell/inner plexiform layer thinning. *Neurology*. 2013;80:47–54.
67. Walter SD, Ishikawa H, Galetta KM, Sakai RE, Feller DJ, Henderson SB, et al. Ganglion cell loss in relation to visual disability in multiple sclerosis. *Ophthalmology*. 2012;119:1250–7.
68. Abegg M, Dysli M, Wolf S, Kowal J, Dufour P, Zinkernagel M. Microcystic macular edema: retrograde maculopathy caused by optic neuropathy. *Ophthalmology*. 2014;121:1422–9.
69. Kaufhold F, Zimmermann H, Schneider E, Ruprecht K, Paul F, Oberwahrenbrock T, Brandt AU. Optic neuritis is associated with inner nuclear layer thickening and microcystic macular edema independently of multiple sclerosis. *PLoS One*. 2013;8, e71145.
70. Gelfand JM, Nolan R, Schwartz DM, Graves J, Green AJ. Microcystic macular oedema in multiple sclerosis is associated with disease severity. *Brain*. 2012;135:1786–93.
71. Gelfand JM, Cree BA, Nolan R, Arrow S, Green AJ. Microcystic inner nuclear layer abnormalities and neuromyelitis optica. *JAMA Neurol*. 2013;70:629–33.
72. Abegg M, Zinkernagel M, Wolf S. Microcystic macular degeneration from optic neuropathy. *Brain*. 2012;135:1–2.
73. Barboni P, Carelli V, Savini G, Carbonelli M, La Morgia C, Sadun AA. Microcystic macular degeneration from optic neuropathy: not inflammatory, not trans-synaptic degeneration. *Brain*. 2013;136, e239.
74. Wolff B, Basdekidou C, Vasseur V, Mauget-Faysses M, Sahel JA, Vignal C. Retinal inner nuclear layer microcystic changes in optic nerve atrophy: a novel spectral-domain OCT finding. *Retina*. 2013;33:2133–8.
75. Schippling S, Balk L, Costelo F, Albrecht P, Balcer L, Calabresi P, et al. Quality control for retinal OCT in multiple sclerosis: validation of the OSCAR-IB criteria. *Mult Scler*. 2015;21(2):163–70.
76. Kerrigan-Baumrind LA, Quigley HA, Pease ME, Kerrigan DF, Mitchell RS. Number of ganglion cells in glaucoma eyes compared with threshold visual field tests in the same persons. *Invest Ophthalmol Vis Sci*. 2000;41:741–8.
77. Mikelberg FS, Yidegilligne HM, Schulzer M. Optic nerve axon count and axon diameter in patients with ocular hypertension and normal visual fields. *Ophthalmology*. 1995;102:342–8.
78. Quigley HA, Dunkelberger GR, Green WR. Retinal ganglion cell atrophy correlated with automated

- perimetry in human eyes with glaucoma. *Am J Ophthalmol.* 1989;107:453–64.
79. Balcer LJ, Miller DH, Reingold SC, Cohen JA. Vision and vision-related outcome measures in multiple sclerosis. *Brain.* 2015;138:11–27.
80. Gabilondo I, Martinez-Lapiscina EH, Fraga-Pumar E, Ortiz-Perez S, Torres-Torres R, Anodra M, et al. Dynamics of retinal injury after acute optic neuritis. *Ann Neurol.* 2015;77:517–28.
81. Knier B, Rothhammer V, Heink S, Puk O, Graw J, Hemmer B, et al. Neutralizing IL-17 protects the optic nerve from autoimmune pathology and prevents retinal nerve fiber layer atrophy during experimental autoimmune encephalomyelitis. *J Autoimmun.* 2015;56:34–44.
82. Toosy AT, Mason DF, Miller DH. Optic neuritis. *Lancet Neurol.* 2014;13:83–99.
83. Llufriu S, Sepulveda M, Blanco Y, Marin P, Moreno B, Berenguer J, et al. Randomized placebo-controlled phase II trial of autologous mesenchymal stem cells in multiple sclerosis. *PLoS One.* 2014;9, e113936.

Elena H. Martínez-Lapiscina,
Bernardo Sanchez-Dalmau, and Pablo Villoslada

Technological Advances Favor the Development of Neuroprotective Therapies

Inflammation, demyelination, and neuroaxonal damage are the pathological mechanisms underlying multiple sclerosis (MS) [1]. The interplay among them explains the MS phenotype, but axonal damage is considered to be the main factor leading to irreversible disability [2]. Thus, new drugs preventing axonal loss such as neuroprotective therapies are essential for MS patients.

The development of these therapies is hampered by technical difficulties for studying the brain. Early on, magnetic resonance imaging (MRI) solved the problem of monitoring inflammation measured as new/enlarging T2 lesions and gadolinium-enhancing lesions. This technological advance has improved the development of current disease-modifying treatments. These drugs target inflammation and decrease the risk of new or enlarging lesions [3] thereby providing secondary neuroprotection due to the reduction of direct axonal damage. Myelin is important to maintain axon integrity. As such, myelin-

reparative/protective strategies may also provide secondary neuroprotection. Full-field and multifocal visual evoked potentials (FF-VEP and MF-VEP) might be very useful to track demyelination and remyelination processes. Anti-LINGO-1 mAb (BIIB033), a drug promoting myelin repair, is under evaluation by using this technology in patients after an acute multiple sclerosis optic neuritis (MSON) episode [4]. Phase 2 of the RENEW study of anti-LINGO-1 in acute MSON has shown improved latency recovery, as measured by the primary endpoint, FF-VEP, among anti-LINGO-1 participants, compared with placebo. Per-protocol participants (those who were treated with at least five of the six doses of anti-LINGO-1) showed a 34 % improvement of 7.55 milliseconds in optic nerve conduction latency at week 24, compared with placebo ($p=0.05$). Further latency recovery was observed at the last study visit (week 32), with a statistically significant 41 % improvement of 9.13 milliseconds, compared with placebo ($p=0.01$) [5].

The development of software to measure non-conventional quantitative MRI outcomes such as brain volumes (in cross-sectional studies) and especially brain atrophy (in longitudinal studies) has favored the evaluation of neuroprotection in MS [6]. Brain atrophy correlates with disability [7] and cognitive impairment in MS [8]. However, brain atrophy not only reflects neuroaxonal damage but also the loss of myelin and glial cells.

E.H. Martínez-Lapiscina, MD, PhD (✉)
B. Sanchez-Dalmau, MD • P. Villoslada, MD, PhD
Center of Neuroimmunology and Neurology
Department, Institute of Biomedical Research August
Pi Sunyer (IDIBAPS) – Hospital Clinic of Barcelona,
Barcelona, Spain
e-mail: HERNANDEZ@clinic.ub.es

Astrogliosis may underestimate neuroaxonal damage in MS. Moreover, the respective contribution of each component to brain atrophy may depend on several factors including MS-related factors, such as disease duration, as well as non-related factors (lifestyle factors and comorbidities) and may differ between individuals [7].

More recently, the technological development of photonic devices such as optical coherence tomography (OCT) has provided a new window into the MS brain [9]. The most widely used OCT outcome has been retinal nerve fiber layer (RNFL) as a measure of axonal damage [10]. However, ganglion cell layer (GCL), as a measure of neuronal damage, is becoming more important [11, 12]. The retina lacks myelin, and retinal measurements, especially GCL, are less affected by astrogliosis. Thus, whereas pathophysiological mechanisms behind brain atrophy are still unclear, OCT is a more specific measurement of neurodegeneration than brain atrophy quantified by MRI. Once again, technological innovation has facilitated scientific research, and different molecules with potentially primary neuroprotective effects, including well-known old drugs such as phenytoin and new ones such as BN201, are under evaluation for acute MSON and MS.

Optical Coherence Tomography for Assessing Neuroprotection

Acute MSON causes retrograde degeneration of retinal ganglion cells (RGC) in the retina that can be monitored by RNFL [13–17] and GCL thickness measurements [11]. RNFL thickness correlates with visual disability [14, 16, 18] although GCL thickness is preferable because it is less affected by edema and astrogliosis [19] and shows a stronger correlation with visual disability [20, 21]. The bulk of the data supports the role of OCT as a tool for monitoring acute neuroaxonal damage due to acute MSON.

Previous studies have provided evidence supporting the existence of primary retinopathy in MS as part of the normal appearing gray matter damage affected by diffuse and chronic neurodegenerative processes [12, 22]. Moreover, retinal

neurodegeneration may also appear as a result of transsynaptic effects due to chronic diffuse damage in the afferent visual pathway [23–26]. OCT captures the effects of both mechanisms, which may explain the correlation between OCT outcomes and neurological disability [27–29] and brain atrophy [27, 30–33]—especially gray matter atrophy [32].

Considering the results discussed earlier, OCT can be used for monitoring neuroprotection in an acute lesion model (6 months) such as acute MSON even with relatively few samples (Table 12.1) [34]. OCT may also address neuroprotection in a chronic model such as diffuse damage in MS. However, the average yearly thinning of RNFL in MS is around 2 μm [29, 35], and therefore longer follow-up and larger sample sizes might be necessary to witness any effect (Table 12.2). Contrary to acute MSON trials that include RNFL thickness as the primary outcome, most studies evaluating neuroprotective effects in MS use brain atrophy as the primary outcome and RNFL thickness as the secondary outcome in the design (Table 12.2).

OCT and AON: Good Partners for Drug Trials for Neuroprotection

First Evidence: RNFL Thickness to Track Neurodegeneration After AON

In 2006, Costello and colleagues provided the first evidence that OCT can be longitudinally performed to track RNFL thinning after acute MSON. They showed that RNFL loss tended to occur within 3–6 months after MSON onset. Moreover, they reported a threshold of RNFL thickness at 6 months (75 μm), below which RNFL measurements predicted persistent visual dysfunction at 6 months [13].

In 2010, Henderson and colleagues corroborated this strong functional-structural correlation and suggested that RNFL thinning appeared earlier, within just 1–2 months after acute MSON [16]. More importantly, they provided sample size calculations for using RNFL loss after 6 months as a suitable outcome in placebo-

Table 12.1 Sample sizes in clinical trials addressing neuroprotection by using RNFL thinning in acute MSON

Trial (phase)	Goal	Drug	Indication	Primary outcome	Secondary outcomes	Alpha error	Power	Effect size	Sample per arm	Status	Ref/NCT
ACTION (RCT Phase II)	Primary neuroprotection	I: Amiloride C: Placebo	iAON MSON	Change in RNFLT between MSON-eye and NON-eye at 6 months	RNFLT at 12 m MRI outcomes ERG, VEP HC/LCVA color NEI-VFQ-25; 10S	-	-	-	23	Ongoing	NCT01802489
Neuroprotection with phenytoin in MSON (RCT Phase II)	Primary neuroprotection	I: Phenytoin C: Placebo	iAON MSON	Change in RNFLT in MSON-eye from baseline to 6 months	MRI ON VEP LCVA color	-	-	50 %	45	Completed benefit	NCT01451593
VISION PROTECT (RCT Phase II)	Primary neuroprotection	I: Erythropoietin + methylprednisolone C: Placebo	iAON MSON	Change in RNFLT in MSON-eye from baseline to 4 months	MRI ON atrophy VF VA and VEP (From 0 to 4 m)	0.01	-	50 %	20	Completed benefit	NCT00355095 [34]
Mino in MSON (RCT Phase II)	Primary neuroprotection	I: Minocycline+DMT C: None+DMT	iAON MSON	RNFLT at 0, 3, 6, and 9 months at MSON-eye	RNFLT and MV Visual outcomes	-	-	-	36 (min)	Withdrawn due to lack of recruitment	NCT01073813
RENEW (RCT Phase II)	Myelin repair Secondary neuroprotection	I: BIIB033 C: Placebo	iAON MSON (Newly diagnosed)	Nerve velocity conduction (FF-VEP) at 6 months for the MSON-eye from the baseline of NON-eye	Change in RNFLT and RGCL/IPL at 6 months for MSON-eye from NON-eye at baseline	0.1	80 %	50 %	41	Completed benefit	NCT01721161

(continued)

Table 12.1 (continued)

Trial (phase)	Goal	Drug	Indication	Primary outcome	Secondary outcomes	Alpha error	Power	Effect size	Sample per arm	Status	Ref/NCT
ACTHAR (RCT Phase IV)	Anti-inflammatory Secondary neuroprotection	I: Acthar gel C: MP iv + oral taper	iAON MSON	RNFLT at 6 months in MSON-eye	RNFL swelling at 1/3 months in MSON-eye	–	–	–	30	Recruiting	NCT01838174
Lipoic acid in acute MSON (RCT Phase I)	Antioxidant Secondary neuroprotection	I: Lipoic acid C: Placebo	iAON MSON	RNFL atrophy in MSON-eye from baseline to 6 months	Change in HCVA LCVA CS CV and VF from 0 to 6 months	–	–	–	27	Recruiting	NCT01294176
Fingolimod in acute MSON (RCT Phase II)	Immunomodulation Myelin protection Secondary neuroprotection	I: Fingolimod C: Placebo	MSON	Change in RNFLT at 6 months for MSON-eye from baseline of NON-eye	LCVA NEI-VFQ-25 % McDonald 2010	0.05	80 %	45 %	63	Withdrawn	NCT01757691
PROTECT (Phase IV)	Immunomodulation Secondary neuroprotection	I: Interferon beta-1a I: Natalizumab	RRMS- MSON	RNFL atrophy in MSON-eye from 1 to 9 months	Same but corrected by NON-eye	–	–	–	25	Withdrawn	NCT00771043

I intervention, C control, RCT randomized clinical trial, AON acute optic neuritis, iAON idiopathic acute optic neuritis, MSON acute optic neuritis in MS patient, RRMS relapsing-remitting multiple sclerosis, DMT disease-modifying treatment, MSON-eye eye with acute MSON, NON-eye fellow eye, RNFLT retinal nerve fiber layer thickness, RGCL/IPL retinal ganglion cell layer/inner plexiform layer, MV macular volume, MRI magnetic resonance imaging, ERG electroretinogram, VEP visual evoked potentials, FF-VEP full-field VEP, HCVA high-contrast visual acuity, LCVA low-contrast visual acuity, CS contrast sensitivity, CV color vision, VF visual field, NEI-VFQ-25 National Eye Institute Visual Function Questionnaire 25 items, Ref Reference, NCT ClinicalTrials.gov

Table 12.2 Sample sizes in clinical trials addressing neuroprotection by using RNFL thinning in multiple sclerosis

Trial (phase)	Goal	Drug	Indication	Primary outcome	Secondary outcomes	Sample per arm	Status	Ref/NCT
Effect of MD1003 in chronic visual loss related to MSON in MS (RCT Phase III)	Not available	I: MD1003 C: Placebo	MS with prior MSON >6 months with VA ≤5/10	HCVA (1 year)	VF, VEP (latency), and RNFLT (1 year)	105 (total)	Ongoing	NCT02220244
FLORIMS (RCT Phase II)	Primary neuroprotection	I: Flupirtine + interferon beta-1b C: Placebo + interferon beta-1b	RRMS	New T2 lesions MRI (1 year)	New Gad + lesions and brain atrophy RNFLT Neurological impairment and disability (1 year)	15	Complete (Results not available)	NCT00623415
MS-SMART (RCT Phase II)	Primary neuroprotection	I: Ibudilast I: Riluzole I: Amitolotide C: Placebo	SPMS	Brain atrophy (2 years)	New/enlarging T2 lesions (2 years) Neurological impairment and disability (1 year)	110	Recruiting	NCT01910259
Andrographolide in P-MS (RCT Phase II)	Primary neuroprotection	I: Andrographolide C: Placebo	PPMS SPMS	Brain atrophy (2 years)	Disability and QoL; new T2 T1 holes and T1 Gad lesions; RNFLT and VF (2 years)	34	Recruiting	NCT02273635
Ibudilast in progressive MS (RCT Phase II)	Primary neuroprotection	I: Ibudilast (MN-166) C: Placebo	PPMS SPMS	Brain atrophy (3 years)	Several MRI outcomes; disability and QoL and RNFLT (3 years)	125	Recruiting	NCT01982942
Neuroprotection with riluzole in early RRMS (RCT Phase II)	Primary neuroprotection	I: Riluzole + interferon beta-1a i.m. C: Placebo + interferon beta-1a i.m.	CIS Early RRMS	Brain atrophy (2 years)	Neurological disability; change in NWMV and NGMV and change in RNFLT (2 years)	43 (total)	Complete No effect	NCT00501943

(continued)

Table 12.2 (continued)

Trial (phase)	Goal	Drug	Indication	Primary outcome	Secondary outcomes	Sample per arm	Status	Ref/NCT
ACTiMuS (RCT Phase II)	Immunomodulation Myelin repair Secondary neuroprotection	I: Early infusion C: Late infusion (Autologous bone marrow therapy)	PPMS SPMS	Global evoked potential (2 years)	Disability measures brain and spinal cord atrophy and lesion load; RNFLT and MV (2 years)	40	Recruiting	NCT01815632
OCT and BIIB017 in RRMS (RCT Phase III)	Immunomodulation Secondary neuroprotection	I: PEGylated interferon beta-1a (BIIB017) C: Placebo	RRMS	% of patients with ↓RNFL $\geq 5 \mu\text{m}$ (2 years)	Other OCT outcomes and different time points (2 years)	–	Withdrawn (Prior to enrollment)	NCT01337427
Tysabri effects on cognition neurodegeneration in MS (NRCT)	Immunomodulation Secondary neuroprotection	I: Natalizumab (MS <2y) I: Natalizumab (MS >2y)	RRMS	Cognition; RNFLT and MRI markers of cognitive dysfunction (2 years)	Not provided	10	Recruiting	NCT01071512
MSCIMS (NRCT Phase I/IIA)	Immunomodulation Secondary neuroprotection	I: Mesenchymal stem cells No control arm	SPMS	Safety (AE-SAE) (13 months)	VA and color; neurological disability; VEP and RNFLT MSON and brain MTR; T1 lesions (13 months)	10	Complete Benefit in VA, VEP No SAE	NCT00395200
CMM-EM (RCT Phase II)	Immunomodulation Secondary neuroprotection	I: Mesenchymal stem cells C: Placebo (Crossover: 6 + 6 months)	RRMS SPMS PPMS	Safety (AE-SAE) Efficacy (new T1Gad+) (12 months)	Neurological disability + QoL MRI outcomes and RNFLT Immunological analysis	9	Complete Benefit in Gad+ No SAE	NCT01228266

I intervention, C control, RCT randomized clinical trial, NRCT non-randomized clinical trial, MS multiple sclerosis, CIS clinically isolated syndrome, RRMS relapsing-remitting multiple sclerosis, SPMS secondary progressive MS, PPMS primary progressive MS, ON optic neuritis, OCT optical coherence tomography, RNFLT retinal nerve fiber layer thickness, MV macular volume, MRI magnetic resonance imaging, NWMV normalized white matter volume, MTR magnetization transfer ratio, VEP visual evoked potentials, VA visual acuity, VF visual field, QoL quality of life, AE adverse effects, SAE serious adverse effects, Ref reference, NCT ClinicalTrials.gov, NA not applicable

Alpha error, statistical power, and size effect were not available for these studies

controlled trials of acute neuroprotection in optic neuritis [16]. Taking into account the comparison of the affected eye follow-up, adjusted for baseline fellow eye RNFL thickness and with 6-month duration, 80 % power, and 30 and 50 % treatment effects, sample sizes were 97 (95 % CI 54,197) and 35 (95 % CI 20, 71). The study design with no adjustment for fellow eye values would be less powerful since a mean of 159 (95 % CI not shown) and 58 (95 % CI not shown) patients per arm would be needed considering equal settings [16]. In 2013, Kupersmith and colleagues found that RNFL loss at 1 month was predictive of the RNFL thinning at 6 months. These results highlighted the importance of the 1-month time point for predicting the outcome after acute MSON [17].

Randomized Clinical Trials Addressing Neuroprotection by Using RNFL Thinning

Considering the aforementioned studies, a number of randomized clinical trials (RCTs) were set up to evaluate molecules with primary or secondary neuroprotective effects in acute MSON by using RNFL thinning as the primary outcome (Table 12.1). Most of these studies are phase II RCT with an average duration of 6 months. These studies require small sample sizes (23–63 participants per arm) for an estimated effect size between 45 and 50 %.

The first RCT that has been published is the *VISION PROTECT* RCT with erythropoietin (EPO) [34]. This study found that patients treated with EPO as add-on therapy to methylprednisolone had lower RNFL thinning after 4 months than those treated only with methylprednisolone. High-contrast visual acuity (HCVA) after the trial was better for those allocated to the interventional arm compared to controls, although the difference was not statistically significant [34]. They used HCVA instead of low-contrast visual acuity (LCVA), which is more effective at capturing visual dysfunction after acute MSON. As such, the use of HCVA instead of LCVA charts may have underestimated this clinical benefit.

The neuroprotection with phenytoin in MSON study found that the average adjusted affected eye RNFL thickness was 7.15 μm higher in the phenytoin group than the placebo group in intention-to-treat analysis, a 30 % protective treatment effect but with no significant between-group difference in visual outcomes [36].

Phase 2 RENEW study of anti-LINGO-1 in acute MSON has shown improved latency recovery by using FF-VEP. However, groups did not differ in RNFL thinning at the end of follow-up [5].

New Findings: Early Retinal Ganglion Cell Layer Atrophy Is Clinically Relevant in AON

In 2011, segmentation of different retinal layers appeared on the scene, and this technological development revealed the importance of GCL thinning after AON [11]. These authors also proposed sample sizes for hypothetical 6-month clinical trials of neuroprotection in acute MSON using percent reduction of the observed mean change in retinal ganglion cell layer+ inner plexiform layer (GCIP) from baseline to 6 months as the outcome instead of RNFL thinning [11]. A neuroprotective agent that would reduce the observed thinning by 40 % would require 68 participants per arm at 80 % power, whereas a drug that would reduce the damage by 50 % would need only 44 subjects per group [11].

More recently, findings from our cohort in Barcelona supported this early retinal atrophy [37]. Our findings suggested that macular RNFL and GCIP thickness decreased in parallel, yet atrophy always occurred more rapidly and more severely for the GCIP complex [37]. These results along with the presence of peripapillary RNFL swelling during the first few months after acute MSON (which prevented an accurate measurement of RNFL loss during this period), prompted the use of GCIP thickness as the primary outcome of neuroprotection instead of RNFL thickness.

However, retinal neuroprotection is only important if it involves clinical benefits. Structural changes are more relevant if accompanied by meaningful clinical outcomes. For this reason, in

the Barcelona cohort, we evaluated the role of the GCIP thinning in ON-eyes during the first month after acute MSON to predict visual impairment at 6 months. We found that GCIP thinning $\geq 4.5 \mu\text{m}$ (6.5 %) predicted poor 2.5 % LCVA and 1.25 % LCVA recovery (defined as inter-eye asymmetry >7 letters) with a sensitivity of 92 % and 93 % and a specificity of 70 % and 88 %, respectively. Moreover, a decrease $\geq 7 \mu\text{m}$ (10 %) in RGC+IPL complex thickness predicted poor VF (MD ≤ -3.00 dB) and color vision (HRR <35) recovery with a sensitivity of 93 % and 100 %, respectively, and specificity of 88 % and 66 %, respectively. We did not find any association with HCVA [37].

Retinal Ganglion Cells and Low-Contrast Visual Acuity: The Best Partners for AON Trials

HCVA measures were successfully used to evaluate visual recovery after acute MSON [38]. However, LCVA has several advantages. First, LCVA is more sensitive and is therefore better at demonstrating visual dysfunction [37, 39, 40]. Second, low-contrast vision correlates with health-related quality of life better than high-contrast vision [41, 42]. LCVA measures are more informative and indicative of the ability of patients to perform daily visual tasks since they capture visual disability rather than visual impairment. Finally, low-contrast vision testing has the capacity to reveal treatment effects [43, 44].

For the design of clinical trials in acute MSON, we propose LCVA as the most sensitive clinical endpoint. Thus, using data from our cohort, we performed sample size estimations to design RCT aimed at preventing retinal atrophy based on GCIP thinning in the MSON-eye during the first month after attack, with an alpha error of 0.05 and beta error of 0.20 (80 % statistical power). Because our model indicates that a GCIP thinning $\geq 4.5 \mu\text{m}$ implies a high probability of visual dysfunction (LCVA) at month 6, we defined our endpoint and optimal power as a decrease in the GCIP thickness $<4.5 \mu\text{m}$. We found that 25 patients with acute MSON per group will have sufficient power

to detect differences between the groups using GCIP thickness as the outcome [37, 40].

Strengths of the Acute Optic Neuritis Model for Evaluating Neurodegeneration in RCT

Addressing neuroprotective effects of drugs in RCTs using acute MSON as an acute model of damage in MS has some advantages. Table 12.3 summarizes these strengths. First, there is strong evidence that OCT can track dynamic changes in the retina after an acute episode of acute MSON [11, 13, 16, 17, 37, 40]. Considering the bulk of the data, we suggest that OCT should be acquired monthly (or even weekly during the first weeks) during the first 3 months and thereafter at 6 months. Second, AON is a dynamic model with remarkable changes in a short period of time. Studies have shown an average RNFL thinning of 20 % relative to unaffected eyes and a mean GCIP thickness decrease of 12–16 % in affected eyes within 6 months [11, 13, 16, 37, 40].

Third, brain atrophy is the most commonly used endpoint in RCT for addressing neuroprotective effects in MS. Yet OCT has some technical advantages compared to MRI since its acquisition is easier, faster, and more cost-efficient. Moreover, OCT needs no image processing except for segmentation, which is completely automatized by OCT software. On the contrary, MRI brain atrophy as an outcome requires image processing to be estimated. More importantly, MRI-based methods available to measure brain volumes usually require lesion segmentation masks to avoid pixel misclassification, which are usually done manually or require correction after running segmentation software (semiautomatically). Fourth, OCT also has biological advantages since it measures neurodegeneration more specifically than MRI brain atrophy, which includes neuroaxonal damage but also myelin loss and astrogliosis. The retina lacks myelin and GCIP thickness might only be slightly affected by astrogliosis.

Finally, acute MSON constitutes a good functional-structural paradigm, and this has favored defining milestones for clinical conse-

Table 12.3 Strengths and challenges of acute optic neuritis model to evaluate neurodegeneration in RCTs

Strengths	Challenges	
	Limit	Proposed solution
Expertise to track retinal atrophy after acute MSON with OCT	Low incidence rate	Collaborative multicenter initiatives
Acute MSON is dynamic model with remarkable changes in OCT across 6 months	Time from clinical onset to baseline is variable and frequently too long	Develop truly integrated neuro-ophthalmology units to facilitate recruitment in RCT
Small sample sizes and short follow-up (Decrease cost of RCT)	Methylprednisolone therapy in AON is variable	Use methylprednisolone for all participants Big data approach for effectiveness
OCT is easier, faster, and more cost-efficient than MRI. No image processing	Differences in devices, acquisition and segmentation algorithms, and scan qualities add variability and reduce accuracy of outcomes	A multi-platform segmentation algorithm in a reading center
Retinal atrophy by OCT is more specific as neurodegeneration outcome than MRI	Some limitations to discriminate pathologic mechanisms (inner nuclear layer paradigm)	A molecular retinal imaging device such as Raman spectroscopy coupled to structural imaging device
Good functional-structural paradigm with thresholds for clinical consequences	Neurodegenerative biochemical pathway may differ from an acute lesion and chronic and diffuse damage	A molecular retinal imaging photonic device discriminates biochemical pathways

Acute MSON acute multiple sclerosis associated optic neuritis, *OCT* optical coherence tomography, *RCT* randomized clinical trials, *MRI* magnetic resonance imaging

quences, including a minimum of 75 μm of peripapillary RNFL thickness to avoid visual field abnormalities [13] and more recently 4.5 μm of GCIP thinning to avoid poor low-contrast vision recovery [37, 40]. These thresholds are key points to evaluate the efficacy of neuroprotection drugs, not only considering structural changes but, more importantly, functional consequences in the patients' daily life.

Challenges of the Acute MSON Model to Evaluate Neurodegeneration in RCT

Evaluating neuroprotection in RCT using acute MSON as a lesion model with OCT as the outcome also has clinico-epidemiological, technical, and biological challenges. Table 12.3 summarizes these challenges and provides solutions to overcome these limitations.

Regarding clinico-epidemiological challenges, first, we should notice that the incidence rate of acute MSON ranges between 0.56 and 5.1 cases per 100,000 person-years. A recent study setting

in Barcelona from 2008 to 2012 found that the mean annual incidence rate in acute MSON was 5.36 cases per 100,000 person-years [45]. This study suggested that the incidence of acute MSON is rising in Europe; however, it still can be considered as a rare disease. This may be a limitation for the recruitment phase in RCT and supports calls for collaborative initiatives to ensure a large enough sample size.

Even though acute MSON is clinically eloquent, time from clinical onset to baseline OCT and visual testing in cohort studies ranges from an average of 6.4 days (SD: 4.0) in the acute MSON study from Kupersmith and colleagues [46] to a median 16 days in the study from Henderson and colleagues [16]. Other researchers included participants that completed baseline OCT and visual testing within 28 days of acute MSON onset but did not give an average period between onset and baseline visit [11]. Mean (SD) time from acute MSON symptom onset to the first visit (including first dose of anti-LINGO mAb) was 24 days (SD: 3.7) in the *RENEW trial* [47]. This is because this trial decided that study treatment could be initiated within 28 days after

acute MSON onset. Therefore, the time period from onset to baseline visit display varies widely across different studies, and this may hamper comparison of drug efficacy across different molecules and RCT designs. Moreover, taking into account that GCL atrophy appeared as early as the first week after inclusion in a subsample of patients (n: 7) in our Barcelona cohort that was evaluated weekly in the first month (data not show) and that neuroprotective drugs should be administered early to exert their effects, a shorter time period is preferable. For this reason, it may be necessary to develop truly integrated neuro-ophthalmology units to facilitate the quick identification of candidates to RCT.

In 2012, the Cochrane Collaboration initiative stated that randomized trials did not support a conclusive benefit from corticosteroids in terms of vision recovery after acute MSON [48]. However, the lack of evidence does not mean lack of effect, and consequently corticosteroids are often used for moderate to severe acute MSON in clinical practice. They are supposed to shorten symptoms, although it is not possible to rule this as a true secondary neuroprotective effect due to their anti-inflammatory activity. For this reason, some trials have included the condition that all patients should be treated with corticosteroids [34, 47]. Considering the relatively low risk of short-term side effects after methylprednisolone in normal conditions [49], this approach may be appropriate. This may reduce the inclusion of milder forms in RCTs, which would be a limitation for the external validation of results. Nevertheless, participants included in RCTs often differ in some way from those attended to in the clinical setting. Therefore, effectiveness is frequently lower than efficacy. A big data focus on electronic medical record approach will fill this scientific gap [50] (see Chap. 3) for in detail description.

Nowadays, most OCT evaluations are performed using the spectral domain OCT: Cirrus® (Carl Zeiss Meditec) or Spectralis® (Heidelberg Engineering). Both devices have confirmed adequate reproducibility [51] but results are not comparable. OCT acquisitions in MS and acute MSON usually include RNFL thickness and macular volume (MV). Cirrus® includes standard acquisition protocols for RNFL (optic disk

200 × 200) and MV (macular cube 518 × 128). However, Spectralis® allows for manual setting of different parameters (grid size, ART). This confers more flexibility to amend the protocol to specific research objectives but also leads to greater variability in outcomes. Differences in segmentation algorithms from these two devices also add variability. Finally, quality of OCT may differ between explorers and centers. The OSCAR-IB Consensus Criteria for Retinal OCT Quality Assessment was a nice attempt to solve this limitation, but it was designed only for RNFL thickness in cross-sectional studies. Thus, differences in devices, acquisition protocols, segmentation algorithms, and scan qualities add variability and reduce accuracy of retinal layer thickness assessment in a multicenter setting. Variability from devices cannot be completely eliminated, but setting a consensus Spectralis® acquisition protocol similar to Cirrus (e.g., setting 6 mm ETDRS grid instead of 3 mm or 3.45 mm) will facilitate comparisons between outcomes. However, segmentation of bigger grids may have lower reliability than 3 mm. Nevertheless, in order to reduce variability, a critical step will be the assessment of OCT scans with a multi-platform segmentation algorithm in a reading center. This will be further explored in the next chapter of this book (see Chap. 10).

Finally, OCT provides a good in vivo structural retinal image. To that end, OCT has consistently revealed GCL thinning to be neurodegenerative damage after acute MSON. However, *inner nuclear layer* thickening in OCT scans has been associated with inflammatory activity of the disease in some studies [52], whereas others have suggested that this phenotype along with the presence of *microcystic macular edema* (a pathologically related finding) may represent a neurodegenerative change of the retina [53]. This is a technological limitation of OCT as a structural photonic device. However, a molecular retinal imaging photonic device may better and earlier discriminate these mechanisms since functional changes usually appear in an early phase of disease, a key period for neuroprotective drugs.

Lastly, neurodegenerative processes due to an acute inflammatory lesion model, such as acute MSON, may not resemble biochemical

neuroaxonal changes due to chronic and diffuse neuroinflammation in MS. Thus, if the biochemical cascade leading to neurodegeneration is not similar or has a common pathway for both acute and chronic processes, the approved drugs with a favorable neuroprotective profile for acute injury will not be really effective for chronic neurodegeneration. Additionally, it would be barely detectable since both retinal and brain atrophies develop slowly in MS. Here again, molecular imaging would be helpful since it addresses metabolic changes associated with biological processes.

Proposed Design for Evaluating Acute Neuroprotection by Means of acute MSON and OCT

Considering the aforementioned results and discussion, Fig. 12.1 displays the proposed design

for an RCT using acute MSON as a lesion model and OCT as the primary outcome. In the Barcelona cohort, we estimated that 25 participants would be enough for a drug that ensures that the GCIP thinning was $<4.5 \mu\text{m}$ in the first month. This is the biological threshold to avoid visual dysfunction (LCVA) at month 6. Assuming a dropout rate of 20 %, we proposed that 30 participants per arm would be enough to evaluate the neuroprotective effect of a drug in a placebo-controlled trial with a 6-month duration, 80 % power, and alpha error equal to 0.05.

Participants should be diagnosed as having unilateral idiopathic acute MSON or CIS (clinically isolated syndrome) or RRMS (relapsing-remitting MS) newly diagnosed based on the acute MSON episode and MRI findings (dissemination in time and/or space). Participants with a prior episode in the same eye should be excluded since retinal atrophy may not be comparable to naive patients.

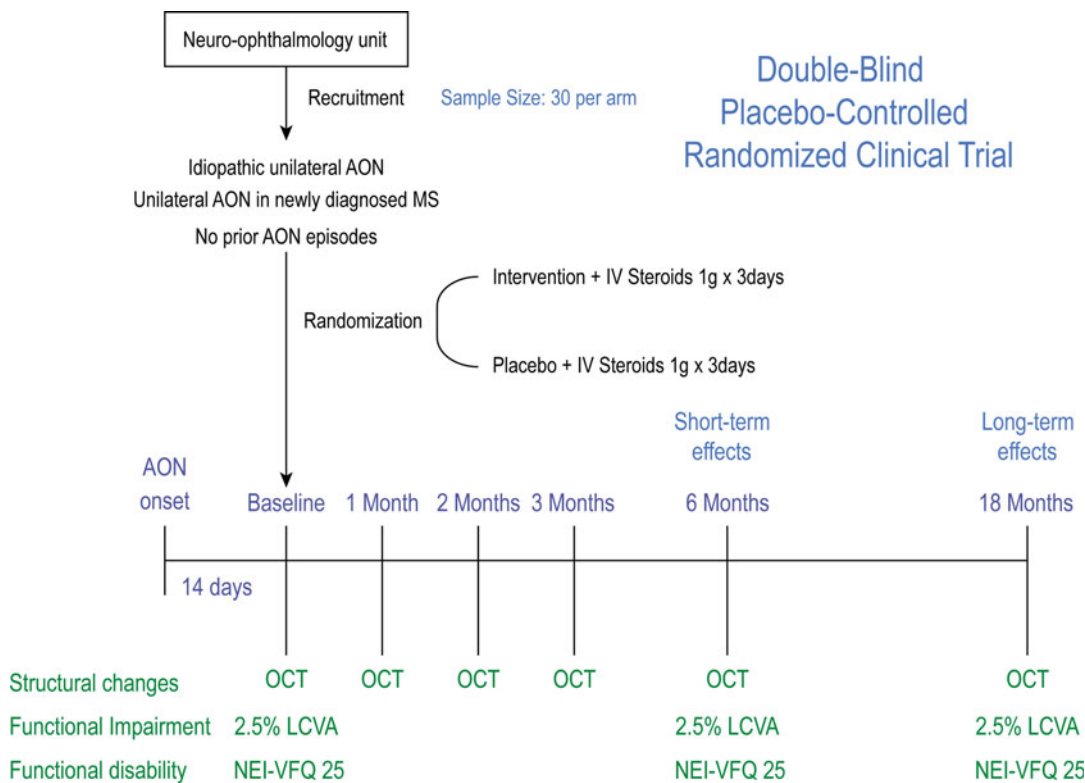


Fig. 12.1 Proposed design for a double-blind placebo-controlled randomized clinical trial. *AON* acute optic neuritis, *MS* multiple sclerosis, *IV* intravenous, *OCT* optical

coherence tomography, *LCVA* low-contrast visual acuity, *NEI-VFQ-25* National Eye Institute Visual Function Questionnaire 25 items

Acute MSON should be diagnosed clinically by the presence of classic symptoms and signs defined in the ONTT [54]. Time between acute MSON onset and baseline visit should be shorter than 28 days. We propose a time period inferior to 14 days similar to those described in different cohort studies [16, 37, 40, 46].

Neurodegenerative structural retinal changes should be monitored by OCT with RNFL and macular acquisitions. We propose to include monocular low-contrast vision by 2.5 % Sloan charts and NEI-VFQ-25 (National Eye Institute Visual Function Questionnaire 25 items) to measure visual impairment and disability, respectively. Other tests such color vision or visual mfVEP may be added to further evaluate neuroprotection.

We suggest performing evaluations at baseline and thereafter at 6 months and 18 months to capture short-term and long-term neuroprotective effects. We have also added OCT performance at the first, second, and third months to track structural changes that, considering previous findings [16, 37, 40, 46], are expected to occur within the first 3 months after acute MSON.

Conclusion and Future Directions

Technological development of photonic-based devices such as OCT has provided a new window into the MS brain. Acute MSON resembles an acute lesion model in MS, and retinal neurodegeneration after acute MSON can be monitored by OCT. Thus, a number of molecules with potentially neuroprotective effects are currently under evaluation by using OCT after acute MSON in RCT with relatively low samples and follow-up. As such, acute MSON and OCT are good partners for drug trials for neuroprotection. However, a collaborative initiative to favor recruitment, a consensus design in RCT, reading centers for OCT, and new technological advances in functional imaging are needed to overcome the clinico-epidemiological, technical, and biological shortcomings of this model.

References

1. Compston A, Coles A. Multiple sclerosis. *Lancet*. 2008;372(9648):1502–17.
2. Tallantyre EC, Bo L, Al-Rawashdeh O, Owens T, Polman CH, Lowe JS, et al. Clinico-pathological evidence that axonal loss underlies disability in progressive multiple sclerosis. *Mult Scler (Houndmills, Basingstoke, England)*. 2010;16(4):406–11.
3. Fazekas F, Soelberg-Sorensen P, Comi G, Filippi M. MRI to monitor treatment efficacy in multiple sclerosis. *J Neuroimaging*. 2007;17 Suppl 1:50S–5.
4. Yang EB, Hood DC, Rodarte C, Zhang X, Odel JG, Behrens MM. Improvement in conduction velocity after optic neuritis measured with the multifocal VEP. *Invest Ophthalmol Vis Sci*. 2007;48(2):692–8.
5. Cadavid D BL, Galetta S, Aktas O, Ziemssen T, Vanopdenbosch L, et al., for the RENEW Study Investigators, editor. Efficacy analysis of the anti-lingo-1 monoclonal antibody biib033 in acute optic neuritis: the renew trial (p7.202). Poster session vii: MS and CNS inflammatory diseases: clinical trials. Washington, DC: American Academy of Neurology; 2015.
6. De Stefano N, Airas L, Grigoriadis N, Mattle HP, O’Riordan J, Oreja-Guevara C, et al. Clinical relevance of brain volume measures in multiple sclerosis. *CNS Drugs*. 2014;28(2):147–56.
7. Jacobsen C, Hagemeyer J, Myhr KM, Nyland H, Lode K, Bergsland N, et al. Brain atrophy and disability progression in multiple sclerosis patients: a 10-year follow-up study. *J Neurol Neurosurg Psychiatry*. 2014;85(10):1109–15.
8. Summers M, Fisniku L, Anderson V, Miller D, Cipelotti L, Ron M. Cognitive impairment in relapsing-remitting multiple sclerosis can be predicted by imaging performed several years earlier. *Mult Scler (Houndmills, Basingstoke, England)*. 2008;14(2):197–204.
9. Parisi V, Manni G, Spadaro M, Colacino G, Restuccia R, Marchi S, et al. Correlation between morphological and functional retinal impairment in multiple sclerosis patients. *Invest Ophthalmol Vis Sci*. 1999; 40(11):2520–7.
10. Petzold A, de Boer JF, Schippling S, Vermersch P, Kardon R, Green A, et al. Optical coherence tomography in multiple sclerosis: a systematic review and meta-analysis. *Lancet Neurol*. 2010;9(9):921–32.
11. Syc SB, Saidha S, Newsome SD, Ratchford JN, Levy M, Ford E, et al. Optical coherence tomography segmentation reveals ganglion cell layer pathology after optic neuritis. *Brain*. 2012;135(Pt 2):521–33.
12. Saidha S, Syc SB, Ibrahim MA, Eckstein C, Warner CV, Farrell SK, et al. Primary retinal pathology in multiple sclerosis as detected by optical coherence tomography. *Brain*. 2011;134(Pt 2):518–33.
13. Costello F, Coupland S, Hodge W, Lorello GR, Koroluk J, Pan YI, et al. Quantifying axonal loss after

- optic neuritis with optical coherence tomography. *Ann Neurol*. 2006;59(6):963–9.
14. Noval S, Contreras I, Rebolledo G, Munoz-Negrete FJ. Optical coherence tomography versus automated perimetry for follow-up of optic neuritis. *Acta Ophthalmol Scand*. 2006;84(6):790–4.
 15. Costello F, Hodge W, Pan YI, Eggenberger E, Coupland S, Kardon RH. Tracking retinal nerve fiber layer loss after optic neuritis: a prospective study using optical coherence tomography. *Mult Scler (Houndmills, Basingstoke, England)*. 2008;14(7):893–905.
 16. Henderson AP, Altmann DR, Trip AS, Kallis C, Jones SJ, Schlottmann PG, et al. A serial study of retinal changes following optic neuritis with sample size estimates for acute neuroprotection trials. *Brain*. 2010;133(9):2592–602.
 17. Kupersmith MJ, Anderson S, Kardon R. Predictive value of 1 month retinal nerve fiber layer thinning for deficits at 6 months after acute optic neuritis. *Mult Scler (Houndmills, Basingstoke, England)*. 2013;19(13):1743–8.
 18. Costello F, Hodge W, Pan YI, Eggenberger E, Freedman MS. Using retinal architecture to help characterize multiple sclerosis patients. *Can J Ophthalmol*. 2010;45(5):520–6.
 19. Green AJ, McQuaid S, Hauser SL, Allen IV, Lyness R. Ocular pathology in multiple sclerosis: retinal atrophy and inflammation irrespective of disease duration. *Brain*. 2010;133(Pt 6):1591–601.
 20. Saidha S, Syc SB, Durbin MK, Eckstein C, Oakley JD, Meyer SA, et al. Visual dysfunction in multiple sclerosis correlates better with optical coherence tomography derived estimates of macular ganglion cell layer thickness than peripapillary retinal nerve fiber layer thickness. *Mult Scler (Houndmills, Basingstoke, England)*. 2011;17(12):1449–63.
 21. Walter SD, Ishikawa H, Galetta KM, Sakai RE, Feller DJ, Henderson SB, et al. Ganglion cell loss in relation to visual disability in multiple sclerosis. *Ophthalmology*. 2012;119(6):1250–7.
 22. Forooghian F, Sproule M, Westall C, Gordon L, Jirawuthiworavong G, Shimazaki K, et al. Electroretinographic abnormalities in multiple sclerosis: Possible role for retinal autoantibodies. *Doc Ophthalmol*. 2006;113(2):123–32.
 23. Heide AC, Kraft GH, Slimp JC, Gardner JC, Posse S, Serafini S, et al. Cerebral n-acetylaspartate is low in patients with multiple sclerosis and abnormal visual evoked potentials. *AJNR Am J Neuroradiol*. 1998;19(6):1047–54.
 24. Rocca MA, Mesaros S, Preziosa P, Pagani E, Stosic-Opincal T, Dujmovic-Basuroski I, et al. Wallerian and trans-synaptic degeneration contribute to optic radiation damage in multiple sclerosis: A diffusion tensor MRI study. *Mult Scler (Houndmills, Basingstoke, England)*. 2013;19(12):1610–7.
 25. Gabilondo I, Martínez-Lapiscina EH, Martínez-Heras E, Fraga-Pumar E, Llufríu S, Ortiz S, et al. Trans-synaptic axonal degeneration in the visual pathway in multiple sclerosis. *Ann Neurol*. 2014;75(1):98–107.
 26. Balk LJ, Steenwijk MD, Tewarie P, Daams M, Killestein J, Wattjes MP, et al. Bidirectional trans-synaptic axonal degeneration in the visual pathway in multiple sclerosis. *J Neurol Neurosurg Psychiatry*. 2014;27.
 27. Sepulcre J, Murie-Fernandez M, Salinas-Alaman A, Garcia-Layana A, Bejarano B, Villoslada P. Diagnostic accuracy of retinal abnormalities in predicting disease activity in ms. *Neurology*. 2007;68(18):1488–94.
 28. Toledo J, Sepulcre J, Salinas-Alaman A, Garcia-Layana A, Murie-Fernandez M, Bejarano B, et al. Retinal nerve fiber layer atrophy is associated with physical and cognitive disability in multiple sclerosis. *Mult Scler (Houndmills, Basingstoke, England)*. 2008;14(7):906–12.
 29. Talman LS, Bisker ER, Sackel DJ, Long Jr DA, Galetta KM, Ratchford JN, et al. Longitudinal study of vision and retinal nerve fiber layer thickness in multiple sclerosis. *Ann Neurol*. 2010;67(6):749–60.
 30. Grazioli E, Zivadinov R, Weinstock-Guttman B, Lincoff N, Baier M, Wong JR, et al. Retinal nerve fiber layer thickness is associated with brain MRI outcomes in multiple sclerosis. *J Neurol Sci*. 2008;268(1–2):12–7.
 31. Siger M, Dziegielewska K, Jasek L, Bieniek M, Nicpan A, Nawrocki J, et al. Optical coherence tomography in multiple sclerosis: thickness of the retinal nerve fiber layer as a potential measure of axonal loss and brain atrophy. *J Neurol*. 2008;255(10):1555–60.
 32. Saidha S, Sotirchos ES, Oh J, Syc SB, Seigo MA, Shiee N, et al. Relationships between retinal axonal and neuronal measures and global central nervous system pathology in multiple sclerosis. *JAMA Neurol*. 2013;70(1):34–43.
 33. Garcia-Martin E, Polo V, Larrosa JM, Marques ML, Herrero R, Martin J, et al. Retinal layer segmentation in patients with multiple sclerosis using spectral domain optical coherence tomography. *Ophthalmology*. 2014;121(2):573–9.
 34. Suhs KW, Hein K, Sattler MB, Gorlitz A, Ciupka C, Scholz K, et al. A randomized, double-blind, phase 2 study of erythropoietin in optic neuritis. *Ann Neurol*. 2012;72(2):199–210.
 35. Serbecic N, Aboul-Enein F, Beutelspacher SC, Vass C, Kristoferitsch W, Lassmann H, et al. High resolution spectral domain optical coherence tomography (SD-OCT) in multiple sclerosis: the first follow up study over two years. *PLoS One*. 2011;6(5), e19843.
 36. Kapoor R RR, Hickman S, Toosy A, Sharrack B, Mallik S, et al. Phenytoin is neuroprotective in acute optic neuritis: results of a phase 2 randomized controlled trial. Washington, DC: American Academy of Neurology; 2015.
 37. Martínez-Lapiscina EH, Fraga-Pumar E, Ortiz-Perez S, Torres-Torres R, Andorra M, Llufríu S, Zubizarreta I, Saiz A, Sanchez-Dalmau B, Villoslada P. Dynamics

- of retinal injury after acute optic neuritis. *Ann Neurol*. 2015;77(3):517–28.
38. Kupersmith MJ, Gal RL, Beck RW, Xing D, Miller N. Visual function at baseline and 1 month in acute optic neuritis: predictors of visual outcome. *Neurology*. 2007;69(6):508–14.
 39. Trobe JD, Beck RW, Moke PS, Cleary PA. Contrast sensitivity and other vision tests in the optic neuritis treatment trial. *Am J Ophthalmol*. 1996;121(5):547–53.
 40. Martínez-Lapiscina EH, Gabilondo I, Fraga-Pumar E, Ortiz-Perez S, Torres-Torres R, Andorrà M, et al. Retrograde axonal and neuronal degeneration of the retina in acute optic neuritis. *Mult Scler (Houndmills, Basingstoke, England)*. 2014;20:357.
 41. Mowry EM, Loguidice MJ, Daniels AB, Jacobs DA, Markowitz CE, Galetta SL, et al. Vision related quality of life in multiple sclerosis: correlation with new measures of low and high contrast letter acuity. *J Neurol Neurosurg Psychiatry*. 2009;80(7):767–72.
 42. Schinzel J, Zimmermann H, Paul F, Ruprecht K, Hahn K, Brandt AU, et al. Relations of low contrast visual acuity, quality of life and multiple sclerosis functional composite: a cross-sectional analysis. *BMC Neurol*. 2014;14(1):31.
 43. Balcer LJ, Galetta SL, Calabresi PA, Confavreux C, Giovannoni G, Havrdova E, et al. Natalizumab reduces visual loss in patients with relapsing multiple sclerosis. *Neurology*. 2007;68(16):1299–304.
 44. Graves J, Galetta SL, Palmer J, Margolin DH, Rizzo M, Bilbruck J, et al. Alemtuzumab improves contrast sensitivity in patients with relapsing-remitting multiple sclerosis. *Mult Scler (Houndmills, Basingstoke, England)*. 2013;19(10):1302–9.
 45. Martínez-Lapiscina EH, Fraga-Pumar E, Pastor X, Gomez M, Conesa A, Lozano-Rubi R, et al. Is the incidence of optic neuritis rising? Evidence from an epidemiological study in Barcelona (Spain), 2008–2012. *J Neurol*. 2014;261(4):759–67.
 46. Kupersmith MJ, Mandel G, Anderson S, Meltzer DE, Kardon R. Baseline, one and three month changes in the peripapillary retinal nerve fiber layer in acute optic neuritis: relation to baseline vision and MRI. *J Neurol Sci*. 2011;308(1–2):117–23.
 47. Cadavid D, Ziemssen F, Butzkueven H, Balcer LJ, Galetta SL, Rahilly A, et al. A phase ii study of the anti-lingo-1 monoclonal antibody, biib033, in subjects with acute optic neuritis: baseline data. *Mult Scler (Houndmills, Basingstoke, England)*. 2014;20(1 suppl):387–8.
 48. Gal RL, Vedula SS, Beck R. Corticosteroids for treating optic neuritis. *Cochrane Database Systematic Reviews*. 2012;4:CD001430.
 49. Lienert C, Schawalder G, Findling O, Kamm CP, Humpert S, Mugglin A, et al. Tolerance of intravenous methylprednisolone for relapse treatment in demyelinating CNS disease. *Swiss Med Wkly*. 2013;143, w13783.
 50. Hoffman S, Podgurski A. The use and misuse of biomedical data: is bigger really better? *Am J Law Med*. 2013;39(4):497–538.
 51. Pierro L, Gagliardi M, Iuliano L, Ambrosi A, Bandello F. Retinal nerve fiber layer thickness reproducibility using seven different OCT instruments. *Invest Ophthalmol Vis Sci*. 2012;53(9):5912–20.
 52. Saidha S, Sotirchos ES, Ibrahim MA, Crainiceanu CM, Gelfand JM, Sepah YJ, et al. Microcystic macular oedema, thickness of the inner nuclear layer of the retina, and disease characteristics in multiple sclerosis: a retrospective study. *Lancet Neurol*. 2012;11(11):963–72.
 53. Burggraaff MC, Trieu J, de Vries-Knoppert WA, Balk L, Petzold A. The clinical spectrum of microcystic macular edema. *Invest Ophthalmol Vis Sci*. 2014;55(2):952–61.
 54. Cleary PA, Beck RW, Anderson Jr MM, Kenny DJ, Backlund JY, Gilbert PR. Design, methods, and conduct of the optic neuritis treatment trial. *Control Clin Trials*. 1993;14(2):123–42.

Ferenc B. Sallo, James V.M. Hanson,
Sebastian Lukas, and Sebastian Wolf

What Is a Reading Center?

The optical coherence tomography (OCT) reading center (RC) is usually an institution that supports the sponsor and the investigational sites of a clinical study in the various aspects of OCT data acquisition, handling, and storage. Typically, such a study can be dissected into three major phases [1–7]: planning, execution, and end of study (EOS), as shown in Fig. 13.1. In the planning phase, the RC helps to establish an appropriate scan protocol, taking into account the needs of the sponsor, tech-

nical feasibility, and available devices. In addition, the RC may help to define the outcome measures with respect to the proposed imaging protocol.

During the execution phase, the RC supports several vital aspects of the study. It provides server infrastructure and a secure upload portal for the acquired data. Once the data acquisition and upload procedure is documented and provided to the participating sites, it supports the investigator with dedicated training on the image acquisition as required, via learning materials, teleconferencing, or on-site training. Operators usually need to undergo a certification procedure, in order to ensure that they understand the scan protocol and are capable of acquiring images of sufficient quality. Typically, as part of the certification process, a healthy volunteer (e.g., a coworker at the study site) is scanned (in longitudinal studies, two consecutive certification scans may be used in order to assess repeatability) and the data uploaded to the RC server for assessment. The RC performs a full quality check (QC) on the data and, if the scan is of sufficient quality, issues a certificate showing that the operator is allowed to scan patients as part of the study. Certification is specific to the member of staff in question and does not cover other workers at the same center. If an operator submits a scan of insufficient quality, the certification procedure must be repeated until successful. Operators may only scan patients in the study after being certified.

F.B. Sallo, MD, PhD (✉)

NIHR Biomedical Research Center for
Ophthalmology of Moorfields Eye Hospital and the
UCL Institute of Ophthalmology, London, UK
e-mail: ferenc.sallo@ Moorfields.nhs.uk

J.V.M. Hanson, PhD

Department of Neurology, Neuroimmunology and
Multiple Sclerosis Research and Neuro-OCT Reading
Centre Zurich, University Hospital Zurich and
University of Zurich, Zurich, Switzerland

Department of Ophthalmology, University Hospital
Zurich, Zurich, Switzerland

S. Lukas, Dipl. Ing. (FH)

Department of Neurology, Neuroimmunology and
Multiple Sclerosis Research and Neuro-OCT Reading
Centre Zurich, University Hospital Zurich and
University of Zurich,
Zurich, Switzerland

S. Wolf

Department of Ophthalmology, Inselspital,
University Hospital Bern, Bern, Switzerland

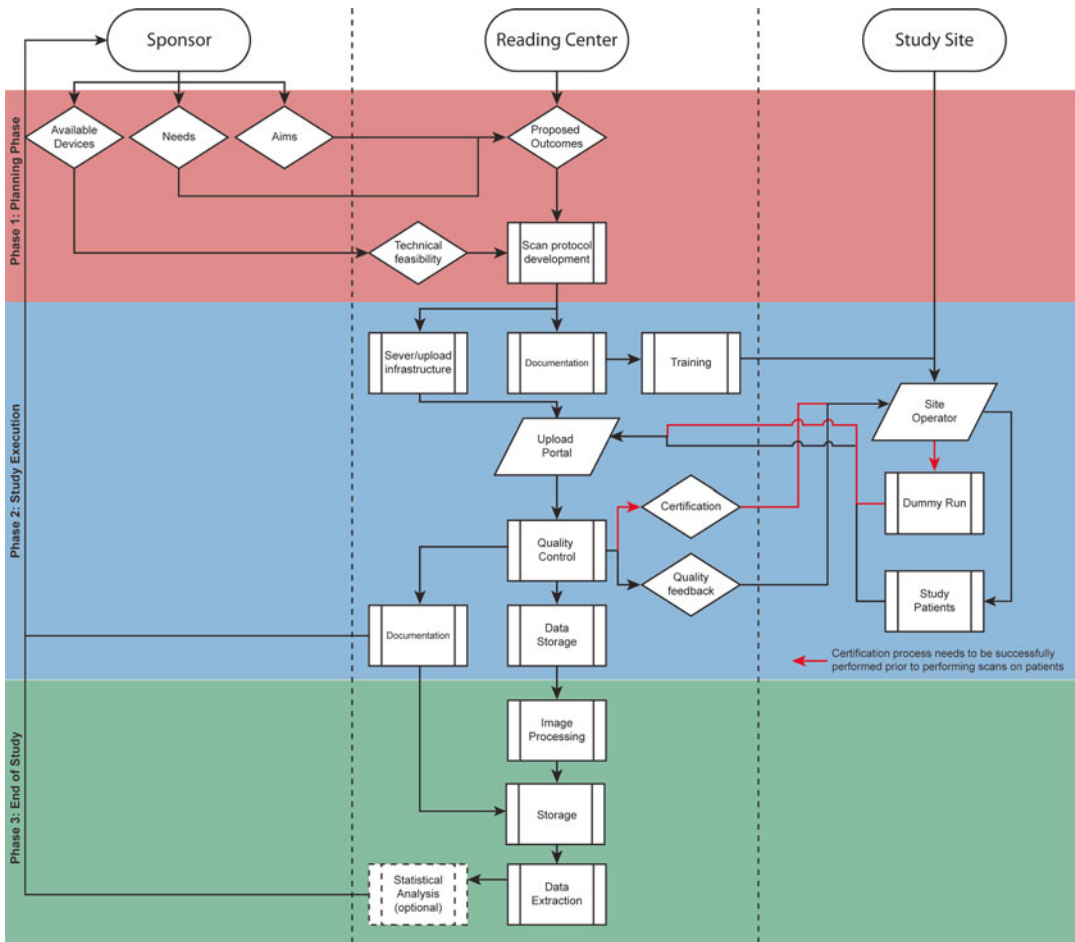


Fig. 13.1 Flowchart showing the three major phases of a study and the involvement of the RC in each of these phases

The procedure to be followed with patients is similar to that during certification, with the operator performing the scans and then uploading the data to the RC and the data being accepted or rejected following QC. If a scan performed on a patient is rejected, it is highly desirable to provide feedback to the operator, listing the grounds for rejection. The sponsor and/or study administrators (if applicable) should also be informed of any rejected scans. If the scan is accepted, the data is stored for subsequent analysis.

The third phase is typically time consuming and work intensive for the RC. At EOS, the complete set of images received during the study must undergo post-processing (e.g., segmentation of multiple retinal layers). The required outcome

measures for each patient are listed on a worksheet and may then be forwarded to the sponsor for statistical analysis or, alternatively, analyzed at the RC.

Challenges of Image Analysis

Image analysis and quantification should ideally be free from systematic errors (accurate) and random errors (precise) and should yield the same results if performed multiple times (repeatable). Since these tasks are performed by human analysts (“graders”), errors are inevitable but must be managed and should be minimized. While random errors are limited in scope and relatively

easy to control, systematic effects/errors (“bias”) may lead to misleading results. Bias may be caused by a multitude of factors.

Sources of Bias

In order to be clinically efficient, medical professionals are trained to collect and synthesize information about a patient from many sources “on the fly” from the very first glance at the patient, noting their posture, movements, fixation, speed and ability to navigate, and general appearance even before performing a full (ophthalmic) examination (from the lids all the way back to the retina). The sum of these observations will steer the clinician’s attention toward potential diagnoses and prompt them to perform specific further tests of structure (imaging) and function (e.g., perimetry, electrophysiology). While this approach is essential in the clinical setting, it may be a source of bias and thus out of place in the context of systematic image analysis. If image analysis is performed by persons with access to clinical information, their interpretation may be influenced by factors other than the data shown in the images (clinical bias). Bias may also be introduced by differences in training or personal opinions at different sites within multicenter studies. It is also part of human nature that investigators with a vested interest—academic, personal, or other (including financial)—may be biased, either unconsciously or consciously, toward a certain outcome of a study. To attain and maintain precision, accuracy, and repeatability over time and between graders, and in order to minimize bias, image analysis requires objectivity and clearly set criteria.

Advantages of Using a Dedicated Reading Center

RCs aim—through their organizational structure and procedures—to eliminate bias in data assessment while still utilizing the unparalleled pattern recognition abilities of the human brain, as well as computerized analysis tools that make grading

easier and quicker. RCs as organizations are independent. Their quality hallmarks are precision, accuracy, repeatability, reliability, and, above all, objectivity, irrespective of the actual findings or final outcome of any specific study. Images are analyzed according to predefined criteria and procedures by consistently trained graders, who only report to the RC and must not have any vested interest of any kind in any specific study they are involved in. Graders are trained to grade only what they can actually see in the specific image being graded. No clinical inferences are made at the point of grading, and graders are completely masked to clinical information, other graders’ data, and typically even their own grading data from previous scans. Graders are geared toward high-quality, rather than high-speed, image analysis. Predefined grading procedures include strategies for quality assurance (multiple primary graders, adjudication by expert clinicians, regular assessment of inter- and intra-grader variability) and also ensure compliance with regulatory standards [8, 9].

Roles of a Reading Center

Study Development

Ideally, the role of an RC begins long before study initiation. RCs can collaborate with the research group or sponsor in developing a study protocol. Once a research question has been formulated and a structural characteristic (or “sign”) of interest identified, appropriate outcome measures need to be found. RCs can help assess which imaging modality is likely to best reflect the structure in question and which equipment and imaging/scan parameters may be suitable in terms of sensitivity, specificity, and repeatability while remaining practically feasible in terms of patient and operator acceptance. For example, high-density raster volume scans may be superior to circular scans in terms of data consistency; however, in patients with neurological disorders and in the presence of tremor, nystagmus, etc., these may not be practicably attainable. RCs can also help develop a grading system, selecting

which morphological descriptors to quantify on which scale (continuous, interval, or categorical). Descriptors may include a wide range of morphological characteristics, including 2D/3D size (diameter, thickness, area, volume), shape (e.g., convexity, roundness), signal intensity, structure, texture, or location. Grading turns structural characteristics into meaningful quantitative or qualitative data that can be used in statistical analyses and serve as a basis for clinical decisions. RCs typically have a thorough knowledge of methods used in previous studies. If precedents can be found and applied to the current problem, established outcome measures (based on evidence rather than opinion) can be used; if not, then new structural (and/or functional) outcome measures need to be developed and evaluated. If necessary, RCs can conduct pilot studies, testing new methods on smaller samples under controlled conditions.

Once the methods have been finalized, the RC can define participant eligibility criteria (e.g., minimum/maximum lesion size, optical media transparency, etc.), which will help standardize patient recruitment. To standardize methods all across the study (at multiple national and/or international clinical study sites), protocols are developed for image acquisition (visit timing; equipment criteria; appropriate scan parameters; scan quality criteria; image/data formats, e.g., TIFF, PNG, DICOM, or proprietary, e.g., E2E) and for image/data management (image anonymization, submission to the RC, tracking). To maintain data uniformity, it is essential that all clinical sites comply fully with the study-specific protocols. Likewise, for use within the RC, a protocol is developed for image analysis (grading standard operating procedure [SOP] or independent review charter, grading forms, paper or electronic data entry) and for how the study is to be managed at the RC (study-specific manual of operations). This deals with issues such as quality assurance, grading data management (NB grading data are managed without grader read access and are held separately from clinical data until all grading is concluded and the database is locked), and data analysis.

The RC may help to ensure that the equipment at each participating clinical site is compliant with the requirements documented in the imaging protocol. The RC may also conduct study-specific clinical site photographer training and certification. Duties at clinical sites are shared between site staff, including the principal investigator, study coordinators, and photographers. The RC provides training for these roles as needed. The PI must be trained in order to know what is expected of their staff at their site as well as the necessary administrative routines for managing a site. Study-specific training and certification may also apply to graders at the RC, according to the grading and data entry protocols.

Study Management (Operational Logistics)

Study Initiation

Once the appropriate study-specific protocols have been developed and agreed on, approvals from relevant regulatory bodies collected, and sites approved in terms of equipment and personnel, the study can be initiated.

Patient Recruitment

Clinical sites identify candidates (according to the clinical inclusion/exclusion criteria, e.g., diagnosis, disease severity, age, comorbidities, previous therapies, etc.), perform the imaging as required by the imaging SOP, and send the (anonymized!) image packages to the RC. The RC may assess participant eligibility based on the predefined imaging criteria. When necessary, expert clinicians are asked to arbitrate questionable or borderline cases. Once the decision whether the patient is eligible or not is made, the site is informed.

Follow-up Phase

Once the baseline image sets are collected, during the follow-up phase of longitudinal studies, the RC may manage image data collection, i.e., ensure that clinical sites obtain and submit image sets of suitable quality within the time frames required by the SOP. The RC provides feedback on protocol compliance and provides assistance to on-site clinical

staff with protocol interpretation when necessary. The RC also makes sure that protocols are kept up to date and made available to on-site clinical staff. The RC manages the submitted images, including data storage, inventory, and tracking. Approved image sets are graded at the RC according to the grading protocol by trained and certified graders. Grading performance is assessed regularly. Grading data are managed independently from graders and held separately from clinical data.

Quality Assurance

Throughout all stages of the study, the RC ensures that QA measures are in place and manages monitoring and audits of progress by sponsor or regulatory bodies [8, 9].

Study Termination

The RC also helps develop protocols for what happens once the projected sample size and duration of the study are reached, including patient end-of-study (EOS) procedures, clinical site staff EOS procedure training, and monitoring clinical staff protocol adherence. Once the last patient has been seen and the last image has been graded, all data collected and graded by the RC will be transferred to the sponsor. The RC may participate in data analysis and reporting in scientific journals or at meetings. The RC also manages image and data archival following study termination.

Working With an RC as a Clinical Site

The uniformity of data content and quality is essential and poses a particular challenge in multicenter studies. Clinical sites may be involved in the planning and design of a study or decide to join at a later stage when the study protocols have already been agreed on. In either case, all sites must adhere to the same protocols. So what is expected from a clinical site?

Site Requirements

Sites must comply with study-specific administrative routines for the management of a study.

Protocols for patient (clinical) data records, data entry, image acquisition, and image transfer must be adhered to. Some of these are managed by the RC.

Imaging Equipment Certification

Prior to certification, the manufacturer, model, type, and serial numbers of the hardware and (where relevant) software versions of your imaging equipment will be recorded and, if necessary, inspected at the study site by RC staff. Image artifacts that may be expected—from, for example, misalignment or contamination of the optics—will be assessed either through sample images or by on-site inspection. The calibration status will be investigated and, if necessary, a new calibration will be performed (by the manufacturer's service provider).

Staff Training and Certification

All site staff are required to have passed training and certification in the guidelines of Good Clinical Practice [1–7]. Photographers are expected to have basic familiarity and experience with the equipment to be used. Study-specific protocols for image acquisition will be provided by the RC. This will specify what equipment to use (manufacturer, model, software versions), whether the pupils should be dilated (mydriasis) prior to imaging, and the specifics of the images to be recorded. In the case of OCT scans, these will include detailed information about required scan parameters (type of scan, e.g., in the case of raster volume scans; size of area to be scanned; B-scan intervals; scan grid placement and orientation; ART frame rate), as well as minimum image quality criteria—this may be expressed in signal to noise ratios (dB) as on the Heidelberg Spectralis or in proprietary units like on the CZM Cirrus (signal strength n/10) or the “Q-factor” on Topcon 3D-OCT devices. It is recommended that the scan parameters are verified before performing each scan, in order to prevent possible errors that may require the scans to be repeated or rejected by the RC. Details of how to anonymize

and export scans will be specified. Most OCT manufacturers are moving toward standardizing image data output to comply with the standards set up within the DICOM framework. Scans may also be exported as a series of images with lossless compression, e.g., TIFF or PNG. BMP images are not recommended due to their large file size. Image exports, however, do not contain information about scan parameters (camera/scanner ID, focus, specifics of the eye being scanned, SNR, etc.). File-naming conventions will also be specified. The procedures for certification of equipment and staff are described in the imaging protocol. The RC may offer a multitude of channels for training, to suit the requirements of the specific site or individual photographer. Once the imaging criteria are clear, a set of scans compliant with the SOP are to be submitted to the RC for certification. These will be used to evaluate photographer performance. Once the study is running, another requirement is that images are obtained within the date intervals defined in the study schedule (e.g., 6 monthly ± 2 weeks). Setting up checklists (“cheat sheets”) for image acquisition showing the scan protocol and examination timeline can be a useful guide. Protocols may in principle be amended while a study is in progress.

Images may be submitted by photographers only. Since most communication is now electronic, this necessitates basic IT skills. Depending on the scope of the study, language skills may also be necessary, as in international studies English is typically the main language of communication. Image submission is mostly electronic, via the Internet, using https or sftp/ftps/ssh protocols. Prior to submission, all patient files must be anonymized or pseudonymized according to the study protocol; it is vital that no information that could enable the RC to ascertain the real identity of the patient is present. This applies to openly visible information as well as to embedded data (in the image header, EXIF comments, IPTC information or other embedded data formats). RCs often provide upload portals with individual login credentials for each certified staff member in the study and drag-and-drop functionality via a standard Web browser (Firefox, Chrome, Opera,

Safari, or other). It is important that these upload portals comply with the US Food and Drug Administration’s (FDA) good manufacturing practices (GMP) standards [10] and Code for Federal Regulations Title 21 Part 11 compliance requirements [11]. Sending images in a timely manner is also important, as the SOP may specify a time limit following the patient visit during which the scans must be uploaded. Once the images have been uploaded, the responsible person at the RC should be notified of the fact, typically via email. In some cases, images may be written to optical or (USB/SD/microSD) flash media and sent via post or courier. In this case, printed hard copy transfer documentation is to be attached and the media need to be clearly labeled. Note that data that has not been anonymized or pseudonymized must *never* be sent from the study site, either electronically or via post.

Reading, understanding, and adhering to protocols are essential for all studies. The RC holds the latest version of the upload and image acquisition protocols and makes them available to clinical sites. In addition, the RC can provide training in image acquisition and/or transfer according to the relevant study-specific protocols to all qualified candidates who wish to be certified. Prior to training, however, it is essential that trainees read and try to understand the relevant protocols so that any potential issues with protocol interpretation can be resolved as quickly as possible. Training may be provided via a set of standard photographs, multimedia training packages, on-site live training, or audio-/videoconferencing in groups or on an individual basis. This is available prior to site certification but also as continued training and recertification as necessary due to employee turnover (e.g., new personnel, return following absence, etc.), protocol breach, or on request.

Communication with the RC

Following site certification, communication between the RC and sites is usually via email. Most RCs provide centralized or study-specific email addresses (e.g., submission@RC.ac.uk) that are monitored by multiple members of the

RC team. The RC also provides sites with a list of staff members who can be contacted personally via email, phone, or post. If needed, RC/site conference calls may be arranged via telecom or VOIP (Skype, Viber) or dedicated secure conferencing systems. The RC must preserve all records of communication with study centers (e.g., feedback following certification scans, email traffic), and typically this is preserved along with all patient data at EOS for 10–15 years, at the trial master file (TMF) of the study sponsor.

Documentation and Quality Assurance

Just as at the RC, clinical sites must also preserve a clear audit trail. Staff CVs, job descriptions, training and certification records, equipment certificates, image acquisition, and transmission logs including feedback from the RC must all be maintained. Communication logs should also be retained. Sites must be aware that regulatory or sponsor monitoring visits may be also conducted at individual clinical sites.

Procedures at the RC

In the planning phase of a study, documentation is created at the RC that must include at a minimum the study protocol, which outlines the study requirements and is developed by the sponsor or study group in cooperation with the RC; the safety reference manual, specifying the safety aspects of the study intervention(s); the regulatory (ethics) approval(s) provided by the sponsor; a study-specific manual of procedures (MOP), which describes the work performed at the RC (staff assignment, roles, and responsibilities); the planned image and data storage and archiving procedures; the image acquisition protocol (described earlier); and the image grading protocol.

The grading protocol defines the aims of grading and details equipment criteria, e.g., grading screen parameters, routines for color management (e.g., screen calibration) necessary for accurate color (and grayscale) reproduction,

hardware tools for grading (e.g., stereo viewers), and software tools for viewing and grading images (including making measurements). Finally, the grading SOP defines the grading data entry procedures. Nowadays grading data are entered directly into a dedicated data entry tool tailored to the complexity of the specific grading, to maximize speed and minimize the risk of grader error. All database management systems employed should be compliant with the Code for Federal Regulations (CFR) Title 21, Part 11, issued by the US Food and Drug Administration (FDA) [11].

During the Implementation Phase of the Study

Preparation of Images for Grading

During the execution phase of the study, image sets submitted by clinical sites are downloaded from the transfer server (or CD/flash media). Images received are inspected and checked against the transmittal form to ensure that the correct number and types of images were received, visit intervals were as prescribed in the study protocol, appropriate file formats were used, the labels/file names comply with the SOP, the patient study identifiers are correct (when receiving follow-up scans for a particular patient, it can be useful to compare previous fundus images to those in the new scans in order to confirm that a patient has not been scanned under an incorrect study ID), and no data enabling identification of the patients' real name or clinical status are present (if so, the site and the sponsor are informed, the data are immediately deleted, and a resubmission request is sent) (Fig. 13.2). Images are then uploaded to an image file server that is accessible to graders, an acknowledgement of receipt is sent to the submitting site (indicating any issues or, if necessary, requesting resubmission), and the images are entered into the grading queue (i.e., the graders are notified). All steps in this process are documented in the relevant SOP. Common errors observed by the RC in uploaded scans include incorrect or incomplete study or center ID, patient visit outside the schedule specified in the study

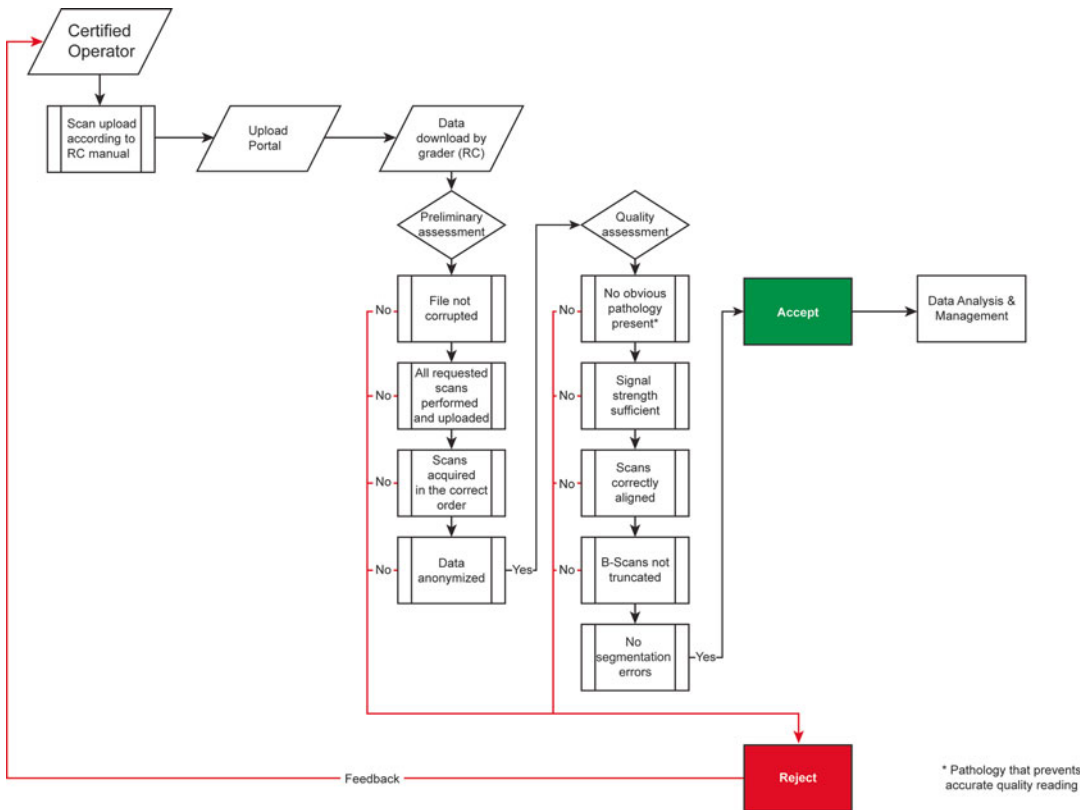


Fig. 13.2 Workflow quality assessment

protocol, incorrect scan protocol, and incomplete anonymization or pseudonymization. The importance of these factors cannot be overstated to study sites. In particular, an incorrect study ID input for the OCT scan will result in the data for that patient being ascribed to another participant, potentially distorting the results and thus the study outcome. A “zero tolerance” approach to study ID errors is therefore recommended, with any scans that have invalid or incorrect IDs immediately being rejected and resubmission with the correct details requested.

Image Grading

Initial image analysis (grading) is performed by primary graders according to the grading SOP within a predefined time period following receipt of the images. Grader hierarchy and the adjudication process are defined in the MOP. Some graders may only be authorized to determine participant eligibility or to perform primary grading. More

senior graders can also perform secondary grading, i.e., reanalyze cases where primary gradings are inconclusive or discrepant. Graders are selected for appropriate roles based on their experience. All graders receive uniform study-specific training. Persisting grading controversies are resolved by an adjudicator who may be the principal investigator or other nominated senior expert clinician. Image grading begins with the recording of grader ID, grading date and time, and an image quality grading (with scans of insufficient quality being rejected). This is followed by a grading of the relevant features of the phenotype, according to the SOP. Once an image (set) has been graded, it is locked, i.e., no longer available to graders, other than for secondary grading or adjudication. Revision of grading is possible but must be fully documented and done under the supervision of a more senior grader, with preservation of the original grading data along with the revised data and a description of the reason for the revision. A subset

of images (typically 10 %, depending on the overall sample size) may be graded multiple times (with a minimum interval of 4 weeks) and by multiple graders. This makes it possible to compare gradings and calculate intra- and inter-grader repeatability. Intra-grader repeatability shows how consistently a grader performs over time. A typical phenomenon is “drift,” which is a gradual change in grading over time, partly due to the learning curve but possibly also to further insight gained during the study. Nevertheless it is important to ensure that grading remains as consistent as possible. Inter-grader repeatability demonstrates how similarly different graders perform. Good initial training is the most important factor ensuring high inter-grader repeatability (see also Chap. 3). Variability in excess of predefined acceptable levels may necessitate re-training or even full recertification of graders.

Image and Data Management

Data safety and access control are managed by local IT support staff. Access control is key to ensuring subject and study confidentiality; i.e., patient data must be masked to reduce grading bias but also to protect the privacy of the participant. Processes must be in place to deal with premature unmasking of study personnel. Grading logs and image tracking may be automated or manual, depending on the size/complexity/scope of the study. Data safety is guaranteed by the redundancy built into the system, through multiple levels of backup servers and a policy for data backup at regular intervals. Most data storage solutions are now cloud-based services; when selecting a service provider, it should be kept in mind that regulators (e.g., the FDA [11] or the European Medicines Agency, EMA [12]) may have restrictions regarding the location of the hosting servers (EU/USA) as well as the routing of data.

At the End of a Study Cycle

Once the last image set has been graded, variable levels of error checking (“database cleaning”) may be necessary, depending on the quality of the implementation of the grading data entry software

(e.g. filtering of impermissible values or blank data cells at the point of entry) and on the level of continuous data maintenance. Once database maintenance is concluded, the grading database is finalized and locked (i.e., no further changes are permitted). Grading and clinical databases may be merged and are sent to the sponsor as well as made available for final analyses. At this point, graders may be unmasked to patient and clinical data and may participate in data analyses and reporting in scientific journals or at meetings.

Data Archiving

Study images, grading data, and administrative records must be archived for extended periods (typically 5–25 years, depending on the preferences of the sponsor and the relevant legislation and regulatory guidelines). Archival also has a purpose beyond regulatory compliance and QA considerations. Often, the results of a study may prompt new research ideas long after the study has been concluded, and so the image database must be kept intact and available for future analyses. Technically this is achieved by an individually optimized combination of online (supporting frequent, very rapid access to data) and near-line (safe, long-term, with infrequent access to data) cloud storage.

QA Measures

Reading centers operate within the framework of Good Clinical Practice [1–7]. All activities must be transparent and well documented, including clear definitions of roles, authorizations and responsibilities of personnel, and procedures relevant to the study. Records of all activities must be kept up to date. Staff must be capable of implementing the necessary work on the study according to SOPs and the MOP but also in how to recognize and report protocol breaches and how to analyze and adjust routines in order to avoid future occurrences. Frequent communication with the research team (and with regulators if necessary) is essential throughout the study

cycle to avoid or at least identify and manage (potential) protocol breaches at an early stage. Prior to initiation, meetings are held with the sponsor's operational staff, followed by an RC orientation meeting/initiation meeting and start-up meetings with investigators and research group staff. Agendas and minutes are recorded for all study meetings. Internal and external audits are conducted, and based on the audit reports, root cause analyses (RCAs) are performed and corrective and preventive action (CAPA) plans are developed. The activities of the RC are also subject to monitoring visits by the sponsor and regulatory bodies. Regulatory inspections may be conducted with or without notice, so preparedness for monitoring visits (at the RC and at clinical sites) is essential.

References

1. World Health Organization. Handbook for good clinical research practice. Guidance for implementation. 2002. http://apps.who.int/prequal/info_general/documents/GCP/gcp1.pdf. Accessed 13 Apr 2015.
2. ICH. E6(R1) Good clinical practice. 1996. <http://www.ich.org/products/guidelines/efficacy/efficacy-single/article/good-clinical-practice.html>. Accessed 13 Apr 2015.
3. US Food and Drug Administration. Clinical trials and human subject protection. <http://www.fda.gov/ScienceResearch/SpecialTopics/RunningClinicalTrials/>. Accessed 13 Apr 2015.
4. Medicines & Healthcare products Regulatory Agency (MHRA). Good clinical practice for clinical trials. 2014. <https://www.gov.uk/good-clinical-practice-for-clinical-trials>. Accessed 13 Apr 2015.
5. Medical Research Council (MRC). MRC guidelines for good clinical practice in clinical trials. 1998. <http://www.mrc.ac.uk/documents/pdf/good-clinical-practice-in-clinical-trials/>. Accessed 13 Apr 2015.
6. Official Journal of the European Union. Commission Directive 2005/28/EC of 8 April 2005 laying down principles and detailed guidelines for good clinical practice as regards investigational medicinal products for human use, as well as the requirements for authorisation of the manufacturing or importation of such products. <http://eur-lex.europa.eu/LexUriServ/LexUriServ.do?uri=OJ:L:2005:091:0013:0019:en:PDF>. Accessed 13 Apr 2015.
7. European Commission. EudraLex – Volume 10 Clinical trials guidelines. 2006. <http://ec.europa.eu/health/documents/eudralex/vol-10/>. Accessed 13 Apr 2015.
8. Tewarie P, Balk L, Costello F, Green A, Martin R, Schippling S, et al. The OSCAR-IB consensus criteria for retinal OCT quality assessment. *PLoS One*. 2012;7(4), e34823.
9. Schippling S, Balk LJ, Costello F, Albrecht P, Balcer L, Calabresi PA, et al. Quality control for retinal OCT in multiple sclerosis: validation of the OSCAR-IB criteria. *Mult Scler*. 2015;21(2):163–70.
10. US Food and Drug Administration. Facts about the current good manufacturing practices (CGMPs). <http://www.fda.gov/Drugs/DevelopmentApprovalProcess/Manufacturing/ucm169105.htm>. Accessed 13 Apr 2015.
11. US Food and Drug Administration. Code of Federal Regulations Title 21, Part 11. <http://www.accessdata.fda.gov/scripts/cdrh/cfdocs/cfcfr/CFRSearch.cfm?CFRPart=11&showFR=1> <http://www.accessdata.fda.gov/scripts/cdrh/cfdocs/cfcfr/CFRSearch.cfm?CFRPart=11&showFR=1>. Accessed 13 Apr 2015.
12. European Medicines Agency. <http://www.ema.europa.eu/ema/>. Accessed 13 Apr 2015.

Index

A

Achiasma, 65–66
ACTHAR, 174
Acthar gel, 174
ACTiMuS, 176
ACTION, 173
Active multiple sclerosis, 104, 115, 148
Against aquaporin 4 (AQP4), 85, 90, 93, 156
AION. *See* Anterior ischemic optic neuropathy (AION)
Algorithm, 28, 31, 36–41, 93, 114, 118, 153, 179, 180
Alzheimer's disease (AD), 79–80
Amiloride, 173, 175
Andrographolide, 175
Angiovue, 25, 26
Anonymized, 188, 190
Anterior ischemic optic neuropathy (AION), 25, 31, 40, 60, 61, 153
Anterograde, 76, 104, 115, 116
Anti-aquaporin 4, 63, 85, 90, 93
A-scan, 26
Astrocytes, 9–11, 13–15, 90, 120
Audit, 43–44, 191, 194
Autoantibodies, 63, 85, 117
Autofluorescence (AF), 24, 29, 30, 41, 66, 75
Autoimmunity, 1
Automated segmentation, 31, 37, 43, 70, 118
Axial resolution, 10, 21, 26
Axonal damage, 51, 99, 103, 161, 164, 171, 172
Axonal degeneration, 7, 14, 47, 50, 52, 71, 73, 74, 76, 79, 80, 104, 109, 113, 115, 116, 119
Azathioprine, 63, 135

B

BIIB017, 176
BIIB033, 173
Bi-directional trans-synaptic axonal degeneration, V, 105
Biomarkers, 91, 93
Blood–brain barrier, 113, 117, 120, 135
Branch retinal artery occlusion (BRAO), 70–72
Bruch membrane, 4, 12, 78
Bruch membrane opening (BMO), 24, 77
B-scan, 2, 24, 28–30, 32, 33, 36–41, 59, 63, 71, 142, 189

C

Canon OCT HS-100, 25, 26
Central nervous system (CNS), 1, 3, 11, 13–15, 62, 63, 78, 80, 85, 97–99, 101–109, 113–115, 126, 128
Central retinal artery occlusion, 71
Cerebrospinal fluid (CSF), 14, 15, 47, 78, 144, 164
Chiasmitis, 64–65
Chronic inflammatory optic neuropathy, 98
Chronic relapsing inflammatory optic neuropathy (CRION), 60, 63, 64, 88
Cirrus, 24–26, 48, 93, 114, 123, 180, 189
Clinical isolated syndrome (CIS), 50, 61, 62, 97–109, 121, 128, 163, 176, 181
Clinical trial, 2, 31, 33, 38, 41, 42, 52, 127, 148, 165, 173–179, 181
CMM-EM, 176
Cocaine, 69, 70
Cognition, 22–23, 41, 59, 176, 187
Colour vision, 6, 37, 47, 52, 59, 61, 63, 65, 98–100, 117, 163, 164, 174, 178, 182
Conduction block, 99, 106
Copernicus HR, 25, 26
CRAO, 40
CRION. *See* Chronic relapsing inflammatory optic neuropathy (CRION)
CSF. *See* Cerebrospinal fluid (CSF)

D

3D 2000, 25, 26
Dementia, 26
Demyelination, 1, 47, 50, 101, 104–107, 113, 115, 116, 127, 136, 161, 163, 171
Devic, 85
Disease modifying therapies, 51, 113, 120
3D OCT 1000, 25
Doppler OCT, 26, 31
DRI OCT Atlantis, 25
Drusen, 30, 38, 40, 41, 44
Dyschromatopsia, 62, 64, 73, 74, 80, 98

- E**
 Early Treatment Diabetic Retinopathy Study (ETDRS), 24, 48, 62, 146, 147, 180
 Electrodiagnostic testing, 65, 74
 Electroretinogram/electroretinography (ERG), 116, 117, 119, 122, 173, 174
 Erythropoietin, 173
 ETDRS. *See* Early Treatment Diabetic Retinopathy Study (ETDRS)
 Ethics, 191
 Examiner, 21–23
 Expanded disability status scale (EDSS), 91, 103, 119, 151
 Eye-Tracker, 28, 29
 Eye tracking, 24, 25
- F**
 Fingolimod, 7, 124, 164, 174
 Fixation, 22, 23, 26, 28, 38, 42, 117, 187
 Floater, 23, 39, 41, 65
 FLORIMS, 175
 Fluorescence angiography (FA), 24, 31, 48, 75
 Flupirtine, 175
 Foveola, 12, 29, 30, 38, 39, 65, 66, 123
- G**
 Glare, 62, 122
 Glia, 11, 13
 Glycosylation, 31
- H**
 Heidelberg Engineering, 24, 118, 180
- I**
 Ibudilast, 175
 Immunology, 85, 176
 Indocyanine green angiography (ICGA), 24
 Inflammation, 1, 47, 61, 63, 67, 97–102, 104–106, 108, 109, 113, 115, 117, 119, 120, 122, 123, 125–127, 129, 135, 153, 164, 171
 Interferon, 174–176
 Interferon beta-1a, 174, 175
 Interferon beta-1b, 175
 Isolated optic neuritis (ION), 60, 62–65
 IVue, 24–26
- K**
 Kuppersmith, 31
- L**
 Lamina cribrosa, 10, 13–15, 29, 49, 73, 113, 115
 Layer
 ganglion cell layer, 1, 2, 8–10, 12, 13, 49, 51–53, 59, 90, 99, 104, 114, 121, 126, 139, 143, 144, 152–154, 172, 174, 177–178
 inner nuclear layer, 7–9, 11–13, 59, 74, 87–90, 99, 104, 105, 107, 114, 116, 124, 126, 139, 142–144, 151, 152, 154, 155, 157, 164, 179, 180
 inner plexiform layer (IPL), 7–9, 11, 12, 31, 33, 48, 51, 52, 59, 71, 88–90, 114, 118, 121, 138, 139, 144, 151, 173, 174, 178
 outer nuclear layer (ONL), 6–7, 13, 32, 33, 36, 37, 41, 43, 61, 71, 78, 88, 90, 114, 117, 118, 122, 124–126, 128, 144
 outer plexiform layer, 7, 8, 12, 13, 61, 90, 114, 117, 118, 151
 photoreceptor layer, 5, 6, 13, 117
 pigment epithelium, 4–6
 retinal nerve fibre layer. (*see* Retinal nerve fibre layer (RNFL))
 Leber's hereditary optic atrophy, 61, 98, 122, 153, 164
 Lipoic acid, 174
 Longitudinal, 2, 24, 25, 31, 39, 41, 43, 51, 53, 63, 64, 69, 73, 76, 93, 103–104, 109, 120–122, 127, 129, 139, 144–148, 165, 171, 185, 188
- M**
 Macular, V, 2, 7, 11–12, 27–28, 37, 39, 48, 53, 55, 61, 66, 71–72, 75–77, 81, 86, 87, 89, 99, 114, 130–132, 136, 140, 144–145, 149, 151, 163, 166–169, 173, 174, 180–188, 194–196
 Macular (o)edema, 7, 122, 164
 Maculopathy, 61, 74, 75, 90
 Magnetic resonance imaging (MRI), 1, 47, 61, 86, 91, 101, 107, 123–127, 143, 171, 174, 176, 179
 McDonald criteria, 1, 97, 102
 MD1003, 175
 Meta-analysis, 49, 100, 102
 Microcystic macular (o)edema, 48, 88–90, 100, 105, 142, 151–157, 180
 Microcysts, 28, 66, 69, 77, 80, 105, 156, 164
 Microsaccades, 80
 Minocycline, 173
 Mitochondrial, 74, 136
 Mobility, 22
 MSCIMS, 176
 MSON. *See* Multiple sclerosis associated optic neuritis (MSON)
 MS-SMART, 175
 Muller cell, 6, 7, 10–12, 90, 93, 125, 156, 158
 Multifocal VEP (mfVEP), 107, 108, 163, 182
 Multiple sclerosis, 1, 22, 47, 59, 61–62, 85, 97, 113, 135–136, 151, 161, 165, 171
 Multiple sclerosis associated optic neuritis (MSON), 36–38, 47–55, 59–81, 87, 98–100, 102, 103, 137–139, 142, 145, 146, 148
- N**
 NAION, 69, 70, 75, 76
 Natalizumab, 52, 174, 176
 NCRT, 176
 Network, 13, 109

Neurodegeneration, 21, 31–33, 44, 80, 99, 101, 104, 114–117, 120, 123–125, 127–129, 135, 143, 165, 172, 176, 178–182
 Neurodegenerative diseases, 1, 79–81, 151
 Neurofilament, 31
 Neuromyelitis optica (NMO), 2, 40, 65, 85, 86, 98, 152, 153, 156, 164
 Neuro-ophthalmology, 29, 47, 179, 180
 Neuroprotection, 52, 99, 103, 127–129, 171–182
 Neuroprotective, 2, 31, 50, 51, 94, 104, 109, 114, 127, 128, 144, 145, 148, 165, 171–172, 177, 178, 181, 182
 Nidek, 25
 Nitrosylation, 31
 NMO. *See* Neuromyelitis optica (NMO)
 Nystagmus, 22, 65, 187

O

OCT/SLO, 25
 Oligodendrocytes, 13–15, 115, 127
 Optic atrophy, 9, 61, 73, 78–80, 116, 153, 164
 Optic disc, 98, 100
 Optic disc swelling, 98
 Optic nerve, 3–15, 24–27, 29, 40–42, 48–51, 53, 61, 63, 73, 74, 85, 88, 90–92, 94, 97, 98, 101, 104, 105, 107, 108, 113–117, 119, 120, 122, 125, 127, 128, 139, 142, 151, 153, 161, 163, 171
 Optic neuritis, 1, 2, 9, 14, 24, 25, 31, 47–55, 59–64, 67, 68, 73, 85–90, 92, 93, 98–102, 106, 107, 109, 115, 121–123, 137–141, 144, 151–153, 155, 161, 162, 165, 171, 173, 174, 176–179, 181
 Optic neuropathy, 2, 25, 31, 47, 61, 63, 69, 73–77, 88, 98, 105, 115, 116, 119, 127, 128, 152–156, 158, 161, 164
 Optopol Technology, 25
 Optos, 25
 Optovue, 24, 25
 OSCAR-IB, 33, 37, 40, 41, 165, 180
 Outcome measure, 9, 52, 86, 104, 127, 128, 165, 166, 185–188

P

Papilloedema, 9, 66, 69
 Perimetry, 49, 99, 100, 187
 Phenytoin, 173
 Phosphorylation, 31
 Pitfalls, 31–32
 Plasticity, 99
 Polarization sensitive OCT (PS-OCT), 31, 100
 Post-translational modification, 31
 Power calculation, 93
 Prednisone, 73, 74, 98
 Primary progressive multiple sclerosis (PPMS), 50, 97, 103, 113, 120, 135, 137–139, 143–147, 175, 176
 PROTECT, 174
 Protein aggregate, 31
 Protocol, 22, 26–31, 33, 38, 41, 44, 103, 136, 137, 165, 171, 180, 185, 187–194

Pulfrich, 62
 Pupil size, 25–26, 33

Q

Quality control (QC), 2, 31, 32, 43

R

Reading centre, 187–188
 Relapsing isolated optic neuritis (RION), 60, 63, 152, 153
 Relapsing remitting multiple sclerosis (RRMS), 50, 53, 86, 87, 97, 103, 104, 107, 109, 113–129, 135–139, 142, 144, 147, 148, 151, 174–176, 181
 Relative afferent pupil/pupillar defect (RAPD), 52, 63, 64, 71, 73, 74, 80, 98
 RENEW, 173
 Resolution, 2, 6, 8, 10, 21, 25, 26, 52, 67, 69, 73, 106, 113, 117, 118, 156, 164
 Retina, V, 1, 3, 5, 10, 21, 31, 48, 59, 86, 98, 114, 136, 151, 155, 161, 172, 186
 Retinal nerve fibre layer (RNFL), 1, 29, 34, 36–38, 43, 44, 48, 50–51, 53–55, 59, 77, 98, 99, 114, 119–121, 123, 126, 127, 138–141, 143, 161, 162, 172, 177
 Retinopathy, 40, 48, 61, 154, 156, 172
 Retrograde, 7, 14, 73, 74, 77, 79, 80, 88, 90, 94, 100, 104, 105, 115, 116, 119, 122, 127, 142, 151–158, 163, 164, 172
 Retrograde maculopathy, 77, 80, 142, 151–158
 Riluzole, 175
 Ring Scan, 24, 26, 28, 29, 31–33, 35–38, 42, 44, 59, 62, 67, 69, 73, 76, 77, 141
 RION. *See* Relapsing isolated optic neuritis (RION)
 Risk factors, 60, 71, 73, 117, 154
 RRMS. *See* Relapsing remitting multiple sclerosis (RRMS)
 RS-3000, 25, 26

S

Scanning laser ophthalmoscopy (SLO), 25, 141, 142, 164
 Scanning laser polarimetry, 31
 Scanning speed, 25, 26
 Secondary progressive multiple sclerosis (SPMS), 50, 97, 103, 113, 135, 137–139, 141, 143–148, 175, 176
 Segmentation, 2, 24, 25, 28, 31, 32, 36, 37, 43, 49, 51–52, 63, 70, 71, 93, 100, 104, 107, 114, 118, 119, 122, 124–126, 128, 129, 136, 139, 144, 164, 178–180, 186
 SLE. *See* Systemic lupus erythematosus (SLE)
 SLO. *See* Scanning laser ophthalmoscopy (SLO)
 Spectralis, 24–28, 92, 93, 118, 180, 189
 SPMS. *See* Secondary progressive multiple sclerosis (SPMS)
 Steroids, 52, 53, 60, 63, 66, 73, 158
 Stratus, 25, 26
 Systemic lupus erythematosus (SLE), 40, 60, 61

T

Team, 41–42, 44, 191, 193
Topcon, 25, 189
Training, 41, 43, 44, 185, 187–193
Trans-synaptic, 14, 71, 73, 74, 79, 80, 88, 90, 94,
104–105, 116, 125, 163, 172
Treatment, 2, 24, 31, 40, 47, 48, 52, 63, 73, 98, 113, 124,
127, 135, 144, 148, 152, 157–158, 161–166, 171,
174, 177–179
Tubulin, 31
Tysabri, 176

U

Uthoff, 59, 62, 99

V

VISION, 173
Vision, 3, 6–8, 10, 11, 22, 23, 26, 37, 47, 48, 50–53, 59,
61–66, 73–76, 98–100, 108, 109, 117, 158, 163,
164, 166, 173, 174, 177–180, 182
Visual evoked potentials (VEP), 74, 94, 102, 106–108,
119, 163, 173–176
Visual field, 8, 13, 22, 47, 48, 65, 69–71, 73, 75, 91, 98,
100, 106–108, 117, 158, 163, 164, 174, 176, 179
Vitamin B12, 60

Z

Zeiss, 24, 93, 123, 180